Carbon dynamics in Arctic vegetation

Lorna Street

PhD Thesis

University of Edinburgh
School of GeoSciences

March 2011

Declaration

I declare that this thesis has been composed by myself and has not been submitted for any other degree. The work described is my own, except where otherwise indicated.

Lorna E Street

March 2011

Abstract

Rapid climate change in Arctic regions is of concern due to important feedbacks between the Arctic land surface and the global climate system. A large amount of organic carbon (C) is currently stored in Arctic soils; if decomposition is stimulated under warmer conditions additional release of CO_2 could result in an accelerating feedback on global climate. The strength and direction of Arctic C cycle - climate feedbacks will depend on the growth response of vegetation; if plant growth increases some or all of the extra CO_2 emissions may be offset. Currently the Arctic is thought to be a small net sink for CO_2, the expected balance of terrestrial C sinks and sources in the future is unknown. In this thesis I explore some of the critical unknowns in current understanding of C cycle dynamics in Arctic vegetation.

Quantifying gross primary productivity (GPP) over regional scales is complicated by large spatial heterogeneity in plant functional type (PFT) in Arctic vegetation. I use data from five Arctic sites to test the generality of a relationship between leaf area index (LAI) and canopy total foliar nitrogen (TFN). LAI and TFN are key drivers of GPP and are tightly constrained across PFTs in Low Arctic Alaska and Sweden, therefore greatly simplifying the task of up-scaling. I use data from Greenland, Barrow and Svalbard to asses the generality of the LAI-TFN relationship in predicting GPP at higher Arctic latitudes.

Arctic ecosystems are unique among biomes in the large relative contribution of bryophytes (mosses, liverworts and hornworts) to plant biomass. The contribution of bryophytes to ecosystem function has been relatively understudied and they are poorly represented in terrestrial C models. I use ground based measurements in Northern Sweden to fill an existing data gap by quantifying CO_2 fluxes from bryophytes patches in early spring and summer, and develop a simple model of bryophyte GPP. Using the model I compare bryophyte GPP to that of vascular plants before, during and after the summer growing season, finding that productive bryophyte patches can contribute up to 90 % of modelled annual GPP for typical vascular plant communities at the same

site, and that the relative magnitude of bryophyte GPP is greatest in spring whilst the vascular plant canopy is still developing.

Understanding how GPP relates to plant growth is important in relating remotely sensed increases in Arctic 'greenness' to changes in plant C stocks. I use a ^{13}C pulse-labelling techniques to follow the fate of recently fixed C in mixed vascular and bryophyte vegetation, with a focus on quantifying the contribution of bryophytes to ecosystem carbon use efficiency (CUE). I show that bryophytes contribute significantly to GPP in mixed vegetation, and act to increase ecosystem CUE. I highlight the importance of including bryophytes, which do not have roots, in aboveground: belowground partitioning schemes in C models.

To further explore C turnover in bryophytes, I use the results of a second ^{13}C labelling experiment to develop a model of C turnover in two contrasting Arctic mosses (*Polytrichum piliferum* and *Sphagnum fuscum)*. I find significant differences in C turnover between *Polytrichum piliferum* which respires or translocates about 80 % of GPP, while *Sphagnum fuscum* respires 60 %. This analysis is the first to explicitly model differences in C partitioning between Arctic bryophyte species.

Finally, I discuss the implications of each chapter for our understanding of Arctic C dynamics, and suggest areas for further research.

Acknowledgments

I am enormously grateful to my supervisor Prof. Mathew Williams for his support and guidance over the past years. I particularly appreciate that he has tirelessly responded to my relentless self-doubt with positivity and encouragement. He is a great mentor and has been a huge help to me at difficult moments. I am also very grateful to my supervisor from the Macaulay Institute, Dr. Martin Sommerkorn, both for his help with my studies and for his and his family's hospitality in Aberdeen. Despite moving to a demanding job outside of academia mid-way through my second year, he still found the time to make helpful, thoughtful comments on every chapter. My only disappointment is that we never did any ski-touring. Thanks also go to my second supervisor at Edinburgh, Dr. Caroline Nichol, whom I hold in high regard as an excellent role model for women in science.

Very important thanks go to two scientists from whom I have learnt enormous amounts whilst having a really fun time. I was lucky enough to work with Dr. Jens-Arne Subke during the design and execution of both isotope-labelling experiments; he also ran hundreds of my samples at York and has generally been fantastically helpful in the production of two of my manuscripts. A big thank you also goes to Dr. Paul Stoy for his valuable intellectual input and thorough commenting on manuscript drafts, but also for being a brilliant person to work with in the field.

I would like to thank Gus Shaver, Ed Rastetter and Mark van Wijk for providing data for my first chapter and for continuing to work with me even after I ceased to be their RA. Much of the isotope work would not have happened were it not for Prof. Phil Ineson's kind loan of his mass-spectrometer with the additional support of Andreas Heinemeyer and Harry Vallack. I would also like to thank Barry Thornton and the support staff at the Macaulay Institute for their help with isotope analysis and administrative things. I owe nearly all the data I collected to the assistance of the staff at Abisko Research Station (especially Linnea, Annika and Anders) and at Kevo Research Station (especially Elina, Risto and Esa). The following people helped me

with weighing, sorting and grinding samples: Soraya Bishop, Michael Starkey, Veronica Lussier and Laura Packham. Thanks also to Helene Ducrotoy, Carole Lowther, Katie Walker and Rosyln MacDonald for their help and good company during fieldwork. I have very fond memories of my PhD field trips and for that I also heartily thank my ABCAUS colleagues and many other wonderful people; Frida, Ben, Victoria, Rachel T…to name a few.

I am very grateful to my friends Casey and Tim for offering all sorts of valuable help and advice whenever needed, and to Mikael and Harriet for the happy home I've had for the past four years. I thank Nancy for proof-reading, for being an excellent office-mate and friend, and then for showing up when I least expected. I thank Catherine, Hazel, Alun and Robert (1 yr) for always being there when I needed them.

Finally, I dedicate this thesis to my parents, Victoria and David, and thank them for providing me with the opportunities to further my education right from the very beginning.

Contents

1. Introduction

Thesis context: Arctic ecosystems are changing

Arctic regions are especially vulnerable to climate change

Recent trends in global climate warming are now unequivocal. The IPCC strengthened their position in the 4th Assessment Report stating that anthropogenic emissions of greenhouse gases (GHGs) were '*very likely*' to be the primary cause of recent warming (Solomon *et al.*, 2007), meaning an 'assessed probability of occurrence' of > 90 %. In December 2010 the globally averaged concentration of CO_2 in the atmosphere reached 390 p.p.m., the highest in 800,000 years (Dr. Pieter Tans, NOAA/ESRL). In June 2010, the twelve month running mean of average global surface temperature reached a record high (Hansen *et al.*, 2010). Changes in global climate are felt most strongly in the polar regions due to amplification of warming at high latitudes. This occurs due to regional changes in heat transport and radiative forcing, and due to decreases in albedo as a result of melting ice and snow. Polar amplification was predicted by global circulation models (GCMs) more than a decade ago (Polyakov *et al.*, 2002) but has only recently been confirmed in the observational record (Bekryaev *et al.*, 2010). If average annual global temperatures increase by 4 °C by the end of the century, large swathes of the terrestrial Arctic are predicted to experience warming of at least 6 °C (Sanderson *et al.*, 2011).

The potential impacts of a changing climate on Arctic regions are wide-ranging, including melting of sea-ice and glaciers, loss of habitat for Arctic species, cultural and economic impacts on indigenous communities, severe coastal erosion, and damage to infrastructure through subsidence of permafrost. Some changes will create economic opportunity, for example increasing marine access for shipping and natural resource extraction (ACIA, 2005). Recent assessments suggest that 30 % of the world's undiscovered gas, and 12 % of undiscovered oil reserves are located offshore above the Arctic circle (Gautier *et al.*, 2009). In 2009, for the first time in history, commercial vessels navigated the north-east passage through ice-free waters. Increasing

accessibility to the Arctic regions and evolving knowledge of their complex geography will also have profound geopolitical implications, for example in competing claims over sovereignty and navigation rights (Ebinger & Zambetakis, 2009).

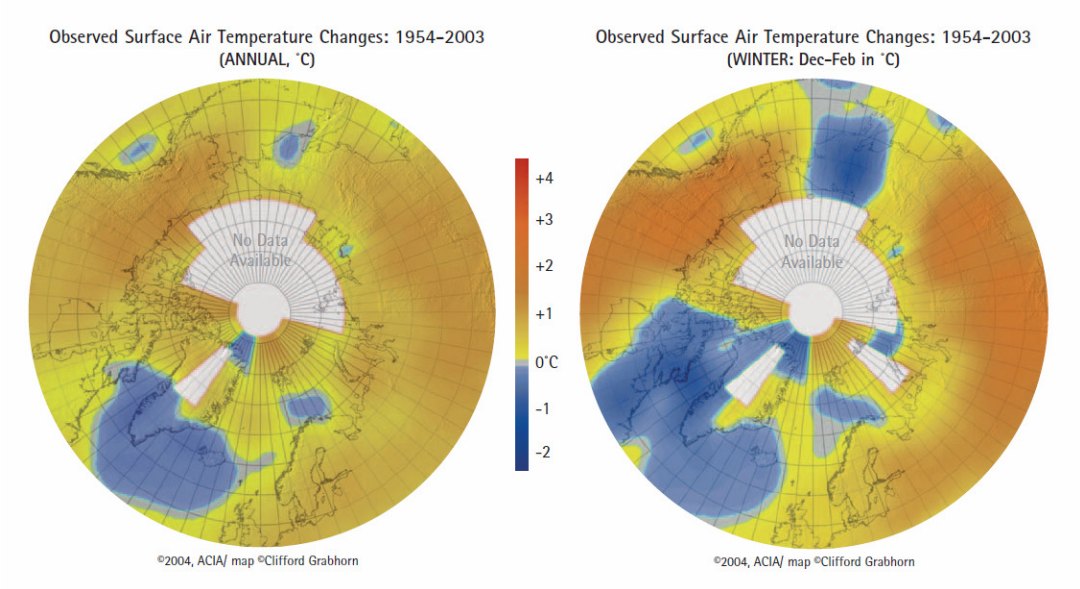

Figure 1. Observed annual and winter Arctic surface air temperature change 1954-2003. Modified from the Arctic Climate Impact Assessment (ACIA) 2005.

Changes in climate are affecting the structure and function of Arctic ecosystems both on land and in the ocean (Post *et al.*, 2009). Critically, shifts in ecosystem function may change the complex nature of feedbacks between the biosphere and the climate system potentially accelerating rates of change by increasing the net strength of positive feedbacks (Arneth *et al.*, 2010; Friedlingstein *et al.*, 2006). Reduction in the extent of summer sea ice for example, reduces the ability of the region to reflect solar radiation and has a regional heating effect, though production of aerosols from open sea water may increase cloudiness and result in cooling (McGuire *et al.*, 2006). There is some evidence that degradation of permafrost under the coastal Arctic ocean may lead to the release of CH_4 from methane hydrate deposits and other geological sources (Shakhova *et al.*, 2010). Release of C stored in permafrost soils either as CO_2 or CH_4 due to enhanced decomposition or methanogenesis, could add further GHG to the atmosphere (McGuire *et al.*, 2009). The complexity and interdependence of Arctic

climate feedbacks makes quantifying the net effect on the climate system extremely challenging. However, this knowledge is critical; both for the identification of 'safe' targets for human GHG emissions and for our ability to anticipate and adapt to unprecedented changes in climate globally.

The complexity of Arctic C cycle - climate feedbacks

Feedbacks between climate and the terrestrial C cycle in the Arctic are of particular importance due to the large amounts of C stored in terrestrial ecosystems. Most of this C is stored in soils as organic material, typically attributed to the limiting effects of cold temperatures and anaerobic conditions on decomposition (Hobbie *et al.*, 2000; Shaver *et al.*, 2006; Wallenstein *et al.*, 2009). The northern circumpolar region is estimated to contain about 1600 Pg of carbon in soils (Tarnocai *et al.*, 2009), with about 60-70 Pg stored in vegetation (McGuire *et al.*, 2009). These C stores are vulnerable to the effects of warming, for example if heterotrophic respiration increases with increasing soil temperature (Davidson & Janssens, 2006). For illustration, if the Arctic loses 10 % of stored terrestrial C to the atmosphere as CO_2 by 2100, this would be equivalent to approximately 25 years' worth of additional fossil fuel emissions of CO_2 over the same period, at current emission rates (Denman *et al.*, 2007).

Currently the Arctic is thought to be a small net sink for CO_2 on the basis of remote sensing and process modelling studies (McGuire *et al.*, 2009; McGuire *et al.*, 2010; Sitch *et al.*, 2007). Modelled estimates of the net balance between CO_2 uptake by vegetation and loss through ecosystem respiration, fall within the large uncertainty range of bottom-up estimates based on surface measurements, which are highly spatially and temporally variable (Griffis *et al.*, 2000; Groendahl *et al.*, 2007; Kwon *et al.*, 2006; Lund *et al.*, 2010). Under future Arctic climate scenarios CO_2 uptake through enhanced photosynthesis is generally expected to partially or fully compensate for the temperature stimulation of soil respiration. Plant productivity is likely to increase if nutrients become more available due to more rapid N mineralisation in soils (Rustad *et al.*, 2001), while rising CO_2 concentrations are expected to have significant positive effects on plant productivity through CO_2 fertilisation (Sitch *et al.*, 2008). A 'greening'

trend in remote sensing data suggests that Arctic vegetation is already becoming more productive (Jia *et al.*, 2003, 2009; Myneni *et al.*, 1997). A recent comparison of 10 coupled climate-carbon cycle models by Qian *et. al.* (2010) predicts that the Arctic will continue to be a net CO_2 sink for the next 100 years as increases in plant productivity and associated litter input to soils outweigh increases in soil organic matter decomposition.

Forecasts of a future Arctic carbon sink are not always consistent with observational evidence. For instance, latitudinal (Wilmking *et al.*, 2006) and altitudinal (Sjogersten & Wookey, 2009) encroachment of the tree line appears to result in lower total ecosystem C storage. Both of the above studies indicate that conversion of tundra to forest reduces belowground C storage by increasing rates of decomposition (but see Kammer et al. (2009)). Long-term nutrient addition experiments have also resulted in lower ecosystem C storage, due to changes in rooting depth and the lifting of N limitation on decomposition (Mack *et al.*, 2004). Artificial warming has also resulted in both positive and negative CO_2 sink responses, dependant on water level position (Huemmrich *et al.*, 2010b).

Current carbon-cycle climate models inadequately represent many biologically mediated C cycle processes which we know are important in determining ecosystem C balance (Chapin *et al.*, 2009). These include but are not limited to 1) controls over the allocation of recently photosynthesised C to growth versus respiration, and between aboveground and belowground productivity in vascular plants 2) interactions between belowground plant C allocation and soil biogeochemistry 3) interactions between C, N and H_2O cycles and the implications for C cycle sensitivity to climate. Many terrestrial C cycle processes unique to cold environments are also absent from global models (Qian *et al.*, 2010), for example permafrost melt and peatland C dynamics. Release of C from melting permafrost has been shown to overwhelm positive plant growth responses over periods of decades (Schuur *et al.*, 2009; Vogel *et al.*, 2009). Experimental results also indicate that old C in deep peat deposits may be vulnerable to decomposition constituting a large potential positive feedback on warming (Dorrepaal

et al., 2009). The effect of increases in disturbance events such as fires and the outbreaks of insects contribute significantly to CO_2 fluxes, but are also poorly represented (Sitch *et al.*, 2007; Wolf *et al.*, 2008).

Arctic C cycle feedbacks include the potential effects of increasing methane emissions, of particular concern due to the greater radiative forcing potential of CH_4 compared to CO_2 (Solomon *et al.*, 2007). The Arctic is currently a source of methane; satellite measurements of global atmospheric CH_4 concentrations suggest the increase in global atmospheric concentration between 2003-2007 was consistent with warming of mid-latitude and Arctic wetlands (Bloom *et al.*, 2010). Arctic climate feedbacks are also further complicated by evidence that increased growth of shrubs and trees is accompanied by decreases in albedo which may act to more than offset any increased sequestration in long lived plant material (Chapin *et al.*, 2005). Shrubs also enhance the retention of snow over the landscape, insulating the soil from low temperatures in winter and increasing rates of winter respiration, a significant part of the annual C budget (Grogan & Jonasson, 2005). Current understanding of the role of vegetation and vegetation change in controlling interactions between climate and the terrestrial C cycle does not currently extend to predicting the net direction, magnitude or timing of climate feedbacks .

The nature of Arctic vegetation

Arctic tundra vegetation is characterised by the absence of trees and high spatial heterogeneity. Patches of vegetation dominated by evergreen or deciduous shrubs, graminoids, bryophytes or lichens can occur over scales of less than 1m (Williams *et al.*, 2008). The leaf area index (LAI) of these communities is also highly variable; for example ranging between 0.1 and 3.6 at 0.2 m resolution and between 0.1 and 1.6 at ~10 m resolution in European sub-arctic heath (Spadavecchia *et al.*, 2008). Heterogeneity in Arctic vegetation composition and structure complicates the task of scaling up experimental (plot) level understanding of C cycle processes, as it requires either knowledge of the spatial distribution of vegetation across the landscape, or identification of general relationships which are independent of vegetation type.

Many important C cycle processes are strongly dependant on the functional type composition of vegetation, for example in determining the ration of aboveground to belowground C allocation, rooting depths (Wookey *et al.*, 2009) and litter quality (Cornelissen *et al.*, 2007b). The presence of a wide range of functional types also allows for large functional shifts if species composition changes under an altered climate. Functional shifts are accompanying recent increases in vegetation productivity; deciduous shrubs replacing graminoid tundra in low Arctic tundra (Forbes *et al.*, 2010; Hallinger *et al.*, 2010; Molau, 2010; Sturm *et al.*, 2001; Tape *et al.*, 2006). New evidence from repeat sampling of historic experimental sites in high Arctic systems however, show increases in plant biomass without major shifts in species composition (Hill & Henry, 2011; Hudson & Henry, 2010).

Arctic vegetation is also characterised by large abundances of bryophytes (mosses, liverworts and hornworts). Where estimates have been made, aboveground biomass of bryophytes is about 30 % that of vascular plants. Bryophytes play an important role in Arctic ecosystems, they can account for significant photosynthetic carbon uptake (Douma *et al.*, 2007; Sommerkorn *et al.*, 1999) and produce litter which is resistant to decomposition so strongly influence the organic matter content and dynamics of soils (Hobbie *et al.*, 2000). Bryophytes are also important in regulating the thermal

environment of the soil due to their effects on ecosystem energy balance (Gornall *et al.*, 2007). The impact of bryophytes on photosynthetic carbon fluxes, and on the thermal and hydrological regimes of Arctic ecosystems is currently poorly represented in most regional terrestrial C models (Sitch *et al.*, 2007). The loss of bryophytes from Arctic plant communities is generally expected as a consequence of Arctic warming, due to changes in surface energy balance and increased shading by vascular plants (Shaver *et al.*, 2001; van der Wal *et al.*, 2005; Wookey *et al.*, 2009).

Thesis rationale: a better understanding of Arctic land-atmosphere CO_2 fluxes and the fate of assimilated C

Large uncertainties remain over how the terrestrial Arctic will respond to climate change and the extent to which the net effects of carbon-climate feedbacks will accelerate or decelerate warming. The aim of this thesis is to contribute towards a better understanding of the processes governing Arctic C balance, addressing two main themes: 1) quantification and prediction of GPP in Arctic terrestrial ecosystems and 2) patterns of allocation and turnover of recently photosynthesised C.

A well constrained relationship between gross primary productivity (GPP) and leaf area index (LAI) has been identified at low Arctic tundra sites (Shaver *et al.*, 2007; Street *et al.*, 2007). This relationship demonstrates a 'functional convergence' across PFTs, and is a powerful tool in up-scaling GPP through remotely-sensed estimates of LAI. The convergence in GPP with respect to LAI has been linked to a tightly-constrained relationship between LAI and the total foliar nitrogen (TFN) of plant canopies (Williams & Rastetter, 1999) at the same sites. The generality of the LAI-TFN relationship across sites and latitudes is unknown however, as are the mechanisms by which coupling is achieved. A better understanding of the LAI_TFN relationship and the impact on canopy scale GPP fluxes would improve regional scale GPP prediction for the Arctic and potentially provide new insights into how natural mixed-species canopies are constructed.

While measurements of *in-situ* rates of GPP demonstrate that bryophytes can contributed significantly to photosynthetic fluxes (Douma *et al.*, 2007; Sommerkorn *et al.*, 1999), few attempts have been made to quantify the seasonal drivers of land-surface CO_2 exchange for bryophyte dominated vegetation. In particular, bryophytes may be important in the early growing season, before canopy expansion in vascular vegetation. Simple models relating bryophyte productivity to environmental drivers which extend beyond the growing season and which are supported by *in-situ* data are a required step towards improving the representation of bryophytes in C models.

Interpreting patterns of vegetation change in terms of impacts on terrestrial C storage requires an understanding of 1) the fraction of GPP used for plant growth versus that re-released to the atmosphere through autotrophic respiration (the carbon use efficiency, CUE) 2) the partitioning of photosynthesised C between plant pools, and 3) the longevity of those pools. The role of mosses in the partitioning and turnover of C in Arctic ecosystems is a key uncertainty in terrestrial C models, and critical in understanding the impacts of the loss of bryophytes on Arctic ecosystem function. There is a need for a better understanding of the processes and drivers of plant C allocation and turnover at the ecosystem scale.

Thesis objectives:

The objectives of this thesis are to resolve key uncertainties related to the uptake and turnover of C within Arctic vegetation. Specifically:

In estimating Arctic gross primary productivity:

1. Are there general relationships between leaf area index, total foliar nitrogen and GPP across Arctic terrestrial ecosystems?

2. What is the annual GPP of common bryophyte species in comparison to vascular plants? What are the key drivers of bryophyte GPP?

In understanding the allocation and turnover of assimilated C within vegetation:

3. What role do bryophytes play in C turnover and allocation in Arctic vegetation?

4. What is the CUE and rate of turnover of recently fixed C in common bryophyte species?

Overview of thesis chapters:

The thesis is structured as a series of four papers, either published or intended for publication; all chapters stand alone as research articles. The thesis also includes two appendices presenting data which was collected as part of the thesis work but which

was not included within the research chapters. The content and purpose of each paper are outlined below.

Paper 1.Photosynthetic CO_2 flux and the relationship between leaf area index and total foliar nitrogen across Arctic latitudes

This chapter examines whether a simple relationship identified between LAI and total foliar plant nitrogen (TFN) in Alaska and Sweden (van Wijk *et al.*, 2005), is a universal relationship across sites and latitudes. Our objective was to test the LAI-TFN relationship in high Arctic and coastal tundra environments, and to assess its impact on gross primary productivity (GPP). We use LAI, TFN and GPP data collected between 1997 and 2009 to test the generality of the LAI-TFN relationship. We find differences in parameters representing theoretical top of canopy N concentration, and the degree of uniformity in leaf N concentration with canopy depth. We suggest this is due to between-site differences in total radiation and the fraction of radiation which is diffuse.

Paper 2. Seasonal bryophyte productivity in the sub-Arctic: A comparison with vascular plants

This chapter addresses the importance of bryophyte photosynthesis in seasonal photosynthetic CO_2 flux in Arctic vegetation using measurements and a model. The model is based on independent laboratory light, temperature and moisture photosynthesis response curves, and compared against *in situ* GPP measurements, for *Polytrichum piliferum* and *Sphagnum fuscum*. The flux data presented include the first ever published values of *in situ* bryophyte photosynthesis made in spring *before* the end of the snow season. The paper shows that cumulative GPP through the season for mosses patches is comparable to that of vascular plants, approximately 90 % and 30 % respectively of modelled annual GPP for typical vascular plant communities. We find that the seasonal development of photosynthetic capacity is important in explaining differences in bryophyte photosynthesis between spring and summer.

Paper 3. Recently assimilated C in Arctic vegetation: The importance of non-vascular plants

This chapter quantifies the contribution of mosses to ecosystem CUE and aboveground: belowground C allocation. The paper describes the results of a ^{13}C pulse-labelling experiment in sub-Arctic Finland used to quantify the C turnover in pure stands of *Sphagnum* and *Pleurozium*, and in a mixed dwarf shrub community with a *Pleurozium* understory. The paper demonstrates that neglecting the presence of mosses in Arctic plant communities can result in a underestimation of ecosystem CUE by nearly 10 % and overestimation of the fraction of GPP which is incorporated into belowground plant biomass.

Paper 4. Turnover of recently assimilated C in Arctic bryophytes

This paper describes a new model of C turnover in Arctic bryophytes, parameterised using the results of a ^{13}C pulse-labelling experiment in sub-Artic Sweden and laboratory and *in situ* measurements of *Polytrichum piliferum* and *Sphagnum fuscum* photosynthesis. The model consists of four pools for labile and structural C in photosynthetic and stem tissues with photosynthetic, respiration, translocation and litter fluxes. We demonstrate differences in NPP:GPP ratios and turnover times between moss species. The ratio of aboveground NPP:GPP in *Polytrichum piliferum* was 23 % (CI 9% - 35 %), with an average turnover time of 1.7 days (CI 1.1 - 2.5 days). The aboveground NPP:GPP ratio in *Sphagnum fuscum* was 43 % (CI 19 % - 65 %) with an average turnover time of 3.1 days (CI 1.6 - 6.1 days).

Appendix 1

Appendix 1 presents data on bryophyte biomass from 125 destructive harvests at Abisko (N. Sweden) and Kevo (N. Finland).

Appendix 2

Appendix 2 presents data on the effect of mosses on surface temperature and soil heat flux.

Appendix 3

Appendix 3 present data on the spatial abundance of bryophytes at Kevo (N. Finland).

Appendix 4

Street, L.E., Shaver, G.R., Williams, M., & Van Wijk, M.T. (2007) What is the relationship between changes in canopy leaf area and changes in photosynthetic CO_2 flux in arctic ecosystems? Journal of Ecology, 95, 139-150. This paper contains details of chamber CO_2 flux methods used throughout the thesis.

References

ACIA (2005) *Arctic Climate Impact Assessment - Scientific Report* Cambridge University Press.

Arneth, A., Harrison, S.P., Zaehle, S., Tsigaridis, K., Menon, S., Bartlein, P.J., Feichter, J., Korhola, A., Kulmala, M., O'Donnell, D., Schurgers, G., Sorvari, S., & Vesala, T. (2010) Terrestrial biogeochemical feedbacks in the climate system. *Nature Geoscience*, **3**, 525-532.

Bekryaev, R.V., Polyakov, I.V., & Alexeev, V.A. (2010) Role of Polar Amplification in Long-Term Surface Air Temperature Variations and Modern Arctic Warming. *Journal of Climate*, **23**, 3888-3906.

Bloom, A.A., Palmer, P.I., Fraser, A., Reay, D.S., & Frankenberg, C. (2010) Large-Scale Controls of Methanogenesis Inferred from Methane and Gravity Spaceborne Data. *Science*, **327**, 322-325.

Chapin, F.S., McFarland, J., McGuire, A.D., Euskirchen, E.S., Ruess, R.W., & Kielland, K. (2009) The changing global carbon cycle: linking plant-soil carbon dynamics to global consequences. *Journal of Ecology*, **97**, 840-850.

Chapin, F.S., Sturm, M., Serreze, M.C., McFadden, J.P., Key, J.R., Lloyd, A.H., McGuire, A.D., Rupp, T.S., Lynch, A.H., Schimel, J.P., Beringer, J., Chapman, W.L., Epstein, H.E., Euskirchen, E.S., Hinzman, L.D., Jia, G., Ping, C.L., Tape, K.D., Thompson, C.D.C., Walker, D.A., & Welker, J.M. (2005) Role of land-surface changes in Arctic summer warming. *Science*, **310**, 657-660.

Cornelissen, J.H.C., van Bodegom, P.M., Aerts, R., Callaghan, T.V., van Logtestijn, R.S.P., Alatalo, J., Chapin, F.S., Gerdol, R., Gudmundsson, J., Gwynn-Jones, D., Hartley, A.E., Hik, D.S., Hofgaard, A., Jonsdottir, I.S., Karlsson, S., Klein, J.A., Laundre, J., Magnusson, B., Michelsen, A., Molau, U., Onipchenko, V.G., Quested, H.M., Sandvik, S.M., Schmidt, I.K., Shaver, G.R., Solheim, B., Soudzilovskaia, N.A., Stenstrom, A., Tolvanen, A., Totland, O., Wada, N., Welker, J.M., & Zhao, X.Q. (2007) Global negative vegetation feedback to climate warming responses of leaf litter decomposition rates in cold biomes. *Ecology Letters*, **10**, 619-627.

Davidson, E.A. & Janssens, I.A. (2006) Temperature sensitivity of soil carbon decomposition and feedbacks to climate change. *Nature*, **440**, 165-173.

Denman, K.L., Brasseur, G., Chidthaisong, A., Ciais, P., Cox, P.M., Dickinson, R.E., Hauglustaine, D., Heinze, C., Holland, E., Jacob, D., Lohmann, U., Ramachandra, S., Dias, P.L.d.S., Wofsy, S.C., & Zhang, X. (2007). Couplings Between Changes in the Climate System and Biogeochemistry. In *Climate Change 2007: The Physical Science Basis. Contribution of Working Group I to the Fourth Assessment Report of the Intergovernmental Panel on Climate Change* (eds S. Solomon, D. Qin, M. Manning, Z. Chen, M. Marquis, K.B. Averyt, M.Tignor & H.L. Miller). Cambridge University Press, Cambridge, United Kingdom and New York, NY, USA.

Dorrepaal, E., Toet, S., van Logtestijn, R.S.P., Swart, E., van de Weg, M.J., Callaghan, T.V., & Aerts, R. (2009) Carbon respiration from subsurface peat accelerated by climate warming in the subarctic. *Nature*, **460**, 616-U79.

Douma, J., van Wijk, M.T., Lang, S.I., & Shaver, G.R. (2007) The contribution of mosses to the carbon and water exchange of arctic ecosystems: quantification and relationships with system properties. *Plant, Cell and Environment*, **30**, 1205-1215.

Ebinger, C.K. & Zambetakis, E. (2009) The geopolitics of Arctic melt. *International Affairs*, **85**, 1215-+.

Forbes, B.C., Fauria, M.M., & Zetterberg, P. (2010) Russian Arctic warming and 'greening' are closely tracked by tundra shrub willows. *Global Change Biology*, **16**, 1542-1554.

Friedlingstein, P., Cox, P., Betts, R., Bopp, L., Von Bloh, W., Brovkin, V., Cadule, P., Doney, S., Eby, M., Fung, I., Bala, G., John, J., Jones, C., Joos, F., Kato, T., Kawamiya, M., Knorr, W.,

Lindsay, K., Matthews, H.D., Raddatz, T., Rayner, P., Reick, C., Roeckner, E., Schnitzler, K.G., Schnur, R., Strassmann, K., Weaver, A.J., Yoshikawa, C., & Zeng, N. (2006) Climate-carbon cycle feedback analysis: Results from the (CMIP)-M-4 model intercomparison. *Journal of Climate*, **19**, 3337-3353.

Gautier, D.L., Bird, K.J., Charpentier, R.R., Grantz, A., Houseknecht, D.W., Klett, T.R., Moore, T.E., Pitman, J.K., Schenk, C.J., Schuenemeyer, J.H., Sorensen, K., Tennyson, M.E., Valin, Z.C., & Wandrey, C.J. (2009) Assessment of Undiscovered Oil and Gas in the Arctic. *Science*, **324**, 1175-1179.

Gornall, J.L., Jonsdottir, I.S., Woodin, S.J., & Van der Wal, R. (2007) Arctic mosses govern below-ground environment and ecosystem processes. *Oecologia*, **153**, 931-941.

Griffis, T.J., Rouse, W.R., & Waddington, J.M. (2000) Interannual variability of net ecosystem CO2 exchange at a subarctic fen. *Global Biogeochemical Cycles*, **14**, 1109-1121.

Groendahl, L., Friborg, T., & Soegaard, H. (2007) Temperature and snow-melt controls on interannual variability in carbon exchange in the high Arctic. *Theoretical and Applied Climatology*, **88**, 111-125.

Grogan, P. & Jonasson, S. (2005) Temperature and substrate controls on intra-annual variation in ecosystem respiration in two subarctic vegetation types. *Global Change Biology*, **11**, 465-475.

Hallinger, M., Manthey, M., & Wilmking, M. (2010) Establishing a missing link: warm summers and winter snow cover promote shrub expansion into alpine tundra in Scandinavia. *New Phytologist*, **186**, 890-899.

Hansen, J., Ruedy, R., Sato, M., & Lo, K. (2010) Global Surface Temperature Change. *Reviews of Geophysics*, **48**.

Hill, G.B. & Henry, G.H.R. (2011) Responses of High Arctic wet sedge tundra to climate warming since 1980. *Global Change Biology*, **17**, 276-287.

Hobbie, S.E., Schimel, J.P., Trumbore, S.E., & Randerson, J.R. (2000) Controls over carbon storage and turnover in high-latitude soils. *Global Change Biology*, **6**, 196-210.

Hudson, J.M.G. & Henry, G.H.R. (2010) High Arctic plant community resists 15 years of experimental warming. *Journal of Ecology*, **98**, 1035-1041.

Huemmrich, K.F., Kinoshita, G., Gamon, J.A., Houston, S., Kwon, H., & Oechel, W.C. (2010) Tundra carbon balance under varying temperature and moisture regimes. *Journal of Geophysical Research-Biogeosciences*, **115**.

Jia, G.S.J., Epstein, H.E., & Walker, D.A. (2003) Greening of arctic Alaska, 1981-2001. *Geophysical Research Letters*, **30**.

Jia, G.S.J., Epstein, H.E., & Walker, D.A. (2009) Vegetation greening in the canadian arctic related to decadal warming. *Journal of Environmental Monitoring*, **11**, 2231-2238.

Kammer, A., Hagedorn, F., Shevchenko, I., Leifeld, J., Guggenberger, G., Goryacheva, T., Rigling, A., & Moiseev, P. (2009) Treeline shifts in the Ural mountains affect soil organic matter dynamics. *Global Change Biology*, **15**, 1570-1583.

Kwon, H.J., Oechel, W.C., Zulueta, R.C., & Hastings, S.J. (2006) Effects of climate variability on carbon sequestration among adjacent wet sedge tundra and moist tussock tundra ecosystems. *Journal of Geophysical Research-Biogeosciences*, **111**.

Lund, M., Lafleur, P.M., Roulet, N.T., Lindroth, A., Christensen, T.R., Aurela, M., Chojnicki, B.H., Flanagan, L.B., Humphreys, E.R., Laurila, T., Oechel, W.C., Olejnik, J., Rinne, J., Schubert, P., & Nilsson, M.B. (2010) Variability in exchange of CO2 across 12 northern peatland and tundra sites. *Global Change Biology*, **16**, 2436-2448.

Mack, M.C., Schuur, E.A.G., Bret-Harte, M.S., Shaver, G.R., & Chapin, F.S. (2004) Ecosystem carbon storage in arctic tundra reduced by long-term nutrient fertilization. *Nature*, **431**, 440-443.

McGuire, A.D., Anderson, L.G., Christensen, T.R., Dallimore, S., Guo, L.D., Hayes, D.J., Heimann, M., Lorenson, T.D., Macdonald, R.W., & Roulet, N. (2009) Sensitivity of the carbon cycle in the Arctic to climate change. *Ecological Monographs*, **79**, 523-555.

McGuire, A.D., Chapin, F.S., III, Walsh, J.E., & Wirth, C. (2006) Integrated Regional Changes In Arctic Climate Feedbacks: Implications for the Global Climate System. *Annual Review of Environment and Resources*, **31**, 61-91.

McGuire, A.D., Hayes, D.J., Kicklighter, D.W., Manizza, M., Zhuang, Q., Chen, M., Follows, M.J., Gurney, K.R., McClelland, J.W., Melillo, J.M., Peterson, B.J., & Prinn, R.G. (2010) An analysis of the carbon balance of the Arctic Basin from 1997 to 2006. *Tellus Series B-Chemical and Physical Meteorology*, **62**, 455-474.

Molau, U. (2010) Long-term impacts of observed and induced climate change on tussock tundra near its southern limit in northern Sweden. *Plant Ecology & Diversity*, **3**, 29-34.

Myneni, R.B., Keeling, C.D., Tucker, C.J., Asrar, G., & Nemani, R.R. (1997) Increased plant growth in the northern high latitudes from 1981 to 1991. *Nature*, **386**, 698-702.

Polyakov, I.V., Alekseev, G.V., Bekryaev, R.V., Bhatt, U., Colony, R.L., Johnson, M.A., Karklin, V.P., Makshtas, A.P., Walsh, D., & Yulin, A.V. (2002) Observationally based assessment of polar amplification of global warming. *Geophysical Research Letters*, **29**.

Post, E., Forchhammer, M.C., Bret-Harte, M.S., Callaghan, T.V., Christensen, T.R., Elberling, B., Fox, A.D., Gilg, O., Hik, D.S., Hoye, T.T., Ims, R.A., Jeppesen, E., Klein, D.R., Madsen, J., McGuire, A.D., Rysgaard, S., Schindler, D.E., Stirling, I., Tamstorf, M.P., Tyler, N.J.C., van der Wal, R., Welker, J., Wookey, P.A., Schmidt, N.M., & Aastrup, P. (2009) Ecological Dynamics Across the Arctic Associated with Recent Climate Change. *Science*, **325**, 1355-1358.

Qian, H.F., Joseph, R., & Zeng, N. (2010) Enhanced terrestrial carbon uptake in the Northern High Latitudes in the 21st century from the Coupled Carbon Cycle Climate Model Intercomparison Project model projections. *Global Change Biology*, **16**, 641-656.

Rustad, L.E., Campbell, J.L., Marion, G.M., Norby, R.J., Mitchell, M.J., Hartley, A.E., Cornelissen, J.H.C., & Gurevitch, J. (2001) A meta-analysis of the response of soil respiration, net nitrogen mineralization, and aboveground plant growth to experimental ecosystem warming. *Oecologia*, **126**, 543-562.

Sanderson, M.G., Hemming, D.L., & Betts, R.A. (2011) Regional temperature and precipitation changes under high-end (>= 4 degrees C) global warming. *Philosophical Transactions of the Royal Society a-Mathematical Physical and Engineering Sciences*, **369**, 85-98.

Schuur, E.A.G., Vogel, J.G., Crummer, K.G., Lee, H., Sickman, J.O., & Osterkamp, T.E. (2009) The effect of permafrost thaw on old carbon release and net carbon exchange from tundra. *Nature*, **459**, 556-559.

Shakhova, N., Semiletov, I., Leifer, I., Salyuk, A., Rekant, P., & Kosmach, D. (2010) Geochemical and geophysical evidence of methane release over the East Siberian Arctic Shelf. *Journal of Geophysical Research-Oceans*, **115**.

Shaver, G.R., Bret-Harte, S.M., Jones, M.H., Johnstone, J., Gough, L., Laundre, J., & Chapin, F.S. (2001) Species composition interacts with fertilizer to control long-term change in tundra productivity. *Ecology*, **82**, 3163-3181.

Shaver, G.R., Giblin, A.E., Nadelhoffer, K.J., Thieler, K.K., Downs, M.R., Laundre, J.A., & Rastetter, E.B. (2006) Carbon turnover in Alaskan tundra soils: effects of organic matter quality, temperature, moisture and fertilizer. *Journal of Ecology*, **94**, 740-753.

Shaver, G.R., Street, L.E., Rastetter, E.B., Van Wijk, M.T., & Williams, M. (2007) Functional convergence in regulation of net CO2 flux in heterogeneous tundra landscapes in Alaska and Sweden. *Journal of Ecology*, **95**, 802-817.

Sitch, S., Huntingford, C., Gedney, N., Levy, P.E., Lomas, M., Piao, S.L., Betts, R., Ciais, P., Cox, P., Friedlingstein, P., Jones, C.D., Prentice, I.C., & Woodward, F.I. (2008) Evaluation of the terrestrial carbon cycle, future plant geography and climate-carbon cycle feedbacks using five Dynamic Global Vegetation Models (DGVMs). *Global Change Biology*, **14**, 2015-2039.

Sitch, S., McGuire, A.D., Kimball, J., Gedney, N., Gamon, J., Engstrom, R., Wolf, A., Zhuang, Q., Clein, J., & McDonald, K.C. (2007) Assessing the carbon balance of circumpolar Arctic tundra using remote sensing and process modeling. *Ecological Applications*, **17**, 213-234.

Sjogersten, S. & Wookey, P.A. (2009) The Impact of Climate Change on Ecosystem Carbon Dynamics at the Scandinavian Mountain Birch Forest-Tundra Heath Ecotone. *Ambio*, **38**, 2-10.

Solomon, S., D. Qin, M. Manning, Z. Chen, M. Marquis, K.B. Averyt, Tignor, M., & Miller, H.L., eds. (2007) *Contribution of Working Group I to the Fourth Assessment Report of the Intergovernmental Panel on Climate Change*. Cambridge University Press, Cambridge, UK.

Sommerkorn, M., Bolter, M., & Kappen, L. (1999) Carbon dioxide fluxes of soils and mosses in wet tundra of Taimyr Peninsula, Siberia: controlling factors and contribution to net system fluxes. *Polar Research*, **18**, 253-260.

Spadavecchia, L., Williams, M., Bell, R., Stoy, P.C., Huntley, B., & van Wijk, M.T. (2008) Topographic controls on the leaf area index and plant functional type of a tundra ecosystem. *Journal of Ecology*, **96**, 1238-1251.

Street, L.E., Shaver, G.R., Williams, M., & Van Wijk, M.T. (2007) What is the relationship between changes in canopy leaf area and changes in photosynthetic CO2 flux in arctic ecosystems? *Journal of Ecology*, **95**, 139-150.

Sturm, M., Racine, C., & Tape, K. (2001) Increasing shrub abundance in the Arctic. *Nature*, **411**, 546-547.

Tape, K., Sturm, M., & Racine, C. (2006) The evidence for shrub expansion in Northern Alaska and the Pan-Arctic. *Global Change Biology*, **12**, 686-702.

Tarnocai, C., Canadell, J.G., Schuur, E.A.G., Kuhry, P., Mazhitova, G., & Zimov, S. (2009) Soil organic carbon pools in the northern circumpolar permafrost region. *Global Biogeochemical Cycles*, **23**.

van der Wal, R., Pearce, I.S.K., & Brooker, R.W. (2005) Mosses and the struggle for light in a nitrogen-polluted world. *Oecologia*, **142**, 159-168.

van Wijk, M.T., Williams, M., & Shaver, G.R. (2005) Tight coupling between leaf area index and foliage N content in arctic plant communities. *Oecologia*, **142**, 421-427.

Vogel, J., Schuur, E.A.G., Trucco, C., & Lee, H. (2009) Response of CO2 exchange in a tussock tundra ecosystem to permafrost thaw and thermokarst development. *Journal of Geophysical Research-Biogeosciences*, **114**.

Wallenstein, M.D., McMahon, S.K., & Schimel, J.P. (2009) Seasonal variation in enzyme activities and temperature sensitivities in Arctic tundra soils. *Global Change Biology*, **15**, 1631-1639.

Williams, M., Bell, R., Spadavecchia, L., Street, L.E., & Van Wijk, M.T. (2008) Upscaling leaf area index in an Arctic landscape through multiscale observations. *Global Change Biology*, **14**, 1517-1530.

Williams, M. & Rastetter, E.B. (1999) Vegetation characteristics and primary productivity along an arctic transect: implications for scaling up. *Journal of Ecology*, **87**, 885-898.

Wilmking, M., Harden, J., & Tape, K. (2006) Effect of tree line advance on carbon storage in NW Alaska. *Journal of Geophysical Research-Biogeosciences*, **111**.

Wolf, A., Kozlov, M.V., & Callaghan, T.V. (2008) Impact of non-outbreak insect damage on vegetation in northern Europe will be greater than expected during a changing climate. *Climatic Change*, **87**, 91-106.

Wookey, P.A., Aerts, R., Bardgett, R.D., Baptist, F., Brathen, K.A., Cornelissen, J.H.C., Gough, L., Hartley, I.P., Hopkins, D.W., Lavorel, S., & Shaver, G.R. (2009) Ecosystem feedbacks and cascade processes: understanding their role in the responses of Arctic and alpine ecosystems to environmental change. *Global Change Biology*, **15**, 1153-1172.

2a. Photosynthetic CO_2 flux and the relationship between leaf area index and total foliar nitrogen – a single Arctic relationship?

L. E. Street[1], G. R. Shaver[2], E.B. Rastetter[2], M. T. van Wijk[3], Kaye B. A.[2], M. Williams[1]

[1]School of Geosciences, University of Edinburgh, Edinburgh, EH9 3JN, UK.

[2] Marine Biological Laboratory, Woods Hole, MA 02543, USA.

[3]Plant Production Systems, Wageningen University, Plant Sciences, Haarweg 333, 6709 RZ Wageningen, Netherlands.

(*intended for submission to Journal of Ecology*)

Abstract

The Arctic is characterised by high variability in plant functional type (PFT) composition and productivity. Despite this variability, the two main drivers of canopy photosynthesis are leaf area index (LAI) and total foliar nitrogen (TFN). LAI and TFN have been shown to be tightly coupled across a wide range of PFTs in the sub-Arctic, which simplifies up-scaling by allowing quantification of the main drivers of GPP from remotely sensed LAI. Our objective was to test the LAI-TFN relationship in multiple Arctic environments, and assess the utility of LAI as a predictor of gross primary productivity (GPP) across Arctic latitudes. We find that including PFT as a group factor in a mixed effects model of the LAI-TFN relationship results in only incremental improvements in model fit. Significant improvements however resulted from including site as a random effect in the model. Estimates of the random effects on the parameter for theoretical top-of-canopy N concentration (per unit leaf area) were positively correlated with total SW radiation for the growing season. Random effects for the theoretical extinction of N concentration (per unit leaf area) with canopy depth were negatively correlated with the average fraction of SW radiation which is diffuse. We argue these results indicate a community-level optimisation of N use to fully utilise the available light resource. We find that a single general model relating GPP to LAI is the most appropriate for Arctic vegetation.

Introduction

Recent research has focused on the Arctic as the region most vulnerable to climate change (ACIA, 2005; Anisimov *et al.*, 2007). Northern high latitudes are warming at twice the rate of the rest of the globe, with observed warming of 1.5 °C since 1980 (Holland & Bitz, 2003; Trenberth *et al.*, 2007) and potential warming of > 5 °C by 2100 (Christensen *et al.*, 2007). There are large stocks of terrestrial carbon (C) in these regions; North American Arctic soils alone contain about 98 Pg of organic carbon, one sixth the amount of carbon in the atmosphere (Ping *et al.*, 2008). Mineralization of soil organic C is sensitive to temperature so potentially large amounts of C could be lost to

the atmosphere under warmer conditions, resulting in an important amplifying feedback on global climate (Davidson & Janssens, 2006; Hartley *et al.*, 2008). The effort to build regional-to-global models of the carbon cycle to calculate carbon budgets is complicated by the variability in Arctic vegetation type, hydrology, soil type and climate over many scales. However, there are powerful linkages among biogeochemical, hydrological and climatic variables throughout the Arctic and across the globe (Chapin *et al.*, 2005; McKane *et al.*, 1997a, b). These linkages, if properly understood, provide a means to explain and quantify observed variability and constrain predictions of Arctic C balance and exchanges.

A tightly constrained relationship between total canopy leaf area index (LAI) and total foliar N per m^2 ground area (TFN) has been documented in sub-Arctic tundra vegetation (van Wijk *et al.*, 2005; Williams & Rastetter, 1999). These studies found that average canopy N per unit leaf area (TFN/LAI) at LAI < 1.0 m^2 m^{-2} was 1.9 g N m^{-2} LA across a wide range of vegetation types, and that the variability in average TFN/LAI is less than would be expected if canopies were randomly constructed from the pool of available species. LAI and TFN are the most important drivers of photosynthesis in the Arctic (Williams *et al.*, 2001). If LAI and TFN are tightly coupled, remotely sensed estimates of LAI alone are powerful predictors of GPP. This result has been confirmed in plot scale studies of the same sub-Arctic systems, where LAI alone explains 80 % of the variability in GPP through time and across vegetation types (Shaver *et al.*, 2007; Street *et al.*, 2007). Nutrient availability, which is known to limit plant production in the Arctic (Shaver & Chapin, 1980, 1986; 1991), determines the peak ecosystem LAI across a range of Arctic plant functional types. Williams and Rastetter (1999) demonstrated that a strong correlation between LAI and TFN can optimise GPP by balancing limitations on photosynthesis.

The canopy scale relationship between LAI and TFN, and the corresponding linkages to GPP, have not previously been investigated at higher latitude. In this study we ask the following questions: 1) is there a general LAI-TFN relationship for the Arctic? 2) can LAI be reliably estimated from NDVI across Arctic sites? 3) is there a

general relationship between GPP and LAI across the Arctic? While nutrient availability will dictate landscape patterns in LAI, we expect that lower total irradiance at higher latitudes will modify the optimal development of TFN with respect to LAI. Most nitrogen in leaves is contained within the photosynthetic enzymes (Evans, 1989). We hypothesise that if less light is available during the growing season, less photosynthetic enzyme (and hence leaf N) will be required to fully use the available light resource. A more efficient canopy construction in lower light would be to spread leaf N more thinly over a greater leaf area. We therefore expect the LAI-TFN relationship to be shifted towards lower N per unit leaf area with increasing latitude. This could be achieved by species either having lower average N concentration by mass or by higher specific leaf area (SLA).

We expect any differences in the LAI-TFN relationship between latitudes to affect canopy GPP only under saturating light conditions. At high light levels GPP is limited by the amount of photosynthetic enzyme in leaves, so if canopies at higher latitude have less N per unit leaf area they will also have lower GPP per unit leaf area. However, in conditions where light limits photosynthesis we would expect light use efficiency (moles CO_2 fixed per mole photons), per unit leaf area to be the same across sites.

For the first time we present a comparison between the TFN, LAI, and GPP for whole canopies, across multiple Arctic sites spanning latitudes from 68 – 78 ºN. We supplement previously published data from the sub-Arctic with new measurements from high Artic sites in Svalbard and Greenland, and a coastal tundra site at Barrow, Alaska.

Methods

A list of abbreviations is given in Table 1. The present analysis combines new TFN, LAI, NDVI and GPP data from near Longyearbyen, Svalbard, from Zackenberg, NE Greenland, and from Barrow, Alaska with previously published data from Abisko, northern Sweden and from near Toolik Lake, Alaska (Table 2).

Table 1. List of symbols, abbreviations and units.

Symbol	Definition	Units
LAI	Leaf area index	m^2 leaf m^{-2} ground
TFN	Total foliar nitrogen	g N m^{-2} ground
TLM	Total leaf mass	g leaf m^{-2} ground
LA	Leaf area	m^{-2} leaf
N/LA	Nitrogen per unit leaf area	g N m^{-2} leaf area
N/LM	Nitrogen per unit leaf mass	g N g^{-1} leaf mass
SLA	Specific leaf area	m^2 leaf g^{-1} leaf
PPFD	Photosynthetic photon flux density	µmol photons m^{-2} ground s^{-1}
GPP	Gross primary productivity	µmol CO_2 m^{-2} ground s^{-1}
NDVI	Normalised difference vegetation index	-
LM	Leaf mass	g leaf
NEE	Net ecosystem exchange	µmol CO_2 m^{-2} ground s^{-1}
ER	Ecosystem respiration	µmol CO_2 m^{-2} ground s^{-1}
P_{max}	Theoretical light saturated photosynthetic rate	µmol CO_2 m^{-2} ground s^{-1}
E_o	Initial light use efficiency of photosynthesis	µmol CO_2 µmol^{-1} photons
GPP_{600}	Gross primary productivity at 600 µmol m^{-2} PPFD	µmol CO_2 m^{-2} ground s^{-1}
GPP_{600L}	Gross primary productivity at 600 µmol m^{-2} PPFD per unit leaf area	µmol CO_2 m^{-2} leaf s^{-1}
E_{0L}	Initial light use efficiency of photosynthesis per unit leaf area	µmol CO_2 µmol^{-1} photons m^{-2} leaf
γ	Nitrogen extinction coefficient	m^2 ground m^{-2} leaf
$[N_0]$	Top of canopy N/LA	g N m^{-2} leaf area

Site descriptions

Longyearbyen, Svalbard

We measured CO_2 flux using chamber techniques and sampled vegetation at ten sub-sites, all within approximately 20 km of the town of Longyearbyen, on the island of Spitzbergen (78° 13'N, 15°37'E). Mean annual air temperature (MAT) for Longyearbyen is ~ -5 °C, mean July temperature is ~ 6°C and mean precipitation ~310mm, approximately 30 – 50% falling as snow during the winter (Forland & Hanssen-Bauer, 2000). Vegetation in the fjord (Adventdalen) in which Longyearbyen is situated ranges from salt marsh on the margins of the estuary, to wet sedge meadow (mostly *Dupontia*, *Carex* and *Eriophorum spp.*) on the flat valley bottom, to dwarf shrub heath communities on well drained slopes. Dwarf shrub vegetation is characterized by locally dominant patches of *Cassiope tetragona*, *Dryas octopetala*, and *Salix polaris* communities (Baddeley *et al.*, 1994). Plots were chosen to sample the range of vegetation types within the area. All field measurements were made 14th July - 3rd August 2005.

Zackenberg, Greenland

We measured CO_2 flux using chamber techniques and sampled vegetation at sub-sites, all within approximately 2 km of Zackenberg Research Station (74° 28'N, 20°34'E) and below an elevation of 100 m. Mean annual air temperature (1995 – 2002) for Zackenberg, is –9.75°C with a total annual precipitation of 222 mm (Christiansen, 2004). Vegetation in the area around Zackenberg consists of wet fen and grassland in areas by water tracks, with heath vegetation dominated by *Cassiope tetragona* on better drained level ground. Heath dominated by *Vaccinium uliginosum* or *Dryas* species is more common on exposed slopes. There are also extensive areas of snowbed vegetation dominated by *Salix arctica*. Plots were chosen to sample the range of vegetation types within the area. All field measurements were made between 8th July – 1st August 2006.

Barrow, Alaska

Flux measurements, leaf harvests, and reflectance measurements were made in the Barrow Environmental Observatory (BEO) near Barrow, Alaska (71°18′N, 156°40′W) in July 2009. All measurements were made within a single, shallow, drained and revegetated thaw lake basin and surrounding shoreline ridges. The area was entirely underlain by permafrost with ice-wedge polygons creating local microrelief. Sites were selected to represent vegetation along a soil moisture gradient, from constantly-flooded, emergent wet-sedge vegetation dominated by rhizomatous sedges and grasses to relatively dry ridges dominated by creeping willow species and grasses. Vegetation, soils, and climate in the Barrow region have been thoroughly described in past research (e.g., (Brown *et al.*, 1980)), including at the BEO adjacent to sites used in this research (Hollister *et al.*, 2005). Annual temperature at Barrow is –11°C and the long-term average temperature in July is –4°C although this has increased in recent decades.

Abisko, Sweden

We used leaf harvest data from near Abisko in Northern Sweden (68°18′N,18°51′E) collected between the 15th July and 30th July 2002 (van Wijk *et al.*, 2005). We use CO_2 flux data collected between the 22nd July and 5th August 2004 at two sites nearby the site of vegetation sampling, (the 'Stepps' site and 'Paddus' site), and at another upland site (the 'Latnja' site) (Shaver *et al.*, 2007). MAT at Abisko is -1°C, mean July temperature is 11°C and mean annual precipitation is 225 – 475mm with 47 % falling as snow in the winter (van Wijk *et al.*, 2005).

Toolik, Alaska

We used destructive LAI and TFN data during 1997 as part of the Arctic flux study within the Kuparuk watershed on the northern side of the Brooks Range, AK, USA (Williams & Rastetter, 1999). We used CO_2 flux data collected between 12 July and 4th August 2004 in tussock, dry heath and shrub tundra at Toolik Lake (68º38'N,149º36'W) and nearby at Imnavait Creek (68º37'N,149º19'W) (Shaver *et al.*, 2007). Though at a similar latitude to Abisko, the climate at Toolik is more continental;

MAT at Toolik Lake is -10 °C and mean July temperature is 14 °C. Mean annual precipitation is 200 – 400 mm, 45 % falling as snow in the winter (van Wijk *et al.*, 2005).

Table 2. Summary of data including year, site, number of measurements and literature source.

Data type (plot sizes)	Year	Site	Number of measurements	Source
harvest ($0.03\ m^{2)}$	2009	Barrow, Alaska	23	This study
harvest ($0.03\ m^2$, $0.05\ m^2$, $0.09\ m^2$)	2006	Zackenberg, NE Greenland	28, 26, 24	This study
Harvest ($0.05\ m^2$)	2005	Longyearbyen, Svalbard	48	This study
harvest ($0.04\ m^2$)	2001	Abisko, Sweden	92	Van Wijk *et al.* (2005)
harvest ($0.04\ m^2$)	1997	Kuparuk watershed, Alaska	94	Williams & Rastetter (1999)
GPP light response curve ($1\ m^2$)	2009	Barrow, Alaska	10	This study
GPP light response curve ($1\ m^2$, $0.09\ m^2$)	2006	Zackenberg, NE Greenland	26, 15	This study
GPP light response curve ($1\ m^2$)	2005	Longyearbyen, Svalbard	36	This study
GPP light response curve ($1\ m^2$)	2004	Toolik Lake, Alaska	28	Shaver *et al.* (2007) & Street *et al.* (2007)
GPP light response curve ($1\ m^2$)	2004	Abisko, Sweden	45	Shaver *et al.* (2007)

Measurements

NDVI, LAI and canopy N of harvest plots

We measured the NDVI, LAI, total leaf biomass (TLM) and total canopy N of harvested plots at Svalbard (n = 48) , Zackenberg (n = 78), Barrow (n = 23), Toolik (n = 92) and Abisko (n = 94) . The size of the harvested plots was between 0.03 and 0.09 m^2 (Table 2). At Zackenberg, Svalbard and Barrow we measured the NDVI of each plot before harvesting using a Unispec spectral analyser, following the methods of Street *et al.* (2007) [Appendix 4]. LAI, TLM and TFN were measured destructively, following the methods of Van Wijk *et al.* (2005) and Street *et al.* (2007). For *Cassiope tetragona* we doubled the one-sided projected leaf area (Campioli, 2008). We estimated the percent cover of bryophytes for each plot, and at Svalbard and Zackenberg re-measured NDVI following removal of the vascular plant canopy.

NDVI, LAI and percent cover of flux plots

We measured NDVI of each flux plot following the methods of (2007). We estimated absolute aerial cover in each flux plot for all vascular plants by species (i.e. total cover can be > 100%), and for bryophytes. We did this by placing a 5 × 5 grid (each square = 0.04 m^2) over the plot, and visually estimating cover in each square, then calculated an average species cover for the entire plot. Both harvest and flux plots were classified as either deciduous, evergreen, graminoid or mixed vegetation according to the contribution of each functional type to total biomass (for the harvest plots) or cover (for the flux plots). Plots with cover of a single PFT > 70 % were classified as that type, otherwise plots were classified as mixed.

To estimate the LAI of the flux plots from NDVI we modelled the relationship between LAI and NDVI for each functional type using a model modified from (Steltzer & Welker, 2006).

$$LAI = \frac{1}{Kc} \ln\left(\frac{NDVI_{\min} - NDVI_{\max}}{NDVI - NDVI_{\max}} \right) \qquad (1)$$

Where $NDVI_{min}$ is the minimum measured background NDVI (0.24), $NDVI_{max}$ is a fitted parameter representing the maximum NDVI for a vegetation canopy, and K_c is a fitted extinction co-efficient. We also fitted a second model, in which background $NDVI_{min}$ was proportional to the estimated bryophyte cover, with slope a and intercept b of the measured relationship between bryophyte cover and (minimum) background NDVI for harvested plots (Fig. 1).

$$LAI_B = \frac{1}{Kc} \ln\left(\frac{[(a \times B_c) + b] - NDVI_{max}}{NDVI - NDVI_{max}} \right) \quad (2)$$

Where B_c is bryophyte cover (%), $a = 0.24$ and $b = 0.0024$.

For both Toolik and Alaska we used the previously published values of LAI for each flux measurement plot, using vegetation specific NDVI-LAI calibrations (Street *et al.*, 2007).

Flux measurements

We measured the light response of net ecosystem CO_2 exchange (NEE), and ecosystem respiration (ER) in Svalbard, Zackenberg, Barrow, Toolik and Abisko over 1 m × 1 m patches of vegetation (Table 2). All flux measurements were made with chambers using protocols described in Williams *et al.* (2006) , Street *et al.* (2007) and Shaver *et al.* (2007). In Zackenberg we also measured fluxes for 15 0.3 m × 0.3 m patches using a smaller chamber and destructively sampled the LAI. For the Toolik and Abisko data we chose a sub-set of the data presented in Shaver *et al.* (2007) that coincided with the dates of collection for the Svalbard CO_2 flux data.

Data analysis

LAI and total canopy N

We aimed to find the parameters for a theoretical model that relates LAI to TFN – and then determine whether the fitted parameters differ significantly between sites. It has been argued that an exponential decline in foliar N through the canopy is a plant

strategy for maximizing canopy photosynthesis with respect to canopy nitrogen (Field, 1983; Hikosaka & Hirose, 1998; Hirose & Werger, 1987):

$$[N] = [N]_0 e^{-\gamma L} \tag{3}$$

where [N] is the nitrogen concentration (N/LA) of a leaf in the canopy (g N m^{-2} leaf), $[N]_0$ is the top of the canopy nitrogen concentration (g N m^{-2} leaf), γ an extinction coefficient (m^2 ground m^{-2} leaf), and L is the cumulative leaf area above the leaf (m^2 leaf m^{-2} ground). Total canopy nitrogen (TFN) is then the integral of equation 3:

$$TFN = \int_0^{LAI} ([N])\, d\, L = \frac{[N]_0}{\gamma}\left(1 - e^{-\gamma LAI}\right) \tag{4}$$

where TFN is the total canopy nitrogen (g N m^{-2} ground) and LAI is leaf area index (m^2 leaf m^{-2}ground). Equation 4 would be expected to describe the regional relationship between TFN and LAI if $[N]_0$ and γ are uniform over the region.

CO_2 flux

In order to test the relationship between LAI and canopy photosynthesis, we compare the parameters of fitted GPP light response curves to LAI for each plot. GPP at each light level was calculated by subtracting NEE from ecosystem respiration (ER). The light response of photosynthesis was then modelled with a rectangular hyperbola:

$$GPP = \frac{GPP_{\max} \times I}{\left(\frac{GPP_{\max}}{E_0}\right) + I} \tag{5}$$

where $GPP_{\max}$ is the rate of light saturated canopy level photosynthesis (μmol CO_2 m^{-2} s^{-1}), I is the incident PPFD (μmol photons m^{-2} s^{-1}), E_0 is the initial slope of the light response curve or quantum efficiency at low light levels (μmol CO_2 μmol^{-1} photons). Each fitted light curve was used to predict GPP at 1000 μmol photons m^{-2} s^{-1}

(GPP_{1000}). We compared the relationship between GPP near light saturation (GPP_{1000}) and LAI, using only curves where the maximum PPFD measured during the light curve exceeded 1000 μmol photons m^{-2} s^{-1}. We assume leaf level photosynthesis at 1000 μmol^{-1} photons (P_{1000}) is approximately linearly related to N/LA (Hirose and Werger 1987) and therefore follows an exponential distribution with canopy depth as N/LA, giving an equation analogous to equation 4:

$$GPP_{1000} = \frac{[P]_0}{\gamma_p}\left(1 - e^{-\gamma_p LAI}\right) \quad (6)$$

where GPP_{1000} is canopy-level GPP at 1000 μmol photons m^{-2} s^{-1}, P_0 is top of the canopy leaf level P at 1000 and γ_p is the extinction of leaf level P with canopy depth. We compare the relationship between quantum efficiency E_0 (the initial slope of the light response curve) and LAI, assuming that E_0 is not strongly related to leaf N concentration at low light levels (Hirose and Werger 1987), and therefore follows a uniform distribution with LA from the top of the canopy and a linear relationship to LAI.

Statistical analysis

We model the relationship between LAI and TFN using equation 4. We excluded data from Barrow as radiation data were not available for this site. All data analysis was carried out using the 'nlme' package for R (version 2.12.1). We initially fit a general model to the whole data set (TFN.gnls), and for each PFT individually ($TFN.gnls_{PFT}$) using generalised least squares. We included power variance functions in both 'gnls' models, to account for heteroscedasticity in the data. To assess the effect of site we fitted non-linear mixed effects (NLME) models using maximum likelihood. We included and excluded PFT as a fixed effect ($TFN.nlme_{PFT}$ and TFN.nlme respectively) on N_0 and γ and included site as a random effect (RE) on N_0 alone, γ alone, and N_0 and γ together. Alternative model formulations were compared using Akaike's information criterion (AIC), loglikelihood (LogLik) ratio tests and the root mean square error (RMSE) of model predictions. We included power variance functions in all NLME

models, to account for heteroscedasticity. We used a similar approach to examine the relationship between LAI and GPP_{1000} and E_0, however there was insufficient replication for some PFT/site combinations, so we could not include vegetation fixed effects and site random effects together in a single model. We therefore compared vegetation fixed effects only, and site random effects only, to the general models in each case. It was necessary to include power variance functions to account for heteroscedasticity in the E_0 data, but not in the GPP_{1000} data.

Radiation data

We compare fitted parameters for the canopy N distribution to average solar radiation conditions at Toolik, Abisko, Svalbard and Zackenberg over 7 years between 1996 and 2005 (2001, 2002 and 2004 were excluded because of data gaps). We calculated the sum of hourly short-wave (SW) radiation over the growing season (defined as 1st June to 31st August) for each year, then calculated the mean and standard deviation across years for each site. We calculated the average diffuse radiation fraction by averaging hourly daytime (defined as the period where incident SW > 20 Wm^{-2}) diffuse fraction over the growing season. For Svalbard we used hourly global SW and diffuse SW data from Ny Alesund, approximately 100 km NW of Svalbard (supplied by the Alfred-Wegner Institute http://www.awi.de/en/). For Abisko we used hourly global SW data provided by Abisko Scientific Research Station (www.linnea.com/~ans/) to model hourly diffuse SW fraction based on the ratio of modelled extraterrestrial to measured global SW according to (Erbs *et al.*, 1982). We tested the Erbs *et al.* model with 2.5 weeks of global and diffuse SW data provided by the ABACUS project (www.geos.ed.ac.uk/abacus) (Supplementary Material Fig. 2 [Chapter 2b]). For Toolik we used 10 years of global SW data from the Toolik Lake Long Term Ecological Research (LTER) database (ecosystems.mbl.edu/ARC) to model daily diffuse SW fraction. We tested the Erbs model results at Toolik with 6 weeks of total and diffuse PPFD data from late summer 2008 provided by the Arctic Observing Network (aon.iab.uaf.edu/index.html) (Supplementary Material Fig. 3 [Chapter 2b]). Global SW was estimated from total PPFD data using an empirical

relationship for that site (Supplementary Material Fig. 1 [Chapter 2b]). For Zackenberg we used hourly global SW data provided by the ClimateBasis programme at Zackenberg research station (available at www.zackenberg.dk/data/) to model diffuse fraction according to Erbs *et al.* (1982).

Results

LAI and TFN

LAI was < 1.0 m m^{-2} in 90 % of the 151 harvests carried out at Zackenberg, Svalbard and Barrow reflecting short stature, low LAI plant canopies at higher latitude and coastal tundra vegetation compared to lower latitude sites. The maximum TFN values recorded (across all sites) were in Svalbard with ~ 4.5 g N m^{-2} ground (Fig. 2b). Relationships between TFN and total leaf mass (TLM, g leaf m^{-2} ground area), and between LAI and TLM were less well-constrained than the relationship between LAI and TFN both within and across sites (Fig. 2 a b & c, Fig. 3).

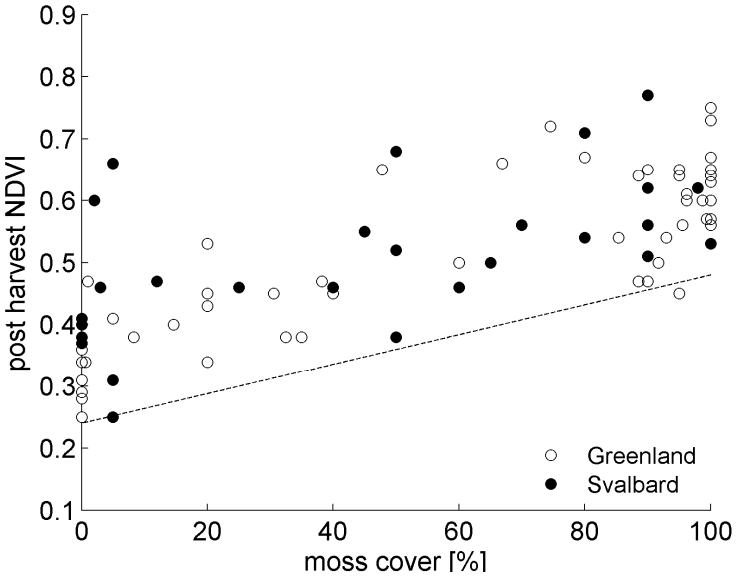

Figure 1. Post harvest NDVI versus percent moss cover for Zackenberg and Svalbard. The dotted line represents the relationship between moss cover (B_c) and $NDVI_{min}$ (equation 2) ($NDVI_{min}$ = 0.24 + 0.0024 B_c)

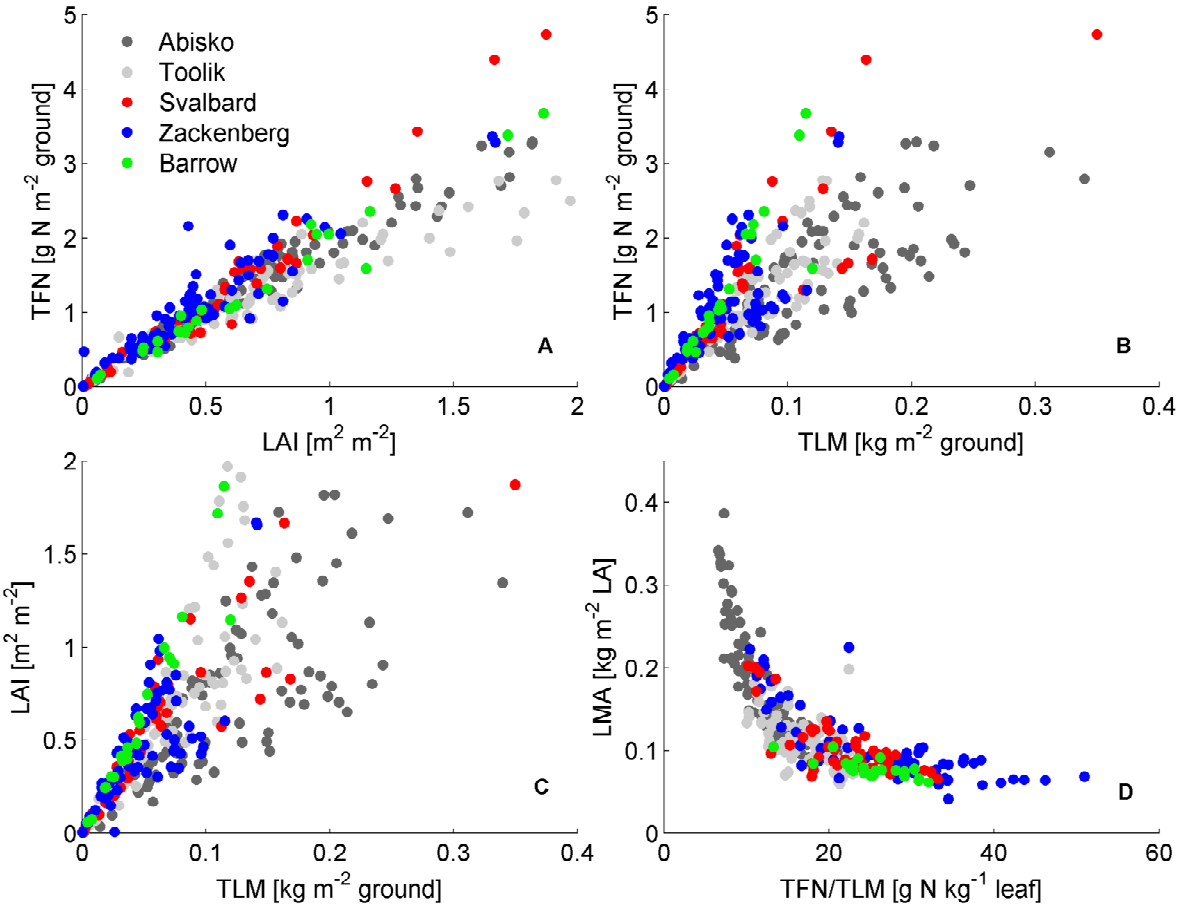

Figure 2. Inter-comparison of relationships between a) TFN and LAI b) TFN and TLM c) LAI and TLM and d) LMA and TFN/TLM for 0.04 m^2 vegetation harvests at Svalbard 2005 (n = 49), Abisko 2002 (n = 92) and Toolik 1997 (n = 94), Zackenberg (n = 78) and Barrow (n = 23)

Canopies with low average N concentration per unit leaf mass, (TFN/TLM) tended to have greater average leaf mass per area (LMA) (Fig. 2d). The highest average canopy foliar N concentrations per unit mass were in Zackenberg where TFN/TLM in several plots was > 35 g N kg^{-1} leaf (Fig. 2d). At LAI <1, average TFN/TLM at each site was greater at Zackenberg (25.8 ± 1.1 g N kg^{-1} leaf), Svalbard (21.4 ± 0.8 g N kg^{-1} leaf) and Barrow (24.8 ± 0.8 g N kg^{-1} leaf) than at the lower latitude sites Toolik (18.8 ± 0.4 g N kg^{-1} leaf) and Abisko (12.1 ± 0.5 g N kg^{-1} leaf).

Leaf-level N/LM varied between 16 mg N g^{-1} (1.6 % by mass) in *Dryas* leaves at Zackenberg, and 38 mg N g^{-1} (3.8 % by mass) in *Polygonum viviparum* at

Zackenberg. Leaf level N/LA varied > 4-fold, from 0.95 g N m^{-2} LA for *Saxifraga cernua* at Barrow, to > 4.0 g N m^{-2} LA in forbs and graminoids at Zackenberg (Table 3).

Table 3. Average specific leaf area (SLA), leaf nitrogen per unit leaf area (N/LA) and leaf nitrogen per unit leaf mass (N/LM) for plant species at Svalbard, Barrow and Zackenberg.. Species for which n < 5 are not included. Plant functional types (PFT) are: D = deciduous, E = evergreen, F = forb, G = graminoid.

Site	Species	n	PFT	N/LA [g m^{-2}]	N/LM [mg g^{-1}]	SLA [m^2 kg^{-1}]
Barrow	Salix phlebophylla	7	D	1.76 ± 0.09	23.3 ± 1.8	13.2 ± 0.3
	Stellaria species	9	F	1.43 ± 0.17	22.4 ± 1.6	17.4 ± 2.2
	Saxifraga cernua	8	F	0.95 ± 0.07	19.4 ± 1.3	20.6 ± 1.0
	Dupontia fisheri	15	G	2.21 ± 0.17	23.1 ± 1.0	11.2 ± 0.8
	Eriophorum scheuchzeri	10	G	2.51 ± 0.23	30.3 ± 1.9	12.5 ± 0.6
	other grasses	9	G	1.73 ± 0.14	19.3 ± 1.0	11.5 ± 0.6
Svalbard	Salix polaris	34	D	1.75 ± 0.05	24.2 ± 0.8	13.9 ± 0.4
	Dryas octopetala	21	E	2.68 ± 0.13	20.2 ± 0.6	8.1 ± 0.8
	Cassiope tetragona	6	E	2.16 ± 0.20	19.8 ± 1.2	4.6 ± 0.2
	Polygonum viviparum	35	F	2.06 ± 0.07	30.8 ± 0.3	15.5 ± 0.5
	other forbs	20	F	1.88 ± 0.20	24.9 ± 1.1	15.1 ± 1.3
	Equisetum species	30	P	3.14 ± 0.18	28.4 ± 1.3	9.5 ± 0.5
	Carex species	9	G	1.90 ± 0.17	19.3 ± 1.3	10.6 ± 0.9
	Dupontia fisheri	5	G	2.09 ± 0.20	16.1 ± 1.3	7.8 ± 0.2
	other graminoids	32	G	2.32 ± 0.10	21.6 ± 0.6	9.7 ± 0.3
Zackenberg	Salix Arctica	58	D	2.18 ± 0.08	30.9 ± 1.0	14.4 ± 0.6
	Arctostaphylos alpina	14	D	2.87 ± 0.20	31.1 ± 2.0	11.1 ± 0.6
	Vaccinium uliginosum	14	D	1.44 ± 0.05	24.6 ± 1.3	16.2 ± 1.5
	Dryas species	23	E	2.12 ± 0.09	16.0 ± 0.7	8.0 ± 0.5
	Cassiope tetragona	22	E	2.15 ± 0.19	23.2 ± 0.6	5.8 ± 0.4
	Polygonum viviparum	37	F	4.01 ± 1.09	38.3 ± 1.0	15.9 ± 1.3
	Stellaria species	16	F	2.15 ± 0.57	27.0 ± 1.5	17.6 ± 1.9
	Pedicularis species	8	F	2.40 ± 0.23	36.2 ± 3.7	16.1 ± 2.5
	Equisetum species	12	P	2.62 ± 0.10	27.3 ± 1.9	10.4 ± 0.5
	Carex species	8	G	2.17 ± 0.22	24.9 ± 1.9	11.8 ± 0.8
	Dupontia species	6	G	2.45 ± 0.21	21.3 ± 2.7	8.6 ± 0.7
	Eriophorum species	6	G	2.47 ± 0.12	25.9 ± 1.6	10.7 ± 0.9
	other graminoids	28	G	4.47 ± 2.03	24.9 ± 1.4	11.1 ± 1.1
	other grasses	18	G	5.07 ± 1.69	28.6 ± 1.6	8.2 ± 0.9
	other sedges	5	G	2.25 ± 0.26	24.9 ± 2.1	11.5 ± 1.2

The data provided most support for the TFN model that included site as a random effect on the LAI-TFN relationship without fixed effects of vegetation type (Table 4). The smallest RMSE 0.18 g N m^{-2} was associated with the $TFN.nlme_{PFT}$ model, which included the fixed effects of PFT, and random effects of site on N_0 and γ. Excluding vegetation fixed effects but retaining site random effects on N_0 and γ (TFN.nlme) did not significantly change the loglikelihood value however, and decreased the AIC, indicating only a marginal loss of fit for the reduction in number of model parameters from 14 to 8. Including site random effects for N_0 alone ($TFN.nlme_a$), or γ alone ($TFN.nlme_b$) significantly reduced the loglikelihood, increased the RMSE and increased the AIC, indicating less support for these models. In the TFN.nlme model the fixed effects value of N_0, the theoretical top of the canopy N/LA was 2.24 g N m^{-2}, and γ was 0.22. The standard deviation of site random effects for N_0 was 0.21 and for γ was 0.31 (Table 4).

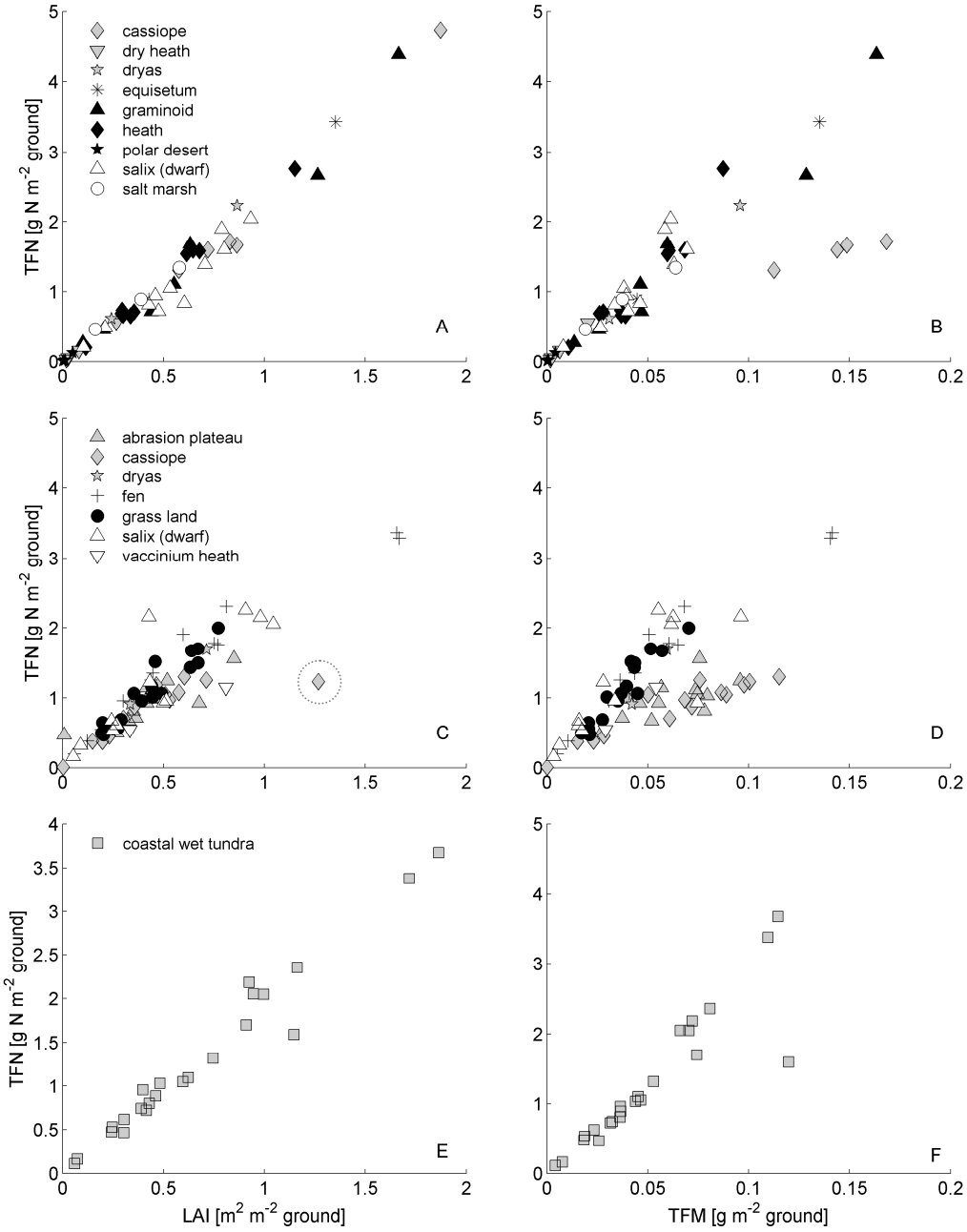

Figure 3. Relationships between total foliar nitrogen (TFN) and LAI (left panels) and TFN and total foliar biomass (TFM) (right panels) for vegetation harvests in Svalbard 2005 (a & b, n = 49), Zackenberg 2006 (c & d, n = 78) and Barrow 2009 (e & f, n = 23). Data points classified by vegetation type. The data point circled in panel C was identified as an outlier and excluded from further analysis.

Table 4. Model structure, Akaike's information criteria (AIC), loglikelihood (LogLik) and root mean square error (RMSE) for alternative TFN model formulations. " - " indicates that site random effects are not included in the model

Model	PFT	PFT fixed effects		Parameter number	SD of site random effects		AIC	LogLik	RMSE [g N m^{-2}]
		N_o	γ		N_o	γ			
TFN.gnls	all	2.34	0.41	3	-	-	-50.7	29.4 *	0.28
TFN.gnls$_{PFT}$	deciduous	2.25	0.41	12	-	-	-69.3	47.6 *	0.26
	evergreen	1.86	-0.21						
	graminoid	2.45	0.30						
	mixed	2.34	0.39						
TFN.nlme	all	2.24	0.22	8	0.21	0.31	-161.4	90.7 $ +	0.19
TFN.nlme$_a$	all	2.27	0.22	7	0.24	-	-119.2	67.6 $ &	0.22
TFN.nlme$_b$	all	2.27	0.23	7	-	0.27	-147.6	81.8 + £	0.20
TFN.nlme$_{PFT}$	deciduous	2.08	0.26	14	0.20	0.27	-150.0	90.5 & £	0.18
	evergreen	2.09	0.06						
	graminoid	2.41	0.24						
	mixed	2.31	0.25						

Radiation conditions

Total growing season SW radiation (± 1 S.D)was lowest for Svalbard was (1310 ± 100 MJ m^{-2}) and greatest at Zackenberg (1707 ± 111 MJ m^{-2}) (Fig. 4a.). The Erbs *et al.* (1982) model of diffuse radiation fraction performed well when tested with measured data from Abisko (Supplementary Material Fig. 2 a & b) though there was a slight bias (daily modelled vs. measured diffuse radiation slope = 1.11, intercept = -0.59, R^2 = 0.86, RMSE = 0.99 MJ m^{-2} day^{-1}). This bias was corrected for when calculating growing season diffuse fraction. We also corrected for bias at Toolik Lake (daily modelled vs. measured diffuse radiation slope = 1.02, intercept = 0.69, R^2 = 0.72, RMSE = 1.38 MJ m^{-2} day^{-1}). Average diffuse fraction was greatest in Svalbard; 81 % of total growing season radiation was diffuse in Svalbard, compared to 67 % in Sweden, 63 % in Alaska and 64 % in Zackenberg. There was a positive trend in fitted values of N_0 (fitted fixed effect plus estimated site random effect) with total growing season radiation. There was a negative trend in fitted values of γ (fitted fixed effect plus estimated site random effect) with increasing diffuse radiation fraction (Fig. 4b).

LAI and NDVI

We found a positive correlation between NDVI after vascular canopy removal and percent moss cover. NDVI for bare ground with no moss cover varied between 0.24 and 0.42, for ground with 100 % moss cover NDVI varied between 0.52 and 0.78 (Fig. 1). There was a clear relationship between NDVI and observed LAI in Svalbard, for plots with both low and high moss cover (Fig. 5a). The relationship between LAI and NDVI was more scattered for Zackenberg, with a clustering of points with > 50 % moss cover at high NDVI values but low LAI values (Fig. 5b).

Including the effect of mosses on $NDVI_{min}$ using equation 2 (parameterised separately for each PFT) we could explain 74 % of the variation in LAI. If we did not include the effect of mosses on $NDVI_{min}$ we could explain 70 %. Including the effect of mosses on $NDVI_{min}$ for Zackenberg, we could explain 49 % of the variation in LAI, excluding the effect of mosses on $NDVI_{min}$ we could explain only 37 %. Data from Barrow were limited so we parameterised the LAI_NDVI relationship for graminoids, and combined

mixed/forb and deciduous vegetation. We could explain 34 % of the variation in LAI at Barrow using NDVI and % moss cover, NDVI alone explained 23 % .

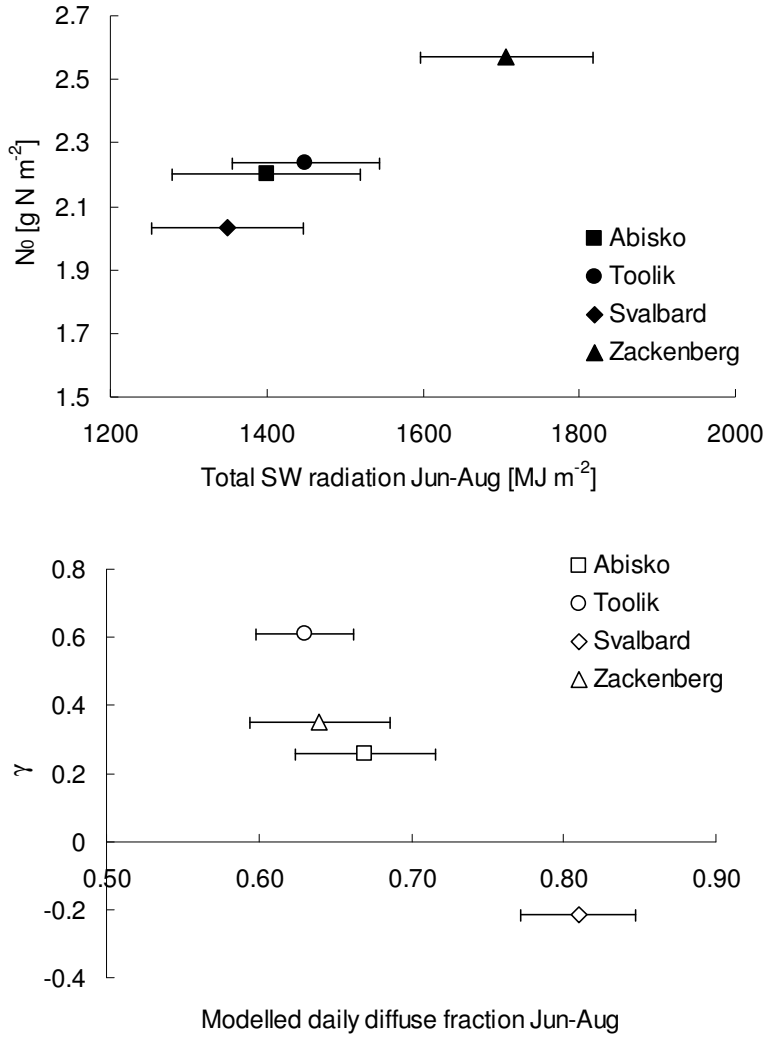

Figure 4. a) Fitted values of N_0 vs. total growing season short wave radiation and b) fitted values of γ versus diffuse radiation fraction at Abisko, Toolik, Svalbard and Zackenberg. Error bars are standard deviation for 7 years of radiation data

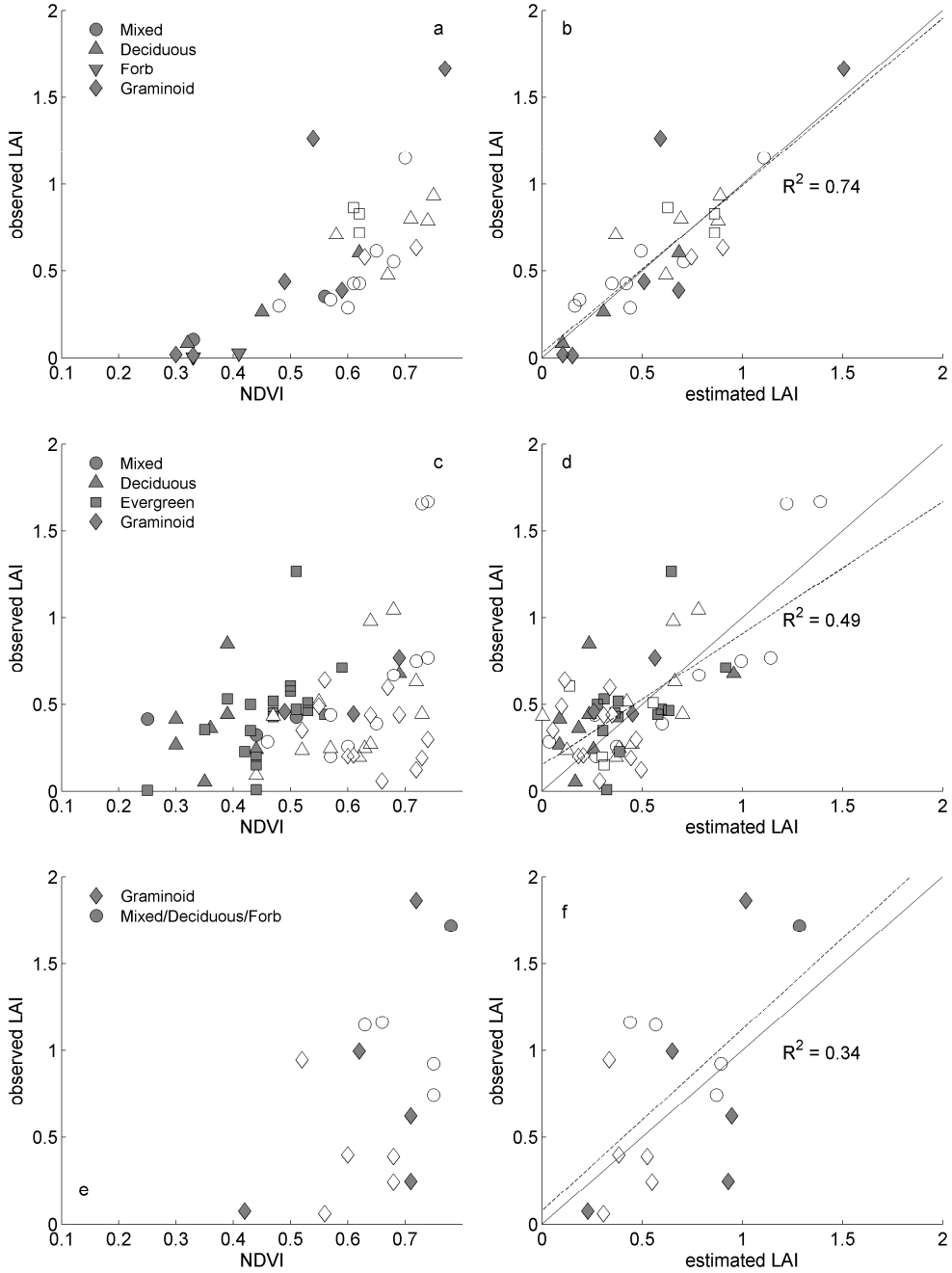

Figure 5. The relationship between NDVI and LAI (left panel) and modelled versus measured LAI (right panels) for a) Svalbard, b) Zackenberg and c) Barrow. Open symbols indicate the moss cover is > 50 %, closed symbols indicate moss cover < 50 %.

LAI, GPP and E_0

For GPP model there was a small increase in the loglikelihood value when including PFT as a fixed effect in the model (and a small decrease in RMSE) but this was non-significant at the 5 % level, and was accompanied by a small increase in AIC compared to the general model, indicating over-parameterisation (Table 5). Including random effects of site in the GPP model resulted in an increase in loglikelihood that was weakly significant ($p < 0.1$) and a marginal decrease is AIC, but the accompanying decrease in RMSE compared to the general model was small (less than 10 %). Fitted P_0 for the general model was 11.8 μmol m^{-2} s^{-1} and γ_p was 0.6 m^{-2} ground m^{-2} leaf (Fig. 6a, Table 5). There was little support for including vegetation fixed effects or site random effects in the linear model between E_0 and LAI (Fig. 6b, Table 6). The general E_0 model was associated with the lowest AIC value and had slope of 0.017 μmol CO_2 μmol^{-1} PPFD and intercept of 0.005 μmol CO_2 μmol^{-1} PPFD.

Table 5. Model structure, Akaike's information criteria (AIC), loglikelihood (LogLik) and root mean square error (RMSE) for alternative GPP model formulations. " - " indicates that site random effects are not included in the model.

Model	PFT	PFT fixed effects		Parameter number	SD site random effects		AIC	LogLik	RMSE [μmol m^{-2} s^{-1}]
		P_0	γ_p		P_0	γ_p			
GPP.gnls	all	11.8	0.63	3	-	-	379.3	-186.6 *	2.06
GPP.gnls$_{PFT}$	D	10.5	0.33	9	-	-	380.8	-181.4	1.94
	E	23.0	4.1						
	G	12.1	0.29						
	M	11.4	0.61						
GPP.nlme	all	13.7	1.0	5	5.3	1.0	379.2	-176.9 *	1.87

* indicates nested models where log likelihood ratio test significant at 0.10 level. NB only used light curves where PPFD over 1000 μmol m^{-2} s^{-1}

Table 6. Model structure, Akaike's information criteria (AIC) and root mean square error (RMSE) for alternative E_0 model formulations. " - " indicates that site random effects are not included in the model

Model	PFT	PFT fixed effects		Param number	SD site random effects		AIC	LogLik	RMSE [μmol m^{-2} s^{-1}]
		Slope	intercept		Slope	intercept			
E_0.gnls	all	0.0166	0.0049	3	-	-	-928.7	468.3	0.0061
E_0.gnls$_{PFT}$	D	0.0034	0.0024	9	-	-	-918.4	469.2	0.0061
	E	0.0213	0.0079						
	G	0.0017	0.0021						
	M	0.0050	-0.0001						
E_0.nlme	all	0.0163	0.0050	5	8.6×10^{-4}	3.5×10^{-7}	-924.0	469.0	0.0060

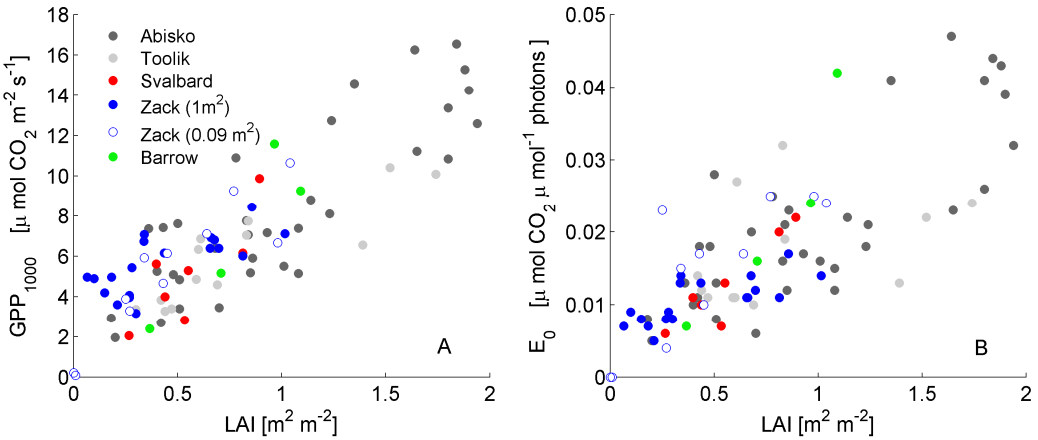

Figure 6. a) The relationship between GPP_{1000} and LAI and b) E_0 and LAI for Svalbard, Abisko Toolik, Zackenberg and Barrow

Discussion

The relationship between LAI and TFN in Arctic vegetation

The average fitted value for top of canopy nitrogen concentration (N_0) across sites was 2.2 g N m^{-2}, with a standard deviation across sites of 0.2 g N m^{-2} and coefficient of variation (CV) 9 %. Our estimate of N_0 is slightly higher than the average canopy N/LA of 1.9 g N m^{-2} reported by van Wijk *et al* (2005) for a subset of the same data (Abisko and Toolik data sets) because of the extinction of N/LA within the canopy as LAI increases. The average fitted TFN extinction coefficient γ was 0.22, with standard deviation across sites of 0.31 or CV of 140 %. The extinction of N/LA with canopy depth was more variable across sites than top of the canopy N/LA. The fit of the TFN model could not be improved by adding the effects of PFT composition, supporting the conclusions of Van Wijk *et al* (2005) and Campioli *et al.* (2009) that the relationship between LAI and TFN converges for a wide range of vegetation types.

The large variability in fitted γ compared to N_0 is apparent in the data (Fig. 2a), with the degree of overlap between sites decreasing with increasing LAI. The overlap in LAI-TFN relationship across sites at low LAI (Fig. 2a) occurs despite differences between sites in average leaf N concentration by mass (TFN/TLM); average TFN/TLM at Zackenberg, Svalbard and Barrow was greater than at Toolik and Abisko (Fig. 2d). Higher metabolite concentrations in colder climates can be expected as an acclimation response to lower rates of enzyme activity (Chapin & Oechel, 1983), or because of passive lack of dilution resulting from slower growth (Weih & Karlsson, 2001). Alternatively, the shorter growing season in Svalbard and Zackenberg may favour short-lived leaves, which tend to be thinner (Shipley *et al.*, 2006) forcing canopies to concentrate N (per unit mass) to achieve optimal N per unit leaf area. The result is differences in how LAI-TFN coupling is achieved across sites; in Svalbard and Zackenberg leaves are thinner with higher N concentration by mass (*Cassiope tetragona*, the only abundant evergreen shrub, being the exception), whereas in Sweden, for example, leaves are thicker, with lower N concentration by mass (corresponding to vegetation dominated by *E. hermaphroditum*). Leaf characteristics at

Toolik are intermediate between these extremes (Fig. 2d). Trade-offs between leaf properties have been well investigated within and across species (Reich & Oleksyn, 2004; Wright *et al.*, 2004) but this is the first time such trade-offs have ever been documented at the level of whole plant communities.

The influence of radiation

Much work has been done on modelling and measuring the vertical distribution of N and its effect on canopy level C gain (Hirose, 2005; Niinemets, 2007), mostly within single species. Where light extinction is greatest, models predict the optimal N distribution to follow an exponential decline. *In vivo* the actual distribution of N is often found to be more uniform than is optimal; however, differences in light extinction through plant canopies is a plausible explanation for differences in N extinction (γ) and hence the extent of curvature in the LAI-TFN relationship. Factors that effect the light gradient within canopies include the relative amount of incident beam and diffuse radiation (Gu *et al.*, 2002). Under cloudy sky conditions all incident radiation is diffuse, reducing the amount of shading within the canopy, and increasing light penetration to deeper layers (Roderick *et al.*, 2001). Lower sun angles at high latitude also increase the diffuse fraction. We find a negative relationship between modelled daily diffuse radiation and γ, but contrary to our expectations this did not follow a latitudinal pattern. Diffuse radiation at Zackenberg, although at higher latitude, was the same as that at Toolik with Svalbard having the highest diffuse fraction.

Difference in diffuse radiation between sites can be explained by differences in cloudiness; remotely sensed maps of cloud frequency (Wylie 2010) show high cloud cover (approaching 100%) over the polar oceans and around Svalbard. Cloud frequency over Greenland is lower (around 60 %) than that of terrestrial Arctic at lower latitudes presumably because of the influence of the ice cap on cloud formation. Cloud cover over northern Alaska appears slightly lower than over northern Sweden, though local weather patterns will have an impact. There are other important influences on canopy light penetration, such as canopy height, leaf angle and geometry. (Anten *et al.*, 1995) showed that the optimal N distribution in monocotyledonous species followed a

more uniform N distribution than dicotyledonous species because erect leaf angles allowed greater light penetration into the canopy. The lack of significant improvements in model fit when incorporating PFT in the model ($TFN.nlme_{PFT}$) however suggests that the properties of incident radiation are more important controls over the distribution of N within canopies.

Despite relatively small variations in N_0 between sites compared to the mean, N_0 was positively correlated to the total amount of SW radiation available over the growing season, as we initially expected. The relationship also did not follow a latitudinal pattern; Zackenberg had the highest total SW radiation (because of the combination of longer days with lower diffuse fraction), and Svalbard had the lowest total SW. Although we can not exclude other factors that affect soil N availability across sites, such as soil type, depth, moisture and temperature, as explanations for differences in N_0, it could be argued that these factors are more likely to affect *whole plant*, or *whole canopy* TFN than top of canopy N/LA. The highest TFN values recorded were in grass dominated communities in Svalbard underneath cliffs, perhaps because of nutrient enrichment by sea birds or run off from snow melt from plateaus above.

Predicting LAI from NDVI: the importance of bryophytes

We found a positive relationship between the % cover of mosses and the NDVI of the ground surface after the vascular canopy had been removed. Including the effect of mosses on background NDVI reduced error in LAI prediction in all cases, and at Zackenberg by 10 %. This improvement is surprising considering the inaccuracies inherent in visually estimating percent cover, and the probable variability in moss NDVI with water content and species. The large abundances of mosses at Zackenberg (pers. obs) may also increase the impact of structural vegetation properties on the LAI-NDVI relationship, because of the effects of canopy structure on the degree to which underlying mosses are visible from above. Without including the effects of vegetation and moss cover at Zackenberg, NDVI was able to explain only 17 % of the variation in LAI.

Using LAI to predict GPP across latitudes

We found no significant improvement in model fit by including vegetation functional type as a factor in models of GPP_{1000} and E_0. Functional convergence of PFTs in Arctic vegetation has previously been reported, and we argue that this is a direct result of the close convergence of the LAI-TFN relationship within a site (Shaver *et al.*, 2007; Street *et al.*, 2007; Williams *et al.*, 2006). We found a slight but insignificant improvement in the GPP model fit by including site level effects, which we suggest may be the result of differences in the LAI-TFN relationship between sites. However we did not measure GPP fluxes in plots with LAI >1 at Zackenberg, Svalbard and Barrow; at scales of 1 × 1 m vegetation with LAI > 1 is unusual at these sites. The LAI-TFN relationship largely overlaps across sites below an LAI of 1, so it might be expected that site level differences in the relationship between GPP and LAI would be difficult to detect. The effects of air temperature, phenology, and VPD will also control GPP (Rastetter *et al.*, 2010) contributing to variation in the relationship between GPP and LAI, and masking any effect of site.

Conclusions

The close coupling between LAI and TFN indicates that Arctic plant canopies must follow a narrowly constrained set of rules that dictate the development of LAI with respect to TFN. The route by which LAI-TFN coupling is achieved however differs between sites, with a trade-off between average leaf N concentration and leaf mass per unit area. The relationship between TFN and LAI appears to be affected by differences in radiation environment as a result of differences in cloudiness and day length. Predicted increases in cloudiness as a result of global climate change may therefore increase uniformity in the distribution of N in Arctic vegetation. We show that GPP can be predicted from LAI across Arctic latitudes by a single relationship, and although some site level differences are apparent, the improvement in model fit by including site effects is small. We also show that predicting LAI from NDVI at sites where LAI is low and moss abundance is high requires information on the type of vegetation and the extent of moss cover.

Acknowledgements

This work was supported by grants from the US National Science Foundation to the Marine Biological Laboratory including grants # OPP-0352897, DEB-0423385, and DEB-0444592. We thank Jim Laundre at the MBL and the staff at Toolik Field Station and Abisko Scientific Research Station for their help and support. Bob Douma and Celine Ronfort assisted with fieldwork in Sweden and Svalbard. We acknowledge Glenn Scott from AON, Siegrid Debatin from the Alfred Wegener Institute Foundation for Polar and Marine Research, and Jonathan Evans from the ABACUS project for providing radiation data. We also thank Paul Stoy and Adrian Rocha for their valuable comments on a previous version of this manuscript.

References

ACIA (2005) *Arctic Climate Impact Assessment - Scientific Report* Cambridge University Press.

Anisimov, O.A., Vaughan, D.G., Callaghan, T.V., Furgal, C., Marchant, H., Prowse, T.D., Vilhjálmsson, H., & Walsh, J.E. (2007) *Polar regions (Arctic and AntArctic).* Cambridge University Press, Cambridge.

Anten, N.P.R., Schieving, F., & Werger, M.J.A. (1995) Patterns of Light and Nitrogen Distribution in Relation to Whole Canopy Carbon Gain in C-3 and C-4 Monocotyledonous and Dicotyledonous Species. *Oecologia*, **101**, 504-513.

Baddeley, J.A., Woodin, S.J., & Alexander, I.J. (1994) Effects of Increased Nitrogen and Phosphorus Availability on the Photosynthesis and Nutrient Relations of 3 Arctic Dwarf Shrubs from Svalbard. *Functional Ecology*, **8**, 676-685.

Brown, J., Miller, P.C., Tieszen, L.L., & Bunnell, F.L. (1980) An Arctic Ecosystem: The coastal tundra at Barrow, Alaska. . In US IBP Synthesis Series, Vol. 12, pp. 571. Dowden, Hutchinson, and Ross, Stroudsburg, PA.

Campioli, M. (2008) Carbon allocation in ecosystems: an experimental and modelling approach for tundra and forest vegetations, Universiteit Gent, Gent.

Chapin, F.S. & Oechel, W.C. (1983) Photosynthesis, Respiration, and Phosphate Absorption by Carex-Aquatilis Ecotypes Along Latitudinal and Local Environmental Gradients. *Ecology*, **64**, 743-751.

Chapin, F.S., Sturm, M., Serreze, M.C., McFadden, J.P., Key, J.R., Lloyd, A.H., McGuire, A.D., Rupp, T.S., Lynch, A.H., Schimel, J.P., Beringer, J., Chapman, W.L., Epstein, H.E., Euskirchen, E.S., Hinzman, L.D., Jia, G., Ping, C.L., Tape, K.D., Thompson, C.D.C., Walker, D.A., & Welker, J.M. (2005) Role of land-surface changes in Arctic summer warming. *Science*, **310**, 657-660.

Christensen, J.H., Hewitson, B., Busuioc, A., Chen, A., Gao, X., Held, I., Jones, R., Kolli, R.K., Kwon, W.-T., Laprise, R., Rueda, V.M., Mearns, L., Menéndez, C.G., Räisänen, J., Rinke, A., Sarr, A., & Whetton, P. (2007). Regional Climate Projections. In *Climate Change 2007: The Physical Science Basis. Contribution of Working Group I to the Fourth Assessment Report of the Intergovernmental Panel on Climate Change* (eds S. Solomon, D. Qin, M. Manning, Z. Chen, M. Marquis, K.B. Averyt, M. Tignor & H.L. Miller). Cambridge University Press, Cambridge, United Kingdom and New York, USA.

Christiansen, H.H. (2004) Meteorological control on interannual spatial and temporal variations in snow cover and ground thawing in two northeast greenlandic circumpolar-active-layer-monitoring (CALM) sites. *Permafrost and Periglacial Processes*, **15**, 155-169.

Davidson, E.A. & Janssens, I.A. (2006) Temperature sensitivity of soil carbon decomposition and feedbacks to climate change. *Nature*, **440**, 165-173.

Erbs, D.G., Klein, S.A., & Duffie, J.A. (1982) Estimation of the Diffuse-Radiation Fraction for Hourly, Daily and Monthly-Average Global Radiation. *Solar Energy*, **28**, 293-302.

Evans, J.R. (1989) Photosynthesis and Nitrogen Relationships in Leaves of C-3 Plants. *Oecologia*, **78**, 9-19.

Field, C. (1983) Allocating Leaf Nitrogen for the Maximization of Carbon Gain - Leaf Age as a Control on the Allocation Program. *Oecologia*, **56**, 341-347.

Forland, E.J. & Hanssen-Bauer, I. (2000) Increased precipitation in the Norwegian Arctic: True or false? *Climatic Change*, **46**, 485-509.

Gu, L.H., Baldocchi, D., Verma, S.B., Black, T.A., Vesala, T., Falge, E.M., & Dowty, P.R. (2002) Advantages of diffuse radiation for terrestrial ecosystem productivity. *Journal Of Geophysical Research-Atmospheres*, **107**.

Hartley, I.P., Hopkins, D.W., Garnett, M.H., Sommerkorn, M., & Wookey, P.A. (2008) Soil microbial respiration in Arctic soil does not acclimate to temperature. *Ecology Letters*, **11**, 1092-1100.

Hikosaka, K. & Hirose, T. (1998) Leaf and canopy photosynthesis of C-3 plants at elevated CO2 in relation to optimal partitioning of nitrogen among photosynthetic components: theoretical prediction. *Ecological Modelling*, **106**, 247-259.

Hirose, T. (2005) Development of the Monsi-Saeki theory on canopy structure and function. *Annals of Botany*, **95**, 483-494.

Hirose, T. & Werger, M.J.A. (1987) Maximizing Daily Canopy Photosynthesis with Respect to the Leaf Nitrogen Allocation Pattern in the Canopy. *Oecologia*, **72**, 520-526.

Holland, M.M. & Bitz, C.M. (2003) Polar amplification of climate change in coupled models. *Climate Dynamics*, **21**, 221-232.

Hollister, R.D., Webber, P.J., & Bay, C. (2005) Plant response to temperature in Northern Alaska: Implications for predicting vegetation change. *Ecology*, **86**, 1562-1570.

McKane, R.B., Rastetter, E.B., Shaver, G.R., Nadelhoffer, K.J., Giblin, A.E., Laundre, J.A., & Chapin, F.S. (1997a) Climatic effects on tundra carbon storage inferred from experimental data and a model. *Ecology*, **78**, 1170-1187.

McKane, R.B., Rastetter, E.B., Shaver, G.R., Nadelhoffer, K.J., Giblin, A.E., Laundre, J.A., & Chapin, F.S. (1997b) Reconstruction and analysis of historical changes in carbon storage in Arctic tundra. *Ecology*, **78**, 1188-1198.

Niinemets, U. (2007) Photosynthesis and resource distribution through plant canopies. *Plant Cell And Environment*, **30**, 1052-1071.

Ping, C.L., Michaelson, G.J., Jorgenson, M.T., Kimble, J.M., Epstein, H., Romanovsky, V.E., & Walker, D.A. (2008) High stocks of soil organic carbon in the North American Arctic region. *Nature Geoscience*, **1**, 615-619.

Rastetter, E.B., Williams, M., Griffin, K.L., Kwiatkowski, B.L., Tomasky, G., Potosnak, M.J., Stoy, P.C., Shaver, G.R., Stieglitz, M., Hobbie, J.E., & Kling, G.W. (2010) Processing Arctic eddy-flux data using a simple carbon-exchange model embedded in the ensemble Kalman filter. *Ecological Applications*, **20**, 1285-1301.

Reich, P.B. & Oleksyn, J. (2004) Global patterns of plant leaf N and P in relation to temperature and latitude. *Proceedings Of The National Academy Of Sciences Of The United States Of America*, **101**, 11001-11006.

Roderick, M.L., Farquhar, G.D., Berry, S.L., & Noble, I.R. (2001) On the direct effect of clouds and atmospheric particles on the productivity and structure of vegetation. *Oecologia*, **129**, 21-30.

Shaver, G.R. & Chapin, F.S. (1980) Response to Fertilization by Various Plant Growth Forms in an Alaskan tundra: Nutrient accumulation and growth. *Ecology*, **61**, 662-675.

Shaver, G.R. & Chapin, F.S. (1986) Effect of fertilizer on production and biomass of tussock tundra, Alaska, U.S.A. *Arctic And Alpine Research*, **18**, 261-268.

Shaver, G.R. & Chapin, F.S. (1991) Production - Biomass Relationships And Element Cycling In Contrasting Arctic Vegetation Types. *Ecological Monographs*, **61**, 1-31.

Shaver, G.R., Street, L.E., Rastetter, E.B., Van Wijk, M.T., & Williams, M. (2007) Functional convergence in regulation of net CO2 flux in heterogeneous tundra landscapes in Alaska and Sweden. *Journal of Ecology*, **95**, 802-817.

Shipley, B., Lechoweicz, M.J., Wright, I., & Reich, P.B. (2006) Fundamental trade-offs generating the worldwide leaf economics spectrum. *Ecology*, **87**, 535-541.

Steltzer, H. & Welker, J.M. (2006) Modeling the effect of photosynthetic vegetation properties on the NDVI-LAI relationship. *Ecology*, **87**, 2765-2772.

Street, L.E., Shaver, G.R., Williams, M., & Van Wijk, M.T. (2007) What is the relationship between changes in canopy leaf area and changes in photosynthetic CO2 flux in Arctic ecosystems? *Journal of Ecology*, **95**, 139-150.

Trenberth, K.E., Jones, P.D., Ambenje, P., Bojariu, R., Easterling, D., Tank, A.K., Parker, D., Rahimzadeh, F., Renwick, J.A., Rusticucci, M., Soden, B., & Zhai, P. (2007). Observations: Surface and Atmospheric Climate Change. In *Climate Change 2007: The Physical Science Basis. Contribution of Working Group I to the Fourth Assessment Report of the Intergovernmental Panel on Climate Change* (eds S. Solomon, D. Qin, M. Manning, Z. Chen, M. Marquis, K.B. Averyt, M. Tignor & H.L. Miller). Cambridge University Press, Cambridge, United Kingdom and New York, USA.

van Wijk, M.T., Williams, M., & Shaver, G.R. (2005) Tight coupling between leaf area index and foliage N content in Arctic plant communities. *Oecologia*, **142**, 421-427.

Weih, M. & Karlsson, P.S. (2001) Growth response of Mountain birch to air and soil temperature: is increasing leaf-nitrogen content an acclimation to lower air temperature? *New Phytologist*, **150**, 147-155.

Williams, M. & Rastetter, E.B. (1999) Vegetation characteristics and primary productivity along an Arctic transect: implications for scaling up. *Journal of Ecology*, **87**, 885-898.

Williams, M., Rastetter, E.B., Shaver, G.R., Hobbie, J.E., Carpino, E., & Kwiatkowski, B.L. (2001) Primary production of an Arctic watershed: An uncertainty analysis. *Ecological Applications*, **11**, 1800-1816.

Williams, M., Street, L.E., van Wijk, M.T., & Shaver, G.R. (2006) Identifying Differences in Carbon Exchange among Arctic Ecosystem Types. *Ecosystems*, **9**, 288-304.

Wright, I.J., Reich, P.B., Westoby, M., Ackerly, D.D., Baruch, Z., Bongers, F., Cavender-Bares, J., Chapin, T., Cornelissen, J.H.C., Diemer, M., Flexas, J., Garnier, E., Groom, P.K., Gulias, J., Hikosaka, K., Lamont, B.B., Lee, T., Lee, W., Lusk, C., Midgley, J.J., Navas, M.L., Niinemets, U., Oleksyn, J., Osada, N., Poorter, H., Poot, P., Prior, L., Pyankov, V.I., Roumet, C., Thomas, S.C., Tjoelker, M.G., Veneklaas, E.J., & Villar, R. (2004) The worldwide leaf economics spectrum. *Nature*, **428**, 821-827.

2b. Photosynthetic CO_2 flux and the relationship between leaf area index and total foliar nitrogen – a single Arctic relationship? – supplementary material

L. E. Street[1], G. R. Shaver[2], E.B. Rastetter[2], M. T. van Wijk[3], Kaye B. A.[2], M. Williams[1]

[1]School of Geosciences, University of Edinburgh, Edinburgh, EH9 3JN, UK.

[2] Marine Biological Laboratory, Woods Hole, MA 02543, USA.

[3]Plant Production Systems, Wageningen University, Plant Sciences, Haarweg 333, 6709 RZ Wageningen, Netherlands.

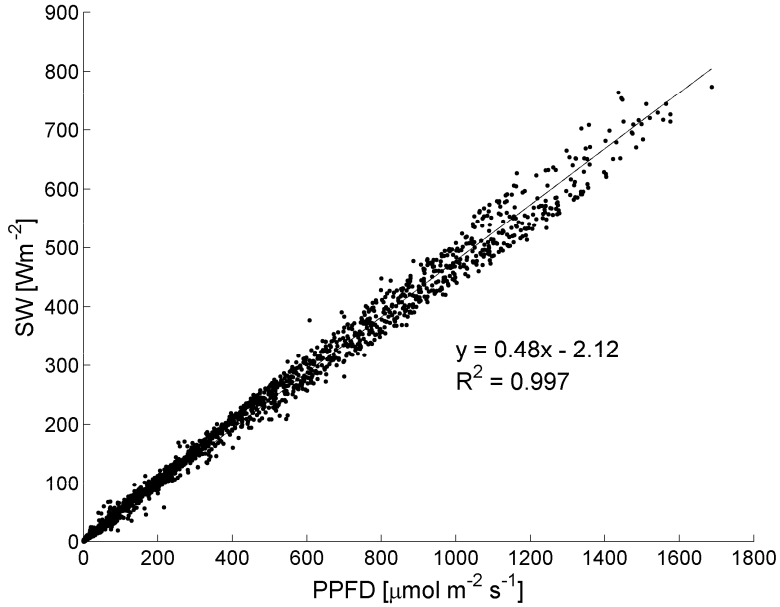

Figure 1. SW vs. PPFD radiation data from Toolik Lake Field station for 12th July to 13th September and 24th October to 26th November 2008

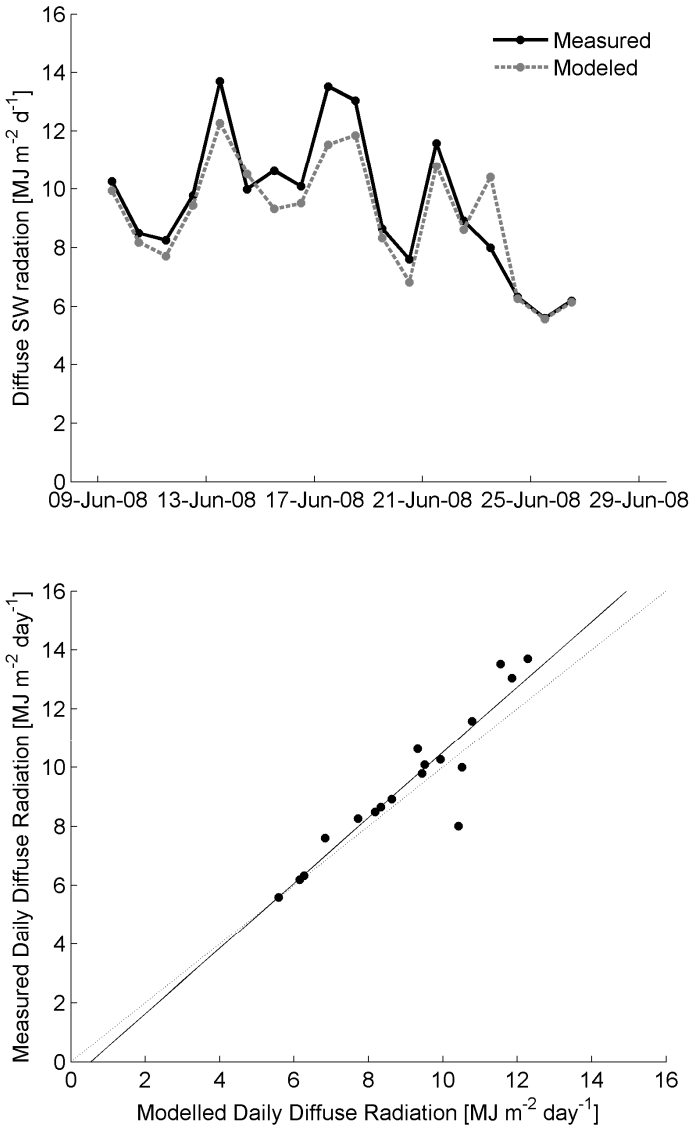

Figure 2. a) Total daily diffuse radiation through time at a Abisko b) linear regression of modelled vs. measured diffuse radiation at Abisko

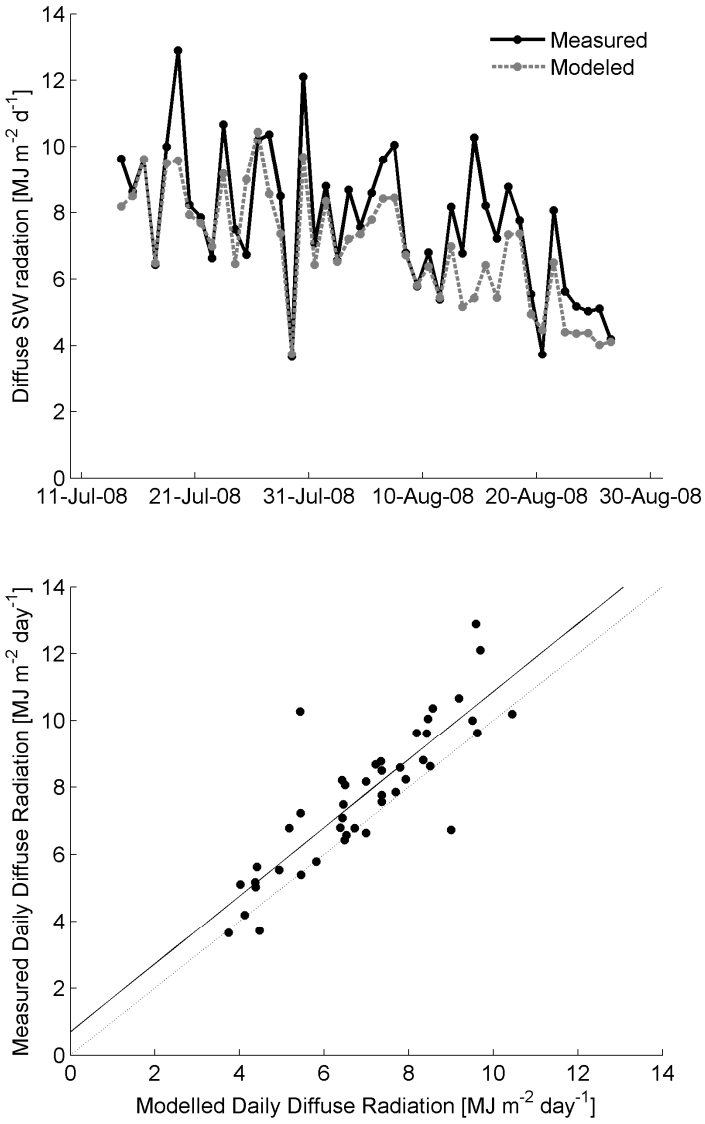

Figure 3. a)Total daily diffuse radiation through time at Toolik Lake, for a 8 week period in late summer 2008. b) linear regression of modelled vs. measured diffuse radiation.

3. Seasonal bryophyte productivity in the sub-Arctic: A comparison with vascular plants

L.E. Street [1], P. Stoy[2], M. Sommerkorn[3], B. Fletcher[4], V. Pope[4], T.C. Hill[1], M. Williams[1]

[1]School of Geosciences, University of Edinburgh, Edinburgh, EH9 3JN, UK

[2] Dept. of Land Resources and Environmental Sciences, Montana State University, Bozeman, MT 59717, USA

[3]Macaulay Land Use Research Institute, Craigiebuckler, Aberdeen, AB15 8QH, UK

[4]Department of Animal and Plant Sciences, The University of Sheffield, Sheffield, ST10 2TN, UK

(*Intended for submission to Arctic, Antarctic and Alpine Research*)

Abstract

Arctic ecosystems are experiencing rapid climate change, which could result in positive feedbacks on climate warming if ecosystem carbon loss exceeds uptake. Bryophytes are an important component of Arctic vegetation, but are not currently well-represented in terrestrial C models and their seasonal C metabolism compared to vascular vegetation is poorly understood. Our objective was to quantify CO_2 fluxes from bryophytes patches in early spring and summer and to develop a simple model of seasonal bryophyte GPP to compare against vascular plant GPP. Total annual GPP for *Polytrichum* was 362 g C m^{-2} and for *Sphagnum* was 112 g C m^{-2}, approximately 90 % and 30 % respectively of modelled annual GPP for typical vascular plant communities at the same site. Bryophyte GPP was nearly 300 % of vascular GPP in spring while the vascular plant canopy was still developing. Moss turf water content did not strongly control GPP due to the physiological adaptations of the species studied. Seasonal changes in photosynthetic capacity were more important in determining GPP for both bryophyte species.

Introduction

The Arctic climate is changing at a faster rate than the rest of the globe. Surface temperatures in the Arctic have increased by approximately 0.4°C per decade between 1966 and 2003 (McBean *et al.*, 2005), and this trend is predicted to continue with a potential annual mean temperature increase of > 5°C by 2100 (Christensen *et al.*, 2007). Increases in Arctic surface temperature will be accompanied by shifts in ecosystem function, and could potentially result in the net release to the atmosphere of stored organic carbon as CH_4 or CO_2 from the vast stores (1672 Pg) of organic C in northern permafrost soils (Tarnocai *et al.* (2009). Enhanced plant productivity through greater availability of nutrients, and extension of the growing seasons, may partially offset increases in respiratory CO_2 flux which may result from warmer soils and melting permafrost (Schuur *et al.*, 2009).

Current understanding of photosynthesis in vascular plant canopies is well developed, with strong relationships demonstrated between vascular plant traits, such as leaf area, leaf N content, and gross primary productivity (GPP) (Shaver *et al.*, 2007; Street *et al.*, 2007; Williams *et al.*, 2006). Bryophytes, however, are an important component of Arctic plant communities that have received relatively little research attention [but see e.g. (Cornelissen *et al.*, 2007a; Douma *et al.*, 2007)]. Existing estimates suggest that bryophytes account for a significant fraction of land surface C uptake; the ratio of bryophyte net primary productivity (NPP) to total aboveground NPP is around 25-30% for Alaskan tussock tundra (Chapin *et al.* (1995), coastal tundra near Barrow, AK (Miller *et al.* (1980) and for Scandanavian tundra heath in the late summer (Campioli *et al.* (2009b). Bryophytes can dominate photosynthetic carbon fluxes where they form continuous cover (Douma *et al.*, 2007). Sommerkorn *et al.* (1999), showed that bryophytes assimilate as much as 51% to 98% of the daily CO_2 released from tundra soils through respiration, suggesting that bryophytes can act as an important buffer against soil CO_2 losses to the atmosphere.

Bryophyte physiology differs to that of vascular plants with important consequences for land-atmosphere CO_2 and H_2O fluxes. Bryophytes do not have stomata and lose water readily from their tissues (Proctor, 2000), they also lack roots so are unable to extract water from depth within the soil profile. Bryophytes instead depend on the availability of water in the environment, either directly from humid air, the surface substrate or from precipitation. Many species are adapted to survive long periods of desiccation. It follows that where bryophytes are a significant component of vegetation the influence of external environmental conditions on photosynthesis will differ from those of vascular plant dominated vegetation.

Recognition of the importance of bryophytes in the land-atmosphere exchange of CO_2 and H_2O is growing (Huemmrich *et al.*, 2010a; Wania *et al.*, 2009a, b) but the data supporting model representations are sparse. Much of the existing literature on Arctic bryophyte photosynthesis is based on laboratory measurements (Oechel & Collins, 1976) or on field measurements on excised shoots where the natural structure of the

bryophyte had been disturbed (Harley *et al.*, 1989; Murray *et al.*, 1989). Few *in-situ* CO_2 flux data sets are available to provide flux data per unit area of the land surface, and none cover the period during or immediately after snow melt (Douma *et al.*, 2007; Miller *et al.*, 1976; Oechel, 1976; Sommerkorn *et al.*, 1999). Recent studies in the high Arctic that indicate the important bryophyte contribution to GPP (Arndal *et al.*, 2009), especially after vascular plant senescence (Uchida *et al.*, 2010), do not explicitly partition ecosystem CO_2 fluxes into bryophyte and vascular components.

In this paper we quantify photosynthetic CO_2 fluxes for two common Arctic bryophyte species and extrapolate *in-situ* bryophyte GPP measurements through time using simple models parameterised from laboratory observations. These models account for the influence of irradiance, moss water content, snow cover and phenology on bryophyte photosynthesis. We also estimate vascular plant GPP using a previously published model parameterized at the Abisko, Sweden study site. We combine measurements and models to address the questions: 1) what are the controls over bryophyte GPP in these species? and 2) how does bryophyte GPP compare to the GPP of vascular plants across the growing season at the same site? We hypothesise that seasonal changes in photosynthetic capacity in bryophytes are less important than seasonal fluctuations in surface moisture content in controlling photosynthesis over the course of a year. We also expect that the relative contribution of bryophytes to GPP is largest from March to May, the period during which the vascular plant canopy has yet to develop, but when moisture availability is high due to snow melt and surface temperatures exceed freezing due in part to the relatively low bryophyte albedos. This study is the first to present *in-situ* data on bryophyte GPP before snow melt in the sub-Arctic.

Materials and Methods

Field measurements

Site description

Our field site was located near Abisko in Northern Sweden, on a hillside approximately 6 km south of Lake Torneträsk (68°18′N,18°51′E). Mean annual temperature in the Abisko valley is -1 °C, mean July temperature is 11 °C and annual precipitation averages *ca.* 300 mm (Abisko Research Station, ANS). We chose to measure CO_2 flux on two common bryophyte species, both of which grow in continuous patches at the site: *Sphagnum fuscum* ((Schimp.) H. Klinggr.) forms hummocks in poorly drained areas, and *Polytrichum piliferum* (Hedw.) is locally abundant in rocky areas with thin organic soils. The vascular vegetation at the site is dominated by ericaceous tundra heath composed of evergreen *Empetrum nigrum* (previously known as *Empetrum hermaphroditum* (Hagerup)), with dwarf shrubs *Betula nana* (L.) and *Salix spp.* in sheltered depressions, and barren cryptogam-dominated areas on exposed ridges.

Environmental conditions

Environmental conditions for patches of *Polytrichum* and *Sphagnum* were monitored from June 2007 to August 2009 at one flux plot for each species (as indicated in Table 1). Bryophyte temperature was measured at ~2 cm depth below the surface and air temperature ~3 cm above the surface (with appropriate shielding from radiation) using HOBO 8-bit temperature sensors. Volumetric water content (VWC, m^3 m^{-3}) was measured for the top 1-5 cm of bryophyte carpet using HOBO ECH_2O soil moisture probes, and surface wetness was measured using HOBO leaf wetness sensors. Data were recorded every 5 minutes using HOBO Micro-Station data loggers (Onset Inc, Massachusetts, USA). We calibrated the soil moisture probes to convert logged VWC to destructively measured VWC and relative water content (RWC) as a percentage dry mass using:

$$VWC = \frac{(M_w - M_d)/\rho}{V_T} \quad (1)$$

$$RWC = \frac{M_w - M_d}{M_d} \times 100 \quad (2)$$

where M_w is wet mass (kg) and M_d is dry mass (kg), V_T is turf volume (m^3) and ρ is the density of water (kg m^{-3}). To avoid the effects of removing and replacing the probes for calibration (a potentially large source of error in the measurement), we removed an entire bryophyte turf of each species (approximately 20 × 20 cm to depth of 10 cm) with the probes *in-situ*. We then carefully transported the turf and probe to the laboratory, and wetted the turf to maximum saturation. After wetting we placed the samples on a wire grid until dripping ceased, then transferred the turfs to plastic tubs, with plastic packaging around the turf edges to prevent drying from the sides. We then logged the VWC of the turfs at frequent intervals as they air-dried, and also measured the weight of the tub, probe and turf. Turf dimensions were recorded to calculate volume as the turfs desiccated. After the turf had dried to below the lowest VWC measured in the field we removed the moisture probe and dried the turf at 80°C until constant weight. We then subtracted the weight of the probe and tub to calculate turf wet weight, VWC and RWC (equations 1 & 2).

We estimated light transmission through the snow pack on 2nd, 13th, 15th and 20th April 2008. To do this we removed cut a block from the snow of approximately 15 cm × 15 cm area to a depth within a few cm of the ground surface. We then placed a PPFD sensor (Skye Instruments, UK) parallel to the ground surface under the remaining snow. We replaced the block of snow to measure light transmission and compared it to ambient light levels. For snow and ice less than 5-6 cm in height, we removed a small portion of the snow pack and placed it directly on top of the levelled sensor.

Field CO_2 fluxes

We measured the net ecosystem exchange (NEE) of CO_2 on 3 replicate bryophyte patches of *Sphagnum* and *Polytrichum* using a closed chamber system, on five dates from 21st June to 15th August 2007, and on 11 dates between 30th March and 25th April 2008. We used a 0.2 × 0.2 × 0.13 m clear acrylic chamber connected to an infrared gas analyser (IRGA); a smaller version of mobile tundra vegetation chambers used in previous studies (Douma *et al.*, 2007; Shaver *et al.*, 2007; Street *et al.*, 2007; Williams *et al.*, 2006). Air in the chamber was mixed by a small battery powered fan. To make a measurement, the chamber was placed on top of a 0.2 m × 0.2 m clear acrylic frame, which had been sealed to the ground surface before the measurement by weighting an attached clear plastic skirt using lengths of chain. During the spring measurements we also used snow on top of the skirt to improve the seal. For each replicate plot we made a series of NEE measurements under ambient and manipulated light conditions (see below) to create NEE light response curves. We subtracted ecosystem respiration (NEE measured under fully darkened conditions) from the net fluxes to calculate GPP.

A LI-6400 IRGA (LICOR, Lincoln, Nebraska) was used for the June - August 2007 measurement period. We first measured three replicates of NEE under ambient light conditions, followed by 4-7 measurements under sequentially reduced light conditions, created using layers of optically neutral shade cloth. We then made three replicate measurements under fully darkened conditions to quantify ecosystem respiration (ER). During the spring 2008 measurement period we followed the methods of Grogan & Jonasson (2006), and removed snow from the plots to measure surface flux. We allowed at least 35 minutes post snow removal before making a measurement. We used a CIRAS-1 IRGA (PP systems, Amesbury, Massachusetts) connected to the same 0.2 m × 0.2 m chamber, and did not make corrections for vapour pressure changes as the rate of vapour pressure change inside the chamber did not exceed 0.02 mb s^{-1} (Grogan & Jonasson, 2006; Hooper *et al.*, 2002) (the maximum rate of water vapour change recorded was 0.008 mb s^{-1}). For the cold season measurements we altered the measurement sequence, making additional measurements of ER before decreasing the

light level from ambient in stages, then re-measured respiration and repeated the sequence from ambient light back to zero (Fig. 6). We did this to detect any potential chamber effects on the background rate of ecosystem respiration, a particular concern under cold conditions and after snow removal. Where possible we took a small sample of bryophyte tissue to measure bryophyte RWC. In March - April 2008 we made 3 measurements of ambient NEE, followed by 3 ER measurements, on five replicate plots dominated by *Empetrum* at the same site (Table 1) to ascertain the differences between vascular and bryophyte-dominated vegetation during the shoulder season. We used the 0.2 m × 0.2 m chamber and followed the same procedure as for the bryophyte flux measurements.

We calculated the NEE of CO_2 from the rate of change of CO_2 concentration within the chamber using:

$$NEE = \frac{\rho V dC / dt}{A} \qquad (3)$$

Where *NEE* is net CO_2 flux (μmol m^{-2} s^{-1}), ρ is air density (mol m^{-3}), *V* is the chamber volume (m^3), d*C*/d*t* is the change in chamber CO_2 concentration over time (μmol mol^{-1} s^{-1}) and *A* is the chamber surface area (m^2). We fitted rectangular hyperbola GPP light response curves to the data using non-linear least squares curve-fitting in Matlab 7.1:

$$GPP = \frac{P_{max} I}{I + K} \qquad (4)$$

where P_{max} is the rate of light saturated photosynthesis (μmol CO_2 m^{-2} s^{-1}), *K* is the half-saturation constant of photosynthesis (μmol PAR m^{-2} s^{-1}) and *I* is the incident PPFD (μmol PAR m^{-2} s^{-1}).

Laboratory measurements

GPP response curves

We used laboratory based CO_2 exchange measurements on samples of *Polytrichum* and *Sphagnum* to parameterise the bryophyte flux (BF) model. We harvested ~ 7 × 7 cm turfs of *Polytrichum* and *Sphagnum* on the 24th of August 2007 and placed the turfs within controlled growth room facilities in the UK within 4 days. Conditions within the growth rooms were maintained at 12 °C with a 16/8 hour light/dark cycle until the beginning of November 2007. CO_2 flux measurements were made using a Walz gas analyser (Walz GmbH, Effeltrich, Germany) connected to a transparent 'mini-cuvette' in continuous differential mode. Turfs were trimmed to 4 cm × 4 cm and placed within the cuvette. The CO_2 flux was allowed to stabilise for 2 - 3 minutes before a measurement was recorded. Light was supplied by two small halogen lamps, the intensity of which was adjusted using multiple sheets of optically neutral tissue paper placed over the cuvette. Air temperature, bryophyte turf temperature and light intensity were monitored inside the cuvette.

Turfs of each species were fully wetted by soaking in distilled water. CO_2 fluxes at 630 and 0 μmol m^{-2} s^{-1} PPFD were then measured at intervals as each turf dried. We measured the total weight of each turf before and after measurement and subtracted CO_2 flux at zero light to calculate GPP. We dried the *Sphagnum* bryophytes sufficiently to observe a decrease in photosynthetic activity but did not allow the turfs to become fully desiccated to avoid damage to tissues. After the driest measurements the turfs were re-wetted overnight. After re-wetting we measured the light response of GPP at 12°C, then 5°C then 20°C. At each temperature GPP measurements were made at 500, 200, 100, 50, 1000, then 0 μmol m^{-2} s^{-1} PPFD. During these measurements the turfs were kept at water contents optimal for photosynthesis (identified from measurements at decreasing water content, and measured by sample weight) by supplying small amounts of water to the base of the turf, and misting the top of each turf, after a measurement. After measurements were completed we removed the green *Polytrichum* photosynthetic tissue and the *Sphagnum* capitula and weighed after drying

at 70 ºC for 3 days. There is very little photosynthetic activity below the capitulum region for this *Sphagnum* species (Street *et al.* (2011)),

Modelling

Bryophyte flux (BF) model

The basic bryophyte flux (BF) model consists of a rectangular hyperbola response of GPP to irradiance (equation 4), with the theoretical light-saturated rate of photosynthesis (P_{max}) varying as an Arrhenius function of temperature (equations 5 and 6) (Warren & Dreyer, 2006).

Where:

$$P_{\max} = \frac{P_{Tref} e^{\left[\frac{E_a}{RT_{ref}} \times \left(1 - \frac{T_{ref}}{T}\right)\right]}}{1 + e^{\left[\frac{\Delta ST - E_d}{RT}\right]}} \left(1 + e^{\left(\frac{\Delta ST_{ref} - E_d}{RT_{ref}}\right)}\right) \quad (5)$$

And where:

$$T_{opt} = \frac{-E_d}{R \ln\left(\frac{-E_a}{E_a - E_d}\right) - \Delta S} \quad (6)$$

Where $P_{\max}$ is the theoretical light-saturated rate of photosynthesis (μmol CO_2 m^{-2} s^{-1}), I is irradiance (μmol m^{-2} s^{-1} PPFD), K is the half-saturation constant (μmol photons m^{-2} s^{-1}), P_{Tref} is $P_{\max}$ measured at the reference temperature T_{ref} (in this case 278 K), T is temperature (K), ΔS is an entropy term (J K^{-1} mol^{-1}), E_a (J mol-1) is the activation energy, E_d is the deactivation energy (J mol^{-1}) R is the gas constant (8.3143 J K^{-1} mol^{-1}) and T_{opt} is the temperature optimum for photosynthesis (K).

Modifications for moss water content

To account for the effect of turf moisture content on GPP we added a polynomial water content adjustment factor (*W*) to the basic BF light-temperature model. W varied between 0 and 1, dependant on the relative water content (RWC) of the bryophyte turf:

$$[BF_W] \qquad GPP = \frac{P_{max} I}{I + k} W \qquad (7)$$

Where:

$$W = w_a X^2 + w_b X + w_c \qquad (8)$$

Where W is the RWC adjustment factor, X is RWC of the top 4 cm of the bryophyte surface (% dry weight), and w_a, w_b and w_c are parameters. BF_W is the BF model adjusted for RWC.

Modifications for impact of snow on irradiance

To account for the effect of snow on light transmission, we add a snow depth/*I* function that was parameterized in the field:

$$[BF_S] \qquad GPP = \frac{P_{max} I_s}{I_s + k} \qquad (9)$$

Where:

$$I_s = \begin{cases} I & ; \text{if S = 0 cm} \\ I \times \tau & ; \text{if 0 cm < S < 3 cm} \\ 0 & ; \text{if S > 3 cm} \end{cases} \qquad (10)$$

Where I_s is estimated irradiance under snow (μmol m^{-2} s^{-1} PPFD) (see below), I is incident radiation (μmol m^{-2} s^{-1} PPFD), τ is light transmission through the snow pack

(%) and *S* is snow depth (cm). The *BF* model with subscript S indicates that modelled GPP includes the effect of snow cover.

We did not have continuous direct observations of snow cover over the plots and albedo and snow depth measurements at a nearby eddy covariance station cannot account for the heterogeneous patterns of melt across the tundra landscape. We instead used measurements of air temperature at 3 cm (1 sensor located above 1 flux plot for each species) and 1.5 m above the surface (at met station ~ 50 m away) to estimate the presence or absence of snow over the plots for each species. For each day of the year (DOY) we assumed the temperature sensors at 3 cm were covered by snow, and the snow depth was therefore > 3 cm, if and only if: 1) the daily maximum air temperature at 1 m was > 0 °C, but the 3 cm maximum air temp was ≤ 0 °C), and 2) the amplitude of daily air temperature fluctuations were greater at 1 m than at 3 cm. Otherwise we assumed snow depth was < 3cm. After the final predicted snow day of each winter, we assumed all snow had melted from the plots once the minimum air temperature at 3 cm > 1 ºC. If snow depth > 3 cm the irradiance under snow was assumed to be 0. If snow depth was < 3 cm but > 0cm we estimated irradiance under snow to be 40 %, assuming 3 cm snow depth. The transmission of light though the snow over time varies continuously as snow melts and accumulates. The effect of these assumptions on modeled GPP are described later in a formal uncertainty analysis.

Parameterizing the BF, BF_W and BF_S models

We parameterised the BF model using laboratory flux data. For each sample we fitted a light response curve (equation 4) at each temperature (5, 12 and 20°C). We then fitted the Arrhenius temperature response curves to the P_{max} values at each temperature (equations 5 and 6). We estimated parameters E_a and E_d by assuming a GPP temperature optimum of 30 °C for each species following Longton (1988), who reported increasing *gross* photosynthesis up to 30 ºC for *Polytrichum alpinum* at Barrow; Harley (1989), who reported a temperature optimum for S*phagnum* in Alaskan tussock tundra of > 30 °C, & Skre and Oechel (1981), who reported a temperature optimum for *Sphagnum* of > 25 °C in interior Alaskan taiga. To ensure the fitted curve

had a defined optimum we included an assumed zero point for photosynthesis at 65 °C when fitting the Arrhenius function. T_{ref} was 5 °C and P_{Tref} was the measured P_{max} for each sample at the reference temperature.

To calculate the parameters w_a, w_b and w_c, which define the shape of the turf RWC-GPP response curve, we used fitted values of K to calculate P_{max} for each of the turfs when measured during the drying experiment (during this part of the experiment we measured GPP only at a constant PPFD of 630 μmol m^{-2} s^{-1}). We then normalised the resulting P_{max} - RWC response curves by the P_{max} for each turf, and fitted equation 8 for each sample. All curve-fitting was carried out using non-linear least-squares in Matlab 2009a.

We used the variability in fitted parameters to represent natural variability between bryophyte patches within the BF model. We generated normal distributions for parameters E_a, E_d, K, w_a, w_b and w_c using the mean and standard deviation (SD) of fitted parameters from laboratory data. To account for covariance between parameters we generated multivariate normal distributions based on the covariance matrices between the light and temperature response parameters (E_a, E_d, K and P_{Tref}) and between the parameters controlling the RWC response (w_a, w_b and w_c). We then ran the model 300 times using random combinations of parameters drawn from these distributions. Modelled GPP is presented as the median, 10^{th} and 90^{th} percentile confidence interval (CI) of the 300 model runs.

Modifications for seasonal changes in photosynthetic capacity

Initial analysis using the BF_W model configuration gave unrealistically high GPP in the spring (March – April) causing poor model fit (Table 2). We therefore included a further factor (D) to represent a linear seasonal development in photosynthetic capacity between spring and summer.

$$[BF_D] \qquad GPP = D \times \frac{P_{max} I}{I + k} \qquad (12)$$

With

$$D = \begin{cases} d & ; \text{if } 0 < DOY < DOY_{min} \\ \left(\frac{1-d}{DOY_{max} - DOY_{min}}\right)(DOY_{min} - DOY_{max}) + 1 & ; \text{if } DOY_{min} < DOY < DOY_{max} \\ 1 & ; \text{if } DOY_{max} < DOY < 365 \end{cases} \qquad (13)$$

Where DOY_{min} is the date of onset of the increase photosynthetic capacity (assumed to be the day after the last spring measurement, *DOY* 115) and DOY_{max} the date at which the maximum capacity is reached (assumed to be the day before the first summer measurement, DOY 172). We made a first approximation of the value of *d* by calculating the ratio between the average P_{max} (for light curves where the maximum ambient PPFD > 800 µmol m^{-2} s^{-1}) over the spring and summer measurement periods for each species (for *Polytrichum*, *d* was 0.14; for *Sphagnum*, *d* was 0.04). We assumed no decrease in photosynthetic capacity after the end of the summer season (Hicklenton & Oechel, 1977). The impact of the values of *d*, DOY_{min}, and DOY_{max}, and alternative forms for equation 13, examined in detail in the section 'Model Sensitivity'.

Vascular flux (PLI) model

We modelled vascular plant GPP using the GPP model of Shaver *et al.* (2007) (hereafter referred to as the 'photosynthesis - light - irradiance' model, or *PLI* model) to simulate vascular plant GPP for heath vegetation (dominated by *Empetrum hermaphroditum*) and dwarf birch (*Betula nana)* dominated vegetation. This model has been tested against eddy-covariance flux measurements in tundra ecosystems in early season (Rastetter *et al.*, 2010). The model is driven by two inputs, leaf area index (*LAI*) and irradiance (*I*):

$$GPP = \frac{P_{maxL}}{k} \times \ln\left(\frac{P_{maxL} + E_0 \times I}{P_{maxL} + E_0 \times I \times e^{-k \times LAI}}\right) \quad (14)$$

where P_{maxL} is the light-saturated photosynthetic rate per unit leaf area (µmol m^{-2} leaf s^{-1}), k is the Beer's law extinction coefficient (m^2 ground m^{-2} leaf), and E_0 is the initial slope of the light response curve (µmol C $µmol^{-1}$ photons). Model parameters for *Betula* and *Empetrum* dominated vegetation were taken from Table 7 of Shaver *et al.* (2007). We used the parameter standard deviations given in Table 7 of Shaver *et al.* (2007) to generate normal distributions of parameters and ran the model 300 times with random combination of these parameters to quantify model uncertainty.

For the 2008-2009 period we ran the vascular plant GPP model using a generalised seasonal time series of vascular LAI for both species. To account for uncertainty in the estimate of seasonal LAI development we synthesised data from 1) NDVI measurements in 2005 (Street *et al.*, 2007) 2) destructive LAI measurements in 2007 (Campioli *et al.*, 2009a) 3) NDVI measurements in 2007 (unpublished data, J. Gornall) 4) destructive LAI measurements in 2007 (unpublished data, B. Fletcher) 5) date of bud-burst in 2007 and 2009 (unpublished data, V. Sloan) 6) modelled LAI 2007, based on destructive and phenology data (unpublished data, B. Fletcher). All the above LAI data were obtained from with approximately 1km of our field site. We linearly interpolate between peak season LAI and end of season LAI, where we assume LAI = 0. For *Betula* we assume leaf abscission (i.e. LAI = 0) occurs between the 31st August,

when signs of senescence first become visible (pers. obs) and the third week of September (Karlsson, 1989). For *Empetrum* we assume the earliest date of zero effective LAI is the 31st August, and the maximum date is when the maximum daily temperature falls below 0°C (9th October in 2008). We derive an upper and lower envelope for the LAI time-course, based on the above data. We ran the GPP model for the upper and lower LAI estimates and the mean estimate, assuming the timing of LAI development is the same for the 2008-2009 simulation years.

Results

Field measurements

Environmental conditions

There was a linear relationship between the sensor VWC and mass-based VWC (Fig. 1a) and the slopes of the regression lines were significantly different than 1 for both *Polytrichum* (slope = 0.58 ± 0.07) and *Sphagnum* (slope = 0.64 ± 0.1). The sensor VWC vs. mass-based RWC calibration relationships differed significantly between the two species ($P < 0.001$) reflecting that *Sphagnum* held more water per unit volume of turf than *Polytrichum* (Fig. 1b).

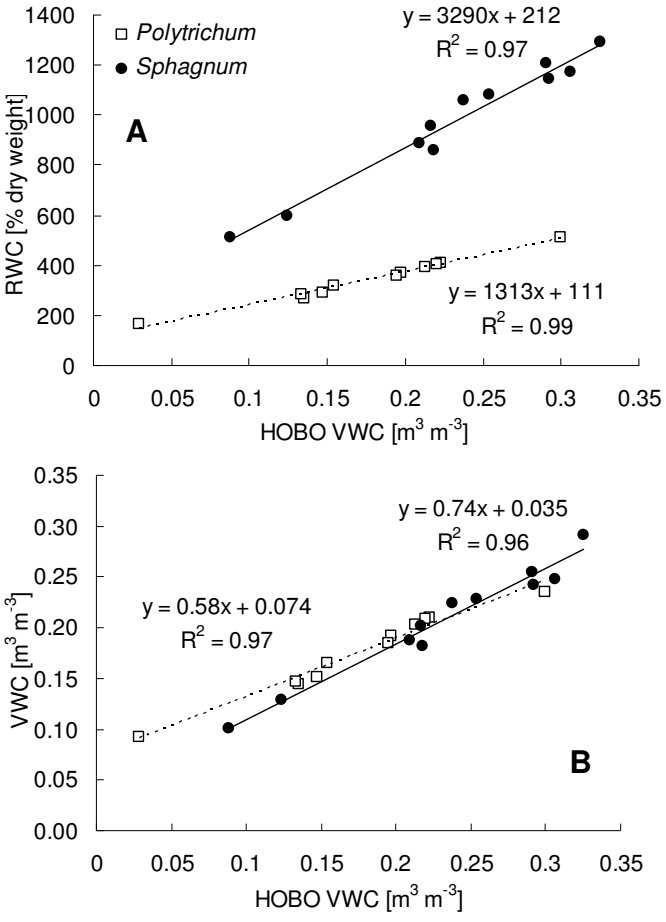

Figure 1. (overleaf) ECH_2O moisture probe calibrations for *Polytrichum* and *Sphagnum* bryophyte turfs for A) relative water content (RWC) by weight [%] b) volumetric water content (VWC) [m^3 m^{-3}].

Maximum and minimum predicted values of RWC *in-situ* during summer (June - August) 2008 were 203 % and 337 % for *Polytrichum*, and 616 and 1082 % for *Sphagnum* (Fig. 2). There was an increase in the water content of the bryophyte surface during the snow melt period; *Polytrichum* RWC exceeded 540 % in April 2008 and *Sphagnum* RWC exceeded 1300 % in April 2009 (Fig. 2).

The predicted number of days where snow depth > 3 cm for the *Polytrichum* logger site was 18 for March-May 2008 and 27 for March-May 2009 (Fig. 3). The predicted number of snow days for the *Sphagnum* logger site was 51 for March-May 2008 and 48 for March-May 2009. Snow depth observations in 2008 were consistent with the predicted patterns of snow cover; on 25th April 2008 no snow was observed at the *Polytrichum* logger site and 9 cm of snow was present at the *Sphagnum* logger site (Table 1). The first predicted snow day in 2008 was 29th October (DOY 302) and the predicted date of complete snow melt for *Polytrichum* and *Sphagnum* was 29th April (Fig. 3). The RWC of *Polytrichum* leaves during April was on average 256 %, with minimum of 114 % on 31st March (Table 1). Measured transmission of light through the snow pack was highly variable when snow pack depth was less than 5 cm. At 1 cm depth, transmission varied between 20 % and 80 % of incoming radiation (Fig. 4). Using an exponential regression ($R^2 = 0.64$), predicted transmission of light was 6 % at 10 cm depth and 42 % at 3 cm dept

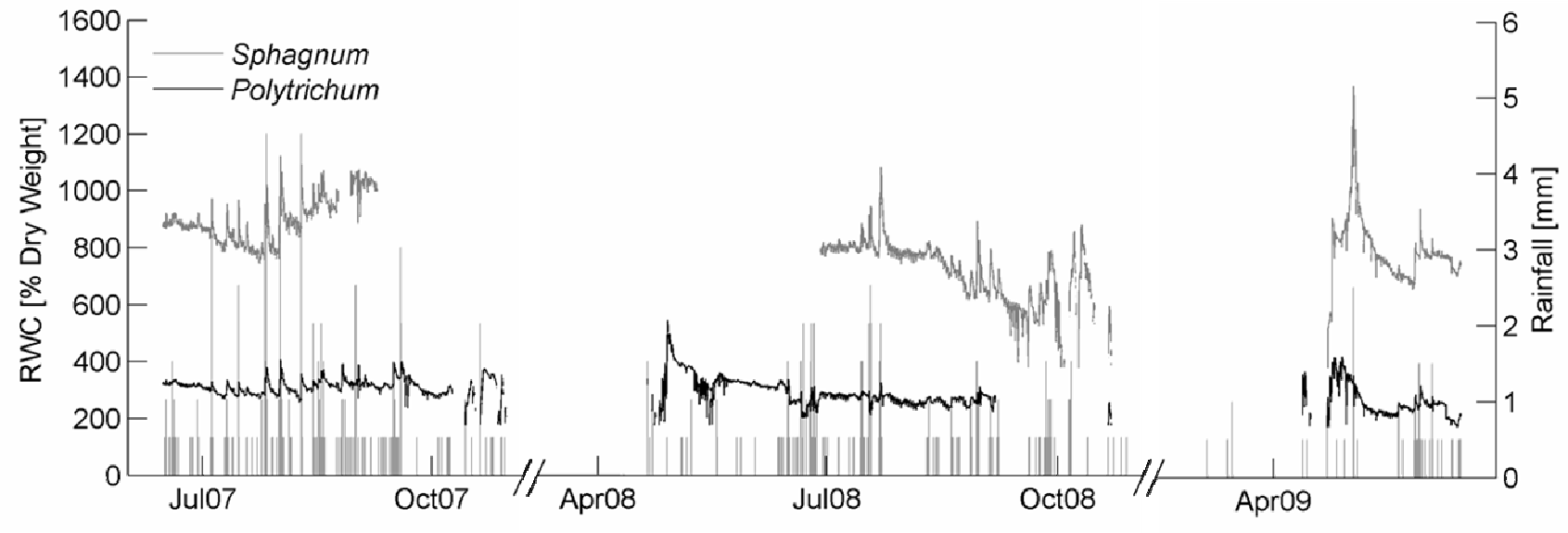

Figure 2. Relative water content (RWC) of the *Polytrichum* and *Sphagnum* bryophyte carpets measured at the Abisko, Sweden study site at 0-4 cm depth. Data gaps occur when bryophyte temperature is below freezing, and for *Sphagnum* in early summer 2008 due to datalogger malfunction.

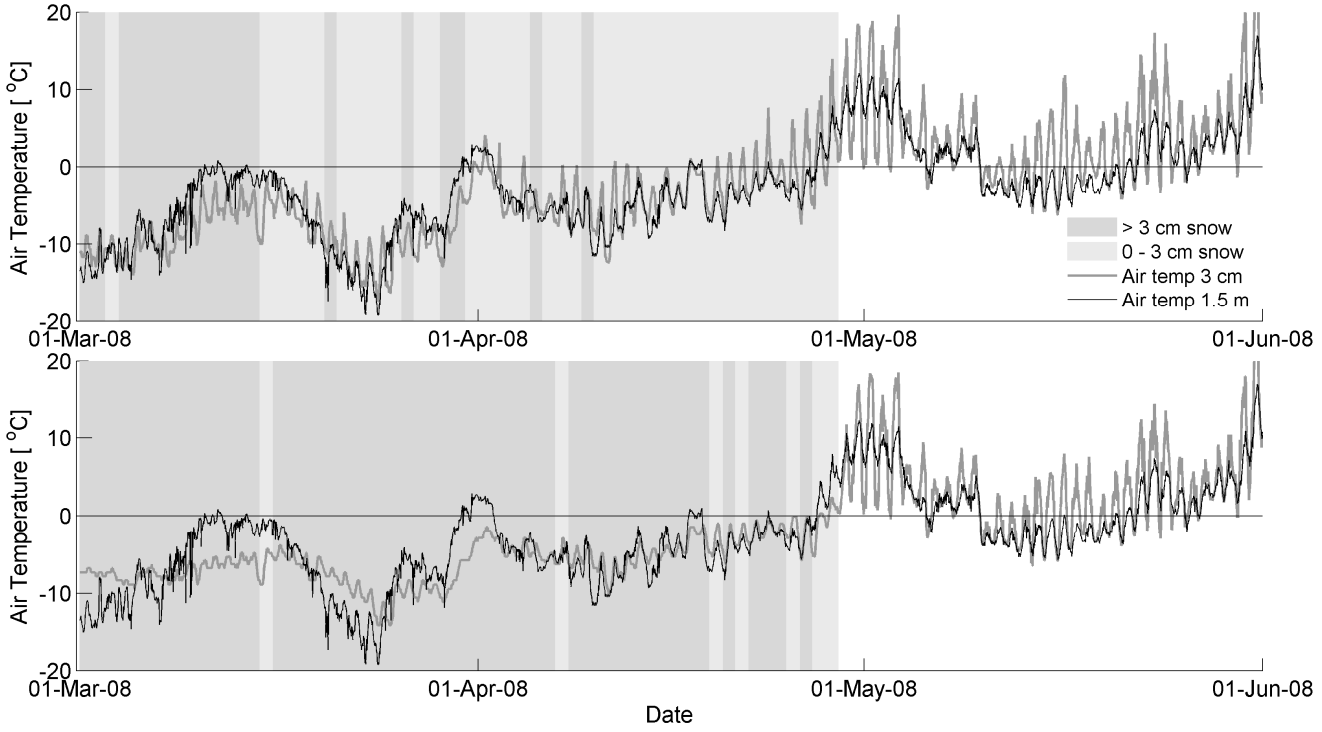

Figure 3. Abisko, Sweden bryophyte plot air temperature at 1.5 m and at 3 cm for March – May 2008 for A) *Polytrichum* and B) *Sphagnum* with predicted snow cover days shaded in grey.

Table 1. Plot descriptions with snow depths. Relative water content (RWC) of photosynthetic tissues given in parentheses. Abisko 2008

		Snow Depth (RWC)										
Plot	**Species**	**31Mar**	**02Apr**	**03Apr**	**10Apr**	**11Apr**	**12Apr**	**13Apr**	**15Apr**	**20Apr**	**22Apr**	**25Apr**
1	Sphagnum	10						0	2			0
2	Sphagnum		12		12					11		
*3	Sphagnum			9						9		9
4	Polytrichum	2.5 (114)						0 (226)	1 (218)	0 (333)		0.5(284)
*6	Polytrichum		0 (356)						1 (200)	0 (285)		0 (291)
7	Polytrichum		6.5		8							
27	Empetrum					0						
41	Emp. + Vac.						0					
47	Empetrum						0					
57	Empetrum										1	
58	Empetrum										0	

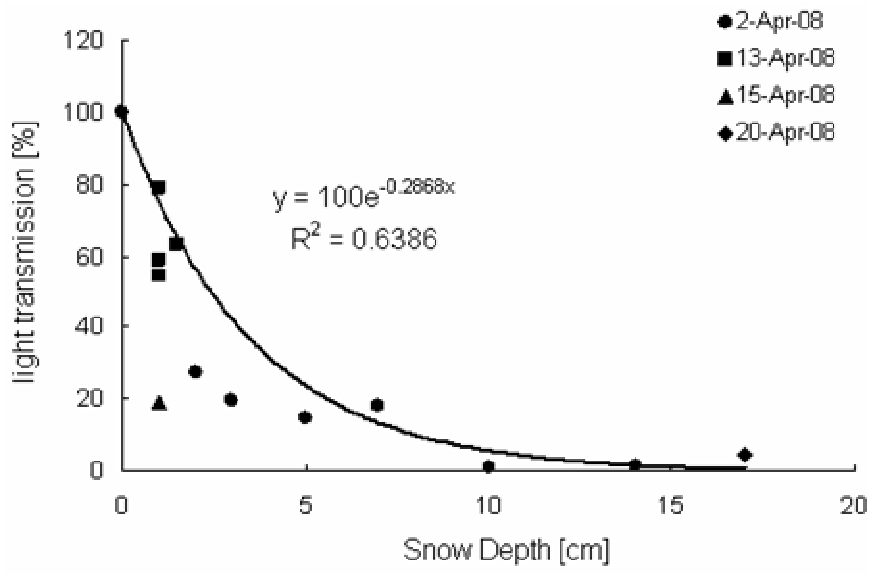

Figure 4. Light transmission through snow layers of different depths as a percentage of incident radiation

Field CO_2 fluxes

Typical values of *Polytrichum* GPP at ambient light levels were in excess of 4 μmol m^{-2} s^{-1} during June-August. *Sphagnum* GPP was generally lower with typical values between 1 and 3 μmol m^{-2} s^{-1} (Figs. 5a & 8a). Average light-saturated GPP (P_{max}) during June-August for *Polytrichum* (n = 3) was 6.5 ± 0.7 μmol m^{-2} s^{-1} and for *Sphagnum* 2.4 ± 0.3 μmol m^{-2} s^{-1} (n = 4). *Polytrichum* GPP in April at ambient light levels was up to 0.5 μmol m^{-2} s^{-1} (Figs. 5b & 8b), which corresponded to a net C uptake by the bryophyte surface of up to -0.3 μmol m^{-2} s^{-1} (Fig. 6a). *Sphagnum* GPP did not exceed 0.1 μmol m^{-2} s^{-1} in April (Fig. 6b). GPP for *Empetrum* during March-April was not significantly different from zero (– 0.01 ± 0.03 μmol m^{-2} s^{-1}, data not shown). The average variance of repeated ER measurements (usually three) for light curves measured in June-August indicated an average measurement error variance of 0.26 μmol m^{-2} s^{-1}. Measurements of ER in the spring season before, during and after the light response curve indicated that the chamber effect on ER over the course of the light curve was small (Fig. 6). During March-April the average error variance on repeated measurements of ER (usually between four and seven) for each light curve was 0.01 μmol m^{-2} s^{-1}.

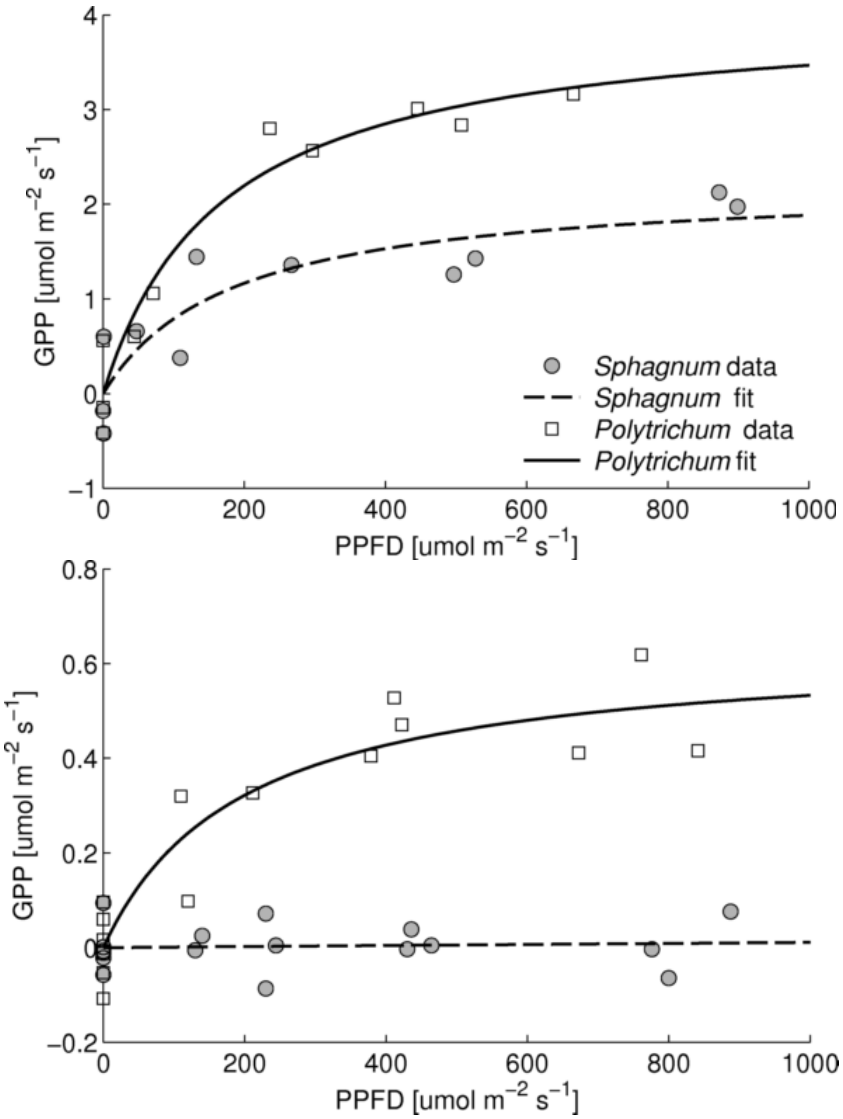

Figure 5. Light response curves for gross primary productivity (GPP) in *Polytrichum* and *Sphagnum* in Abisko, Sweden on A) 15th August 2007 and B) 25th April 2008. Note the difference in the y-axis scales.

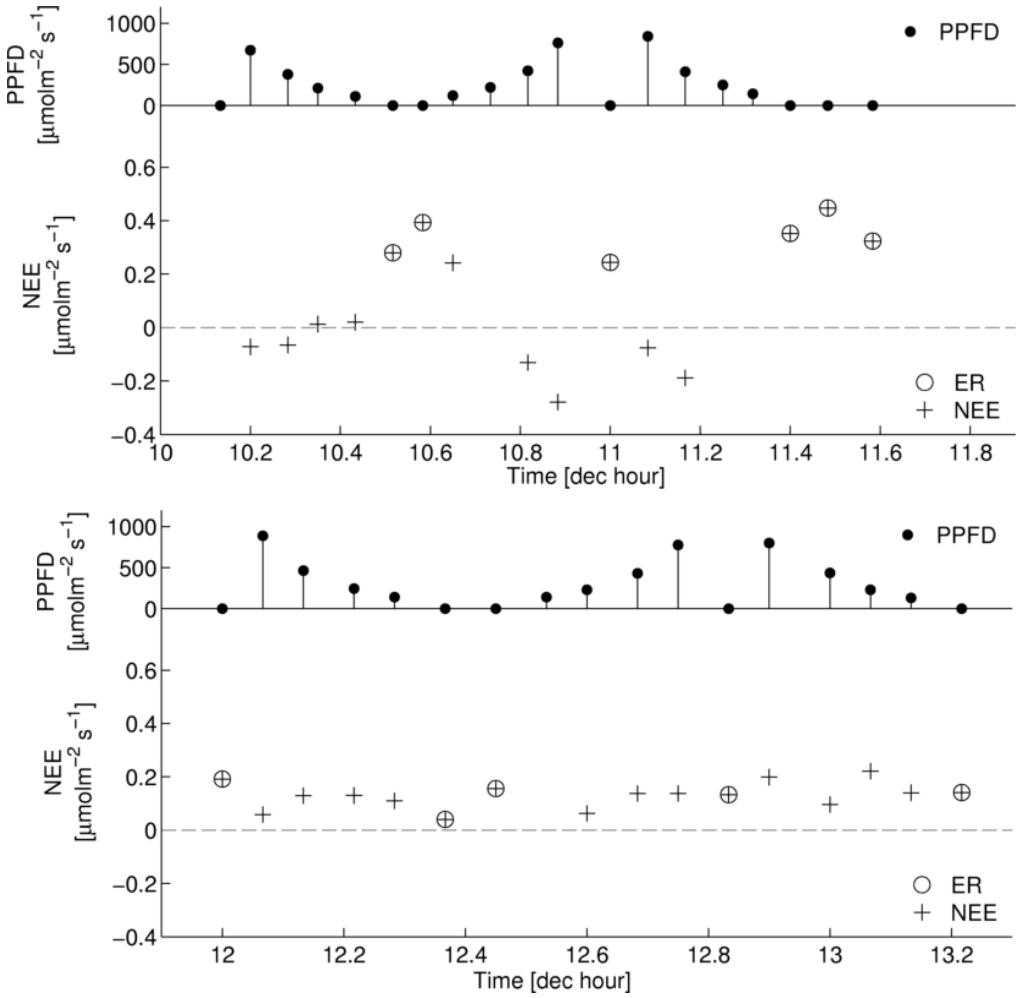

Figure 6. GPP light response curves plotted through time for example curves on A) *Sphagnum* and B) *Polytrichum* plots on 25th April 2008. Crosses with circles are respiration measurements.

Laboratory measurements

Differences in photosynthetic activity between *Polytrichum* and *Sphagnum* in the field were also apparent in the laboratory data; *Polytrichum* had higher rates of gross photosynthesis. P_{max} at 20 ºC for *Polytrichum* varied between 4.2 and 6.0 μmol m^{-2} s^{-1} and for *Sphagnum* between 1.0 and 3.2 μmol m^{-2} s^{-1} (Fig. 7a). The maximum and minimum fitted values of E_a and E_d for *Polytrichum* were 11 and 22 kJ mol^{-1} and 200 and 1302 kJ mol^{-1}. For *Sphagnum* E_a was between 23 and 40 kJ mol^{-1} and E_d between 175 and 1230 kJ mol^{-1}. The fitted optimum turf RWC for photosynthesis was between 181 % and 273 % for *Polytrichum* and 185 % and 701 % for *Sphagnum* (Fig. 7b). The mean turf RWC response curves for each species indicated that 90% photosynthetic capacity was reached when *Polytrichum* RWC was between 170 % and 320 % and *Sphagnum* RWC was between 390 % and 800 %. Average photosynthetic tissue (green 'leaf') biomass for the *Polytrichum* flux samples was 193 ± 10 g m^{-2}, capitulum biomass for *Sphagnum* was 211 ± 30 g m^{-2}.

Modelling

The Bryophyte Flux model

Initial analysis indicated that the BF_W model overestimated the magnitude of bryophyte GPP fluxes during spring. The inclusion of *D*, a factor representing seasonal development of photosynthetic capacity into the model BF_{DW}, increased the R^2 of model vs. measured fluxes for *Polytrichum* from 0.49 to 0.79 and for *Sphagnum* from 0.62 to 0.76 (Table 2). The predicted total GPP for March-May decreased by more than two-thirds for both species as a result of including *D*. Inclusion of the turf RWC adjustment factor, *W*, did not improve the fit of the model (Table 2) we therefore did not include the factor *W* in further analysis. The BF_D model configuration, which accounted for seasonal increases in photosynthetic capacity, but no turf RWC response, explained 81% of the variation in measured fluxes for *Polytrichum* and 81% for *Sphagnum*, with root mean square error (RMSE) of 1.0 and 0.49 μmol m^{-2} s^{-1} (Table 2 & Fig. 8.).

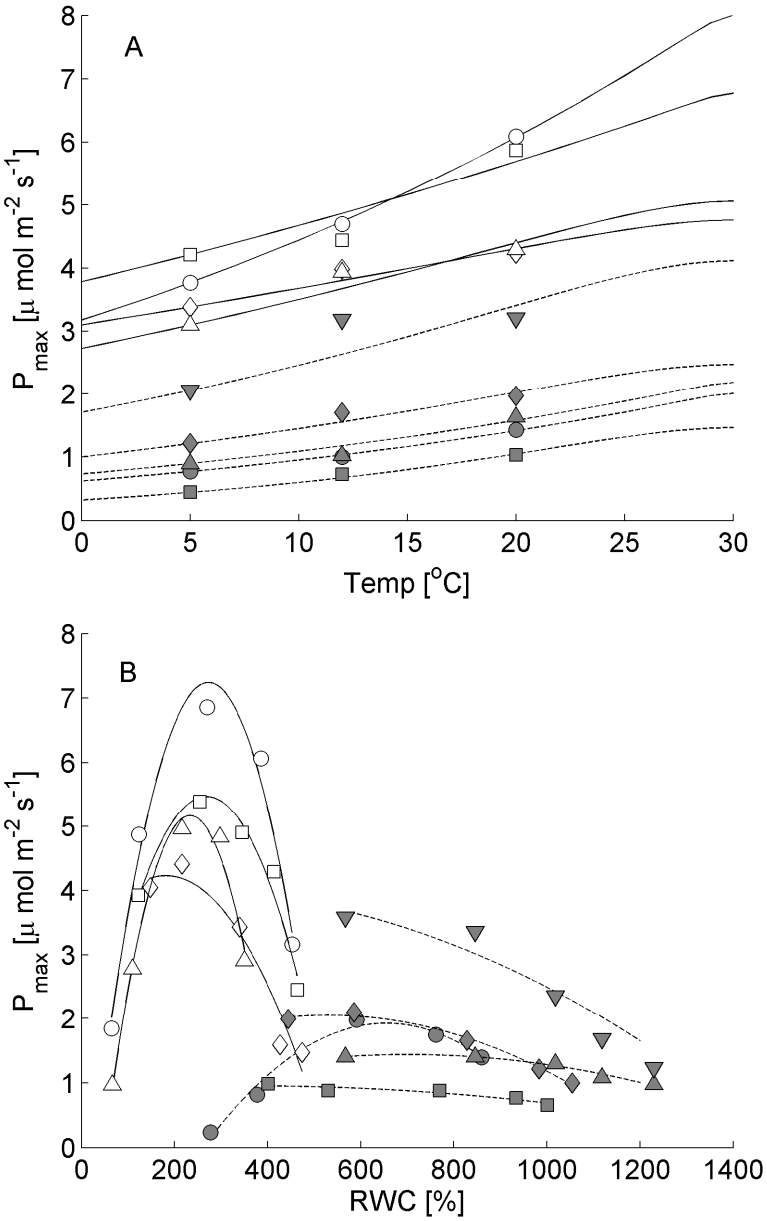

Figure 7. Fitted light-saturated photosynthesis (P_{max}) for laboratory measured *Sphagnum* and *Polytrichum* in response to A) temperature and B) relative water content (RWC). Different symbols indicate different sample turfs.

Table 2. Root mean squared error (RMSE) and r^2 for linear regression of model *vs*. measured gross primary productivity (GPP) for different configurations of the bryophyte flux (BF) model. Subscript D indicates a model includes a phenological response. Subscript W indicates a model that includes bryophyte water content response. Subscript S indicates a model that includes snow data with a light attenuation routine. For each configuration of the BF model, total GPP (g C m^{-2}) with 10^{th} and 90^{th} percentile confidence interval is given for the spring season (March – May), summer season (June – August) and autumn season (September – November) periods.

BF Model	Species	r^2	RMSE (umol m^{-2} s^{-1})	GPP (g C m^{-2}) Mar-May 08	GPP (g C m^{-2}) Jun-Aug 08	GPP (g C m^{-2}) Sep-Nov 08
BF_W	Po	0.49	2.0	131.2 (100.8, 162.6)	234.4 (191.2, 278.5)	83.5 (69.6, 98.6)
	Sp	0.62	0.76	41.0 (10.2, 74.2)	73.0 (22.3, 122.3)	24.2 (4.1, 43.5)
BF_{DW}	Po	0.79	1.1	40.0 (30.9, 49.4)	227.6 (189.5, 270.1)	84.1 (70.7, 97.9)
	Sp	0.76	0.63	9.9 (2.7, 17.0)	71.7 (21.3, 117.5)	25.7 (7.0, 44.3)
BF_D	Po	0.81	1.0	46.4 (39.0, 54.6)	238.0 (199.2, 281.8)	85.2 (71.3, 100.3)
	Sp	0.81	0.49	9.4 (2.2, 16.0)	72.9 (19.8, 118.8)	24.8 (5.9, 42.4)
BF_{DS}	Po	-	-	46.2 (39.1, 53.7)	235.3 (197.4, 281.3)	84.8 (71.6, 98.5)
	Sp	-	-	9.7 (2.4, 16.8)	75.7 (21.0, 121.5)	25.8 (6.3, 44.9)
PLI model				**GPP (g C m^{-2}) Mar-May 08**	**GPP (g C m^{-2}) Jun-Aug 08**	**GPP (g C m^{-2}) Sep-Nov 08**
Max LAI	Heath			91.5 (85.8, 97.2)	379.8 (344.5, 418.5)	55.0 (50.9, 59.4)
	Betula			11.9 (11.4, 12.5)	386.2 (338.9, 433.5)	37.1 (34.2, 40.1)
Mid LAI	Heath			28.9 (27.4, 30.6)	340.1 (309.2, 368.7)	21.8 (20.5, 23.1)
	Betula			6.3 (6.0, 6.5)	359.0 (328.3, 391.8)	45.8 (42.9, 49.1)
Min LAI	Heath			0 (0,0)	262.7 (244.9, 280.2)	0.14 (0.13, 0.14)
	Betula			0 (0,0)	295.1 (271.5, 319.1)	0.19 (0.18, 0.19)

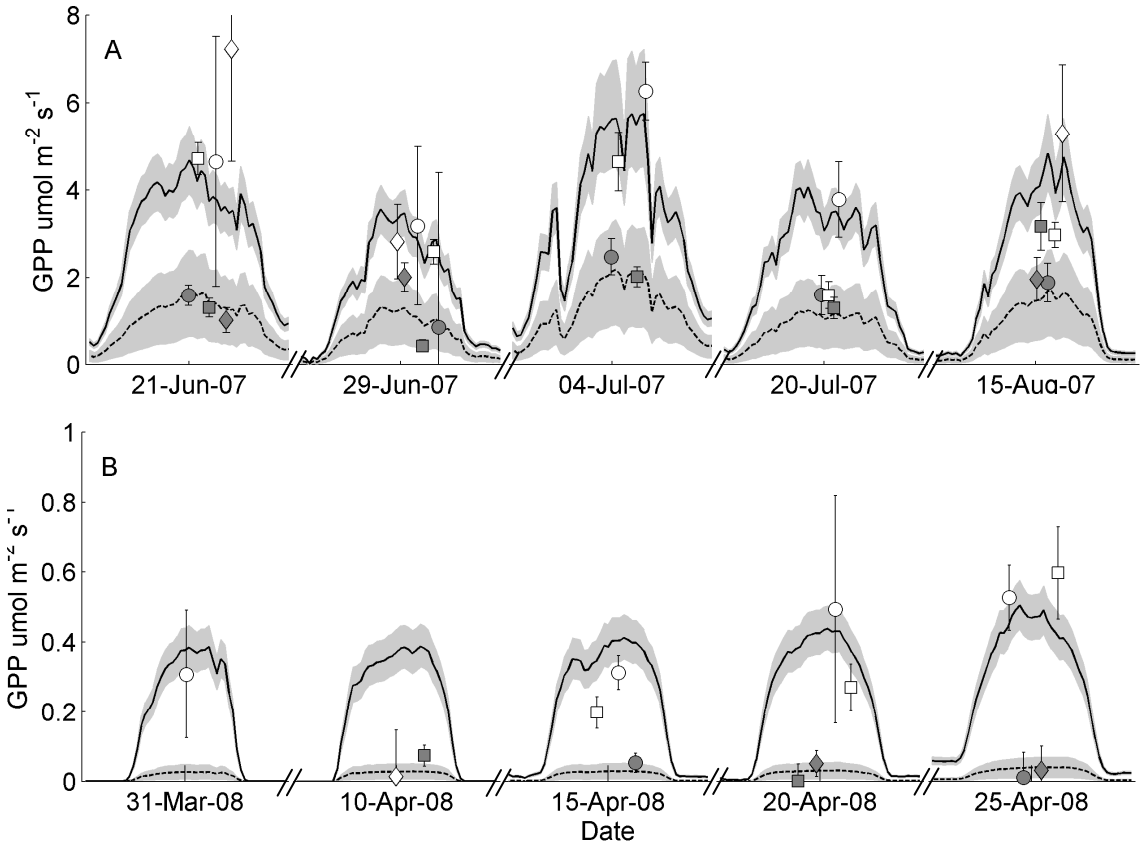

Figure 8. Modelled GPP and measured GPP (corrected for ambient light conditions) for a) June -August 2007 and b) March – April 2008. Open symbols and solid lines represent *Polytrichum*, grey symbols and dashed lines represent *Sphagnum*, and different shaped symbols indicate different plots. Errors bars are the 90% confidence interval for the GPP light response curve. Grey shaded areas show the 10th - 90th percentile of modelled GPP.

Including the effect of snow had no significant impact on the March – May, or September – November seasonal GPP totals (Table 2), assuming negligible light transmission at snow depths > 3cm, and 40 % light transmission at snow depths < 3 cm. The BF_{DS} model predicted total annual (summer plus shoulder seasons) photosynthetic carbon uptake for *Polytrichum* of 366 g C m^{-2} (10th – 90th percentile CI of 308 – 434 g C m^{-2}) and for *Sphagnum* 111 g C m^{-2} (10th – 90th percentile CI of 30 – 183 g C m^{-2}). Spring season (March – May) uptake of carbon by *Polytrichum* was 20 % of summer season (June – August) carbon uptake, and spring season C uptake by *Sphagnum* was 13 % of summer season uptake, assuming a linear increase in photosynthetic capacity between the end of April (DOY 115) and the 3rd week of June (DOY 172). Assuming no decline in photosynthetic capacity after the end of the summer season, total modelled GPP for September – November was 36 % of total summer season GPP for *Polytrichum* and 34 % for *Sphagnum* (Table 2).

The PLI model

Peak growing season LAI for *Betula* was between 1.5 (Street *et al.*, 2007) and 3.0 m^2 m^{-2} (Campioli, 2008). *Empetrum* peak season LAI was lower, between 1.25 (Street *et al.*, 2007) and 2.0 m^2 m^{-2} (ABACUS project, unpublished data) (Fig. 9). PLI predicts zero GPP when LAI is zero. The maximum LAI estimates gave a March-May GPP estimate of 11 g C m^{-2} for *Betula* and a 91 g C m^{-2} estimate for *Empetrum*. Growing season estimates of GPP for maximum and minimum LAI values were more constrained in a relative sense, ranging from 263 – 380 g C m^{-2} for *Empetrum* heath and 295 – 386 g C m^{-2} for *Betula* communities (Table 2). Using the mean estimates of LAI, total annual C uptake by *Betula* dominated communities was 411 g C m^{-2}, 2 % of which occurred during spring (March – May) and 11 % during autumn (September – November). Total annual C uptake by *Empetrum* dominated communities was 391 g C m^{-2}, 7 % of which occurred during spring (March – May) and 6 % during autumn (September – November, Table 2).

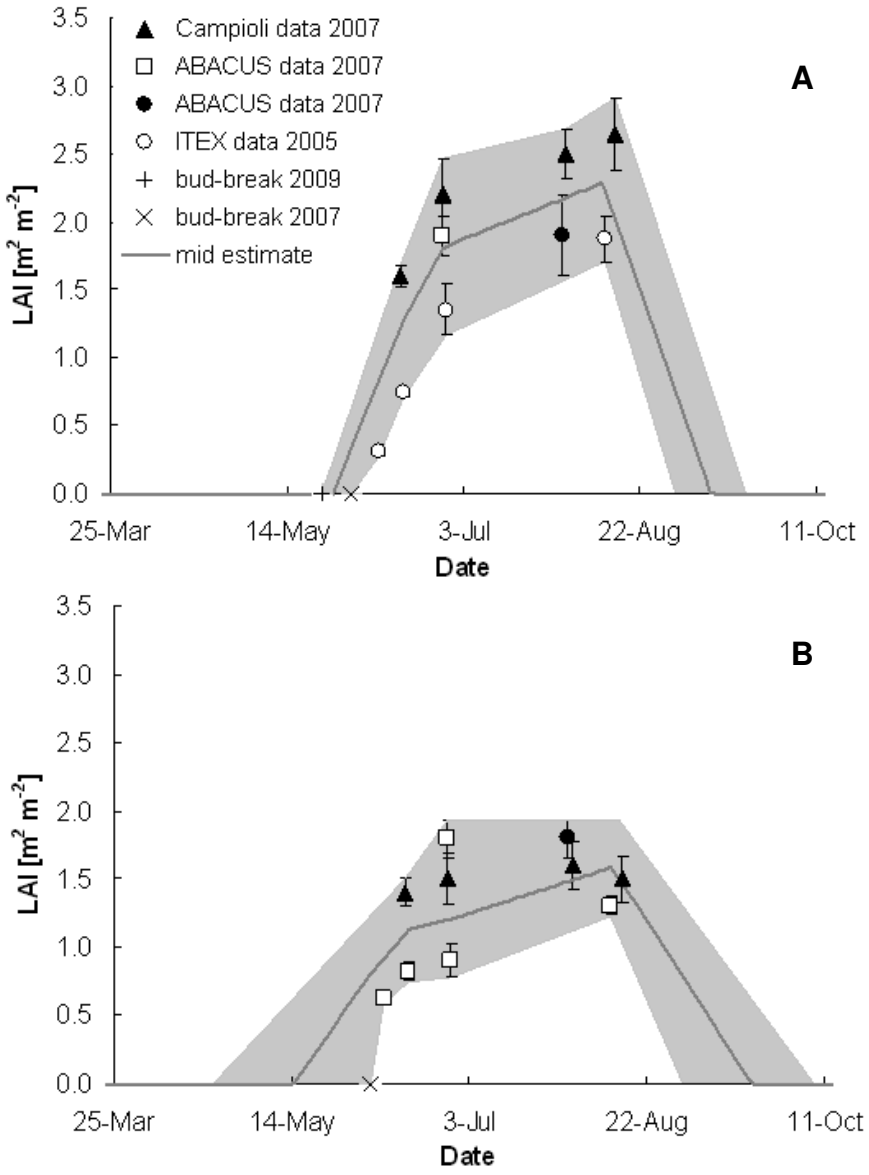

Figure 9. Leaf area index (LAI) estimates used as input to the PLI model for A) *Betula* and B) *Empetrum* heath dominated vegetation. The grey shaded area shows the estimated LAI 'envelope' based on maximum and minimum values from all available data sources. Closed symbols are based on destructive measurements of LAI, open symbols are based on indirect estimates of LAI from NDVI. Cross symbols show observed dates of bud-break.

Comparing bryophyte and vascular GPP

Again assuming that LAI development followed the mean estimate, total growing season *Polytrichum* GPP was ca. 90 % of that for shrub tundra vegetation and *Sphagnum* GPP was ca. 30 % of shrub vegetation (Tables 2 and Fig. 10). *Polytrichum* GPP in March-May was 160 % of the GPP estimate for *Empetrum* and 780 % for *Betula* (assuming again the mean estimate of LAI). *Sphagnum* GPP in March-May was 33 % of the GPP estimate for *Empetrum* and 150 % of that for *Betula* (Tables 2 and Fig. 10).

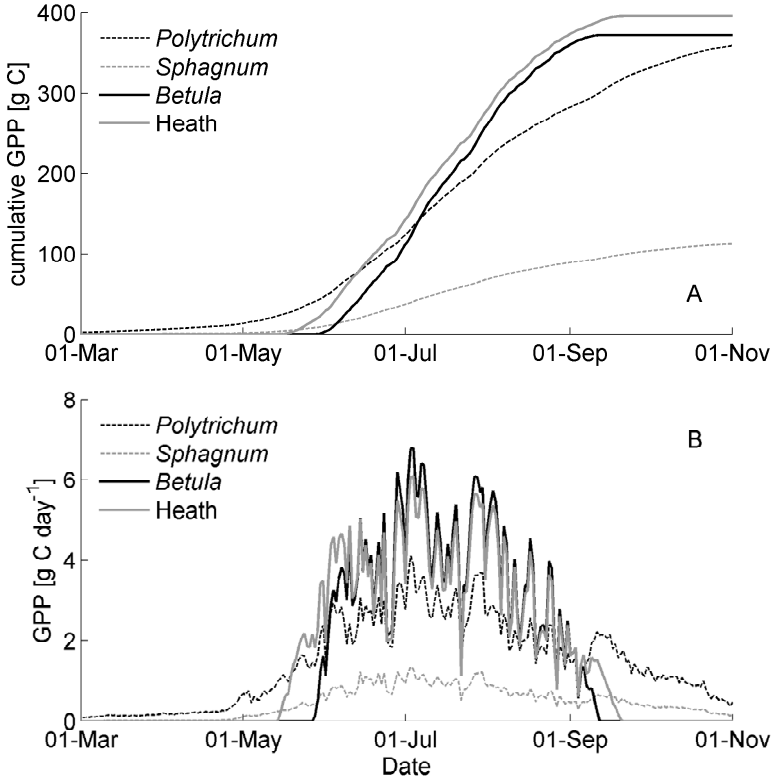

Figure 10. A) cumulative modelled gross primary productivity (GPP, g C m^{-2}) and B) daily GPP (g C m^{-2} day^{-1}) for *Polytrichum*, *Sphagnum*, *Betula* and heath vegetation for March – November 2008.

Bryophyte flux model sensitivity analysis

We explored the sensitivity of the model outputs to both changes in major model assumptions (Table 3), and to one-dimensional perturbations in model parameters (Table 4).

Model assumptions

1. Photosynthesis at low temperatures

We assumed that the Arrhenius temperature response was applicable below 5 °C despite a lack of laboratory data or literature information on nature or the response of photosynthesis to temperature at low temperatures. The Arrhenius fits however, predicted photosynthetic activity at temperatures below literature values for the minimum temperature of physiological activity for *Polytrichum* and *Sphagnum*. We tested this model assumption by setting photosynthesis to zero below the minimum values of -7.5 °C for *Polytrichum* (Longton, 1988) and -1 °C for *Sphagnum* (Gaberščik & Martinčič, 1987). The effect of this model assumption on total spring GPP was negligible (< 3g C m^{-2}) (Table 3).

2. The time-course of development of photosynthetic capacity

We assumed a linear increase in photosynthetic capacity between the end of the spring (March-May) measurement period and the beginning of the summer (June – August) measurement period. We test two alternative scenarios meant to represent end-members: 1) full photosynthetic capacity is reached 3 days after snow melt (BF_{DS_early}) and 2) full photosynthetic capacity is reached 3 days before the first summer measurement (BF_{DS_late}). These scenarios significantly effect the spring (March – May) GPP totals: the early scenario lead to an approximate doubling of the total GPP for both species; the late scenario resulted in spring totals for *Polytrichum* of 20 g C m^{-2} and for *Sphagnum* of 1.6 g C m^{-2} (Table 3).

3. Light transmission through snow

We assumed that either 3 cm (40 % light transmission), > 3cm (negligable light transmission) or 0 cm snow (100 % transmission) covered the bryophyte surface, based on air temperature measurements at the location of the flux plots. We tested the impact of this assumption by increasing the light transmission through > 3 cm

snow to 20 %, and transmission through < 3 cm to 100%. The effect on modelled total spring GPP was negligible (< 1g C m^{-2})(Table 3).

Model parameters

We carried out a one-dimensional sensitivity analysis on the parameters of the BF_{DS} model by increasing or decreasing each parameter by 50 % while keeping the other parameters constant (Table 4). The model was most sensitive to changing values of P_{Tref}. A 50 % increase or decrease in P_{Tref} lead to a 50 % increase or decrease in modelled seasonal GPP and RMSE. Model RMSE also increased with an increase in E_a, though the seasonal sums of GPP were only slightly affected, with summer GPP changing by < 10 %. The model was relatively insensitive to changes in E_d or K (Table 4).

Table 3. Test of BF model assumptions. Subscript D indicates that the model includes a phenological response and subscript S indicates that the model includes snow data with a light attenuation routine. For each configuration of the BF model, total GPP (g C m^{-2}) with 10^{th} and 90^{th} percentile confidence interval is given for the spring season (March – May 2008 & 2009), summer season (June – August 2008) and autumn season (September – November) periods.

BF Model	Description	Species	GPP (g C m^{-2}) Mar-May 08	GPP (g C m^{-2}) Jun-Aug 08	GPP (g C m^{-2}) Sep-Nov 08
BF_{DS}	BF_{DS} model without change	Po	46.2 (39.1, 53.7)	235.3 (197.4, 281.3)	84.8 (71.6, 98.5)
		Sp	9.7 (2.4, 16.8)	75.7 (21.0, 121.5)	25.8 (6.3, 44.9)
BF_{DS_zero}	Photosynthesis set to zero below -7.5 °C (*Po*) and -1 °C (*Sp*)	Po	44.1 (37.6, 50.9)	238.1 (199.4, 279.2)	83.8 (71.1, 96.8)
		Sp	8.9 (2.4, 15.5)	75.0 (22.5, 124.8)	20.8 (5.7, 36.4)
BF_{DS_early}	Maximum photosynthetic capacity reached instantaneously 3 days after snow melt	Po	82.6 (70.7, 95.6)	242.3 (202.4, 285.1)	84.7 (72.2, 98.3)
		Sp	21.7 (6.6, 36.1)	78.4 (27.1, 123.3)	26.0 (7.8, 43.6)
BF_{DS_late}	Maximum photosynthetic capacity reached instantaneously 3 days before first summer measurement	Po	20.7 (17.4, 24.4)	201.1 (168.8, 237.3)	83.5 (70.2, 98.0)
		Sp	1.6 (0.4, 2.9)	63.5 (18.2, 101.5)	25.7 (6.4, 44.0)
BF_{DS_trans}	Transmission through > 3cm snow increased to 20 %, through < 3cm snow increased to 100 %.	Po	45.8 (38.9, 53.2)	233.5 (197.6, 275.9)	83.9 (71.3, 97.6)
		Sp	10.2 (3.1, 16.8)	78.7 (27.9, 124.1)	27.0 (8.1, 44.5)

Table 4. Sensitivity analysis for the Polytrichum and Sphagnum parameterisations of the bryophyte flux with seasonality and snow (BFDS) model. Each row gives the root mean square error (RMSE) and r2 for the linear regression of modeled vs. measured gross primary productivity (GPP), and the total GPP (mol C m-2) for the pre-summer season (March – May 2008 & 2009), the summer season (June – August 2008) and the post-summer season (September – October). Numbers in bold are for the average (nominal) parameter set (in brackets after the parameter symbol). Single parameters are increased or decreased by 50 % while all other parameters are held at the nominal value.

Parameter	**value**	**r^2**	**RMSE (umol m^{-2} s^{-1})**	**GPP (g C m^{-2}) Mar-May 08**	**GPP (g C m^{-2}) Jun-Aug 08**	**GPP (g C m^{-2}) Sept -Nov 08**
Polytrichum (nominal)		0.81	1.03	44.3	218.2	81.8
E_a (1.6×10^4)	2.3×10^4	0.79	1.04	43.7	235.9	80.7
	7.8×10^3	0.81	1.18	45.3	202.4	83.3
E_d (7.5×10^5)	1.1×10^6	0.81	1.03	44.3	218.2	81.8
	3.7×10^5	0.81	1.03	44.3	218.2	81.8
K (107)	161	0.81	1.10	39.8	195.3	67.7
	54	0.80	1.01	51.2	252.8	108.9
P_{Tref} (3.6)	5.4	0.81	1.48	66.5	327.3	122.7
	1.8	0.81	1.95	22.2	109.1	40.9
Sphagnum (nominal)		0.81	0.45	12.8	78.6	25.5
E_a (2.8×10^4)	4.2×10^4	0.78	0.49	12.1	90.4	24.0
	1.4×10^4	0.81	0.59	13.8	68.8	27.4
E_d (6.0×10^5)	9.0×10^5	0.81	0.45	12.8	78.6	25.5
	3.0×10^5	0.81	0.45	12.8	78.5	25.5
K (77)	115	0.81	0.47	11.7	71.7	21.4
	38	0.81	0.43	14.5	88.7	33.3
P_{Tref} (1.1)	1.6	0.81	0.60	19.2	117.8	38.3
	0.5	0.81	0.85	6.4	39.3	12.8

Discussion

Magnitude of bryophyte GPP

Our results indicate that bryophytes can contribute substantially to Arctic land surface photosynthetic C fluxes. Total annual GPP for *Polytrichum* was ca. 90 % of the modelled GPP for a deciduous shrub with a peak season LAI over 2 m^2 m^{-2}, which is towards the upper limit of the range of LAI values found in the tundra ecosystems of Abisko (Spadavecchia *et al.*, 2008). High rates of productivity per unit ground area for *Polytrichum*, observed in our laboratory and *in-situ* measurements, were consistent with previous studies on excised shoots in which net assimilation was up to 7.5 g CO_2 g^{-1} dry weight for *Polytrichum* species (Oechel & Collins, 1976; Penny & Bayfield, 1982). *Sphagnum fuscum* had lower rates of photosynthesis than *Polytrichum*, but total GPP was still 30 % of GPP model estimates for shrub vegetation. The early onset of photosynthetic activity in bryophytes, and delayed senescence in autumn, contributed to large GPP sums in comparison to vascular plants during shoulder seasons. Our results are comparable with studies in northern spruce forests which show that bryophytes can account for 10 - 50 % of whole-forest gross CO_2 uptake (Goulden & Crill, 1997) and can exceed forest over-story NPP in some cases (Frolking *et al.*, 1996).

Polytrichum piliferum occurs on ridge-tops, often with little or no snow cover at our Abisko, Sweden site which is characterised by high winds. *Polytrichum* patches are often the first to emerge during snowmelt at this site (pers. obs.). *Polytrichum* was able to photosynthesise almost immediately after snow had been removed from the flux plots, and patches which were snow free during measurement periods were found to be photosynthetically active. Where *Polytrichum* patches are present, photosynthetic C uptake can occur and lead to net carbon gain by the ecosystem, *before* the snowmelt occurs across the wider landscape. *Polytrichum* GPP flux rates of up to 0.6 μmol m^{-2} m^{-1} during April exceeded the rates of GPP observed for evergreen shrubs after snow removal in spring (up to 0.26 μmol m^{-2} m^{-1}, Starr & Oberbauer (2003)). *Sphagnum* was also able to photosynthesise after snow removal, but rates of GPP were much lower (< 0.1 μmol m^{-2} m^{-1}). *Sphagnum* retains large

amounts of water within capillary spaces between the stems, and the surface was often frozen beneath the snow. This presumably restricted diffusion of CO_2 into and out of tissues and may explain low photosynthetic rates. The *Sphagnum* plots were less frequently without snow cover during April; this species grows in less well-drained areas of the landscape which are less exposed to wind scouring in areas where snow tends to accumulate.

Controls over bryophyte CO_2 flux

We were unable to replicate the magnitude of spring CO_2 fluxes for *Polytrichum* without including an increase in photosynthetic capacity between April and June; spring fluxes were over-estimated if photosynthetic activity was assumed to be equivalent to that of samples collected in late August even after taking into account the direct effect of temperature. In late June, however, the model was able to correctly predict the magnitude of *Polytrichum* GPP. This was contrary to our expectation of no strong seasonal signal in bryophyte GPP. The increase in photosynthetic activity during May and June could be the result of either: 1) increases in the biomass of photosynthetic tissues per m^2 ground through new growth; 2) increased photosynthetic capacity due to increased allocation of resources to the photosynthetic apparatus (Williams & Flanagan, 1998); or 3) shifts in the temperature optimum of P_{max} (Oechel, 1976; Sveinbjornsson & Oechel, 1983), which we assumed to be constant throughout the season. Depression of photosynthetic rates in spring was not due to low leaf water content (mean tissue RWC was 260 %), despite the bryophyte turf being frozen below leaf level.

Contrary to the initial hypothesis, including the water content of the bryophyte turf did not improve the explanatory power of the model. Drying of the surface was not observed during the relatively wet growing seasons; the longest period without at least 0.5 mm of precipitation during the June-August 2007 was 4 days. Both *Polytrichum* and *Sphagnum* also have physiological adaptations to avoid drought conditions. Bryophytes of the genus *Polytrichum* are able to transport water from the substrate via internal conducting tissues, have some cuticular resistance to water loss, and can appress leaves against the stem when turgor is lost (Thomas *et al.*, 1996). *Sphagnum fuscum* is able to hold large amounts of water within tissues due to its

dense growth form and the presence of hyaline cells, and has a broad optimum for photosynthesis allowing survival on hummocks which are elevated above the water table and more exposed to dry conditions (Rydin & McDonald, 1985). During the two-year measurement period neither species experienced *in-situ* turf water contents that were lower than the range over which P_{max} was 90 % of the optimum value measured in the laboratory. Turf water contents exceeded the upper limit of this range for both species, but any limiting effect on the modelled seasonal totals for GPP was minor. The combination of environmental conditions and physiological adaptations meant that including bryophyte turf water content did not increase the explanatory power of the model during the period studied.

BF model sensitivity

We identified the extent of light transmission though snow, the response of moss photosynthesis to temperature below freezing, and the time-course of seasonal development of photosynthetic capacity as the major uncertainties in our model formulation. Exploration of the sensitivity of the model to these assumptions indicated that total GPP was most sensitive to the timing of changes in photosynthetic capacity between spring and summer. It is difficult to separate the effects of inadequate representation of the temperature response below freezing (or potential shifts in the temperature optimum for photosynthesis), from the effect of increases in photosynthetic capacity. The *Polytrichum* plots however became visually greener between spring and summer supporting our conclusion that photosynthetic capacity increased. These results suggest that future research should focus on phenological and physiological mechanisms underlying GPP seasonality in *Polytrichum*.

The parameters to which the model results were most sensitive were P_{Tref}, which controls the magnitude of photosynthetic activity, and E_a, which controls the shape of the P_{max} temperature response below the optimum temperature. Insensitivity of the model to E_d was unsurprising as this parameter controls the shape of the curve above the optimum temperature for photosynthesis and such temperatures were infrequently experienced in the field. The physiological activity of the bryophyte tissue will also be affected by freeze/thaw cycles (Kennedy, 1993), likewise not included in the

model. Including this effect would suppress photosynthetic uptake following periods of extreme cold, but we note that seasonal GPP sums were insensitive to model assumptions in the early season. While we take into account the presence of snow, we did not include the effects of elevated CO_2 concentrations below the snow pack (Sommerkorn, 2000) which could act to increase rates of bryophyte photosynthesis.

Seasonality of vascular GPP

The size of the LAI envelope created from multiple data sources is a reflection of both inter-annual variability in the timing and extent of canopy development and spatial heterogeneity in LAI for the two species. The early and late season LAI for *Betula* was well-constrained by estimated dates of leaf bud-burst and leaf-fall, but there was large uncertainty in the LAI for *Empetrum* before and after the summer growing season. We treated LAI for the evergreen *Empetrum* as 'effective' LAI, which we assumed was zero until the end of April. We did not observe GPP before this date using our chamber system, though this is contrary to the findings of other studies (Starr & Oberbauer, 2003). Lack of measurable GPP may have been due to the exposed nature of the site; the snow cover was < 1 cm over the *Empetrum* heath patches we measured, perhaps exposing the plants to very low temperatures compared to the Starr and Oberbauer (2003) results. Our latest date for the onset of *Empetrum* LAI development was set as the date of current year's leaf bud-break (5th June in 2009, V. Pope pers. com.), but previous year's leaves will have been photosynthetically active before this date (Street *et al.*, 2007). Differences in seasonal GPP estimates for the maximum and minimum seasonal LAI estimates exceeded variability in the model output due to parameter uncertainty reported by Shaver *et. al.* (2007).

The contribution of bryophytes to C exchange of Arctic landscapes

Quantification of the total contribution of these bryophyte species to landscape-scale fluxes requires an estimate of abundance over the landscape and knowledge of landscape-level meteorology. Whereas *Polytrichum* is a highly productive species, its abundance as a fraction of the land surface is probably small, though potentially significant in exposed areas with low cover of vascular plants. The cover of *Sphagnum* as a proportion of ground area in tundra ecosystems is more significant,

being frequently found in poorly drained areas. Other bryophyte species also contribute significantly to ground cover in these ecosystems. We would expect therefore, even though generally photosynthetic rates in other species will be somewhat less than in *Polytrichum* (Longton, 1988) the bryophyte layer makes a large contribution to CO_2 fluxes, especially in spring.

Our study implies that models of C dynamics in Arctic vegetation must include a bryophyte component if such models are intended to predict the effects of shortening or lengthening growing season, or changes in vegetation composition, on the Arctic C balance. We suggest that the expected loss of bryophytes from Arctic vegetation as climate warms, may result in a significant decrease in early season ecosystem carbon gain.

Acknowledgements

We would like to thank Katie Walker and Rachel Turton for their help with spring fieldwork, and ANS for the provision of meteorological data and the invaluable support from their staff. We also thank Jonathan Evans at Centre for Ecology and Hydrology, Wallingford, UK for providing access to field equipment. This work was supported by NERC PhD studentship to L. Street and the NERC funded ABACUS project.

References

Arndal, M.F., Illeris, L., Michelsen, A., Albert, K., Tamstorf, M., & Hansen, B.U. (2009) Seasonal Variation in Gross Ecosystem Production, Plant Biomass, and Carbon and Nitrogen Pools in Five High Arctic Vegetation Types. *Arctic Antarctic And Alpine Research*, **41**, 164-173.

Campioli, M. (2008) Carbon allocation in ecosystems: an experimental and modelling approach for tundra and forest vegetations, Universiteit Gent, Gent.

Campioli, M., Michelsen, A., Samson, R., & Lemeur, R. (2009a) Seasonal variability of leaf area index and foliar nitrogen in contrasting dry-mesic tundras. *Botany-Botanique*, **87**, 431-442.

Campioli, M., Samson, R., Michelsen, A., Jonasson, S., Baxter, R., & Lemeur, R. (2009b) Nonvascular contribution to ecosystem NPP in a subarctic heath during early and late growing season. *Plant Ecology*, **202**, 41-53.

Chapin, F.S., Shaver, G.R., Giblin, A.E., Nadelhoffer, K.J., & Laundre, J.A. (1995) Responses Of Arctic Tundra To Experimental And Observed Changes In Climate. *Ecology*, **76**, 694-711.

Christensen, J.H., Hewitson, B., Busuioc, A., Chen, A., Gao, X., Held, I., Jones, R., Kolli, R.K., Kwon, W.-T., Laprise, R., Rueda, V.M., Mearns, L., Menéndez, C.G., Räisänen, J., Rinke, A., Sarr, A., & Whetton, P. (2007). Regional Climate Projections. In *Climate Change 2007: The Physical Science Basis. Contribution of Working Group I to the Fourth Assessment Report of the Intergovernmental Panel on Climate Change* (eds S. Solomon, D. Qin, M. Manning, Z. Chen, M. Marquis, K.B. Averyt, M. Tignor & H.L. Miller). Cambridge University Press, Cambridge, United Kingdom and New York, USA.

Cornelissen, J.H.C., Lang, S.I., Soudzilovskaia, N.A., & During, H.J. (2007) Comparative cryptogam ecology: A review of bryophyte and lichen traits that drive biogeochemistry. *Annals of Botany*, **99**, 987-1001.

Douma, J., van Wijk, M.T., Lang, S.I., & Shaver, G.R. (2007) The contribution of mosses to the carbon and water exchange of arctic ecosystems: quantification and relationships with system properties. *Plant, Cell and Environment*, **30**, 1205-1215.

Frolking, S., Goulden, M.L., Wofsy, S.C., Fan, S.M., Sutton, D.J., Munger, J.W., Bazzaz, A.M., Daube, B.C., Crill, P.M., Aber, J.D., Band, L.E., Wang, X., Savage, K., Moore, T., & Harriss, R.C. (1996) Modelling temporal variability in the carbon balance of a spruce/moss boreal forest. *Global Change Biology*, **2**, 343-366.

Gaberščik, A. & Martinčič, A. (1987) Seasonal Dynamics of Net Photosynthesis and Productivity of *Sphagnum Papillosum*. *Lindbergia*, **13**, 105-110.

Goulden, M.L. & Crill, P.M. (1997) Automated measurements of CO2 exchange at the moss surface of a black spruce forest. *Tree Physiology*, **17**, 537-542.

Grogan, P. & Jonasson, S. (2006) Ecosystem CO_2 production during winter in a Swedish subarctic region: the relative importance of climate and vegetation type. *Global Change Biology*, **12**, 1479-1495.

Harley, P.C., Tenhunen, J.D., Murray, K.J., & Beyers, J. (1989) Irradiance and Temperature Effects on Photosynthesis of Tussock Tundra Sphagnum Mosses from the Foothills of the Philip Smith Mountains, Alaska. *Oecologia*, **79**, 251-259.

Hicklenton, P.R. & Oechel, W.C. (1977) Influence of Light-Intensity and Temperature on Field Carbon-Dioxide Exchange of Dicranum-Fuscescens in Subarctic. *Arctic And Alpine Research*, **9**, 407-419.

Hooper, D.U., Cardon, Z.G., Chapin, F.S., III, & Durant, M. (2002) Corrected calculations for soil and ecosystem measurements of CO_2 flux using the LI-COR 6200 portable photosynthesis system. *Oecologia*, **132**, 1-11.

Huemmrich, K.F., Gamon, J.A., Tweedie, C.E., Oberbauer, S.F., Kinoshita, G., Houston, S., Kuchy, A., Hollister, R.D., Kwon, H., Mano, M., Harazono, Y., Webber, P.J., & Oechel, W.C. (2010) Remote sensing of tundra gross ecosystem productivity and light use efficiency under varying temperature and moisture conditions. *Remote Sensing of Environment*, **114**, 481-489.

Karlsson, P.S. (1989) Insitu Photosynthetic Performance of 4 Coexisting Dwarf Shrubs in Relation to Light in a Subarctic Woodland. *Functional Ecology*, **3**, 481-487.

Kennedy, A.D. (1993) Photosynthetic Response of the Antarctic Moss Polytrichum-Alpestre Hoppe to Low-Temperatures and Freeze-Thaw Stress. *Polar Biology*, **13**, 271-279.

Longton, R.E. (1988) *Biology of Polar Bryophytes and Lichens* Cambridge University Press, Cambridge.

McBean, G., Alekseev, G., Chen, D., Førland, E., Fyfe, J., Groisman, P.Y., King, R., Melling, H., Vose, R., & Whitfield, P.H. (2005). Arctic climate: past and present. In *Arctic Climate Impact Assessment: Scientific Report*, pp. 21–60. Cambridge University Press, Cambridge, UK.

Miller, P.C., Oechel, W.C., Stoner, W.A., & Sveinbjornsson, B. (1976) Simulation of CO_2 Uptake and Water Relations of Four Arctic Bryophytes at Point Barrow, Alaska. *Photosynthetica*, **12**, 7-20.

Miller, P.C., Webber, P.J., Oechel, W.C., & Tieszen, L.L. (1980). Biophysical Processes and Primary Production In *An Arctic Ecosystem: the Coastal Tundra at Barrow, Alaska.* (eds J.M. Brown, P.C. Miller, L.L. Tieszen & F.L. Bunnell), pp. 66-101. Dowden, Hutchinson & Ross, Inc., Stroudsburg, PA.

Murray, K.J., Harley, P.C., Beyers, J., Walz, H., & Tenhunen, J.D. (1989) Water-Content Effects on Photosynthetic Response of Sphagnum Mosses from the Foothills of the Philip Smith Mountains, Alaska. *Oecologia*, **79**, 244-250.

Oechel, W.C. (1976) Seasonal Patterns of Temperature Response of CO_2 Flux and Acclimation in Arctic Mosses Growing i*n Situ*. *Photosynthetica*, **10**, 447-456.

Oechel, W.C. & Collins, N.J. (1976) Comparative CO_2 Exchange Patterns in Mosses from 2 Tundra Habitats at Barrow, Alaska. *Canadian Journal of Botany-Revue Canadienne De Botanique*, **54**, 1355-1369.

Penny, M.G. & Bayfield, N.G. (1982) Photosynthesis in Desiccated Shoots of Polytrichum. *New Phytologist*, **91**, 637-645.

Proctor, M.C.F. (2000) The bryophyte paradox: tolerance of desiccation, evasion of drought. *Plant Ecology*, **151**, 41-49.

Rastetter, E.B., Williams, M., Griffin, K.L., Kwiatkowski, B.L., Tomasky, G., Potosnak, M.J., Stoy, P.C., Shaver, G.R., Stieglitz, M., Hobbie, J.E., & Kling, G.W. (2010) Processing arctic eddy-flux data using a simple carbon-exchange model embedded in the ensemble Kalman filter. *Ecological Applications*, **20**, 1285-1301.

Rydin, H. & McDonald, A.J.S. (1985) Tolerance of Sphagnum to Water Level. *Journal of Bryology*, **13**, 571-578.

Schuur, E.A.G., Vogel, J.G., Crummer, K.G., Lee, H., Sickman, J.O., & Osterkamp, T.E. (2009) The effect of permafrost thaw on old carbon release and net carbon exchange from tundra. *Nature*, **459**, 556-559.

Shaver, G.R., Street, L.E., Rastetter, E.B., Van Wijk, M.T., & Williams, M. (2007) Functional convergence in regulation of net CO2 flux in heterogeneous tundra landscapes in Alaska and Sweden. *Journal of Ecology*, **95**, 802-817.

Skre, O. & Oechel, W.C. (1981) Moss Functioning in Different Taiga Ecosystems in Interior Alaska .1. Seasonal, Phenotypic, and Drought Effects on Photosynthesis and Response Patterns. *Oecologia*, **48**, 50-59.

Sommerkorn, M. (2000) The ability of lichens to benefit from natural CO_2 enrichment under a spring snow-cover: a study with two arctic-alpine species from contrasting habitats. *Bibliotheca Lichenologica*, **75**, 365-380.

Sommerkorn, M., Bolter, M., & Kappen, L. (1999) Carbon dioxide fluxes of soils and mosses in wet tundra of Taimyr Peninsula, Siberia: controlling factors and contribution to net system fluxes. *Polar Research*, **18**, 253-260.

Spadavecchia, L., Williams, M., Bell, R., Stoy, P.C., Huntley, B., & van Wijk, M.T. (2008) Topographic controls on the leaf area index and plant functional type of a tundra ecosystem. *Journal of Ecology*, **96**, 1238-1251.

Starr, G. & Oberbauer, S.F. (2003) Photosynthesis of arctic evergreens under snow: Implications for tundra ecosystem carbon balance. *Ecology*, **84**, 1415-1420.

Street, L.E., Shaver, G.R., Williams, M., & Van Wijk, M.T. (2007) What is the relationship between changes in canopy leaf area and changes in photosynthetic CO2 flux in arctic ecosystems? *Journal of Ecology*, **95**, 139-150.

Sveinbjornsson, B. & Oechel, W.C. (1983) The Effect of Temperature Preconditioning on the Temperature Sensitivity of Net Co2 Flux in Geographically Diverse Populations of the Moss Polytrichum-Commune. *Ecology*, **64**, 1100-1108.

Tarnocai, C., Canadell, J.G., Schuur, E.A.G., Kuhry, P., Mazhitova, G., & Zimov, S. (2009) Soil organic carbon pools in the northern circumpolar permafrost region. *Global Biogeochemical Cycles*, **23**.

Thomas, R.J., Ryder, S.H., Gardner, M.I., Sheetz, J.P., & Nichipor, S.D. (1996) Photosynthetic function of leaf lamellae in Polytrichum commune. *Bryologist*, **99**, 6-11.

Uchida, M., Kishimoto, A., Muraoka, H., Nakatsubo, T., Kanda, H., & Koizumi, H. (2010) Seasonal shift in factors controlling net ecosystem production in a high Arctic terrestrial ecosystem. *Journal of Plant Research*, **123**, 79-85.

Wania, R., Ross, I., & Prentice, I.C. (2009a) Integrating peatlands and permafrost into a dynamic global vegetation model: 1. Evaluation and sensitivity of physical land surface processes. *Global Biogeochemical Cycles*, **23**.

Wania, R., Ross, I., & Prentice, I.C. (2009b) Integrating peatlands and permafrost into a dynamic global vegetation model: 2. Evaluation and sensitivity of vegetation and carbon cycle processes. *Global Biogeochemical Cycles*, **23**.

Warren, C.R. & Dreyer, E. (2006) Temperature response of photosynthesis and internal conductance to CO2: results from two independent approaches. *Journal of Experimental Botany*, **57**, 3057-3067.

Williams, M., Street, L.E., van Wijk, M.T., & Shaver, G.R. (2006) Identifying Differences in Carbon Exchange among Arctic Ecosystem Types. *Ecosystems*, **9**, 288-304.

Williams, T.G. & Flanagan, L.B. (1998) Measuring and modelling environmental influences on photosynthetic gas exchange in Sphagnum and Pleurozium. *Plant Cell And Environment*, **21**, 555-564.

4a. The fate of assimilated carbon in Arctic vegetation: the importance of non-vascular plants

Lorna E. Street [1], Jens-Arne Subke[2,3], Martin Sommerkorn[4], V. Sloan[5], H. Ducrotoy[6], G. K. Phoenix[5], MathewWilliams[1]

[1]School of Geosciences, University of Edinburgh, Edinburgh, EH9 3JN, UK

[2]Stockholm Environment Institute York, Environment Department, University of York, York, YO10 5DD, UK

[3]School of Biological and Environmental Sciences, University of Stirling, Stirling, FK9 4LA, UK

[4]Macaulay Land Use Research Institute, Craigiebuckler, Aberdeen, AB15 8QH, UK

[5]Department of Animal and Plant Sciences, The University of Sheffield, Sheffield, ST10 2TN, UK

[6]Institute of Geography and Earth Sciences, Aberystwyth University, Aberystwyth, UK

(intended for submission to Arctic, Antarctic and Alpine Research)

Abstract

Mosses contribute substantially to plant biomass at high latitudes, but their impact on ecosystem carbon use efficiency (CUE) and the allocation of fixed carbon within ecosystems is largely unknown. We use a ^{13}C pulse-labelling experiment to quantify the C turnover in pure stands of *Sphagnum* and *Pleurozium*, and in a mixed dwarf shrub community with a continuous *Pleurozium* understory. CUE in *Sphagnum* was 68 – 71% and in *Pleurozium* was between 62 – 81 % of gross photosynthesis (P). We show that C turnover in *Pleurozium* is dependant on tissue moisture content, indicated by an increase in the respiratory return of $^{13}CO_2$ linked to rainfall events after several days of dry weather. When present as an understory in dwarf shrub vegetation *Pleurozium* contributed to 25 % ± 14 % of gross primary productivity (GPP) during the labelling period and ca. 34 % of label retention 19 days after labelling. We find that in the community studied, the presence of a moss understory increased community CUE from 49 % to 58 % and reduces the percentage of GPP allocated to net primary productivity (NPP) belowground from 27 % to 10 %. Our results highlight the importance of including mosses in C models for realistic representation of C turnover in vegetation at high latitudes.

Introduction

There is growing evidence that climate change is driving shifts in the productivity and composition of Arctic vegetation. Remotely sensed data indicate a 'greening' of the land-surface (Myneni *et al.*, 1997; Verbyla, 2008) and ground-based observations suggest that the range of tundra shrubs is expanding (Forbes *et al.*, 2010; Tape *et al.*, 2006). Increases in plant growth have been attributed to rising air temperatures leading to earlier snow melt and a lengthening of the growing season (Groendahl *et al.*, 2007), as well as greater availability of nutrients due to accelerated decomposition and deepening of the active layer. Enhanced plant productivity may partially offset increases in respiratory CO_2 flux which may result from warmer soils and melting permafrost (Schuur *et al.*, 2009). Terrestrial Arctic C stocks are large (1600 Pg in permafrost soils (Tarnocai *et al.*, 2009) and 60-70 Pg in vegetation including boreal forests within the permafrost region (McGuire *et al.*, 2009)) so loss

of carbon from the terrestrial biosphere to the atmosphere, either as CO_2 or CH_4, could represent an important accelerating feedback on climate warming. Modelling studies indicate that the Arctic has been a slight sink for CO_2 over the last 25 years (McGuire *et al.*, 2000); the future C balance of the Arctic will be determined by how much long-term C storage results from the greening trend.

Despite low species diversity in comparison to other biomes (Gaston, 2000), Arctic vegetation is characterised by high spatial heterogeneity in plant functional type (PFT) (Chapin *et al.*, 1996). Evergreen shrubs, deciduous shrubs, sedges, grasses or forbs can be locally dominant over scales of under a metre (Spadavecchia *et al.*, 2008). Non-vascular plants (bryophytes and lichens) also contribute significantly to Arctic plant biomass and have important roles in biogeochemical cycling, producing recalcitrant litter (Cornelissen *et al.*, 2007a) and regulating the hydrologic and thermal regimes of soils (Beringer *et al.*, 2001; Gornall *et al.*, 2007). Shifts in species abundance may therefore be accompanied by pronounced changes in ecosystem function as one PFT is replaced by another (Wookey *et al.*, 2009); for example altering surface energy balance through albedo and surface roughness (Chapin *et al.*, 2000) as well as modifying trace gas fluxes (Johansson *et al.*, 2006) and decomposition rates (Cornelissen *et al.*, 2007b). Changes in the composition of vegetation arise from differential responses to changes in the environment at the species level (Bret-Harte *et al.*, 2001) and general patterns from climate manipulation experiments suggest that deciduous shrubs and grasses are most responsive to elevated temperatures (Dormann & Woodin, 2002). Bryophytes are generally expected to respond negatively to climate warming (van Wijk *et al.*, 2004; Walker *et al.*, 2006; Wookey *et al.*, 2009) though in High Arctic ecosystems bryophyte biomass has increased with warming (Hudson & Henry, 2010).

A key difficulty in interpreting patterns of vegetation change in terms of terrestrial C balance is determining how gross photosynthetic C uptake relates to C storage. This equates to quantifying 1) the fraction of photosynthesised C (or GPP, gross primary productivity) used for growth versus that re-released to the atmosphere through autotrophic respiration (the carbon use efficiency, or CUE) 2) the partitioning of photosynthesised C between plant pools, and 3) the longevity of those

pools. It has often been assumed, largely based on the work of Waring *et. al.* (1998) and Gifford (1994, 2003), that the percentage of GPP used for growth, is well-constrained at around 50 %. While the 50 % figure may represent a central tendency, large differences in CUE have been reported between ecosystems (Zhang *et al.*, 2009) or forest types (DeLucia *et al.*, 2007), species (Albrizio & Steduto, 2003) and stages of plant development (Van Iersel, 2003). Controls over the partitioning of C between plant pools, particularly the fluxes of C to aboveground versus belowground biomass, remain a critical uncertainty in global C models (Chapin *et al.*, 2009; Litton & Giardina, 2008). Constant fractions are often assumed in coupled-climate models (Ise *et al.*, 2010) even though observations suggest that C partitioning varies with forest type, stand age and resource supply (Gower *et al.*, 2001; Litton *et al.*, 2007).

Recent work suggests that C allocation in mosses can be highly variable. In a high Arctic study Woodin *et al.* (2009) find 70 % retention of a ^{13}C tracer in photosynthetic tissues after 4 - 6 weeks in *Calliergon richardsonii*, due to high rates of allocation to recalcitrant pools. By contrast only 20 % of recently assimilated C in *Polytrichum piliferum*, a highly productive species, is retained in aboveground tissues; 80 % is respired or translocated Street *et al.* (2011) [Chapter 5].

Rates of tissue turnover and respiratory C demand for growth and maintenance differ between plant tissue types; large respiratory costs are associated with metabolically active tissues which turnover rapidly (e.g. inflorescences) (McCutchan & Monson, 2001). Tissues which contain large amounts of structural material, such as wood, turnover more slowly and demand less energy for maintenance respiration (Ryan *et al.*, 1995). Differences in CUE between forest types have been attributed to differences in foliar biomass relative to stem biomass (Cannell & Thornley, 2000; DeLucia *et al.*, 2007). Mosses have very little non-photosynthetic supportive tissue in comparison to vascular plants; it follows that whole plant respiratory demand may be more strongly coupled to the respiratory demand of photosynthetic tissues, which we hypothesise will be a greater proportion of fixed C for tissues with higher metabolic and photosynthetic activity.

The objective of this study is to determine the fate of assimilated carbon in Arctic vegetation, and assess the effect of bryophytes on ecosystem CUE and belowground

C fluxes. We use a ^{13}C pulse-labelling experiment to follow the fate of ^{13}C in *Pleurozium* and *Sphagnum* species, and a mixed vascular heath community with a *Pleurozium* understory. We measure the ^{13}C content of respired CO_2 over 19 days, and the ^{13}C content of plant tissues for up to 1 year. Specifically we ask: 1) what fraction of GPP is accounted for by the moss understory in heath vegetation? 2) what fractions of moss GPP and vascular plant GPP are respired autotrophically? and 3) once incorporated, how much C remains in mosses vs. vascular plants after 1 year? We hypothesise that mosses account for a small but significant amount of gross C uptake and we expect that the fraction of recently fixed C respired in mosses is positively related to the time integrated photosynthetic rate over several days. We expect that longer term turnover of C in non-vascular plants is intermediate between that of evergreen shrub species (which have long lived woody stems) and herbaceous vascular species (which turnover all leaf and stem tissues annually).

Methods

Site description

Our field site was located approximately 50 km south of Kevo, in northern Finland (69° 29′ N, 27° 14′ E). The site lies in the sub-Arctic forest-tundra zone just north of the permanent pine forest tree line at an elevation of about 250 m. Mean annual temperature at Kevo is -2 °C (-16 °C in January, and 13°C in July) (The Kevo Research Station website: http://www.kevo.utu.fi/en/location/). Our plots were situated within 50 m of each other in an area typical of the transition between wetland and birch forest, the two dominant land cover types in the region. The vegetation was characterised by dwarf shrubs such as *Betula nana, Empetrum nigrum* and *Vaccinium vitis-idaea* and feather mosses growing on top of raised hummocks, with wetter *Sphagnum* dominated patches in between.

Overview of experimental set-up

We pulse-labelled four replicate plots of three types with $^{13}CO_2$: 1) *Sphagnum* sect. *Acutifolia* with vascular plant canopy removed (*Sp 1-4*) 2) *Pleurozium schreberi* with vascular plant canopy removed (*Pl 1-4*) and 3) *P. schreberi* with an intact vascular canopy of *Empetrum nigrum*, *Vaccinium vitis-idaea* and *Rubus*

chamaemorus (V 1-4). We measured the ^{13}C content of ecosystem respiration (ER) over 19 days, and used these values to model the $^{13}CO_2$ respiratory flux using ER-temperature response curves, based on chamber measurements of ER on the same plots. We also sampled moss and vascular plant tissues for ^{13}C content over time, and compared the loss of ^{13}C from tissues against the total modelled $^{13}CO_2$ respiratory flux. We used independent measurements of moss GPP on extracted turfs of *Pleurozium* and *Sphagnum* to model cumulative GPP through time for each species, and compared average daily moss GPP and moss CUE to previously published values.

^{13}C pulse-labelling

12 plots in total (3 vegetation types with 4 replicates) were pulse-labelled with 98 atom% $^{13}CO_2$ at 370 ppm from 1300hrs to 1800hrs local time (GMT +2) on 7th July 1008. Labelling followed the methods of Street *et al.* (2011); one half of the 0.55 m × 0.55 m clear acrylic chamber was darkened in order to quantify the non-biological back-diffusion of ^{13}C from the surface (Subke *et al.*, 2009). 24 hours prior to labelling we inserted 20 cm diameter '^{13}C return collars' to a depth of 15 cm on the 'dark' and 'light' side of the labelled plots; these collars were then used to collect samples of respired CO_2 for ^{13}C analysis. We did not insert the collars in plots *V1-4* to avoid severing roots and stems growing into the plot, instead we sealed the collars to the surface using plumber's putty. Prior to labelling, all plots were watered to ensure mosses were hydrated. The *Pleurozium* (*Pl 1-4*) hoods were also removed for approximately 10 seconds, at the mid-point of the labelling period in order to apply further water.

Measurements

Environmental conditions

Environmental conditions for nearby patches of *Pleurozium* and *Sphagnum* were monitored from June 2008 to August 2009. Moss temperature was measured at 2 cm depth below the surface using thermocouples connected to CR1000 data loggers (Campbell Scientific, Logan, USA). Surface wetness was measured using HOBO leaf wetness sensors and recorded every 5 minutes using HOBO Micro-Station data

loggers (Onset Inc, Massachusetts, USA). Precipitation and photosynthetic photon flux density (PPFD) were measured at a nearby meteorological station (about 200 m from the labelled plots) as part of the ABACUS project (http://www.abacus-ipy.org/).

Ecosystem respiration

We measured ER fluxes on the 'light' and 'dark' treatment ^{13}C return collars using a LI-COR 8100 Soil CO_2 flux system (LI-COR, Nebraska , USA) on 6 occasions between the 6th and 10th July. Most measurements were made between 1300hrs and 1700hrs; measurements on the 10th were also made at 0700hrs. The temperature range over which the respiration measurements were taken was 6 – 22 °C.

^{13}C content of ecosystem respiration

We measured the atom% of ER fluxes from the isotope return collars at discrete time intervals of 0 (immediately after labelling), 0.3, 0.5, 1, 1.5, 2, 3, 4, 6, 10,11, 19, 42 days after labelling (shortened to L + 0, L + 0.3 etc.) Measurements on day 10 included only half of the replicates as a lightening storm interrupted sampling. For measurements, collars were closed using PVC lids of identical diameter to the collars installed in plots. These were secured and sealed with 4 cm wide rubber seals. An 18 ml gas sample was taken through a septum in the seal immediately after closing the chambers, and a further two samples 30 minutes after chamber closure. Each gas sample was immediately injected into an evacuated glass Exetainer (Labco Ltd, High Wycombe, UK), for storage and subsequent analysis. Within 1 month of collection, all gas samples were returned to the University of York (UK) for total CO_2 concentration and $\delta^{13}C$ determinations using a continuous-flow isotope ratio mass spectrometry (CF-IRMS; SIRAS Series2, Micromass, UK, Pro-Vac Services, Crewe, UK).

Isotope Calculations

All calculations to derive isotopic mixing ratios were based on absolute isotopic concentrations of $^{12}CO_2$ and $^{13}CO_2$ in gas samples, as determined by mass spectrometry. Mixing ratios are expressed as atom% ^{13}C, i.e.

$$^{13}C = \frac{[^{13}C]}{[^{13}C]+[^{12}C]} \times 100 \quad (1)$$

where ^{13}C is the isotopic fraction of ^{13}C in CO_2 expressed as atom%, $[^{13}C]$ and $[^{12}C]$ are the absolute concentration of $^{13}CO_2$ and $^{12}CO_2$ (respectively) in gas samples. The concentrations of soil-derived CO_2 in the isotope flux chambers 30 min after lid closure were calculated as:

$$[C_{resp}] = [C_{sample}] - [C_{air}] \quad (2)$$

where $[C_{resp}]$, is the CO_2 concentration derived from soil and vegetation derived respiration, $[C_{sample}]$ is the CO_2 concentration of samples obtained after 30 minutes of chamber closure, and $[C_{air}]$ is the CO_2 concentrations of samples taken immediately after closing chambers, assumed to represent ambient atmospheric CO_2 conditions.

The ^{13}C:^{12}C isotopic mixing ratio of respiration-derived CO_2 ($^{13}C_{resp}$) was then calculated using a two-source mixing model:

$$^{13}C_{resp} = \frac{([C_{sample}] \times {}^{13}C_{sample}) - ([C_{air}] \times {}^{13}C_{air})}{[C_{resp}]} \quad (3)$$

where $^{13}C_{resp}$ and $^{13}C_{air}$ are the $^{13}C/^{12}C$ isotopic mixing ratios in CO_2 of soil-derived gas and ambient air respectively.

^{13}C content of moss and vascular plant tissues

We sampled moss tissues on days L + 0, 0.5, 1, 2, 3, 4, 6, 10, 19, 42 and 407 (L + 0 was 7th July 2008, L + 407 was 18th August 2009). At each sampling for *Sphagnum* we removed several stems and separated the capitula (cap.) from the next 1 cm of stem, or sub-capitula (sub-cap.). For *Pleurozium* (in plots *Pl 1 – 4* and *V 1 – 4*) we separated the tip of the frond which included current year's (CY) growth (which was

approx. the top 2cm) from the previous year's (PY) growth (the next 2 – 4cm), though the previous year's growth will have included small amounts of new growth (Benscoter & Vitt (2007)). On day L + 407 we also sampled deeper 2 cm sections along the *Sphagnum* stem (2 – 3cm from surface and 3 – 4cm from surface) and senescing brown *Pleurozium* material (SM) below the green layer which was beginning to degrade. Leaves of *Empetrum* (n = 4 for all dates), *Vaccinium* ($n \geq 3$ for all dates except L + 2 (n = 2), L + 6 (n = 1), and L + 10 (n = 2)) and *Rubus* ($n \geq 3$ except for L + 10 (n = 2)) were also sampled at L + 0, 0.5, 1, 2, 3, 4, 6, 10, 19, 42 and 407. On day L + 4 and L + 42 we sampled stems, coarse roots (> 1 mm) and fine roots (< 1 mm) for *Empetrum* (n = 4), *Vaccinium* (n = 2) and *Rubus* (n = 3) from plot (*V1-4*) outside of the ^{13}C return collars. On day L + 407 we harvested entire turfs from the *V1-4* ^{13}C return collars and separated leaves, stems, coarse roots and fine roots for ^{13}C content and biomass (see below).

Tissue samples were collected and immediately sealed in small plastic bags then placed on ice in a cooler, before being transported back to the laboratory and frozen at -18 °C within 4 hours. Samples were removed from the freezer, transferred to paper bags then dried at 70 °C for 3 days before being milled for isotope analysis (Mixer Mill MM200, Retsch, Haan, Germany). A total of 890 plant tissue samples were analysed for ^{13}C content. We also measured the RWC of every labelled moss sample (equation 1) by measuring the wet (after the samples had been frozen) and dry weights.

Differences between tissue ^{13}C contents were tested for statistical significance using paired t-tests in Matlab 7.1 (with Bonferonni correction for multiple comparisons).

Vegetation biomass

On days L + 42 and L + 407 we took 4 cm × 4 cm cores from the moss plots (*Sp1-4* and *Pl 1-4*) to quantify biomass. For *Sphagnum* we sorted the cores into cap, sub-cap, 2 - 3 cm and 3 - 4 cm sections and for *Pleurozium* CY, PY and SM. On day L + 407 we harvested the vascular plants from the return collars and separated the leaves, stems and coarse roots to measure total biomass. As large a sample of fine root material as possible was collected for each species for ^{13}C analysis (at least 15g), by

removing fine roots which were still attached to the plant. The total fine root biomass within the return collars was estimated from a calibration relationship between vascular plant LAI and fine root biomass (V. Sloan, unpublished data). Plant tissue biomass data are provided in Supplementary Material Tables S1 and S2.

Photosynthesis and respiration of moss turfs

We measured net photosynthesis and respiration of *Sphagnum* and *Pleurozium* turfs following the closed-chamber methods of Douma *et al.* (2007), with the exception that the moss turfs were removed and placed on to a clear acrylic sheet before measurement. Turfs were cut from the soil using a bread knife and placed into aluminium trays. We wet the plots with mire water until they were fully waterlogged, excess water was allowed to drain from the sides of the trays. CO_2 fluxes were then measured using a LI-COR 6400 portable photosynthesis system (LI-COR Inc., Lincoln, Nebraska,USA) connected to a 0.2 × 0.2 × 0.13 m clear acrylic chamber. To create a light response curve we took three measurements at full light, followed by two measurements at three successive levels of shading, followed by three measurements in full darkness. The shading was achieved by using layers of black netting. For full darkness we used an opaque black plastic sheet. PPFD was recorded inside the chamber. We made light response curves at repeated intervals as the mosses dried, every day during the first week after wetting, and once every two days in the following days. We calculated gross photosynthesis (P) by subtracting dark respiration (R) from the net CO_2 flux. More than 1000 flux measurements were made over a period of 14 days from 5 replicate plots of *Pleurozium* and *Sphagnum*. The weight of the samples was recorded at each measurement to calculate moss relative water content (RWC):

$$RWC = \frac{M_w - M_d}{M_d} \qquad (4)$$

where M_w is wet mass (kg) and M_d is dry mass (kg). Turfs were dried at 70°C once the measurements were complete. In between measurements the turfs were stored outside under an open transparent shelter to ensure that light levels and humidity were similar to field conditions.

Modelling

Moss photosynthesis

We used the closed chamber measurements of moss photosynthesis to develop a simple 6 parameter model based on the response of gross photosynthesis (*P*) to light, temperature and moss relative water content:

$$P = \frac{P_{\max} I}{I + k} \times W \quad (5)$$

where:

$$P_{\max} = p_t \times T + p_c \quad (6)$$

and:

$$W_p = w_a X^2 + w_b X + w_c \quad (7)$$

where X is moss RWC (% dry weight), T is moss temperature, p_t, p_c are parameters controlling the response of P_{max} to temperature, k is the half saturation constant of photosynthesis, W is an RWC adjustment factor, and w_a w_b w_c are parameters controlling the response of P to moss RWC. We fitted equation 2 to the chamber flux data using non-linear least squares curve-fitting procedures in Matlab 7.1.

Pleurozium respiration

In order to improve our estimates of ER from the *Pleurozium* (*Pl1-4*) and heath plots (*V1-4*) we modelled moss respiration for the *Pleurozium* turfs. Our chamber measurements of ER on the ^{13}C return collars were made under ambient conditions between 6th and 10th July when the mosses were dry; on wetting mosses would contribute further respiratory CO_2 flux which would not otherwise not have been included leading to an underestimation of total ER and thus $^{13}CO_2$ flux. The *Pleurozium* respiration model was based on a temperature and moisture response where:

$$R = ae^{-bT} \times W_r \quad (8)$$

Where:

$$W_r = w_{ar} X^2 + w_{br} X + w_{cr} \quad (9)$$

R is moss respiration, a and b are parameters controlling the response of R to temperature, W_r is a RWC adjustment factor, and w_{ar} w_{br} w_{cr} are parameters controlling the response of respiration to RWC.

Ecosystem respiration

We used chamber ER data to fit exponential ER-temperature response curves for each plot which we then used to calculate total ER over the 19-day period following labelling using air temperature data. We added modelled *Pleurozium* respiration to our ER estimates, based on moss temperature and RWC data. We used surface wetness as a proxy variable for *Pleurozium* RWC, assuming that when the surface wetness probe recorded 100 %, moss RWC was 600 % (the maximum value recorded by the authors in the field; data not shown) and when the surface wetness probe recorded 0 % moss moisture content was 20 %, a typical value for feather mosses at equilibrium with humid air (Dilks & Proctor, 1979). We did not explicitly include the effect of water content on *Sphagnum* as water contents did not change appreciably over the 19 days following labelling (Fig. 1c).

^{13}C concentrations

All values for moss and CO_2 ^{13}C concentrations are given in units of atom% excess above natural abundance (NA) (except in Supplementary Material Fig. 1 [Chapter 4b]) i.e. atom% *pulse-derived* ^{13}C. We normalised ^{13}C atom % excess values across plots to a 10 atom% labelling concentration, based on the linear regressions in Supplementary Material Figure S1, in order to compare recoveries across plots. The ^{13}C content for vascular stems, coarse roots and fine roots were assumed to be zero at L + 0; we linearly interpolated atom% values between L+0, L + 4 and L + 42.

Respiratory $^{13}CO_2$ flux and biomass ^{13}C pool sizes

To calculate $^{13}CO_2$ respiratory flux we multiplied modelled ER by $^{13}CO_2$ atom% linearly interpolated across time points (ER plus modelled *Pleurozium* R for plots *Pl 1-4* and *V 1-4*). The number of moles of ^{13}C in each biomass pool (in moles, pulse-derived and normalised) was calculated by multiplying ^{13}C atom% by biomass C content in moles. Biomasses for vascular leaves, stems and coarse roots were based on harvests taken at L + 407. Biomass pool sizes for mosses were based on harvests taken at L + 42 and L + 407 (see Supplementary Material, Table 1 [Chapter 4b]). We expressed $^{13}CO_2$ flux and biomass ^{13}C pools as percentage of the total pulse-derived ^{13}C assimilated by assuming that the total photosynthetic ^{13}C uptake was equal to the amount of ^{13}C present at the point of greatest tissue enrichment (at L + 0.5 for *Pleurozium* and vascular plants, and L + 1 for *Sphagnum).*

The relationship between moss GPP and CUE

GPP for *Sphagnum* and *Pleurozium* was calculated as the sum of modelled P from L + 0 to L + 19 based on moss chamber flux data and local meteorological data. % C respired for *Sphagnum* and *Polytrichum* over 5 days at Abisko are from Street *et al.* (2011) and GPP over the same 5 days was estimated from Street *et al.* (in prep) [Chapter 2].

Results

Environmental conditions from L + 0 to L + 19

Average maximum and minimum daily air temperature between L + 0 and L + 19 was 15.2 ºC and 7.8 ºC (Fig1a). PPFD exceeded 1000 µmol m^{-2} s^{-1} on cloud-free days; during the night PPFD was between 2 and 35 µmol m^{-2} s^{-1} (Fig. 1b). No precipitation was recorded between the end of labelling on L + 0 and L + 6. From L + 6 onwards the longest period without recordable (> 0.5mm) rainfall was 2 days and moisture events were recorded on the surface wetness probe every day (Fig. 1d). Not all surface moisture events corresponded to a measurable rainfall event (Figs 1a & d). The maximum measured RWC of *Sphagnum* tissues between L + 0 and L + 19 was 1150 % (at L + 19) and the minimum recorded was 965 % (at L + 3). For

Pleurozium, the maximum recorded RWC was 474 % (at L + 10) and the minimum RWC was 5.4 % (at L + 2) (figs 1a & b).

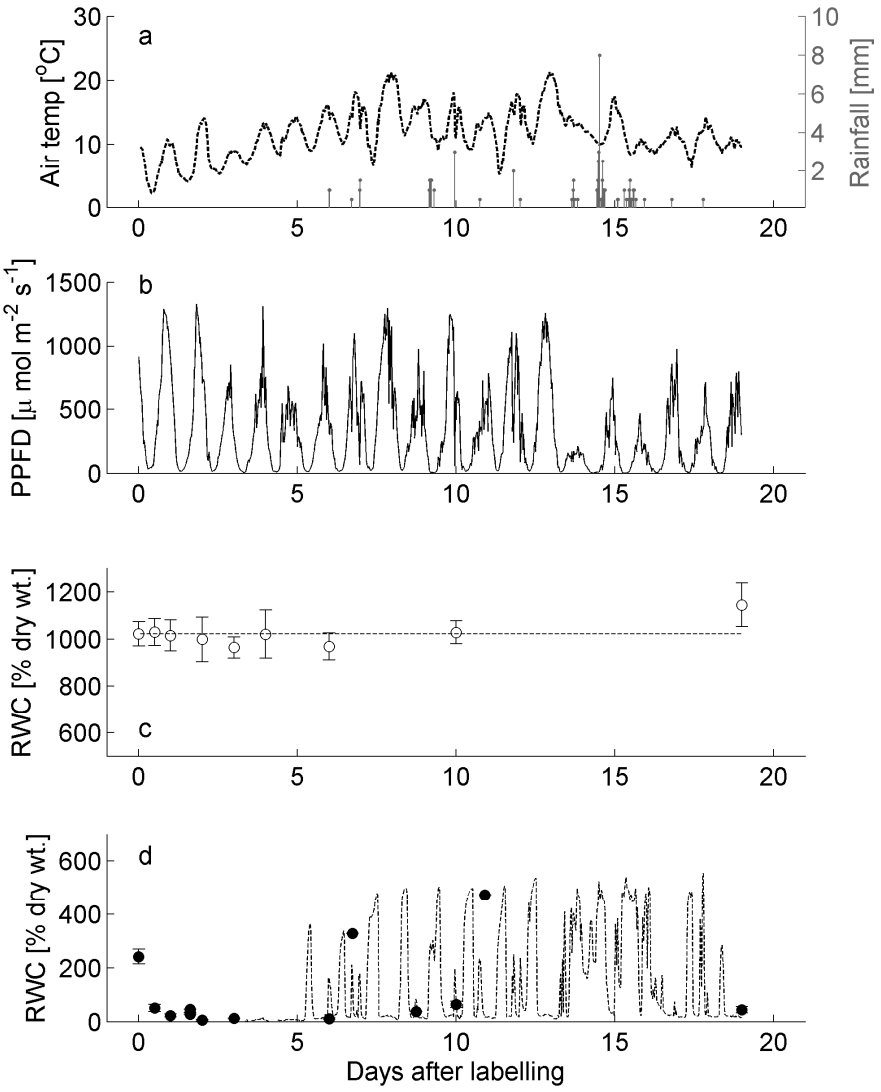

Figure 1. a) air temperature (°C) and rainfall (mm) b) PPFD (µmol m^{-2} s^{-1}) c) *Sphagnum* relative water content (RWC) and d) *Pleurozium* RWC (% dry weight) for 19 days following labelling.

Moss photosynthesis

We measured *Sphagnum* photosynthesis over a range of decreasing RWCs from 2340 % to 280 %, and *Pleurozium* from 590 % to 7 %. The moss *P* model was able to explain > 70 % of the variation in measured moss turf *P* (R^2 for modelled vs. measured P was 0.71 for *Sphagnum* and 0.72 for *Pleurozium*, Supplementary Material Fig. 2a). Maximum rates of P for *Sphagnum* were slightly higher, at up to 3 µmol m^{-2} s^{-1}, than *Pleurozium* for which maximum *P* was 2.2 µmol m^{-2} s^{-1} (Fig. 2a).

Sphagnum had a broad optimum for *P* at around 980 %; the best-fit parameters (w_a, w_b and w_c) for the RWC adjustment factor (*W)* (equation 4) did not cause a reduction in photosynthesis by more than 10 % unless RWC was < 450% or > 1500 %. *Pleurozium* photosynthesis was positively related to RWC, we did not measure any suppression of photosynthesis at the maximum RWC of 590 % (Fig. 2b). The *P* model predicted zero photosynthesis for *Pleurozium* below 35 % RWC.

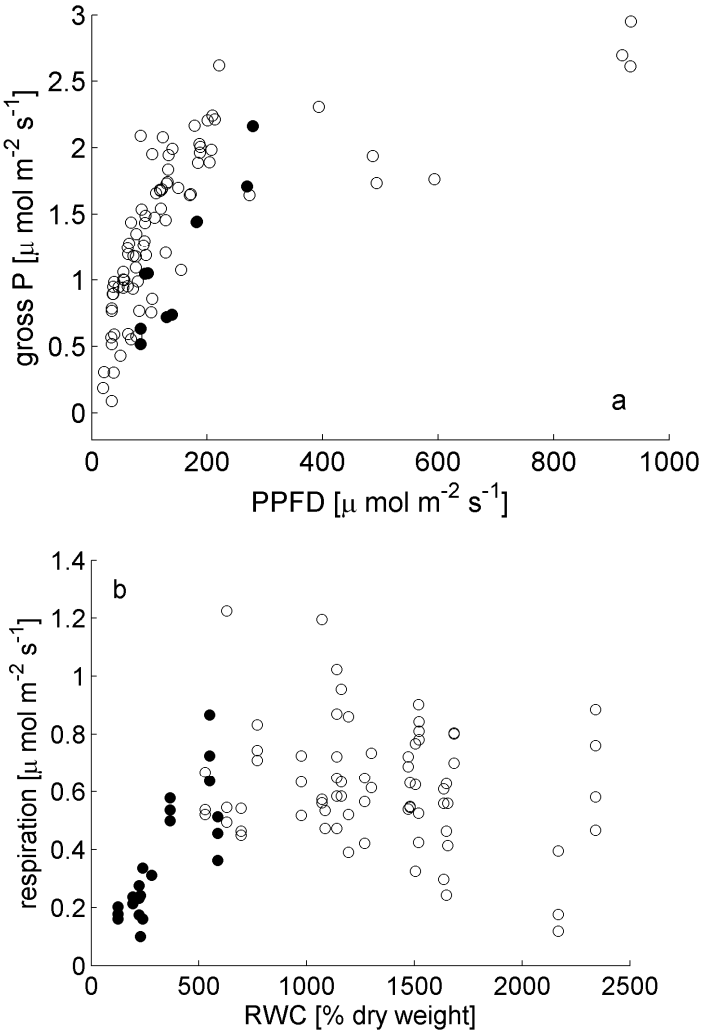

Figure 2. a) gross photosynthesis (P) response to PPFD (μmol m^{-2} s^{-1}) for *Sphagnum* (open symbols), and *Pleurozium* (closed symbols). Water contents for *Sphagnum* are within the range 965 - 1150 % and for *Pleurozium* 300 – 500 % b) gross photosynthesis (at 200 μmol m^{-2} s^{-1} PPFD) response to relative water content (RWC).

^{13}C content of plant tissues

All *Sphagnum* (cap. and sub cap), *Pleurozium* (CY and PY) and vascular plant leaves on the 'light' sides of the plots were enriched in ^{13}C following labelling (top row, Fig. 3). Initial enrichment of photosynthetic tissues was linearly related to hood ^{13}C atom% (e.g. $R^2 = 0.94$ for *Sphagnum* (cap), $R^2 = 0.96$ for *Pleurozium* (CY) and $R^2 = 0.74$ for *Empetrum* leaves, see Supplementary Material Fig. 1 [Chapter 4b]). There was negligible enrichment of tissues on the 'dark' sides of the plots ($9.2 \times 10^{-4} \pm 1.7 \times 10^{-4}$ atom%) which we assumed to be zero in subsequent analysis.

The time point of greatest enrichment for *Pleurozium* and *Empetrum* leaves was 0.5 days after the end of labelling, and L + 1 days after labelling for *Sphagnum*. Enrichment of *Pleurozium* within the heath community appeared to increase slightly until 6 days after labelling. Uncertainty in the measurement of tissue isotope enrichment was large, particularly for *Sphagnum*. This was partly the result of one *Sphagnum* plot (*Sp4*) which had a very low hood labelling concentration (Supplementary Material Fig.1) and therefore high signal to noise ratio. There appeared to be a decreasing trend in *Sphagnum* capitulum isotope enrichment over time (Fig. 3a, *Sp4* not included), however, we found no statistically significant difference in capitulum enrichment between L + 1 and L + 19 (t-test, $p > 0.1$ both including and excluding *Sp4*). *Pleurozium* tissues showed a less consistent downward trend in isotope enrichment, though the lowest enrichment occurred at L + 19 and the difference between L + 0.5 and L + 19 approached statistical significance (paired t-test, $p = 0.07$). *Empetrum* leaves were highly enriched with double the initial enrichment of *Sphagnum* tissues and ten times the initial enrichment of *Pleurozium*. There was a clear decreasing trend in enrichment of *Empetrum* leaves after L + 0.5, but due to large uncertainties the differences in enrichment between L + 0.5 and L + 19 was also non-significant ($p > 0.2$).

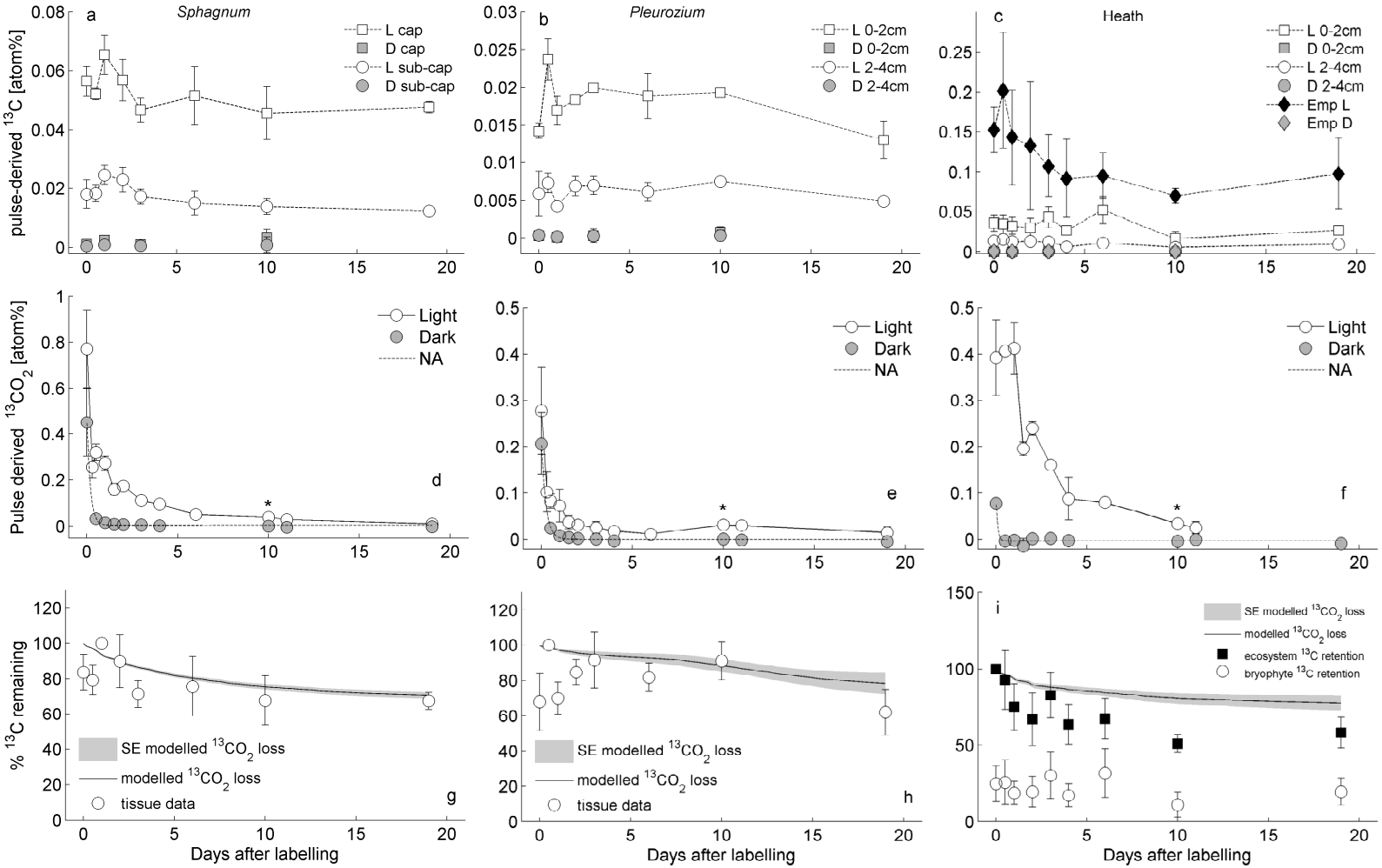
a
Sphagnum
b
Pleurozium
c
Heath
pulse-derived ^{13}C [atom%]
L cap
D cap
L sub-cap
D sub-cap
L 0-2cm
D 0-2cm
L 2-4cm
D 2-4cm
Emp L
Emp D
Pulse derived $^{13}CO_2$ [atom%]
Light
Dark
NA
d
e
f
% ^{13}C remaining
SE modelled $^{13}CO_2$ loss
modelled $^{13}CO_2$ loss
tissue data
ecosystem ^{13}C retention
bryophyte ^{13}C retention
g
h
i
Days after labelling

Figure 3. (overleaf) Top row – normalised pulse-derived ^{13}C content (atom%) of tissues for a) *Sphagnum* capitulum and sub-capitulum, b) *Pleurozium* 0-2 cm and 2-4 cm of frond with vascular canopy removed c) *Empetrum* leaves and *Pleurozium* 0-2 cm and 2-4 cm of frond with canopy intact. Grey symbols are for dark treatments, open symbols are for light treatments. Middle row – normalised pulse-derived ^{13}C content of ecosystem respiration for d) *Sphagnum*, e) *Pleurozium* without vascular canopy and f) *Pleurozium* with vascular canopy. Grey symbols are for dark treatments, open symbols are for light treatments. * indicates n = 2 because sampling was interrupted. Bottom row - % of total label uptake recovered in tissues, based on tissue isotope content (symbols) and modelled loss of ^{13}C in ecosystem respiration (solid line) for g) *Sphagnum* h) *Pleurozium* without vascular canopy and i) *Pleurozium* with vascular canopy. In panel i) closed symbols show total ecosystem recovery and open symbols show bryophyte ^{13}C recovery both as a percentage of total ecosystem uptake.

Respiratory CO_2 fluxes

The maximum ER measured was 3.5 μmol m^{-2} s^{-1} in the heath plots. *Pleurozium* plots tended to have the lowest respiration rates, generally below 1.5 μmol m^{-2} s^{-1} (Supplementary Material Fig. 3 [Chapter 4b]). *Sphagnum* plots had the clearest ER temperature response. Chamber flux measurements indicated maximum rates of *Pleurozium* respiration of up to 0.8 μmol m^{-2} s^{-1}. The R^2 of modelled vs. measured *Pleurozium* respiration was 0.74 (Supplementary Material Fig. 2b [Chapter 4b]). The *Pleurozium* respiration model predicted zero respiration below 15 % RWC.

^{13}C content of ecosystem respiration

ER was enriched in ^{13}C following labelling for both 'light' and 'dark' treatments for all vegetation types (middle row, Fig. 3). The enrichment of 'dark' CO_2 flux was not significantly different to zero by L + 0.5 (t-test, $p > 0.1$) for the vascular plots and by L + 1 for the *Pleurozium* plots (t-test, $p > 0.1$). The CO_2 flux from the dark side of the *Sphagnum* plots remained enriched in ^{13}C until L + 3, though the enrichment was < 0.03 atom% beyond L + 0.5. Enrichment of ecosystem respiration from the 'light' sides of the plots was always greater than from 'dark' sides, though at the first time point for both moss species, abiotic enrichment (i.e. diffusive ^{13}C return from soil pores) was > 50% of total ecosystem $^{13}CO_2$ enrichment. There was a strong decrease in biological ^{13}C return over time, for all species, though problems with leakage for the heath plots meant that much of the data had to be excluded. There appeared to be a slight increase in enrichment between day 6 and day 11 for *Pleurozium* and though not strongly significant (ttest $p = 0.09$), the increase was also indicated by additional (but incomplete) sampling on day 10.

Short-term fate of ^{13}C as % of total ^{13}C assimilated

Total ^{13}C assimilation was calculated to be 4.4 ± 1.4 mol ^{13}C m^{-2} for S*phagnum,* 2 ± 0.2 mol ^{13}C m^{-2} for *Pleurozium*, and 11.3 ± 3.9 mol ^{13}C m^{-2} for the heath plots. Based on the loss of ^{13}C from moss tissues (excluding *Sp4*) *Sphagnum* respired 33 ± 5 % of assimilated ^{13}C by L + 19. The amount of ^{13}C loss based on modelled respiratory $^{13}CO_2$ flux was in close agreement at 29 ± 3 % (Fig. 3g). For *Pleurozium* the loss of ^{13}C from moss tissues (38 % ± 13 %) was greater than the amount of ^{13}C respired (19 % ± 6 %) by L + 19, i.e. about 20 % of the ^{13}C was unaccounted for between L + 0 and L + 19. The difference between the two estimates was not statistically significant (ttest, p = 0.38) (Fig. 3h).

The loss of ^{13}C from plant tissues in plots *V1-4* (including above and below ground vascular and mosses) was 42 % ± 10 % of the initial ^{13}C uptake by L + 19. There was a 20 % discrepancy between the loss of ^{13}C calculated from tissue ^{13}C contents and the measured $^{13}CO_2$ respiratory flux which was 22 % ± 4 % of total ^{13}C uptake. At day L + 0.5, mosses accounted for 25 % ± 14 % of the total heath uptake of ^{13}C. At day L + 19, 58 % of the total uptake of ^{13}C in heath vegetation reamined in plant biomass pools (Fig. 3i); 20 % ± 9 % in mosses, 27 ± 6 % in aboveground vascular tissues and 10 % ± 2 % in belowground vascular tissues. The CUE of the vascular plants alone in the heath plots was 49 %.

Relationship between moss GPP and CUE

Average daily GPP between L + 0 and L + 19 at Kevo was lower for *Pleurozium* (0.4 g C m^{-2} day^{-1}) than for *Sphagnum* (1.4 g C m^{-2} day^{-1}). In comparing the results of this experiment with *Polytrichum piliferum* and *Sphagnum fuscum* GPP and CUE from Street *et al.* (2011) and (Street *et al.* (in prep) [Chapter 2] CUE varied between 23 % and 66 % and average daily GPP varied between 0.4 and 3 g C m^{-2} day^{-1}. There was a non-significant negative relationship between moss CUE and GPP (Fig. 4)

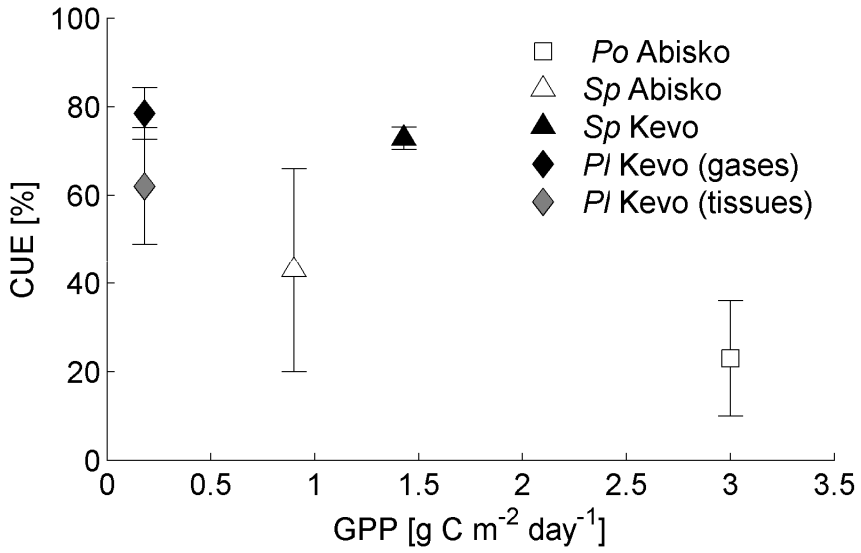

Figure 4. Carbon use efficiency (CUE) and mean daily GPP for *Sphagnum* and *Pleurozium* at Kevo (over 19 days) and *Polytrichum* and *Sphagnum* at Abisko (over 5 days, based on Street *et al.* (2011) and Street et al. (in prep) [Chapter 2].

^{13}C recovery after 1 year

Tissue ^{13}C enrichment and tissue biomass pools are given in the Supplementary Material (Tables 1, 2 and 3). Recovery of ^{13}C between day L + 42 and L + 407 (over 1 year) was greatest for *Sphagnum* at ~80 % and lowest for *Rubus* at ~20 % (Fig. 5a). Differences between species in the % recovery of ^{13}C were non-significant ($p > 0.5$). For *Sphagnum* the ^{13}C content of the capitulum decreased by ~60 % over 1 year, while the sub-capitulum ^{13}C content increased to ~250 % of the amount present at L + 42 (Fig. 5b). Just 3 % of the total ^{13}C present in *Sphagnum* tissues at day L + 42 was recovered below the sub-capitulum at L + 407. For *Pleurozium* in the heath plots ~64 % of ^{13}C was recovered in photosynthetic tissues after 1 year; average recovery in both the PY and CY sections was similar at ~66 % and ~61 % (Fig. 5c). After 1 year *Pleurozium* SM contained 3 % of the total ^{13}C present at L + 42.

For *Empetrum* total ^{13}C recovery between L + 42 and L + 407 was 67 %. The amount of ^{13}C in *Empetrum* stems and coarse roots on average increased between L + 42 and L + 407, though there was large variation between plots. The amount of ^{13}C in *Empetrum* leaves and fine roots decreased. The amount of ^{13}C in senesced leaves after 1 year was ~14 % of the total amount present in green leaves the previous year

(Fig. 5d). We did not recover significant amounts of ^{13}C in *Rubus* tissues, though there was an increase in the amount of ^{13}C in *Rubus* stems between L + 42 and L + 407 and very high ^{13}C atom% in coarse root and rhizome in one of the plots (Fig. 5e).

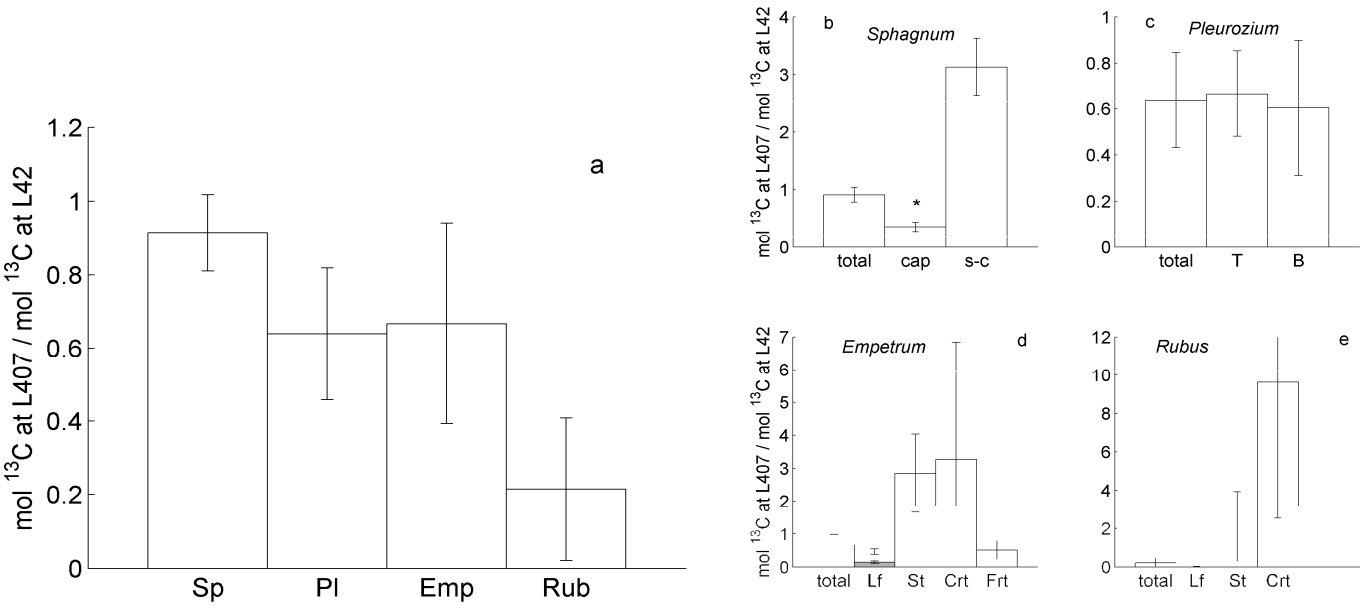

Figure 5. The amount of ^{13}C label (mol ^{13}C m^{-2}) present at L + 407 as a fraction of that present in tissues at L + 42 for a) whole plants and for separate plant tissues of b) *Sphagnum* (Sp), c) *Pleurozium* (Pl) d) *Empetrum* (Emp) and e) *Rubus* (Rub). The grey bar for *Empetrum* shows the contribution of attached, senesced leaves. * indicates a significant difference between ^{13}C content of tissues between L + 42 and L + 407 at 5 % level (with Bonferonni correction for multiple comparisons).

Discussion

Moss CUE efficiency

Using two independent data sources based on: 1) loss of a ^{13}C from labelled plant tissues and 2) respiratory return fluxes of $^{13}CO_2$ from labelled plots we show that *Sphagnum* CUE lies between 68 – 71% of photosynthesised C and *Pleurozium* between 62 – 81 %. These results are higher than the conservative range of 40 – 60 % often assumed for vascular plants and consistent with Woodin *et. al.* (2009) who measure 70 % ^{13}C label retention in mosses in high Arctic systems. For several days after labelling however, the moisture content of *Pleurozium* fell below the minimum required for photosynthetic (and respiratory) activity; our chamber measurements suggested complete cessation of photosynthesis below 35 % RWC and cessation of respiration at water contents slightly lower than this, consistent with other studies (Dilks & Proctor, 1979; Tuba *et al.*, 1998; Williams & Flanagan, 1998). The very rapid decrease of ^{13}C in ecosystem respiration from the *Pleurozium* plots was therefore due in part to a shut down of metabolic activity as the mosses dried. Short-term turnover of C in desiccation tolerant mosses such as *Pleurozium* cannot therefore be modelled as a simple decay function as is a common for vascular plants (Subke *et. al.* in review). *Sphagnum* maintained its RWC close to optimum value by storing water in tissues. Street *et al.* (2011) show that water content is not a strong driver for *Sphagnum fuscum* (sect. *Acutifolia*) photosynthesis under normal conditions, as this species is able to maintain its water content near optimal values. There appeared to be a negative trend in moss CUE with time-averaged photosynthetic rate, though this trend was not statistically significant. Further investigation of additional species, and over a range of controlled moisture conditions would be required to understand if this was a general relationship for bryophytes.

We found that the variability in ^{13}C content of moss tissues was large, probably due to heterogeneity in the moss canopy in terms of photosynthetic capacity and for *Pleurozium*, moisture status of tissues. Measurements of return $^{13}CO_2$ flux integrates the response of the entire moss canopy and so is probably a more reliable measurements of average C turnover. However, we expect that the respiration $^{13}CO_2$ flux for *Pleurozium* may have been underestimated due to underestimation of the time period during which the mosses were moist. The surface wetness probe would almost

certainly have dried more quickly than moss tissues, and feather mosses are also known to absorb some water from underlying organic layers via external wicking and distillation (Carleton & Dunham, 2003).

We assume in our calculations that there is no recycling of ^{13}C label (i.e. re-fixation of respired ^{13}C) which potentially biases our results towards greater structural incorporation of ^{13}C as a fraction of gross *P*. Turetsky & Wieder (1999) quantify C re-fixation in *Sphagnum fuscum* to be 3.5-5.4 %. Re-fixation in *Pleurozium* mats might be expected to exceed that of *Sphagnum*, considering the weft-like structure of the canopy, however re-fixation of CO_2 in feather mosses has not been quantified.

Moss contribution to heath community CUE and aboveground : belowground C partitioning

In the heath plots, *Pleurozium* accounted for ca. 25 % of the initial uptake of $^{13}CO_2$ and after 19 days accounted for ca. 35 % of the label retained in plant tissues. The presence of mosses in the community resulted in a community CUE of 58 %, while the CUE of the vascular community alone was ca. 49 %. The presence of a moss understory therefore increased the CUE of the heath vegetation by almost 10 %. Carbon which is fixed by mosses can not be allocated belowground. The presence of a moss layer in a community therefore increases the fraction of total GPP which is retained in aboveground plant tissues. In this case, including mosses we calculate belowground allocation to be 10 % of ecosystem GPP. Without the presence of mosses, belowground allocation would have been around 27 % of heath community GPP.

We show that CUE of mosses varies considerably between species. The contribution of mosses to ecosystem CUE at the landscape scale therefore requires information on the both the spatial extent of moss abundance *and* species or functional type composition. We also demonstrate that for *Pleurozium*, the processes of C uptake and turnover are strongly dependant on tissue moisture content. To properly represent these communities in C models therefore requires a representation of moss energy balance to relate environmental conditions to non-vascular plant metabolism.

Turnover of structural C pools in Arctic vegetation

In order to estimate longer term C sequestration it is necessary to quantify the rate of turnover (or residence time) of C within plant biomass pools. Over a period of 1 year, we show that the majority of C fixed by mosses is retained within the tissue in which it is fixed, in the case of *Sphagnum* moving downwards in the profile. We could find no significant differences between ^{13}C content of any plant tissues over 1 year (expect for *Sphagnum* capitula which decreased significantly) due to high variability between plots. However we can report qualitative patterns between species. Average recovery of ^{13}C was greatest for *Sphagnum* and lowest for *Rubus*. Only 3 % of the label was recovered in *Sphagnum* below the sub-capitulum, indicating that the shoots grew by a maximum of about 1 cm over the year. The loss of ^{13}C from *Sphagnum* tissues could have occurred through leaching of dissolved organic carbon (Fenner *et al.*, 2004). On average we recovered only 60 % (incl. SM) of *Pleurozium* ^{13}C. The loss of 40 % of the ^{13}C could have been due to a combination of leaching of dissolved organic carbon (Wilson & Coxson, 1999) or respiration of stored carbohydrate after water stress, or due to herbivory by lemmings (Tast, 1991). Recovery of ^{13}C in *Empetrum* was 70 %. The data suggest senescence of at least 14 % of green leaves per year, and indicate some re-allocation of C to stem and coarse roots between growing seasons.

Conclusions

We use two independent measurements, based on moss tissue ^{13}C and respired $^{13}CO_2$ to quantify CUE of *Sphagnum* (68 – 71%) and *Pleurozium* (62 – 81 %). We demonstrate that mosses play an important role in the uptake and retention of C in an evergreen heath community. The presence of a moss understory increases ecosystem CUE and the fraction of GPP which is allocated to aboveground vs. belowground NPP. Our results highlight the need to include mosses within vegetation C models for Arctic ecosystems.

References

Albrizio, R. & Steduto, P. (2003) Photosynthesis, respiration and conservative carbon use efficiency of four field grown crops. *Agricultural and Forest Meteorology*, **116**, 19-36.

Benscoter, B.W. & Vitt, D.H. (2007) Evaluating feathermoss growth: a challenge to traditional methods and implications for the boreal carbon budget. *Journal of Ecology*, **95**, 151-158.

Beringer, J., Lynch, A.H., Chapin, F.S., Mack, M., & Bonan, G.B. (2001) The representation of Arctic soils in the land surface model: The importance of mosses. *Journal of Climate*, **14**, 3324-3335.

Bret-Harte, M.S., Shaver, G.R., Zoerner, J.P., Johnstone, J.F., Wagner, J.L., Chavez, A.S., Gunkelman, R.F., Lippert, S.C., & Laundre, J.A. (2001) Developmental plasticity allows Betula nana to dominate tundra subjected to an altered environment. *Ecology*, **82**, 18-32.

Cannell, M.G.R. & Thornley, J.H.M. (2000) Modelling the components of plant respiration: Some guiding principles. *Annals of Botany*, **85**, 45-54.

Carleton, T.J. & Dunham, K.M.M. (2003) Distillation in a boreal mossy forest floor. *Canadian Journal of Forest Research-Revue Canadienne De Recherche Forestiere*, **33**, 663-671.

Chapin, F.S., BretHarte, M.S., Hobbie, S.E., & Zhong, H.L. (1996) Plant functional types as predictors of transient responses of Arctic vegetation to global change. *Journal of Vegetation Science*, **7**, 347-358.

Chapin, F.S., McFarland, J., McGuire, A.D., Euskirchen, E.S., Ruess, R.W., & Kielland, K. (2009) The changing global carbon cycle: linking plant-soil carbon dynamics to global consequences. *Journal of Ecology*, **97**, 840-850.

Chapin, F.S., McGuire, A.D., Randerson, J., Pielke, R., Baldocchi, D., Hobbie, S.E., Roulet, N., Eugster, W., Kasischke, E., Rastetter, E.B., Zimov, S.A., & Running, S.W. (2000) Arctic and boreal ecosystems of western North America as components of the climate system. *Global Change Biology*, **6**, 211-223.

Cornelissen, J.H.C., Lang, S.I., Soudzilovskaia, N.A., & During, H.J. (2007a) Comparative cryptogam ecology: A review of bryophyte and lichen traits that drive biogeochemistry. *Annals of Botany*, **99**, 987-1001.

Cornelissen, J.H.C., van Bodegom, P.M., Aerts, R., Callaghan, T.V., van Logtestijn, R.S.P., Alatalo, J., Chapin, F.S., Gerdol, R., Gudmundsson, J., Gwynn-Jones, D., Hartley, A.E., Hik, D.S., Hofgaard, A., Jonsdottir, I.S., Karlsson, S., Klein, J.A., Laundre, J., Magnusson, B., Michelsen, A., Molau, U., Onipchenko, V.G., Quested, H.M., Sandvik, S.M., Schmidt, I.K., Shaver, G.R., Solheim, B., Soudzilovskaia, N.A., Stenstrom, A., Tolvanen, A., Totland, O., Wada, N., Welker, J.M., & Zhao, X.Q. (2007b) Global negative vegetation feedback to climate warming responses of leaf litter decomposition rates in cold biomes. *Ecology Letters*, **10**, 619-627.

DeLucia, E.H., Drake, J.E., Thomas, R.B., & Gonzalez-Meler, M. (2007) Forest carbon use efficiency: is respiration a constant fraction of gross primary production? *Global Change Biology*, **13**, 1157-1167.

Dilks, T.J.K. & Proctor, M.C.F. (1979) Photosynthesis, Respiration and Water-Content in Bryophytes. *New Phytologist*, **82**, 97-&.

Dormann, C.F. & Woodin, S.J. (2002) Climate change in the Arctic: using plant functional types in a meta-analysis of field experiments. *Functional Ecology*, **16**, 4-17.

Douma, J., van Wijk, M.T., Lang, S.I., & Shaver, G.R. (2007) The contribution of mosses to the carbon and water exchange of Arctic ecosystems: quantification and relationships with system properties. *Plant, Cell and Environment*, **30**, 1205-1215.

Fenner, N., Ostle, N., Freeman, C., Sleep, D., & Reynolds, B. (2004) Peatland carbon afflux partitioning reveals that Sphagnum photosynthate contributes to the DOC pool. *Plant and Soil*, **259**, 345-354.

Forbes, B.C., Fauria, M.M., & Zetterberg, P. (2010) Russian Arctic warming and 'greening' are closely tracked by tundra shrub willows. *Global Change Biology*, **16**, 1542-1554.

Gaston, K.J. (2000) Global patterns in biodiversity. *Nature*, **405**, 220-227.

Gifford, R.M. (1994) The Global Carbon-Cycle - a Viewpoint on the Missing Sink. *Australian Journal of Plant Physiology*, **21**, 1-15.

Gifford, R.M. (2003) Plant respiration in productivity models: conceptualisation, representation and issues for global terrestrial carbon-cycle research. *Functional Plant Biology*, **30**, 171-186.

Gornall, J.L., Jonsdottir, I.S., Woodin, S.J., & Van der Wal, R. (2007) Arctic mosses govern below-ground environment and ecosystem processes. *Oecologia*, **153**, 931-941.

Gower, S.T., Krankina, O., Olson, R.J., Apps, M., Linder, S., & Wang, C. (2001) Net primary production and carbon allocation patterns of boreal forest ecosystems. *Ecological Applications*, **11**, 1395-1411.

Groendahl, L., Friborg, T., & Soegaard, H. (2007) Temperature and snow-melt controls on interannual variability in carbon exchange in the high Arctic. *Theoretical and Applied Climatology*, **88**, 111-125.

Hudson, J.M.G. & Henry, G.H.R. (2010) High Arctic plant community resists 15 years of experimental warming. *Journal of Ecology*, **98**, 1035-1041.

Ise, T., Litton, C.M., Giardina, C.P., & Ito, A. (2010) Comparison of modeling approaches for carbon partitioning: Impact on estimates of global net primary production and equilibrium biomass of woody vegetation from MODIS GPP. *Journal of Geophysical Research-Biogeosciences*, **115**.

Johansson, T., Malmer, N., Crill, P.M., Friborg, T., Akerman, J.H., Mastepanov, M., & Christensen, T.R. (2006) Decadal vegetation changes in a northern peatland, greenhouse gas fluxes and net radiative forcing. *Global Change Biology*, **12**, 2352-2369.

Litton, C.M. & Giardina, C.P. (2008) Below-ground carbon flux and partitioning: global patterns and response to temperature. *Functional Ecology*, **22**, 941-954.

Litton, C.M., Raich, J.W., & Ryan, M.G. (2007) Carbon allocation in forest ecosystems. *Global Change Biology*, **13**, 2089-2109.

McCutchan, C.L. & Monson, R.K. (2001) Effects of tissue-type and development on dark respiration in two herbaceous perennials. *Annals of Botany*, **87**, 355-364.

McGuire, A.D., Anderson, L.G., Christensen, T.R., Dallimore, S., Guo, L.D., Hayes, D.J., Heimann, M., Lorenson, T.D., Macdonald, R.W., & Roulet, N. (2009) Sensitivity of the carbon cycle in the Arctic to climate change. *Ecological Monographs*, **79**, 523-555.

McGuire, A.D., Clein, J.S., Melillo, J.K., Kicklighter, D.W., Meier, R.A., Vorosmarty, C.J., & Serreze, M.C. (2000) Modeling carbon responses of tundra ecosystems to historical and projected climate: sensitivity of pan-Arctic carbon storage to temporal and spatial variation in climate. *Global Change Biology*, **6**, 141-159.

Myneni, R.B., Keeling, C.D., Tucker, C.J., Asrar, G., & Nemani, R.R. (1997) Increased plant growth in the northern high latitudes from 1981 to 1991. *Nature*, **386**, 698-702.

Ryan, M.G., Gower, S.T., Hubbard, R.M., Waring, R.H., Gholz, H.L., Cropper, W.P., & Running, S.W. (1995) Woody Tissue Maintenance Respiration of 4 Conifers in Contrasting Climates. *Oecologia*, **101**, 133-140.

Schuur, E.A.G., Vogel, J.G., Crummer, K.G., Lee, H., Sickman, J.O., & Osterkamp, T.E. (2009) The effect of permafrost thaw on old carbon release and net carbon exchange from tundra. *Nature*, **459**, 556-559.

Spadavecchia, L., Williams, M., Bell, R., Stoy, P.C., Huntley, B., & van Wijk, M.T. (2008) Topographic controls on the leaf area index and plant functional type of a tundra ecosystem. *Journal of Ecology*, **96**, 1238-1251.

Street, L., Subke, J., Sommerkorn, M., Heinemeyer, A., & Williams, M. (2011) Turnover of recently assimilated carbon in arctic bryophytes. Oecologia. DOI: 10.1007/s00442-011-1988-y.

Subke, J.A., Vallack, H.W., Magnusson, T., Keel, S.G., Metcalfe, D.B., Högberg, P., & Ineson, P. (2009) Short-term dynamics of abiotic and biotic soil (CO2)-C-13 effluxes after in situ (CO2)-C-13 pulse labelling of a boreal pine forest. *New Phytologist*, **183**, 349-357.

Tape, K., Sturm, M., & Racine, C. (2006) The evidence for shrub expansion in Northern Alaska and the Pan-Arctic. *Global Change Biology*, **12**, 686-702.

Tarnocai, C., Canadell, J.G., Schuur, E.A.G., Kuhry, P., Mazhitova, G., & Zimov, S. (2009) Soil organic carbon pools in the northern circumpolar permafrost region. *Global Biogeochemical Cycles*, **23**.

Tast, J. (1991) Will the Norwegian Lemming Become Endangered If Climate Becomes Warmer. *Arctic And Alpine Research*, **23**, 53-60.

Tuba, Z., Protor, M.C.F., & Csintalan, Z. (1998) Ecophysiological responses of homoiochlorophyllous and poikilochlorophyllous desiccation tolerant plants: a comparison and an ecological perspective. *Plant Growth Regulation*, **24**, 211-217.

Turetsky, M.R. & Wieder, R.K. (1999) Boreal bog Sphagnum refixes soil-produced and respired (CO2)-C-14. *Ecoscience*, **6**, 587-591.

Van Iersel, M.W. (2003) Carbon use efficiency depends on growth respiration, maintenance respiration, and relative growth rate. A case study with lettuce. *Plant Cell And Environment*, **26**, 1441-1449.

van Wijk, M.T., Clemmensen, K.E., Shaver, G.R., Williams, M., Callaghan, T.V., Chapin, F.S., Cornelissen, J.H.C., Gough, L., Hobbie, S.E., Jonasson, S., Lee, J.A., Michelsen, A., Press, M.C., Richardson, S.J., & Rueth, H. (2004) Long-term ecosystem level experiments at Toolik Lake, Alaska, and at Abisko, Northern Sweden: generalizations and differences in ecosystem and plant type responses to global change. *Global Change Biology*, **10**, 105-123.

Verbyla, D. (2008) The greening and browning of Alaska based on 1982-2003 satellite data. *Global Ecology and Biogeography*, **17**, 547-555.

Walker, M.D., Wahren, C.H., Hollister, R.D., Henry, G.H.R., Ahlquist, L.E., Alatalo, J.M., Bret-Harte, M.S., Calef, M.P., Callaghan, T.V., Carroll, A.B., Epstein, H.E., Jonsdottir, I.S., Klein, J.A., Magnusson, B., Molau, U., Oberbauer, S.F., Rewa, S.P., Robinson, C.H., Shaver, G.R., Suding, K.N., Thompson, C.C., Tolvanen, A., Totland, O., Turner, P.L., Tweedie, C.E., Webber, P.J., & Wookey, P.A. (2006) Plant community responses to experimental warming across the tundra biome. *Proceedings Of The National Academy Of Sciences Of The United States Of America*, **103**, 1342-1346.

Waring, R.H., Landsberg, J.J., & Williams, M. (1998) Net primary production of forests: a constant fraction of gross primary production? *Tree Physiology*, **18**, 129-134.

Williams, T.G. & Flanagan, L.B. (1998) Measuring and modelling environmental influences on photosynthetic gas exchange in Sphagnum and Pleurozium. *Plant Cell And Environment*, **21**, 555-564.

Wilson, J.A. & Coxson, D.S. (1999) Carbon flux in a subalpine spruce-fir forest: pulse release from Hylocomium splendens feather-moss mats. *Canadian Journal of Botany-Revue Canadienne De Botanique*, **77**, 564-569.

Woodin, S.J., van der Wal, R., Sommerkorn, M., & Gornall, J.L. (2009) Differential allocation of carbon in mosses and grasses governs ecosystem sequestration: a ^{13}C tracer study in the high Arctic. *New Phytologist*, **184**, 944-949.

Wookey, P.A., Aerts, R., Bardgett, R.D., Baptist, F., Brathen, K.A., Cornelissen, J.H.C., Gough, L., Hartley, I.P., Hopkins, D.W., Lavorel, S., & Shaver, G.R. (2009) Ecosystem feedbacks and cascade processes: understanding their role in the responses of Arctic and alpine ecosystems to environmental change. *Global Change Biology*, **15**, 1153-1172.

Zhang, Y.J., Xu, M., Chen, H., & Adams, J. (2009) Global pattern of NPP to GPP ratio derived from MODIS data: effects of ecosystem type, geographical location and climate. *Global Ecology and Biogeography*, **18**, 280-290.

4b. The fate of assimilated carbon in Arctic vegetation: the importance of non-vascular plants – supplementary material

Lorna E. Street [1], Jens-Arne Subke[2,3], Martin Sommerkorn[4], V. Sloan[5], H. Ducrotoy[6], G. K. Phoenix[5], MathewWilliams[1]

[1]School of Geosciences, University of Edinburgh, Edinburgh, EH9 3JN, UK

[2]Stockholm Environment Institute York, Environment Department, University of York, York, YO10 5DD, UK

[3]School of Biological and Environmental Sciences, University of Stirling, Stirling, FK9 4LA, UK

[4]Macaulay Land Use Research Institute, Craigiebuckler, Aberdeen, AB15 8QH, UK

[5]Department of Animal and Plant Sciences, The University of Sheffield, Sheffield, ST10 2TN, UK

[6]Institute of Geography and Earth Sciences, Aberystwyth University, Aberystwyth, UK

(intended for submission to Arctic, AntArctic and Alpine Research)

Table 1. Estimated % cover of mosses and biomass (from 4 cm × 4 cm cores) in labelled plots taken on L + 42 and L + 407.

Species	Tissue	Biomass [g m^{-2}] (± 1SE)		Cover (% ± SE)
		L + 42	L + 402	
Sphagnum	Capitulum (0-1cm)	114.2 ± 6.8	128.5 ± 21.4	100 ± 0
	Sub-capitulum (1-2cm)	112.0 ± 4.2	194.5 ± 22.6	
	2-3cm	-	146.5 ± 19.3	
	3-4cm	-	156.5 ± 23.6	
	Total	-	626 ± 74.2	
Pleurozium (no canopy)	Current year growth	157.3 ± 15.8	5.8 ± 0.6	100 ± 0
	Previous year growth	217.0 ± 29.5	341.8 ± 85.9	
	SM	-	109 ± 30.9	
	Total (excl. SM)	374.5 ± 33.9	347.5 ± 86.1	
Pleurozium (heath canopy)	Current year growth	103.0 ± 31.2	70 ± 16.1	88 ± 13
	Previous year growth	119.5 ± 34.3	108.5 ± 23.4	
	SM	-	45.7 ± 7.3	
	Total (excl. SM)	222.5 ± 65.0	154.3 ± 30.0	

Table 2. Estimated percent cover and biomass of vascular plants in labelled heath plots on L + 407.

Tissue	**Estimated species cover [%] (± 1SE)**			
	Empetrum	Vaccinium	Rubus	Total
All	45 ± 19	14 ± 11	5 ± 4	65 ± 23
Tissue	**Biomass [g m^{-2}] (± 1SE)**			
	Empetrum	Vaccinium	Rubus	Total
Leaves (attached, senesced)	35.6 ± 12.4 (35.8 ± 14.9)	41.4 ± 14.6	11.9 ± 5.9	88.9 ± 29.8 (124.7 ± 43.2)
Stem	102.0 ± 34.0	24.1 ± 4.0	8.4 ± 5.5	134.5 ± 40.0
Coarse roots	34.2 ± 11.2	23.8 ± 5.1	3.4 ± 1.4	61.3 ± 16.7
Fine roots*	225.7 ± 57.6	113.5 ± 9.4	33.5 ± 15.6	372.8 ± 44.3
Total (incl. attached senesced)	433.4 ± 114.3	202.6 ± 28.7	57.3 ± 26.8	693.2 ± 134.8

* estimated from a general relationship between LAI and fine root biomass (V. Sloan unpublished data)

Table 3. ^{13}C enrichment (atom% above natural abundance), ^{13}C content (mmol ^{13}C m^{-2}) and % ^{13}C recovery in plant tissues on days L + 42 (18th Aug 2008) and L + 407 (18th Aug 2009)

Species	^{13}C L+42 (atom % ± 1SE)	^{13}C L+42 (mmol m^{-2} ± 1SE)	^{13}C L+407 (atom % ± 1SE)	^{13}C L+407 (mmol m^{-2} ± 1SE)	% ^{13}C recovery (± 1SE)
Sphagnum					
Capitulum	0.060 ± 0.018	2.62 ± 0.4	0.016 ± 0.0015	0.81 ± 0.2	32 ± 8
Sub-capitulum	0.016 ± 0.012	0.81 ± 0.3	0.021 ± 0.0030	1.52 ± 0.2	253 ± 72
2-3cm stem	n.d.	n.d.	0.0013 ± 0.0004	0.07 ± 0.02	n.d.
3-4cm stem	n.d.	n.d.	0.0004 ± 0.0001	0.02 ± 0.01	n.d.
Total		3.4 ± 0.7		2.4 ± 0.3	78 ± 16
Pleurozium					
Current year	0.0208 ± 0.0023	1.16 ± 0.43	0.0228 ± 0.0074	0.63 ± 0.23	67 ± 19
Previous year	0.0094 ± 0.0009	0.46 ± 0.17	0.0042 ± 0.0013	0.18 ± 0.07	60 ± 29
SM	n.d.	n.d.	0.0015 ± 0.0006	0.03 ± 0.012	n.d.
Total		1.62 ± 0.60		0.84 ± 0.31	67 ± 22
Empetrum					
Leaves (green)	0.0575 ± 0.0141	0.16 ± 0.08	0.0198 ± 0.0079	0.29 ± 0.12	67 ± 31
Leaves (senesced)	n.d.	n.d.	0.0091 ± 0.0027	0.16 ± 0.08	n.d.
Stem	0.0052 ± 0.0016	0.20 ± 0.08	0.0160 ± 0.0111	0.64 ± 0.4	285 ± 119
Coarse root	0.0020 ± 0.0029	0.03 ± 0.03	0.0038 ± 0.0020	0.07 ± 0.05	327 ± 357
Fine root	0.0124 ± 0.0016	1.18 ± 0.35	0.0068 ± 0.0040	0.84 ± 0.53	51 ± 28
Total		2.35 ± 0.73		1.99 ± 1.1	67 ± 32
Vaccinium					
Leaves	0.0141 ± 0.0012	0.23 ± 0.08	0.0123 ± 0.0016	0.36 ± 0.20	135 ± 42
Stem	0.0003 ± 0.0024	0.002 ± 0.02	0.0061 ± 0.0004	0.09 ± 0.01	98 ± 59
Coarse root	0.0068 ± 0.0023	0.064 ± 0.02	0.0026 ± 0.0010	0.02 ± 0.008	47 ± 16
Fine root	0.0010 ± 0.0007	0.054 ± 0.03	0.0017 ± 0.0007	0.08 ± 0.03	108 ± 100
Total		0.34 ± 0.10		0.52 ± 0.24	166 ± 53
Rubus					
Leaves	0.0418 ± 0.0241	0.40 ± 0.32	0.0010 ± 0.0010	0.0053 ± 0.0052	-67 ± 68
Stems	0.0387 ± 0.0182	0.22 ± 0.17	0.0059 ± 0.0045	0.025 ± 0.012	211 ± 181
Coarse root	0.0084 ± 0.0072	0.020 ± 0.02	0.0014 ± 0.0016	0.0028 ± 0.0025	961 ± 707
Total		0.64 ± 0.51		0.033 ± 0.017	22 ± 24

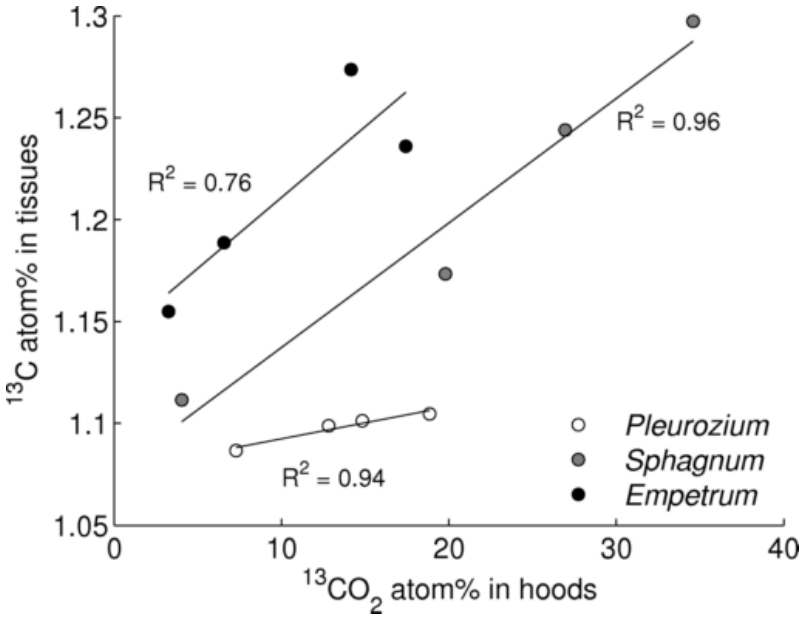

Figure 1. The initial ^{13}C content in tissues (time point L + 0) versus the mean concentration of ^{13}C during labelling.

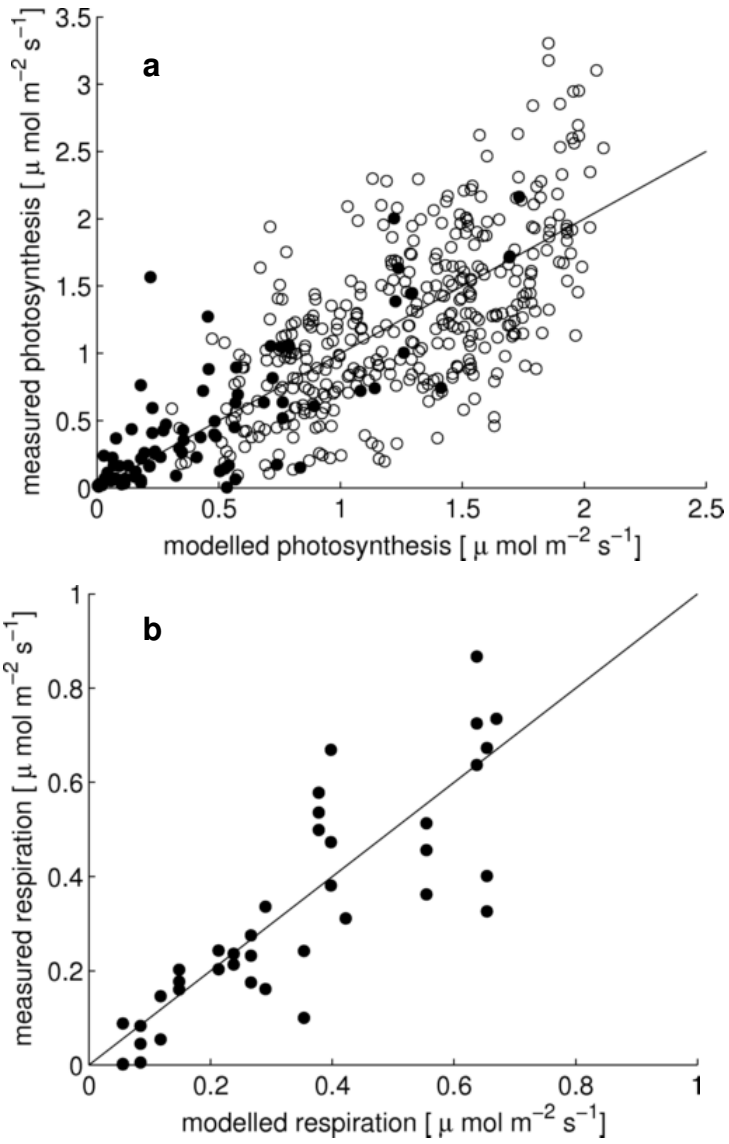

Figure 2. Modelled vs. measured a) gross photosynthesis and b) respiration for *Pleurozium* from 0.2 x 0.2m chamber data. Lines are 1:1 line

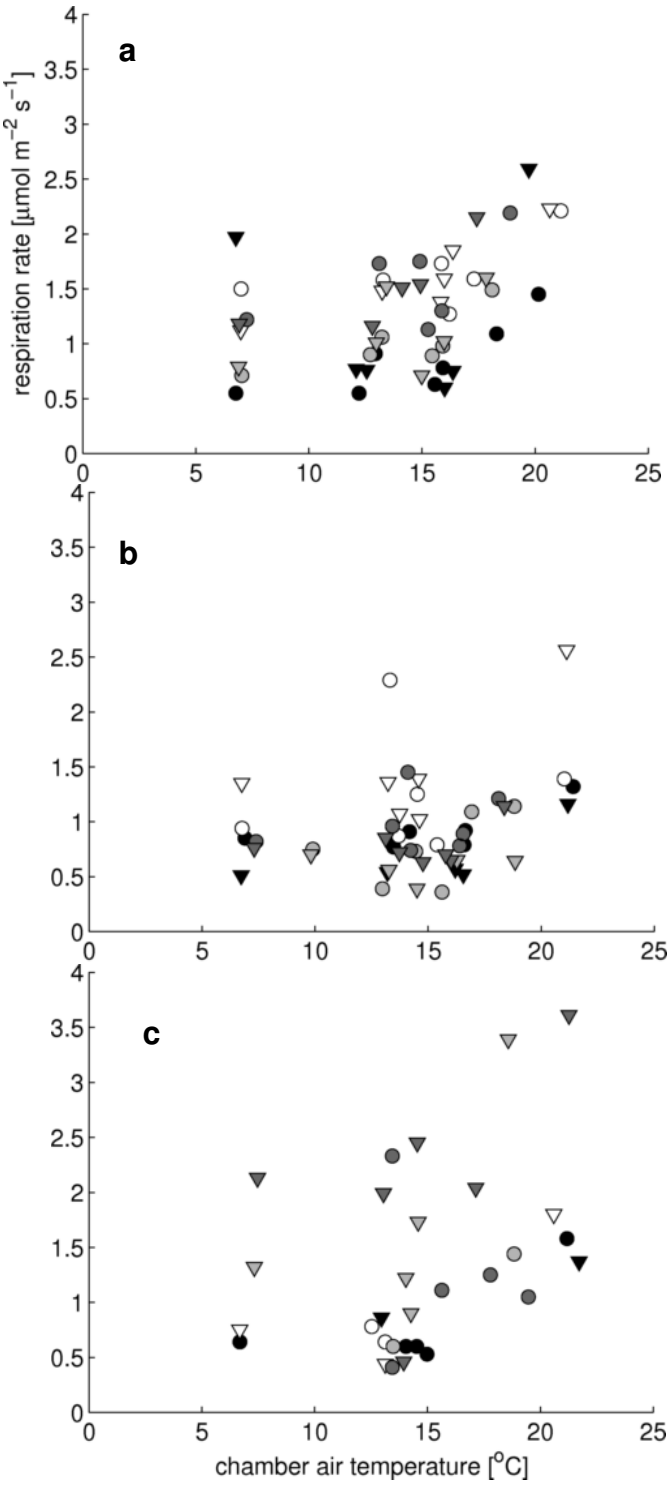

Figure 3. Measurements of ecosystem respiration for a) *Sphagnum* b) *Pleurozium* c) heath plots. Triangles are 'light' treatments, circles are 'dark' treatments, grey shades are different plots

5a. Turnover of recently assimilated carbon in Arctic bryophytes

Lorna E. Street [1], Jens-Arne Subke[2,3], Martin Sommerkorn[4], Andreas Heinemeyer[2], MathewWilliams[1]

[1]School of Geosciences, University of Edinburgh, Edinburgh, EH9 3JN, UK

[2]Stockholm Environment Institute York, Environment Department, University of York, York, YO10 5DD, UK

[3]School of Biological and Environmental Sciences, University of Stirling, Stirling, FK9 4LA, UK

[4]Macaulay Land Use Research Institute, Craigiebuckler, Aberdeen, AB15 8QH, UK

(published in Oecologia as Street, L., Subke, J., Sommerkorn, M., Heinemeyer, A., & Williams, M. (2011) Turnover of recently assimilated carbon in arctic bryophytes. Oecologia. DOI: 10.1007/s00442-011-1988-y.*)*

Abstract

Carbon (C) allocation and turnover in Arctic bryophytes is largely unknown, but their response to climatic change has potentially significant impacts on Arctic ecosystem C budgets. Using a combination of pulse-chase experiments and a newly developed model of C turnover in bryophytes, we show significant differences in C turnover between two contrasting Arctic moss species (*Polytrichum piliferum* and *Sphagnum fuscum).* ^{13}C abundance in moss tissues (measured up to 1 year) and respired CO_2 (traced over 5 days) were used to parameterise the bryophyte C model with four pools representing labile and structural C in photosynthetic and stem tissue. The model was optimised using an Ensemble Kalman Filter to ensure a focus on estimating the confidence intervals (CI) on model parameters and outputs. The ratio of aboveground NPP:GPP in *Polytrichum piliferum* was 23 % (CI 9% - 35 %), with an average turnover time of 1.7 days (CI 1.1 - 2.5 days). The aboveground NPP:GPP ratio in *Sphagnum fuscum* was 43 % (CI 19 % - 65 %) with an average turnover time of 3.1 days (CI 1.6 - 6.1 days). These results are the first to show differences in C partitioning between arctic bryophyte species *in-situ* and highlight the importance of modelling C dynamics of this group separately from vascular plants for a realistic representation of vegetation in Arctic C models.

Introduction

High latitude terrestrial ecosystems are of global importance, because they currently store an estimated 50 % of the total global belowground organic C pool (Tarnocai *et al.* 2009). The Arctic climate has warmed by about 0.4°C per decade since the 1960s (McBean *et al.* 2005), and is forecast to warm by > 5°C by 2100 (Christensen *et al.* 2007). If this warming results in a release of CO_2 or CH_4 to the atmosphere, this could represent an amplifying feedback on global climate change. The C balance of Arctic ecosystems has therefore become the focus of global concern. Bryophytes (the mosses, liverworts and hornworts) are a major component of Arctic vegetation (Walker, 2000). However, in contrast to many vascular plants we lack detailed data on bryophyte C allocation and turnover which is needed to

assess their overall contribution to the C balance of tundra ecosystems, and the likely changes to this contribution following climatic change.

Understanding the C balance of ecosystems requires quantification of the net C uptake and storage by vegetation (Net Primary Productivity, NPP). NPP is the difference between the fixation of CO_2 as sugars in plant leaves through photosynthesis (Gross Primary Productivity, GPP), and the return of a proportion of those sugars as CO_2 through autotrophic respiration (R_a). The ratio of NPP:GPP for whole ecosystems is often assumed to be constrained at or close to 50% (Trumbore, 2006; Waring *et al.*, 1998), though empirical data indicates substantial variation for different ecosystems (Gifford, 2003). There is also large uncertainty over the length of time C resides in different plant pools once incorporated, i.e. how quickly assimilated C is turned over and returned to the atmosphere as CO_2.

Mechanistic representation of GPP in vascular plants at the ecosystem scale is well developed (Shaver *et al.* 2007, Street *et al.* 2007, Williams *et al.* 2006), but allocation of recent photosynthate among plant tissues, and the simulation of R_a and its dependence on temperature, phenology, and plant functional type are not (Cannell & Thornley, 2000). The limited theoretical underpinning of GPP partitioning in models is based exclusively on work in higher plants (Amthor, 2000). However, estimates suggest that bryophyte NPP is a significant fraction of total above ground NPP in the Arctic; for example 0.2 g m^{-2} d^{-1} or about 30% of aboveground NPP in Alaskan tussock tundra (Chapin *et al.* 1995), 0.3 g m^{-2} d^{-1} or about 30% in coastal tundra at Barrow (Miller *et al.* 1980), and 0.5 g m^{-2} d^{-1} or 25% of aboveground NPP in late summer in Scandinavian tundra heath (Campioli *et al.* 2009). Understanding the NPP:GPP ratio, and the storage of C in Arctic vegetation therefore, requires an understanding of C allocation and turnover processes in bryophytes.

Bryophyte ecophysiology differs markedly from vascular plants, though photosynthesis follows a C_3 pathway (Proctor, Raven & Rice, 1992). Bryophytes are smaller and slower growing, with little or no supportive tissue, storage organs or true roots. The genus *Polytrichum* has some internal conducting tissues (Ayres *et al.* 2006), which allow upward movement of water from the substrate, and some active transport of assimilate to belowground parts including emerging shoots (Thomas *et*

al., 1988). *Sphagnum* grows from the shoot apex, and maintains tissue water content by retaining water within metabolically inactive hyaline leaf cells (Vitt & Wieder, 2009). With these different growth strategies, we expect the respiratory costs of tissue growth and maintenance, and therefore the allocation of recently fixed carbon to differ between bryophyte species and to that of vascular plants.

C isotope pulse-labelling has been widely used to track the fate of photosynthesised C through the soil-plant system (Dawson *et al.* 2002, Bowling, Pataki & Randerson, 2008). In order to address the gap in our knowledge regarding the role of bryophytes in Arctic C dynamics, we followed a ^{13}C pulse label in Arctic bryophyte communities, dominated by *Polytrichum piliferum* (Hedw.) and *Sphagnum fuscum* ((Schimp.) H. Klinggr.) *in-situ*. For the first time we continuously measured the respiratory return of $^{13}CO_2$ for 5 days using a field deployed mass spectrometer. We built a simple model of bryophyte photosynthesis and C turnover to address the following questions: 1) what is the ratio of NPP:GPP, 2) what is the turnover time (TT) of recently photosynthesised carbon, and 3) how do differences in C allocation and turnover relate to morphological complexity?

Materials and Methods

Site description

We located our field site near Abisko in Northern Sweden, on a hillside approximately 6 km south of Lake Torneträsk (68°18′N, 18°51′E). Mean annual air temperature in the Abisko valley is -1 °C, mean July temperature 11 °C and annual precipitation around 300 mm. The sun does not set between the beginning of June and mid-July, but photosynthetic photon flux density (PPFD) is low (~25 µmol m^{-2} s^{-1}) at midnight even during mid-summer (Abisko Research Station (ANS) website, http://www.linnea.com/~ans/ans.htm). The vegetation at the site is mainly comprised of ericaceous tundra heath, with deciduous shrubs in sheltered snow beds, and barren cryptogam dominated vegetation on exposed ridges. Where drainage is impeded there are sedge and *Sphagnum* dominated communities. *Sphagnum fuscum* grows in hummocks in the wet sedge areas, and *Polytrichum piliferum* is locally abundant in more freely drained rocky areas with thinner soils.

Overview of experimental set-up

We pulse-labelled four replicate plots of *Sphagnum* (*Sp1 - Sp4*) and *Polytrichum* (*Po1 - Po4*) on 8th July 2007. We monitored the return of ^{13}C in respired CO_2 from these plots over 5 days, and sampled moss tissues for ^{13}C content daily for five days, then at two weeks, six weeks and one year after labelling. The time-series of ^{13}C content in tissues allowed us to parameterise a model of C turnover.

Pulse labelling

We applied CO_2 of 98% atom enrichment in ^{13}C at a concentration of 375 μl l^{-1} from 16:00 to 18:15 local time on 8th July 2007 using 0.55 × 0.55 × 0.2 m clear acrylic labelling hoods. Before labelling all vascular plants were removed from the plots by clipping stems at the level of the bryophyte surface, and manual watering ensured sufficient moisture for photosynthesis (see Online Resource 1 for details on plot preparation). In order to quantify the physical uptake of pulse-derived (PD) $^{13}CO_2$ (through dissolution in surface moisture, or diffusion into surface air spaces) *vs.* biological uptake through photosynthesis, we darkened one half of the labelling hood to prevent photosynthetic uptake by attaching a cardboard partition down the middle and covering one half with black plastic film (see Online Resource 1). PPFD varied between 440 and 870 μmol m^{-2} s^{-1} during labelling on the 'light' side of the plots. We cut around the plots and between the light and dark sides with a knife to a depth of approximately 15 cm to prevent potential lateral translocation of the label. Sampling of bryophyte material, as well as $^{13}CO_2$ flux measurements, was carried out at the centre of plots to avoid edge effects from disturbance to the moss carpet from the Perspex hood and possible light ingression on the 'dark' side. We took gas samples of $^{13}CO_2$ concentration inside hoods once every hour during the labelling period for later analysis.

^{13}C in ecosystem respired CO_2

We began monitoring the return of $^{13}CO_2$ at 18:24 on the day of labelling. We monitored $^{13}CO_2$ from labelled and non-labelled control (natural abundance, NA) plots using 0.2 m diameter opaque collars placed onto the moss surface. Any gaps between the collar and the ground were filled with bubble plastic. The CO_2

concentration and $^{13}C/^{12}C$ isotopic ratio in sample lines from soil chambers were measured directly in the field using isotope ratio mass spectrometry (IRMS), in the "York Mobile Lab". For technical details of the mass spectrometry, see Online Resource 1 and Subke *et al.* (2009). The York Mobile Lab was set up to sample CO_2 from the labelled and NA collars in sequence (*Sp1, Po1, Sp2, Po2, … SpNA1, PoNA1*), with a full sampling cycle taking 1 hour, and composed of the ten collar lines as well as one reference gas and one ambient air line. After two sampling cycles all the collars were switched over to the opposite side of the plot ('light' side to 'dark' side or *vice-versa*). Overnight the number of sampling cycles between switching collars was increased to four. The result was at least one sample of ecosystem respired $^{13}CO_2$ every 2 - 4 hours from all the 'light' sides of the labelled plots measured consecutively, followed by $^{13}CO_2$ samples from the 'dark' sides every hour for 2 - 4 hours. We continued sampling for 5 days until 12:00 on the 12th July, with a gap in sampling from 12:00 - 20:00 11th July. Gas samples from the labelling hoods collected in Exetainers (12 ml gas tight glass vials, Labco, High Wycombe, UK) during labelling were also analysed by the York Mobile Lab after the end of the field deployment (see Online Resource 1).

^{13}C in moss tissues

Samples of moss material were collected daily from the labelled plots during late afternoon from 8th - 12th July, on the 27th July, and 19th August 2007. We sampled tissues from the dark side of the plots on the 8th, 10th and 12th July, and took NA samples on 8th, 10th and 12th July and on 19th Aug 2007. The green leaves of several *Polytrichum* shoots ('photosynthetic' tissue) were sampled, together with the next 1 cm of stem from each shoot ('stem' tissue). For *Sphagnum* we separated the capitulum tissue (approximately the top 0.5 cm of the shoot, hereafter referred to as 'photosynthetic' tissue) from the next 1 cm (the sub-capitulum, for convenience hereafter referred to as 'stem' tissue) of several shoots. Samples were transported from the field and frozen at -20°C within 3 hours of sampling, except for 8th - 10th July, when logistical constraints prevented us from transporting the samples immediately back to the laboratory at ANS. In this case samples were kept in cool storage (below 10°C), in the field and were frozen the following day. On 27th July

2007 and 28th June 2008 we also sampled moss tissues deeper in the profile, in 4 cm × 4 cm cores separated into 1 cm horizontal sections below the *Polytrichum* stem tissue and *Sphagnum* sub-capitulum tissue. In August 2009 we destructively sampled mosses from within the area measured by the collars, and separated into 1 cm horizontal sections to measure total moss biomass in each layer. All samples were stored at -20°C for about 3 weeks and then dried for 3 days at 70°C and milled (Mixer Mill MM200, Retsch, Haan, Germany). The 2007 samples were analysed for $^{13}C/^{12}C$ ratios, and %C content on an IRMS at the Macaulay Land Use Research Institute, 2008 tissue samples were analysed at York University (see Online Resource 1 for technical details).

GPP measurements

To corroborate the GPP component of our bryophyte carbon turnover model we compared modelled GPP based on laboratory measurements (see Online Resource 1) to 26 GPP light response curves measured in the field on the same species nearby the experimental area. We measured net ecosystem exchange (NEE) of CO_2 per unit ground area of three replicate plots of *Polytrichum* and *Sphagnum*, on 21st June, 29th June, 4th July and 20th July using a 20 cm x 20 cm Plexiglas chamber connected to a LI-COR 6400 photosynthesis system in closed system mode. To measure a light response curve we successively darken the chamber using sheets of optically neutral netting. We calculated GPP by adding ecosystem respiration (ER), measured under fully darkened conditions, to the net CO_2 flux. Closed chamber flux methods follow Douma *et al.* (2007).

Bryophyte Turnover (BT) model structure

Following isotopic labelling, the concentration of ^{13}C in bulk photosynthetic tissues decreases over time. While the tissue is alive, the decrease is a result of ^{13}C loss through R_a, any translocation out of the tissue, and potential dilution by new unlabelled photosynthate. To take account of these processes, including the dilution effect of new growth following labelling, we built a simple four-pool model of bryophyte productivity and photosynthate turnover.

The BT model operates on a 10 min time step, and consists of four C pools (Fig. 1): (1) a labile (fast turnover) carbon pool in photosynthetic tissue (2) a structural

(slow turnover) pool in photosynthetic tissue and (3) labile pool in non-photosynthetically active 'stem' tissue and (4) a structural C pool in 'stem' tissue (stem in *Polytrichum*, sub-capitulum tissue in *Sphagnum* (Table 1)). We assume there is no photosynthesis in the 'stem' tissue in *Polytrichum*, and *Sphagnum*. Carbon influx is to the labile C pool in photosynthetic tissue as GPP. There is a translocation flux of labile C from photosynthetic to 'stem' tissue in both species (A_t), and labile C is incorporated into structural C in both photosynthetic and stem components via an allocation flux (A_g and A_s). C loss from the photosynthetic labile pool is via respiration (R_g), from the stem labile pool via respiration and translocation to deeper belowground tissues (R_s and A_d), and from the structural pool via litter loss (L_g and L_s) (Table 1).

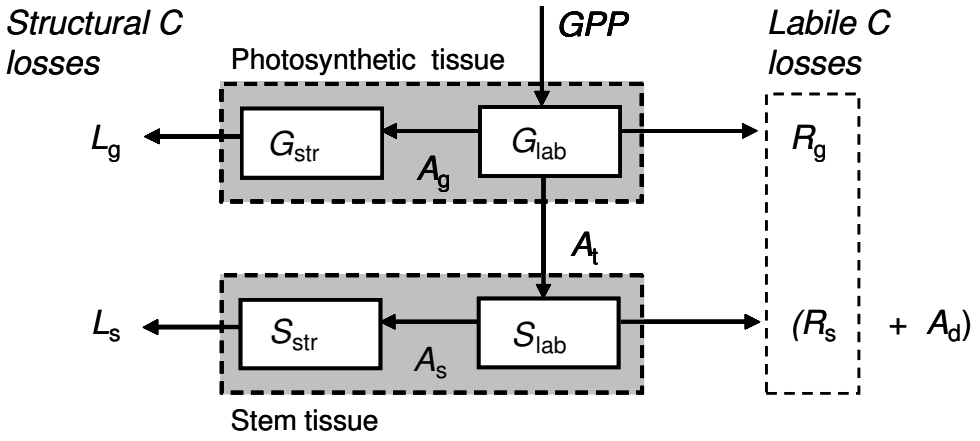

Figure 1. The bryophyte turnover (BT) model. Dashed boxes indicate pools or fluxes for which the bulk carbon isotope ratio was determined following pulse labelling. G_{str} and G_{lab} are structural and labile C pools in photosynthetic tissue. S_{str} and S_{lab} are structural and labile C in non- photosynthetic 'stem' tissue. R_g and R_s are respiration fluxes from the labile C pools. *GPP* is the input of C to the model via photosynthesis. A_g is the allocation flux from labile to structural C in photosynthetic tissues, A_s is the allocation flux from labile to structural C in stem tissues, A_t is the translocation flux of labile C from photosynthetic tissue to stem tissues, A_d is belowground translocation, L_g and L_s are litter loss fluxes from the structural pools.

There are 11 parameters in the model (Table 1). Three are photosynthesis parameters (p_t, p_c, and p_k) describing the response of GPP to light and temperature (equations 1 and 2). These parameters are based on laboratory measurements described in Online Resource 1. Three fitted parameters describe the exponential temperature response of respiration; a basal rate for photosynthetic and stem tissue (r_g and r_s) and the exponent (r_c). We assume that only the basal respiration rate

differs between tissue types, and in stem tissue the basal rate of respiration implicitly includes deeper translocation A_d. A further three fitted parameters are linear coefficients controlling allocation fluxes in photosynthetic (a_g) and stem tissue (a_s) and the translocation of labile C from photosynthetic to stem tissue (a_t). l_g and l_s are fitted litter loss parameters. The model is run in a paired mode. One model version describes ambient natural abundance conditions (the NA model). The other model version simulates the pulse labelling and the fate of that pulse (the PD model). The two models are combined to provide estimates of isotopic fractions over time. Pools, fluxes and parameters for the PD model are given a subscript *l*. For model equations see Table 2.

We modelled the photosynthesis of each moss species using data from the laboratory based CO_2 flux measurements. We modelled GPP with P_{max} as a linear response of temperature:

$$P_{\max} = p_t T + p_c \quad (1)$$

$$GPP = \frac{P_{\max} I}{I + k} \quad (2)$$

where T is moss temperature (°C), I is incident photosynthetically active radiation (μmol m^{-2} s^{-1}), k is the half-saturation constant of photosynthesis (μmol m^{-2} s^{-1}), and p_c and p_t are parameters fitted using linear regression in Matlab 7.1. We were then able to model GPP over the course of the growing season using 10 minute incident radiation data provided by ANS, and local moss temperature data from the field GPP measurement plots, recorded using HOBO Micro Station dataloggers and temperature probes (Onset, MA, USA). During the labelling period we used light and temperature data measured within the hoods using the LICOR 6400.

Table 1. Description of carbon pools, fluxes, parameters and model drivers for the BT model with units. P_{max} is the theoretical light saturated rate of GPP (equation 2)

Pools	Description	Units
G_{lab}	Labile C in photosynthetic tissue	mol C
G_{str}	Structural C in photosynthetic tissue	mol C
S_{lab}	Labile C in stem tissue	mol C
S_{str}	Structural C in stem tissue	mol C
Fluxes		
GPP	Gross photosynthesis	mol C hr^{-1}
R_g	Respiration from photosynthetic tissue	mol C hr^{-1}
R_s	Respiration from stem tissue	mol C hr^{-1}
A_t	Translocation photosynthetic tissue to stem tissue	mol C hr^{-1}
A_d	Translocation to below ground stems and rhizome	mol C hr^{-1}
A_g	Allocation to structural C in photosynthetic tissue	mol C hr^{-1}
A_s	Allocation to structural C in stem tissue	mol C hr^{-1}
L_g	Litter loss photosynthetic tissue	mol C hr^{-1}
L_s	Litter loss stem tissue	mol C hr^{-1}
Drivers		
T	Moss temperature	°C
I	Photosynthetic photon flux density	µmol m^{-2} s^{-1}
E	^{13}C enrichment inside labelling hood*	Atom%
Parameters		
p_t	Slope of P_{max} vs. temperature	mol C mol C^{-1} hr^{-1} $°C^{-1}$
p_c	Intercept of P_{max} vs. temperature	mol C mol C^{-1} hr^{-1}
p_k	GPP light response half-saturation constant	umol m^{-2} s^{-1}
r_g	Basal respiration rate photosynthetic tissue	mol C mol C^{-1} hr^{-1}
r_s	Basal respiration rate stem tissue	mol C mol C^{-1} hr^{-1}
r_c	Exponent respiration temperature response	
a_t	Translocation rate	mol C mol C^{-1} hr^{-1}
a_g	Allocation rate photosynthetic tissue	mol C mol C^{-1} hr^{-1}
a_s	Allocation rate stem tissue	mol C mol C^{-1} hr^{-1}
l_g	Litter loss rate photosynthetic tissue	mol C mol C^{-1} hr^{-1}
l_s	Litter loss rate stem tissue	mol C mol C^{-1} hr^{-1}

*above natural abundance (NA) in air

Table 2. Bryophyte turnover model equations

Natural abundance model	Pulse derived model
Pools	
$G_{lab} = GPP - R_g - A_g - A_t$	$G_{lab\_l} = GPP_l - R_{gl} - A_{gl} - A_{tl}$
$G_{str} = A_g - L_g$	$G_{str\_l} = A_{gl} - L_{gl}$
$S_{lab} = A_t - R_s - A_s$	$S_{lab\_l} = A_{tl} - R_{sl} - A_{sl}$
$S_{str} = A_s - L_s$	$S_{str\_l} = A_{sl} - L_{sl}$
Fluxes	
$GPP = \left(\frac{(p_t T + p_c) I}{I + p_k} (G_{lab} + G_{slow}) \right) * (1 - E)$	$GPP_l = \left(\frac{(p_t T + p_c) I}{I + p_k} (G_{lab} + G_{slow}) \right) * (E)$
$C_{loss} = R_g + R_s + A_d$	$C_{lossl} = R_{gl} + R_{sl} + A_{dl}$
$R_g = r_g e^{(r_c T)} G_{lab}$	$R_{gl} = r_g e^{(r_c T)} G_{lab\_l}$
$R_s = r_s e^{(r_c T)} S_{lab}$	$R_{sl} = r_s + a_d e^{(r_c T)} S_{lab\_l}$
$A_g = a_g G_{lab}$	$A_{gl} = a_g G_{lab\_l}$
$A_t = a_t G_{lab}$	$A_{tl} = a_t G_{lab\_l}$
$A_s = a_s S_{lab}$	$A_{sl} = a_s S_{lab\_l}$
$L_g = l_g G_{str}$	$L_{gl} = l_g G_{str\_l}$
$L_s = l_s S_{str}$	$L_{sl} = l_s S_{str\_l}$

BT model initial conditions

Initial bryophyte biomass in the model was set at a nominal 1 mol C m^{-2}, and the initial fraction of labile carbon was set at 5% (approximated from published values of 6% for non-structural carbohydrate in *Polytrichum alpinum* (Sveinbjornsson & Oechel, 1981) and 3% water-soluble carbohydrates in *Sphagnum fuscum* (Turetsky *et al.* 2008). The ratio of stem to photosynthetic tissue was set at 1:1 in *Polytrichum* and 1:0.81 in *Sphagnum*, based on the relative mass of samples collected in the field. We ran the model for a 2 week 'spin-up' period, before simulating labelling. By the beginning of the labelling period the modelled labile fraction in *Polytrichum* had stabilised to 7 - 9 % and in *Sphagnum* to 4 - 6 %.

Model - data comparison

In order to simulate the turnover of ^{13}C label two identical versions of the BT model were run side by side using the same driving data. The NA version represented the pools and fluxes of C at NA ^{13}C atom%. The second version, the 'pulse-derived' (PD) model represented the flux and turnover of excess ^{13}C supplied during the labelling period. The PD ^{13}C input flux was calculated by multiplying modelled GPP by an enrichment (*E*) in the labelling hoods of 7 % (atom% ^{13}C above the NA of ^{13}C in air). In reality the enrichment in the labelling hoods varied between individual hoods. In order to compare the model to a single field data set for each species, we normalised the PD ^{13}C content in gases and tissues (to a labelling hood head space concentration of 7 atom%) then averaged across replicates. *E* was set to zero after 130 minutes, the duration of the labelling period. During the labelling period the NA GPP flux was multiplied by 1 - *E*. For the five days following labelling, we set *E* to the $^{13}CO_2$ atom% measured in the CO_2 sampling collars, to allow for re-fixation of respired $^{13}CO_2$. The PD model then operated identically to the NA model using the same parameter values but with no further ^{13}C input.

The atom% of PD ^{13}C in photosynthetic (G_{ap}) and stem (S_{ap}) tissue was calculated at each time step from the output of the two models:

$$G_{ap} = \left(G_{lab\_l} + G_{str\_l}\right) / \left(G_{lab\_l} + G_{str\_l} + G_{lab} + G_{str}\right) * 100 \qquad (3)$$

$$S_{ap} = \left(S_{lab\_l} + S_{str\_l}\right) / \left(S_{lab\_l} + S_{str\_l} + S_{lab} + S_{str}\right) * 100 \quad (4)$$

Where *G* is photosynthetic tissue, *S* is stem tissue, *lab* is labile, *str* is structural, *ap* is atom%. The subscript *l* indicates fluxes from the PD model, all other fluxes are from the NA model. See Table 1 for full variable descriptions and units. We calculated the PD ^{13}C content of sampled moss tissues by subtracting NA atom% ^{13}C in each tissue type from measured atom% ^{13}C.

The total PD loss of ^{13}C from labile pools (C_{lossl}) (mol ^{13}C m^{-2} hr^{-1}) in the model was the sum of respiration from the photosynthetic and stem components of the PD model (with deeper translocation implicit in the stem respiration term):

$$C_{loss\,l} = (R_{gl} + R_{sl}) \quad (5)$$

We compared modelled C_{lossl} with the biological respiratory return of ^{13}C ($R_{gl} + R_{sl}$) measured in the field over 5 days following labelling, which we calculated by subtracting the diffusive ^{13}C flux (from the 'dark' side of the plot), from the total biological and diffusive ^{13}C flux from the 'light' side. The ^{13}C flux from the darkened side of the plot also included biological ^{13}C flux at NA, so we assumed that 'light' minus 'dark' ^{13}C flux is entirely biological PD ^{13}C. We linearly interpolated measured $^{13}CO_2$ fluxes to calculate total ^{13}C loss in respiration over 5 days. Gaps in the measured $^{13}CO_2$ flux data were filled by assuming a consistent offset between modelled and measured fluxes. Because occasional gusts of wind caused some leakage of air from the collars, the absolute amount of CO_2 recorded in the sample lines could not be regarded as an accurate estimate of respiration from the area enclosed by the collars. As we could not correct for this loss, respiration fluxes were instead based on temperature regressions for independent closed chamber measurements made with a LI-COR 8100 Soil CO_2 Flux System (LI-COR Inc., Lincoln, Nebraska, USA) attached to a 20 cm diameter survey chamber. These respiration measurements were carried out daily for five days after pulse-labeling. Isotope ratio estimates obtained by the mass spectrometer were valid, however, as ambient air concentrations of ^{12}C and ^{13}C were subtracted from the respective concentrations of the sample gas. Any enrichment in either CO_2 isotope with regard to ambient CO_2 concentrations therefore originated from respiratory processes within

the chamber, and any possible leakage would not affect the isotopic ratio. Since small levels of CO_2 enrichment in the sample gas are prone to larger errors, isotope ratio estimates were only considered if the respiration-derived CO_2 in the sample gas amounted to more than 50 µmol mol^{-1}.

Model optimisation

The BT model (PD and NA versions running simultaneously) was optimised using an Ensemble Kalman Filter (EnKF; Fox *et al.* 2009, Williams *et al.* 2005). The EnKF was chosen because it can determine the uncertainty on resulting parameter estimates and model predictions (se Online Resource 1 for more details on the EnKF analysis). In order to avoid potential bias due to suspected inadequate sample storage over the first 3 days all optimisations were initially carried out using only data from 11th July onwards (4 time points), for which we had full confidence in the sample storage. We also excluded a *Sphagnum* plot which had very low $^{13}CO_2$ enrichment during labelling (< 2%), due to large errors relative to signal in the tissue data. After initial optimization we identified data which fell below the modelled 95% confidence interval (8th July for *Polytrichum*, 8th and 9th July for *Sphagnum*) and repeated the analysis with all the data except for these points. Final optimisation was therefore on tissue data from 9th July onwards for *Polytrichum* (i.e. 6 sampling time points) and 10th July onwards for *Sphagnum* (5 sampling time points). The outcome of the EnKF process was an ensemble of parameter sets statistically consistent with the model, the observations, and their relative errors.

We used modelled GPP and the sum of the allocation fluxes (A_g and A_s) in the natural abundance model to calculate the ratio of NPP to GPP over 5 days following labelling. We define TT to be the time taken for 50% of the recently fixed labile C pool to be either allocated to slow turnover (structural) pools or respired as CO_2. To quantify TT we calculated the time taken for 50% of the PD ^{13}C to be turned over in the model (respired or allocated to structural components). We expressed the measured and predicted amount of PD ^{13}C remaining in the tissue as a percentage of the modelled ^{13}C assimilated during the labelling period.

Model and observation uncertainty

We used the error variance in observed tissue PD atom% ^{13}C across plots for each species to inform the EnKF. The minimum SD was 0.001 atom% ^{13}C and maximum SD was 0.005 atom% ^{13}C for *Sphagnum* and 0.002 atom% ^{13}C and 0.007 atom% ^{13}C for *Polytrichum*. We assessed the model fit for forward runs of each ensemble member by calculating the chi-squared value, with *n-p*-1 degrees of freedom:

$$\chi^2 = \sum_{1}^{n} \frac{1}{\sigma^2_{Yi}} [(y_{i,meas}(x_i) - y_{i,\mathrm{mod}}(x_i : p)]^2 \quad (6)$$

Where n is the total number of measurements (of photosynthetic and stem atom% PD ^{13}C), p is the number of model parameters (8), $y_{i,meas}(x_i)$ is the measured value of output variable y (either G_{ap} or S_{ap}) at the value x_i of the driving variable x, $y_{i,mod}(x_i;p)$ is the modelled value of the output variable (either G_{ap} or S_{ap}) at the value x_i of the driving variable x given the parameters p, and σ^2_{yi} is the maximum measurement error variance for each species. The degrees of freedom for *Sphagnum* were 21 (n = 30, stem and photosynthetic tissue for 5 times points and 3 replicate plots), for *Polytrichum* 39 (n = 48, with stem and photosynthetic tissue for 6 times points and 4 replicate plots). We then retained only those ensemble forward runs with chi-squared values less than the critical value at the 5% level (Williams *et al.*, 2006). We calculated a 90% confidence interval (CI) on NPP:GPP and TT by excluding the most extreme upper 5% and lower 5% of NPP:GPP and TT values which result from forward runs of the ensemble members which pass the chi-square test.

All model parameters and initial conditions were tested for sensitivity by varying each parameter individually by +100% or -50% and assessing the effect on the RMSE and r^2 of modelled vs. predicted PD atom% ^{13}C, the NPP:GPP ratio, and the labile C TT.

Results

Pulse-labelling

The average enrichment (atom% above NA) of $^{13}CO_2$ inside the hoods during pulse-labelling varied between 1.5 and 15.5 atom%, and there was a positive linear correlation with the initial ^{13}C enrichment in the photosynthetic tissues immediately after labelling for both species ($R^2 = 0.98$ for *Polytrichum*, $R^2 = 0.89$ for *Sphagnum*). Darkening the hoods was effective in preventing $^{13}CO_2$ uptake into the tissues via photosynthesis (Fig. 2) in all but one plot (*Po4*). Excluding *Po4*, the average tissue enrichment of *Polytrichum* photosynthetic tissue on the dark side of the plot was 0.0008 ± 0.0008 atom%, and for *Sphagnum* capitula 0.0001 ± 0.0002 atom%. The enrichment of photosynthetic tissue in the dark side of plot *Po4* was < 20% of the enrichment in the light side, and this plot was included in subsequent analysis. We detected pulse-derived ^{13}C in ecosystem respired CO_2 from both the dark and light sides of the labelling plots immediately after labelling (see Fig. 3 for example data for each species). $^{13}CO_2$ enrichment decreased rapidly over the first day, in both 'light' and 'dark sides of the plot, though ^{13}C enrichment of CO_2 was apparent in the 'light' side of some plots 5 days after labelling.

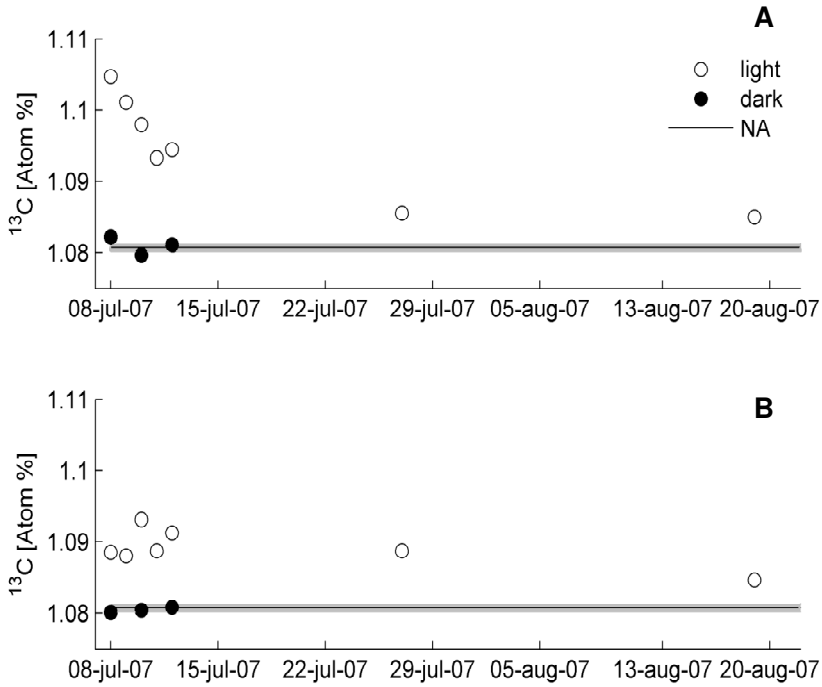

Figure 2. Atom% ^{13}C content of a) *Polytrichum* and b) *Sphagnum* photosynthetic tissues from 'light' and 'dark' treatments. Grey bar indicates NA ± 1SE.

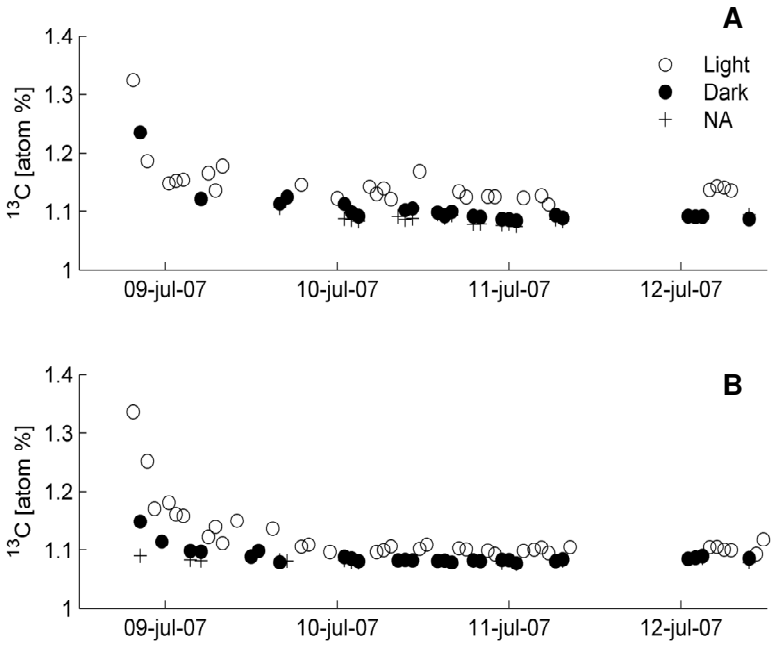

Figure 3. Atom% ^{13}C of ecosystem CO_2 flux from a) *Polytrichum* (*Po2*) and b) *Sphagnum* (*Sp3*) light and dark treatments.

Light response of GPP

The photosynthetic rate in *Polytrichum* was almost 3× that of *Sphagnum*; fitted P_{max} for *Polytrichum* was 0.027 µmol C g^{-1} s^{-1}, and 0.010 µmol C g^{-1} s^{-1} for *Sphagnum* at 20°C (Fig. 4a). Photosynthesis also saturated at lower light levels in *Sphagnum* (the average half-saturation constant, *k*, for *Sphagnum* was 75 µmol m^{-2} s^{-1}, for *Polytrichum* 130 µmol m^{-2} s^{-1}). P_{max} for both species increased with temperature between 5°C and 20°C (Fig. 4a). Modelling GPP using laboratory based light and temperature response curves (on a per unit area basis), produced reasonable results when compared to field data (for *Polytrichum* $r^2 = 0.74$, for *Sphagnum* $r^2 = 0.66$, Fig. 4b).

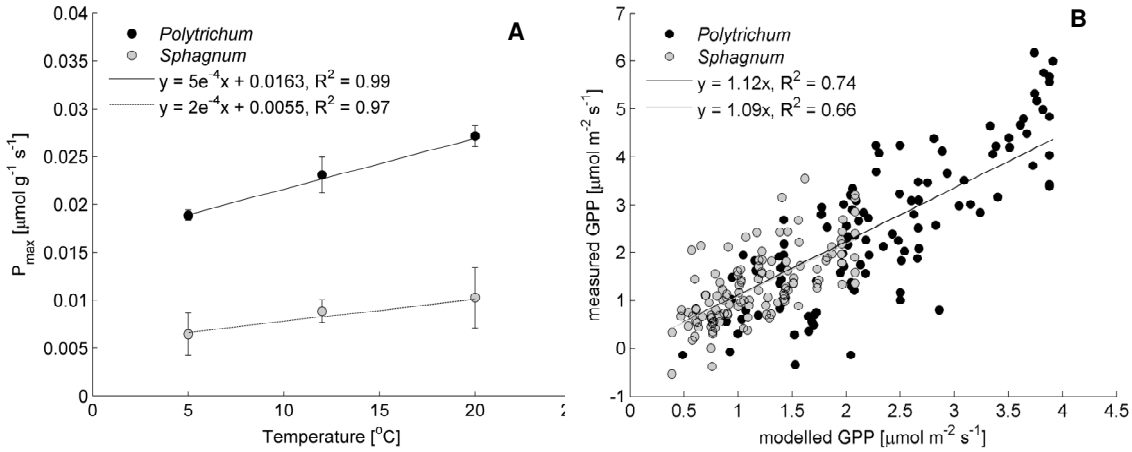

Figure 4. a) Fitted light saturated photosynthesis (P_{max}) from laboratory based GPP light response curves for *Polytrichum* and *Sphagnum* b) Modelled vs. measured GPP for nearby patches of *Sphagnum* and *Polytrichum* between 20th June and 20th July 2007, using the BT GPP model with parameters p_t, p_c, and p_k.

C dynamics in tissues

Using the EnKF we found BT model parameterisations which were consistent with observations of PD atom% ^{13}C in photosynthetic and stem tissue 2 – 42 days after labelling (Fig. 5, and Online Resource 2, top row Tables 1 and 2). For *Polytrichum* 29 ensemble members had acceptable chi-square values at the 5% level, for *Sphagnum* 107 ensemble members had acceptable chi-squared values). For *Polytrichum* the forward run of the average acceptable parameters from the EnKF produced a linear regression of predicted *vs.* measured PD ^{13}C in photosynthetic tissue with an r^2 of 0.96 for a slope of 1.3; for stem tissue the r^2 was 0.83 and the

slope was 1.3. The BT model was also successful in predicting *Sphagnum* tissue ^{13}C content; predicted *vs*. measured PD ^{13}C in capitulum tissue had an r^2 0.94, and a slope 0.76. In stem tissue the r^2 was 0.02 for a slope of 0.27. The low r^2 for *Sphagnum* sub-capitulum tissue can be explained by the small relative magnitude of changes in tissue ^{13}C content relative to measurement error. The first *Polytrichum* tissue sample contained <100 % of the modelled ^{13}C uptake. For *Sphagnum*, samples over the first 2 days had significantly less ^{13}C than that predicted by the model (Fig. 5)

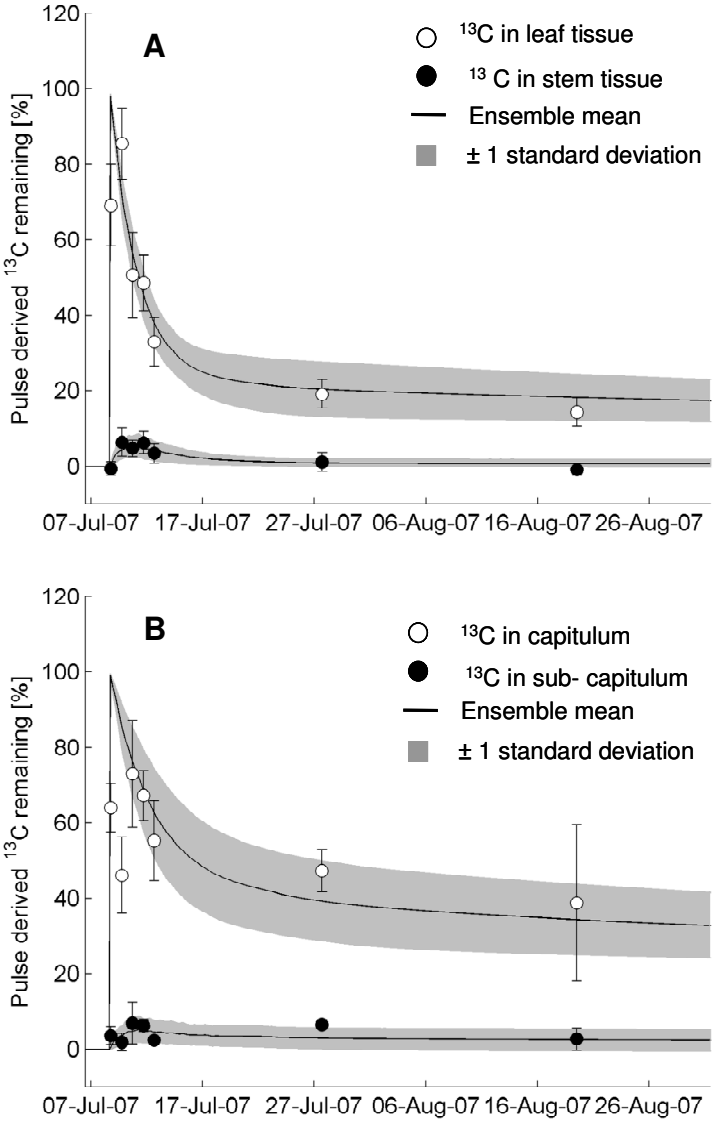

Figure 5. Measured and modelled PD ^{13}C remaining in moss tissues for a) *Polytrichum* and b) *Sphagnum,* expressed as a percentage of modelled PD ^{13}C uptake. The ensemble mean is the average of ensemble members forward runs with acceptable chi-squared values (for *Polytrichum* n = 29, for *Sphagnum* n = 107).

A much lower proportion of recently assimilated C was incorporated into structural tissue in *Polytrichum*; using all acceptable ensemble forward runs, the model predicts an average of 23 % of GPP is allocated to tissue growth over 5 days following labelling, with a 90 % CI of 9 % - 35 %. The average allocation in *Sphagnum* was 43 % of GPP with a 90 % CI of 19 % - 65 %. Turnover times of

assimilated C were also faster in *Polytrichum*; it took on average 1.7 days for 50 % of the initial ^{13}C uptake to be incorporated into structure or respired with a 90 % CI of 1.1 - 2.5 days, for *Sphagnum* turnover times were slightly slower at 3.1 days, 90 % CI 1.6 - 6.1 days. Approximately 21 % in *Polytrichum* and 51 % in *Sphagnum* of PD ^{13}C remained in the photosynthetic tissue plus the top 2 cm of stem tissue 2 weeks after labelling, 20 % in *Polytrichum* and 25 % in *Sphagnum* of PD ^{13}C remained after 1 year (Table 3). Differences in ^{13}C enrichment between NA and labelled plots after 1 year were significant only in photosynthetic tissue (data not shown).

Table 3. Pulse-derived ^{13}C remaining in photosynthetic and stem tissues two weeks and one year after pulse-labelling.

Species	Tissue	% ^{13}C remaining 2 weeks	% ^{13}C remaining 1 year
Polytrichum	Leaves	19.4 ± 8.3	15.5 ± 8.1
	0 - 1 cm stem	2.4 ± 2.4	3.8 ± 1.7
	1 - 2 cm stem	-0.5 ± 1.4	1.1 ± 1.3
	Total	21.3 ± 11.7	20.5 ± 11.0
Sphagnum	Capitulum	31.6 ± 10.1	13.5 ± 4.4
	0 - 1 cm stem	12.2 ± 2.9	9.4 ± 4.8
	1 - 2 cm stem	6.9 ± 3.5	2.4 ± 4.4
	Total	50.7 ± 7.6	25.3 ± 8.8

^{13}C in respiration flux

For *Sphagnum* the BT model predicted that 37 % (CI 24 % – 51 %) of the initial label uptake had been lost from tissues, from the labile pool, after 5 days (Fig. 6b). Total ^{13}C in respired CO_2 calculated from interpolation of measured fluxes was 22 %, suggesting that over 5 days our measurements of the isotopic composition of tissues and respiration left approximately 15 % of the initial ^{13}C uptake unaccounted for. The diurnal temperature signal in the measured fluxes was replicated by the model, though the overall ability of the BT model to predict $^{13}CO_2$ flux over the entire 5 day measurement period was low ($r^2 = 0.13$, Online Resource Table 2). C losses predicted by the model are greater than measured $^{13}CO_2$ fluxes especially 2 - 3 days after labelling (10 - 11th July).

The discrepancy between modelled C losses and biological PD ^{13}C flux was greater for *Polytrichum* than for *Sphagnum*, as modelled losses exceeded measured respiratory $^{13}CO_2$ flux over the entire 5 day period following labelling (Fig. 6a). The BT model predicted that 63 % (CI 50 % – 77 %) of the initial label uptake had been lost from tissues (Fig. 6b). Total ^{13}C in respired CO_2 calculated from the interpolation of measured fluxes was only 11 %, suggesting 52 % of the initial ^{13}C uptake was unaccounted for. Discrepancies between modelled and measured $^{13}CO_2$ fluxes for either species do not have any effect on the partitioning or turnover of labile C in the model nor on our estimates of NPP:GPP ratio or TT, as only tissue data were used during model optimisation.

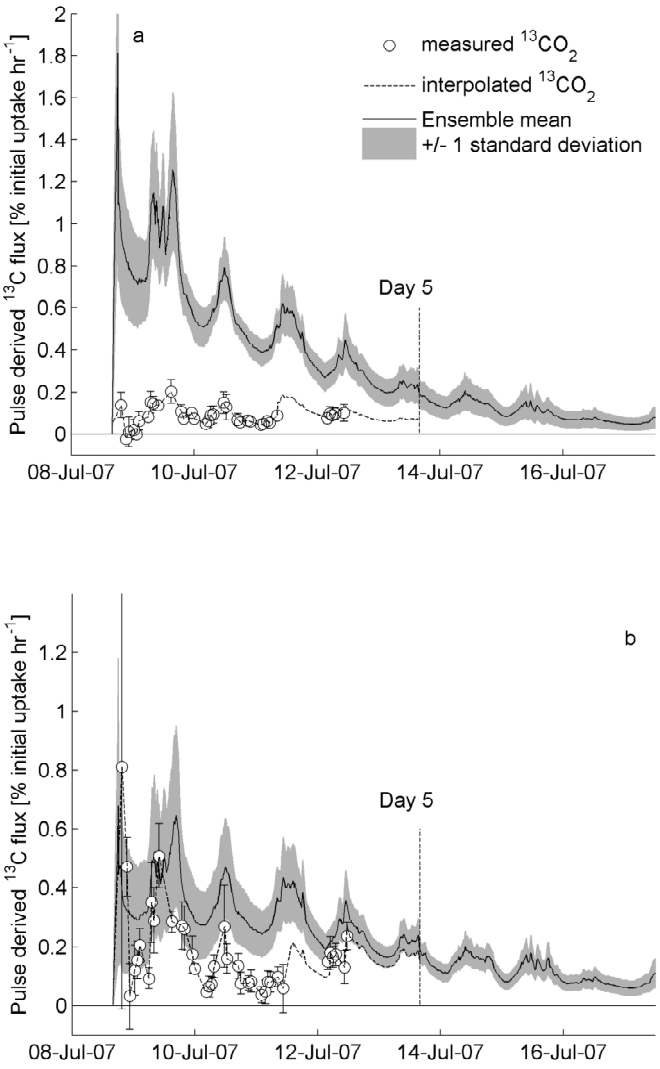

Figure 6. Measured and modelled PD ('light' minus 'dark' treatment fluxes) $^{13}CO_2$ losses (respiration plus belowground translocation) for a) *Polytrichum* and b) *Sphagnum*, expressed as a percentage of modelled total PD ^{13}C uptake. The ensemble mean is the average of ensemble members forward runs with acceptable chi-squared values (for *Polytrichum* n = 29, for *Sphagnum* n = 107).

Model parameters and sensitivity

Modelled aboveground NPP:GPP ratios and TTs were most sensitive to basal respiration rate (r_g), respiration temperature response (r_c) and allocation (a_g) and translocation (a_t) rate constants in photosynthetic tissue (Online Resource 2, Tables 1 and 2). The mean of acceptable fitted allocation rate constants (a_g) was the same between the two species, for *Polytrichum* a_g was 0.69×10^{-3} mol C mol^{-1} C hr^{-1} (S.D. 0.27×10^{-3}) and for *Sphagnum* a_g was 0.69×10^{-3} mol C mol^{-1} C hr^{-1} (S.D. 0.33×10^{-3}). Acceptable translocation rate constants also did not differ significantly between species (for *Polytrichum* $a_t = 0.53 \times 10^{-3}$ mol C mol^{-1} C hr^{-1} (S.D 0.37×10^{-3}) and for *Sphagnum* 0.42×10^{-3} mol C mol^{-1} C hr^{-1} (S.D. 0.28×10^{-3}). For *Polytrichum* the average basal respiration rate (r_g) of acceptable ensemble members was higher (0.0055 mol C mol^{-1} C hr^{-1} (S.D. 0.0027)) than for *Sphagnum* (0.0019 mol C mol^{-1} C hr^{-1} (S.D. 0.0017)) though the temperature sensitivity of respiration was similar for the two species (*Polytrichum* $r_c = 0.056$ (S.D. 0.03) *Sphagnum* $r_c = 0.066$ (S.D. 0.03)) which are equivalent to Q_{10} values for *Polytrichum* of 1.8 and for *Sphagnum* of 1.9. Increasing r_g in the sensitivity analysis reduced the NPP:GPP ratio and decreased TT. The model was relatively insensitive to one-dimensional changes in the photosynthesis parameters in terms of the effect on NPP:GPP ratios or labile C TT (Online Resource 2, Tables 1 and 2).

Discussion

Aboveground C turnover in mosses

The two moss communities showed clear differences in the uptake, storage and turnover of C, though the literature suggests there are no clear differences in net annual productivity for similar species at other locations (approximately 0.4 to 1.2 g g^{-1} for *Sphagnum fuscum* at Stordalen mire, Abisko (Dorrepaal *et al.* 2004), and 0.3 g g^{-1} for *Polytrichum alpinum* in Barrow, Alaska (Sveinbjornsson & Oechel, 1981)). The BT model predicted that *Polytrichum* incorporates only about 23 % of assimilates to new structural material aboveground, and that 77 % of assimilates are either respired or allocated belowground. *Sphagnum,* on the other hand, allocates around 45% of photosynthate to new growth, and retains most newly fixed C within photosynthetic tissues within 2 cm of the surface. The differences in gross photosynthetic rate between the two species are also marked (Fig. 4a).

With calculated 50 % TTs of less than 3 days, after 2 weeks most of the labile C pool will either be respired or allocated to growth. After this period approximately 50 % of PD ^{13}C could be accounted for within 2 - 3 cm of the surface for *Sphagnum* and about 20 % in *Polytrichum* (Table 3). These values are consistent with the modelled NPP:GPP ratios, but are substantially less than the 70 % retention after 4 - 6 weeks in *Calliergon richardsonii* reported by Woodin *et al*. (2009) in a similar high Arctic labelling study. Over a full annual cycle however we found little difference in C retention between the two species in the top 2 - 3 cm of the moss layer, *Sphagnum* retaining 25% ± 9 % of the original label *Polytrichum* retaining 21 % ± 11 %. This suggests that in the period between 2 weeks and 1 year after labelling there was some loss of ^{13}C aboveground, perhaps by re-mobilisation of structural C, or by leaching of dissolved organic carbon (DOC), within *Sphagnum* but not *Polytrichum*. The presence of ^{13}C 1 - 2 cm below the capitulum in *Sphagnum* after 1 year is surprising given annual growth increments of only 0.4 - 1 cm at a nearby site (Dorrepaal *et al.*, 2004). Presence of ^{13}C deeper in the profile suggests some downward movement of label, whether within the stem or as DOC (Fenner *et al.* 2004).

Translocation fluxes

The model predicts much greater loss of $^{13}CO_2$ from aboveground tissues for *Polytrichum* than was measured as respiration (Fig. 6a), suggesting that we were unable to account for 52 % of the assimilated label during the 5 days after labelling. Previous work on other *Polytrichum* species has shown that significant amounts of assimilate can be transported to belowground tissues, especially to the apices of underground shoots (Collins & Oechel, 1974). Sveinbjornsson and Oechel (1981) show that belowground respiration in *Polytrichum alpinum* can account for 30 % of net CO_2 uptake (though any belowground incorporation, if it occurred, would be significantly less than 30 % of *gross* CO_2 uptake). In a ^{14}C tracer study Thomas et al. (1990) show that incorporation of photo-assimilates belowground in *Polytrichum commune* one week after labelling can be between 13 - 21 % of that incorporated aboveground. This would equate to roughly 3 - 5 % of gross photosynthesis, if aboveground incorporation was ~20 % of GPP, as in this case. A ^{14}C labelling study in *P. commune* by Skre et al. (1983) found similar results; after 5 days 80 - 85 % of the label remaining in tissues was in the apical 3 mm of current year's growth. While we therefore can not quantify incorporation of label in deep tissues belowground, we argue that it is unlikely to be more than 10 % of GPP though likely to be strongly dependant on growth stage and variable across months/seasons.

The discrepancy between modelled C loss and measured respiratory flux for *Polytrichum* could also be explained by the following: 1) the comparison between predicted and modelled respiratory $^{13}CO_2$ return requires a conversion from the measured $^{13}CO_2$ flux per unit ground area, to $^{13}CO_2$ return per unit photosynthetic biomass in the collar. This conversion requires an accurate measurement of the total photosynthetic biomass in the collars at the time of $^{13}CO_2$ sampling. We could only destructively harvest the moss from the collars at the end of the experiment (August 2009) so probably over-estimated total photosynthetic biomass in July 2007, due to growth during the interim period. An overestimate of photosynthetic biomass in the collar would result in an underestimate of measured ^{13}C return on a per unit biomass basis. 2) we also detected small amounts of PD ^{13}C in the 'dark' side of the plots, so

the 'light' minus 'dark' subtraction may have resulted in a slight underestimate of biological ^{13}C flux.

Morphological complexity in Polytrichum *and* Sphagnum

Observed differences in C turnover and allocation can be related to differences in morphological complexity between the two species. The Polytrichaceae have highly differentiated leaves with dense chlorophyll-rich lamellae cells on adaxial surfaces (Thomas *et al.*, 1996). The presence of wax on the leaf surface also facilitates rapid conductance of CO_2 into the leaf by repelling water (Proctor, 2009). Highly complex and metabolically active tissues may thus explain greater respiratory energy demand in *Polytrichum*, together with the costs associated with downward translocation of assimilate (similar to phloem loading), or upward movement of nutrients from the soil (Chapin *et al.* 1987). *Sphagnum* by contrast absorbs water and nutrients directly from precipitation. The presence of liquid water on the leaf surface increases diffusive resistance to CO_2 and can limit photosynthesis even at relatively low bulk water content (Williams & Flanagan, 1996, 1998), perhaps in part explaining the lower photosynthetic capacity of this species. Demand for large amounts of structural carbohydrate in *Sphagnum* for the construction of water storing hyaline cells, which are then metabolically inactive, in turn may reduce the demand for tissue maintenance respiration.

Model assumptions

The BT model successfully replicated the quantity of PD ^{13}C label remaining in stem and photosynthetic tissues, but relies on the following assumptions. (1) We assume that no photosynthesis occurs in the sub-capitulum region of the *Sphagnum* stem. Although the canopy of *Sphagnum fuscum* is dense, preventing much light penetration to this part of the plant, photosynthetic activity in the sub-capitulum has been documented in other species of *Sphagnum* (Robroek *et al.* 2009). Therefore the presence of ^{13}C label may indicate a small amount of photosynthetic uptake of the ^{13}C label. (2) We assume that the parameters controlling the response of photosynthesis to light and temperature (p_t, p_c and p_k) remain constant (optimal) throughout the modelled period. This is unlikely to be the case in reality, as sub-optimal water content or the presence of excess water on the leaves following

precipitation, may periodically reduce the photosynthetic capacity of tissues (Lloyd, 2001). We believe that any periods of photosynthetic inhibition over the modelled period were not prolonged enough to affect the turnover of C significantly for two reasons. Firstly, we show that the parameters used in the model provide unbiased predictions of GPP over the growing season (Fig. 6b). Secondly both species are known to be able to regulate tissue water content to some extent, and we would not expect either species to become metabolically inactive for long periods of time unless subject to unusually dry conditions (the maximum time with zero rainfall during the study was one 4-day period). Finally, the sensitivity analyses indicate that the model predictions of the NPP:GPP ratio and TT are relatively insensitive to changes in the photosynthesis parameters.

The lack of adequate sample storage meant our confidence in the initial tissue samples as an accurate measure of total label uptake was low. To avoid resulting bias, we ignored the first 1 - 2 days of sampling for the purpose of model fitting. Because our confidence in the differences in photosynthetic rate between species is high (there was good correspondence between independent lab and field flux data, Fig. 4b), and our confidence in later solid tissue data is also high, the lack of cold sample storage does not affect the conclusions of the study. Samples from the first day, for *Polytrichum* and the first 2 days for S*phagnum* do fall below the modelled values (Fig. 5), which is what would be expected if some ^{13}C in labile components had been lost between sampling in the field and freezing.

Conclusions

We detected significant differences in above ground C allocation and turnover between two common Arctic moss species. Greater photosynthetic rates in *Polytrichum* were associated with higher demands on the labile C pool for respiration or translocation, which we link to greater structural complexity within this species. Our estimate of 23 % allocation of recently fixed C to NPP in *Polytrichum* is lower than the 50 % often assumed for vascular plants. In *Sphagnum* we found 45 % of GPP was allocated to NPP exclusively within the top 2 cm of the moss surface. Consequently C cycle models which aim to quantify regional NPP based only on vascular plant C allocation may significantly overestimate belowground allocation

where *Sphagnum* is present, or overestimate aboveground incorporation where *Polytrichum* species dominate. The *Sphagnum* genus is abundant in northern regions, contributing around 30 % to land surface cover based on estimates of peatland cover (Frey 2007). *Sphagnum* species such as *S. fuscum* can also be important components of shrub and wet-sedge tundra vegetation which may not be classified as peatland in land-cover classification schemes (pers. obs.). *Polytrichum*, while common in dry tundra vegetation, will contribute only a small fraction of the total sub-Arctic land surface, as it is just one of many moss species that contribute to the moss layer in these vegetation types. Further research is required into other common Arctic moss species, and their proportional representation on the land surface, before the implications of C turnover in Arctic bryophytes can be fully understood. However, our modelling results provide the first crucial insights into bryophyte C allocation and turnover and are an important step towards a more complete understanding of the Arctic C cycle.

Acknowledgements

This work was funded by a NERC CASE PhD studentship in partnership with the Macaulay Land Use Research Institute (MLURI), Aberdeen. We thank Barry Thornton (MLURI) for ^{13}C isotope analysis, Sally Eaton for species identification and Veronica Lussier for sample preparation. We thank Harry Vallack for his assistance in setting up the 'York mobile lab' and all the staff at ANS. We particularly thank Roslyn MacDonald for her contribution to the fieldwork. The work was part of the NERC ABACUS Arctic-IPY consortium.

References

Amthor JS (2000) The McCree-de Wit-Penning de Vries-Thornley respiration paradigms: 30 years later. Annals of Botany 86:1-20

Ayres E, van der Wal R, Sommerkorn M, Bardgett RD (2006) Direct uptake of soil nitrogen by mosses. Biology Letters 2:286-288

Bowling DR, Pataki DE, Randerson JT (2008) Carbon isotopes in terrestrial ecosystem pools and CO2 fluxes. New Phytologist 178:24-40

Campioli M, Samson R, Michelsen A, Jonasson S, Baxter R, Lemeur R (2009) Nonvascular contribution to ecosystem NPP in a subarctic heath during early and late growing season. Plant Ecology 202:41-53

Cannell MGR, Thornley JHM (2000) Modelling the components of plant respiration: Some guiding principles. Annals of Botany 85:45-54

Chapin FS, Oechel WC, Vancleve K, Lawrence W (1987) The Role of Mosses in the Phosphorus Cycling of an Alaskan Black Spruce Forest. Oecologia 74:310-315

Chapin FS, Shaver GR, Giblin AE, Nadelhoffer KJ, Laundre JA (1995) Responses Of Arctic Tundra To Experimental And Observed Changes In Climate. Ecology 76:694-711

Christensen JH et al. (2007) Regional Climate Projections. In: Solomon S et al. (eds) Climate Change 2007: The Physical Science Basis. Contribution of Working Group I to the Fourth Assessment Report of the Intergovernmental Panel on Climate Change. Cambridge University Press, Cambridge, United Kingdom and New York, USA

Collins NJ, Oechel WC (1974) Pattern of Growth and Translocation of Photosynthate in a Tundra Moss, Polytrichum-Alpinum. Canadian Journal of Botany-Revue Canadienne De Botanique 52:355-363

Dawson TE, Mambelli S, Plamboeck AH, Templer PH, Tu KP (2002) Stable isotopes in plant ecology. Annual Review of Ecology and Systematics 33:507-559

Dorrepaal E, Aerts R, Cornelissen JHC, Callaghan TV, van Logtestijn RSP (2004) Summer warming and increased winter snow cover affect Sphagnum fuscum growth, structure and production in a sub-arctic bog. Global Change Biology 10:93-104

Douma J, van Wijk MT, Lang SI, Shaver GR (2007) The contribution of mosses to the carbon and water exchange of arctic ecosystems: quantification and relationships with system properties. Plant, Cell and Environment 30:1205-1215

Fenner N, Ostle N, Freeman C, Sleep D, Reynolds B (2004) Peatland carbon afflux partitioning reveals that Sphagnum photosynthate contributes to the DOC pool. Plant and Soil 259:345-354

Fox A et al. (2009) The REFLEX project: Comparing different algorithms and implementations for the inversion of a terrestrial ecosystem model against eddy covariance data. Agricultural and Forest Meteorology 149:1597-1615

Gifford RM (2003) Plant respiration in productivity models: conceptualisation, representation and issues for global terrestrial carbon-cycle research. Functional Plant Biology 30:171-186

Lloyd CR (2001) The measurement and modelling of the carbon dioxide exchange at a high Arctic site in Svalbard. Global Change Biology 7:405-426

McBean G et al. (2005) Arctic climate: past and present. In: Arctic Climate Impact Assessment: Scientific Report. Cambridge University Press, Cambridge, UK, pp 21–60

Miller PC, Webber PJ, Oechel WC, Tieszen LL (1980) Biophysical Processes and Primary Production In: Brown JM, Miller PC, Tieszen LL, Bunnell FL (eds) An Arctic Ecosystem: the Coastal Tundra at Barrow, Alaska. Dowden, Hutchinson & Ross, Inc., Stroudsburg, PA., pp 66-101

Proctor MCF (2009) Physiological Ecology. In: Goffinet B, Shaw AJ (eds) Bryophyte Biology, 2nd edn. Cambridge University Press, Cambridge, pp 273-269

Proctor MCF, Raven JA, Rice SK (1992) Stable Carbon Isotope Discrimination Measurements in Sphagnum and Other Bryophytes - Physiological and Ecological Implications. Journal of Bryology 17:193-202

Robroek BJM, Schouten MGC, Limpens J, Berendse F, Poorter H (2009) Interactive effects of water table and precipitation on net CO2 assimilation of three co-occurring Sphagnum mosses differing in distribution above the water table. Global Change Biology 15:680-691

Shaver GR, Street LE, Rastetter EB, Van Wijk MT, Williams M (2007) Functional convergence in regulation of net CO2 flux in heterogeneous tundra landscapes in Alaska and Sweden. Journal of Ecology 95:802-817

Skre O, Oechel WC, Miller PM (1983) Patterns of Translocation of Carbon in 4 Common Moss Species in a Black Spruce (Picea-Mariana) Dominated Forest in Interior Alaska. Canadian Journal of Forest Research-Revue Canadienne De Recherche Forestiere 13:869-878

Street LE, Shaver GR, Williams M, Van Wijk MT (2007) What is the relationship between changes in canopy leaf area and changes in photosynthetic CO2 flux in arctic ecosystems? Journal of Ecology 95:139-150

Sveinbjornsson B, Oechel WC (1981) Controls on CO_2 exchange in two *Polytrichum* moss species. 2. The implications of belowground plant-parts on the whole-plant carbon balance. Oikos 36:348-354

Tarnocai C, Canadell JG, Schuur EAG, Kuhry P, Mazhitova G, Zimov S (2009) Soil organic carbon pools in the northern circumpolar permafrost region. Global Biogeochemical Cycles 23

Thomas RJ, Ryder SH, Gardner MI, Sheetz JP, Nichipor SD (1996) Photosynthetic function of leaf lamellae in Polytrichum commune. Bryologist 99:6-11

Thomas RJ, Schiele EM, Damberg DT (1990) Translocation in Polytrichum-Commune (Bryophyta) .2. Clonal Integration. American Journal of Botany 77:1569-1573

Thomas RJ, Schiele EM, Scheirer DC (1988) Translocation in Polytrichum-Commune (Bryophyta) .1. Conduction and Allocation of Photoassimilates. American Journal of Botany 75:275-281

Trumbore S (2006) Carbon respired by terrestrial ecosystems - recent progress and challenges. Global Change Biology 12:141-153

Turetsky MR, Crow SE, Evans RJ, Vitt DH, Wieder RK (2008) Trade-offs in resource allocation among moss species control decomposition in boreal peatlands. Journal of Ecology 96:1297-1305

Vitt DH, Wieder RK (2009) Bryophyte-dominated peatlands. In: Goffinet B, Shaw AJ (eds) Bryophyte Biology, 2nd edn. Cambridge University Press, Cambridge, pp 357-392

Walker DA (2000) Hierarchical subdivision of Arctic tundra based on vegetation response to climate, parent material and topography. Global Change Biology 6:19-34

Waring RH, Landsberg JJ, Williams M (1998) Net primary production of forests: a constant fraction of gross primary production? Tree Physiology 18:129-134

Williams M, Schwarz PA, Law BE, Irvine J, Kurpius MR (2005) An improved analysis of forest carbon dynamics using data assimilation. Global Change Biology 11:89-105

Williams M, Street LE, van Wijk MT, Shaver GR (2006) Identifying Differences in Carbon Exchange among Arctic Ecosystem Types. Ecosystems 9:288-304

Williams TG, Flanagan LB (1996) Effect of changes in water content on photosynthesis, transpiration and discrimination against (CO2)-C-13 and (COO)-O-18-O-16 in Pleurozium and Sphagnum. Oecologia 108:38-46

Williams TG, Flanagan LB (1998) Measuring and modelling environmental influences on photosynthetic gas exchange in Sphagnum and Pleurozium. Plant Cell and Environment 21:555-564

Woodin SJ, van der Wal R, Sommerkorn M, Gornall JL (2009) Differential allocation of carbon in mosses and grasses governs ecosystem sequestration: a ^{13}C tracer study in the high Arctic. New Phytologist 184:944-949

5b. Turnover of recently assimilated carbon in Arctic bryophytes – supplementary material

Lorna E. Street [1], Jens-Arne Subke[2,3], Martin Sommerkorn[4], Andreas Heinemeyer[2], MathewWilliams[1]

[1]School of Geosciences, University of Edinburgh, Edinburgh, EH9 3JN, UK

[2]Stockholm Environment Institute York, Environment Department, University of York, York, YO10 5DD, UK

[3]School of Biological and Environmental Sciences, University of Stirling, Stirling, FK9 4LA, UK

[4]Macaulay Land Use Research Institute, Craigiebuckler, Aberdeen, AB15 8QH, UK

(published in Oecologia as Street, L., Subke, J., Sommerkorn, M., Heinemeyer, A., & Williams, M. (2011) Turnover of recently assimilated carbon in arctic bryophytes. Oecologia. DOI: 10.1007/s00442-011-1988-y.*)*

Online Resource 1

Methodological details

1) Labelling plot preparation

Vascular plants removed from *Sphagnum* plots consisted of mostly sedges and grasses with some evergreens such as *Andromeda polifolia*. For *Polytrichum* plots, most vascular plants were prostrate evergreen shrubs with small quantities of *Betula nana*. Estimated total surface cover of vascular plants before removal was less than 20% for all plots. We watered each plot twice, at 5 and 1.5 hours before labelling, to ensure photosynthesis for both species was not moisture limited. Watering delivered 2 l of water to each plot using a watering can, equivalent to approximately 6 mm of rain. Measurements of moss water content following labelling indicated average water contents, as a percentage of dry weight, of 570 % for *Sphagnum* and 71 % for *Polytrichum*. We sealed the labelling hoods to the moss surface using weighted clear plastic skirts attached to the lower edge of the hood and by stuffing air gaps with bubble wrap and placing flat stones around the outer edges. We left a gap in the cardboard partition between 'light' and 'dark' sides in order to allow the $^{13}CO_2$ to flow into each side of the hood, and split the flow of gas inside the hood using a T-piece see Fig. OR1.

We used a LI-COR 6400 photosynthesis system (LI-COR Inc., Lincoln, Nebraska, USA) to monitor temperature and photosynthetic photon flux density (PPFD) in the 'light' side of one of the hoods. In a separate short experiment we monitored light levels in the darkened side of a hood under similar conditions and found PPFD to be consistently below 12 μmol m^{-2} s^{-1}.

2) Laboratory GPP measurements

Five samples of each species were collected as intact turfs on 23rd August 2007, and then shipped by airfreight back to the UK over two days. The turfs were stored in growth room facilities for three months at a temperature of 12°C with a dark period of eight hours every day. The turfs were watered daily to avoid drying out. CO_2 flux

measurements were made using a Walz gas analyser (Walz GmbH, Effeltrich, Germany) connected to a transparent 'mini-cuvette' in continuous differential mode. 4 × 4 cm turfs were placed in the cuvette and CO_2 flux was allowed to stabilise for 2 - 3 minutes before measurement. Light was supplied by two small halogen lamps, the intensity of which was adjusted using multiple sheets of optically neutral tissue paper placed over the cuvette. Air temperature, moss leaf temperature and light intensity were also monitored inside the cuvette.

We measured CO_2 flux on each species at optimum water content, determined by previous measurements on the same turfs at a range of water contents (measurements were made without allowing the turfs to become fully desiccated). We quantified the light response of GPP by measuring net fluxes over a range of light levels then subtracting total turf respiration measured under fully darkened conditions. We measured a GPP light response curve for each turf at 5°C, 12°C and 20°C, and fitted the light saturated rate of photosynthesis (P_{max}) per gram dry weight at each temperature using least-squares curve fitting in Matlab 7.1.

After making gas exchange measurements *Polytrichum* leaves, and *Sphagnum* capitula were removed, dried at 70°C and weighed. We expressed GPP per unit dry weight of leaf tissue in *Polytrichum* and per unit dry weight capitulum tissue in *Sphagnum*.

3) Mass spectrometry

The "York Mobile Lab" constitutes a gas handling unit for switching between the 16 input lines, connected to a Continuous Flow-Gas Chromatograph-Isotope Ratio Mass Spectrometer unit (CF-GC-IRMS). A standard laboratory gas chromatograph is coupled to a 12 cm radius magnetic sector mass spectrometer (SIRAS Series2, Micromass, UK), NIER (Non-Ionizing Electromagnetic Radiation) type ion impact source, triple faraday collector system, rotary/turbo-molecular pumping vacuum system, interfaced to Microsoft Windows™ data system (model name "PVS12", built by Pro Vac Services, Crewe, UK). The CF-GC-IRMS, together with a temperature control system and gas supplies for CO_2 reference and helium carrier gas, has been custom built to fit into a modified twin-axle trailer unit (Model 'Towavan', Indespension Ltd., Bolton, U.K.), thus providing the unique opportunity

to conduct isotope ratio measurements in real time and under field conditions, with no need for off-line sampling and associated problems of gas handling and storage. Power for running the instrumentation of the York Mobile Lab in the field was provided by two propane fuelled generators (Honda EU10i, converted for propane use; Honda Motor Co., Ltd., Tokyo, Japan) with a total power output of 1.8 kW.

For Exetainer gas sample analysis (taken from the labelling hoods) a custom built autosampler replaced the line flow interface, with the CF-GC-IRMS set-up otherwise unchanged to the field sampling mode.

Tissue samples from 2008 were analysed at York University on an elemental analyser (FlashEA1112, ThermoFinnigan, Germany) connected to a custom built isotope ratio mass spectrometer (constructed by Pro-Vac Services Ltd., Crewe, UK). The instrumental output was calibrated against NIST standard ANU8542 (sucrose).

Tissue samples from 2007 were analysed at the Macaulay Land Use Research Institute using a Flash EA 1112 Series Elemental Analyser connected via a Conflo III to a DeltaPlus Advantage isotope ratio mass spectrometer (Thermo Finnigan, Bremen, Germany). The isotope ratios were calculated with respect to CO_2 reference gases injected with every sample and traceable to IAEA reference materials USGS40 and USGS41 (both L-glutamic acid). The C content of the samples were calculated from the area output of the mass spectrometer calibrated against National Institute of Standards and Technology (NIST) standard reference material 1547 peach leaves which were analysed with every batch of ten samples.

4) EnKF analysis

The 8 unconstrained parameters (i.e. all except the 3 photosynthesis parameters) were included in the EnKF augmented model state vector, so that they could be constrained by the data. There are 4 pools and 8 fluxes for both the NA and PD models, thereby giving an augmented state vector of 32 elements. A 300 member ensemble was used to represent the probability density function of the carbon model states and parameters. We chose to focus on parameter estimation with the EnKF,

rather than on state estimation. Thus, model uncertainties on the state variables were set low relative to parameter uncertainties. The standard deviation on each state variable ensemble was estimated at 0.001 % of the mean. The uncertainties on the 8 parameters were set larger, with ensemble standard deviations set at 0.5 % of their mean values, allowing parameters to adjust significantly over 10 - 100s of time steps. The initial uncertainties on the state vector ensembles were set using standard deviations of 10 % of the mean on state variables and 5 % of the mean on parameters included the state vector. The EnKF updated the model parameters so that model predictions best matched observations, according to the weightings provided by the model versus observation uncertainties.

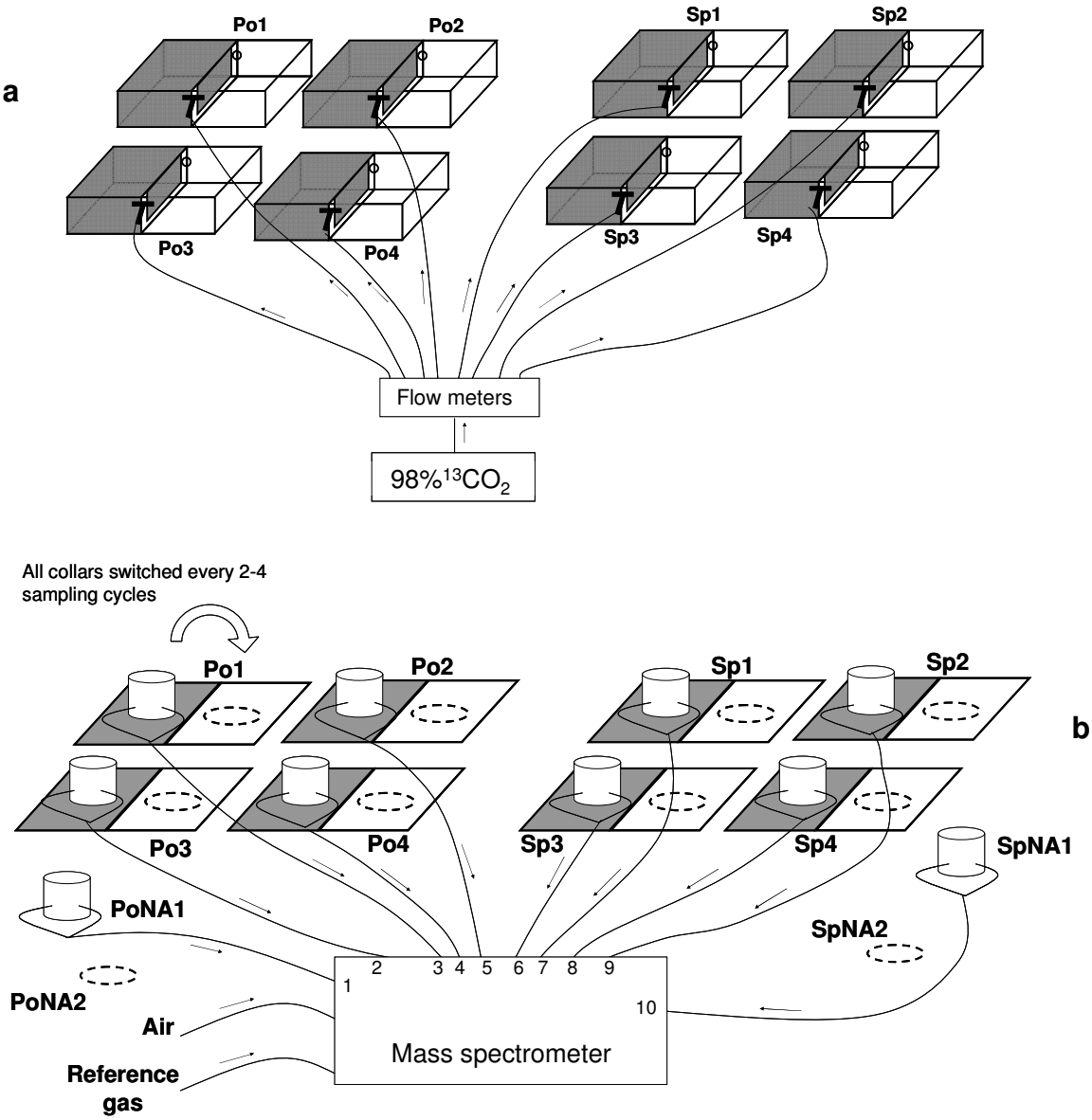

Figure 1 Schematic of a) pulse labelling set-up showing the 8 labelling hoods with dark and light sections. The flow of enriched CO_2 was split inside the hood with a T-piece to ensure equal supply of label to each side. b) Pulse chase experimental set-up. The mass spectrometer sampled from lines 1-10 as well as air and reference lines in sequence, an entire sampling cycle taking 1 hour. The return collars were switched from dark to light side (and NA from NA1 to NA2) or vice versa every 2-4 sampling cycles.

Online Resource 2

Sensitivity analyses

Table 1 Sensitivity analysis for the *Polytrichum* parameterisation of the BT model. Each row gives the root mean square error (RMSE) and R^2 for linear regression of model *vs*. measured tissue enrichment and $^{13}CO_2$ flux, the NPP:GPP ratio and turnover time (TT, time taken for 50 % of the labile C pool to be allocated to growth or respired) for a single model forward run. Numbers in bold are for the average (nominal) parameter set (in brackets after the parameter symbol). Single parameters are adjusted (multiplied or divided by 2) while all other parameters are held at the nominal value.

Polytrichum piliferum		**Leaf ^{13}C (atom%)**		**Stem ^{13}C (atom%)**		**$^{13}CO_2$ (mol hr^{-1})**		**NPP :GPP**	**TT (days)**
Parameter	**Adjusted value**	**r^2**	**RMSE ($\times 10^{-3}$)**	**r^2**	**RMSE ($\times 10^{-4}$)**	**r^2**	**RMSE ($\times 10^{-6}$)**		
(Nominal)		0.96	2.3	0.83	4.4	0.25	2.1	0.24	1.5
p_t (5.28×10^{-5})	1.06×10^{-4}	0.96	4.9	0.83	6.7	0.25	3.3	0.24	1.5
	2.64×10^{-5}	0.96	4.6	0.83	6.1	0.25	1.6	0.24	1.5
p_c (1.56×10^{-3})	3.12×10^{-3}	0.96	6.7	0.83	9.3	0.25	3.8	0.23	1.5
	7.8×10^{-4}	0.96	5.6	0.83	7.1	0.25	1.3	0.24	1.5
p_k (130)	260	0.96	4.1	0.83	5.7	0.25	1.7	0.24	1.5
	65	0.96	1.9	0.83	4.2	0.25	2.4	0.24	1.5
r_g (5.5×10^{-3})	0.011	0.95	6.1	0.85	6.7	0.21	3.3	0.15	0.9
	2.8×10^{-3}	0.91	3.9	0.77	5.4	0.28	1.3	0.33	2.2
r_s (0.013)	0.026	0.96	2.3	0.83	8.2	0.22	2.2	0.23	1.5
	6.5×10^{-3}	0.96	2.3	0.69	7.7	0.25	2.0	0.25	1.5
r_c (0.058)	0.12	0.95	6.8	0.69	11.3	0.33	3.3	0.14	0.8
	0.029	0.94	2.7	0.72	7.2	0.16	1.7	0.29	1.8
a_t (5.3×10^{-4})	1.1×10^{-3}	0.97	3.3	0.85	10.1	0.24	2.2	0.21	1.2
	2.7×10^{-4}	0.95	2.2	0.82	8.8	0.25	2.1	0.25	1.7
a_g (6.9×10^{-4})	1.4×10^{-3}	0.96	3.2	0.85	4.7	0.23	2.0	0.37	1.2
	3.4×10^{-4}	0.96	2.6	0.81	4.4	0.26	2.2	0.14	1.7
a_s (2.2×10^{-4})	4.4×10^{-4}	0.96	2.3	0.81	5.1	0.24	2.1	0.25	1.5
	1.1×10^{-4}	0.96	2.3	0.84	4.2	0.25	2.1	0.23	1.5
l_g (3.2×10^{-5})	6.4×10^{-5}	0.96	2.3	0.83	4.5	0.25	2.0	0.24	1.5
	1.6×10^{-5}	0.96	2.3	0.83	4.3	0.25	2.1	0.24	1.5
l_s (1.7×10^{-5})	3.4×10^{-5}	0.96	2.3	0.83	4.3	0.25	2.1	0.24	1.5
	8.6×10^{-6}	0.96	2.3	0.83	4.4	0.25	2.1	0.24	1.5

Table 2 Sensitivity analysis for the *Sphagnum* parameterisation of the BT model. Each row gives the root mean square error (RMSE) and r^2 for linear regression of model *vs*. measured tissue enrichment and $^{13}CO_2$ flux, the NPP:GPP ratio and TT for a single model forward run. Numbers in bold are for the average (nominal) parameter set (in brackets after the parameter symbol). Single parameters are adjusted (multiplied or divided by 2) while all other parameters are held at the nominal value.

Sphagnum fuscum		**Capitulum ^{13}C (atom%)**		**Stem ^{13}C (atom%)**		**$^{13}CO_2$ (mol hr^{-1})**		**NPP :GPP**	**TT (days)**
Parameter	**Adjusted value**	**r^2**	**RMSE ($\times 10^{-3}$)**	**r^2**	**RMSE ($\times 10^{-4}$)**	**r^2**	**RMSE ($\times 10^{-6}$)**		
(Nominal)		0.94	0.8	0.02	4.6	0.13	1.1	0.42	2.6
p_t (2.4×10^{-5})	1.06×10^{-4}	0.94	3.9	0.02	5.1	0.13	1.1	0.41	2.6
	2.64×10^{-5}	0.93	2.0	0.02	5.5	0.13	1.1	0.42	2.6
p_c (5.23×10^{-4})	3.12×10^{-3}	0.94	4.1	0.02	5.3	0.13	1.1	0.40	2.6
	7.8×10^{-4}	0.93	2.1	0.02	5.6	0.13	1.1	0.44	2.6
p_k (75)	260	0.93	1.1	0.02	4.9	0.13	1.1	0.43	2.6
	65	0.94	1.0	0.02	4.4	0.13	1.1	0.41	2.6
r_g (1.9×10^{-3})	4.0×10^{-3}	0.95	1.9	0.05	5.4	0.25	1.1	0.30	1.8
	1.0×10^{-3}	0.92	1.3	0.01	4.2	0.01	1.1	0.51	3.2
r_s (0.013)	0.026	0.94	0.8	0.08	6.6	0.09	1.1	0.40	2.6
	0.0075	0.94	0.8	0.00	5.3	0.19	1.0	0.44	2.6
r_c (0.065)	0.13	0.95	2.4	0.16	8.0	0.23	1.1	0.24	1.7
	0.033	0.93	1.0	0.00	4.9	0.06	1.1	0.50	3.0
a_t (4.2×10^{-4})	8.4×10^{-4}	0.94	1.4	0.04	6.3	0.05	1.1	0.37	2.1
	2.1×10^{-4}	0.93	1.0	0.02	6.7	0.19	1.0	0.45	2.9
a_g (6.9×10^{-4})	1.4×10^{-3}	0.96	1.0	0.04	5.2	0.18	1.0	0.59	1.8
	3.5×10^{-4}	0.92	1.7	0.01	4.2	0.09	1.1	0.27	3.2
a_s (6.1×10^{-4})	1.2×10^{-3}	0.94	0.8	0.01	3.8	0.14	1.1	0.44	2.6
	3.0×10^{-4}	0.94	0.8	0.03	5.5	0.12	1.1	0.40	2.6
l_g (2.8×10^{-5})	5.6×10^{-5}	0.93	0.8	0.02	4.6	0.13	1.1	0.42	2.6
	1.4×10^{-5}	0.94	0.8	0.02	4.5	0.13	1.1	0.41	2.6
l_s (2.9×10^{-5})	5.8×10^{-5}	0.94	0.8	0.02	4.4	0.13	1.1	0.42	2.6
	1.5×10^{-5}	0.94	0.8	0.02	4.6	0.13	1.1	0.42	2.6

6. Discussion and key conclusions

The objective of this thesis was to resolve key uncertainties related to the uptake and turnover of C in Arctic vegetation. These uncertainties include how process-based understanding at the species or plot level can be scaled to landscapes or regions; relevant to calculating carbon budgets for the Arctic, and also the contribution of bryophytes Arctic productivity. Key uncertainties also exist relating to the fate of carbon once it is fixed by photosynthesis; the partitioning of carbon between plant pools (vascular versus non-vascular, aboveground versus belowground) and the rates of turnover of these carbon pools. To address these uncertainties my thesis answers the following questions relating to:

I) Predicting gross primary productivity in the Arctic:

1. Are there general relationships between leaf area index, total foliar nitrogen and GPP across Arctic terrestrial ecosystems?
2. What is the annual GPP of common bryophyte species in comparison to vascular plants? What are the key drivers of bryophyte GPP?

II) Understanding the allocation and turnover of C in arctic vegetation:

3. What role do bryophytes play in C turnover and allocation in Arctic vegetation?
4. What is the ratio of net primary productivity to gross primary productivity (NPP:GPP ratio) and rate of turnover of recently fixed C in common bryophyte species?

I now review the key conclusions of the these work under the above headings. I discuss the implications for modelling the C cycle in the Arctic. I also highlight new research questions which arise from the key conclusions of each chapter.

I) Predicting gross primary productivity in Arctic ecosystems

The distribution of total foliar nitrogen in Arctic canopies with respect to leaf area index is tightly constrained. The constraints operate largely independently of vegetation type but differ between geographic locations, which we link to differences in the average total and diffuse fraction of short-wave radiation for the growing season. A single general relationship between GPP and LAI is most appropriate for Arctic ecosystems.

In 1999 a study by Williams & Rastetter identified a tightly constrained relationship between leaf area index (LAI) and total foliar nitrogen (TFN) in Alaskan vegetation. Van Wijk *et al.* (2005) confirmed a similar tightly constrained relationship in Northern Sweden. Van Wijk *et al.* (2005) argue that this relationship is a surprising emergent property of the plant

canopy, which usefully simplifies wide variability in leaf traits at the species level . My objective in Chapter 2 of the thesis was to test whether the same LAI-TFN relationship, and therefore the same constraints over canopy construction, exist across the wider Arctic; including higher latitude and coastal tundra sites. A further objective in Chapter 2 was to test whether a single general model could describe the relationship between canopy GPP and LAI; simplifying the task of up-scaling GPP over the pan-Arctic.

Information on vegetation type produced only small improvements in the ability to predict TFN from LAI, confirming the results of van Wijk *et al.* (2005). I find, however, important differences in the LAI-TFN relationship between sites, indicating that the controls over the development of TFN with respect to LAI are dependant on geographic location. At high LAI the relationship at different sites diverges. This divergence appeared to be driven by differences in diffuse radiation conditions with higher diffuse radiation fraction at site associated with a more linear LAI-TFN relationship; implying a more uniform vertical distribution of N within the canopy. It is well established that vertical gradients in leaf level N, and hence photosynthetic capacity, exist within canopies. These gradients follow the extinction of light and act to increase the efficiency of canopy C gain (Bond *et al.*, 1999; Ellsworth & Reich, 1993; Hollinger, 1996; Meir *et al.*, 2002). Most of this work, critical to our understanding of how leaf level processes can be scaled in whole canopy models, has focussed on the internal effects of canopy structure on light extinction (Niinemets, 2010). This chapter provides evidence that geographic location is important in determining the distribution of N within canopies, through the effects of the average properties of incident radiation.

Interesting questions emerge relating to how multi-species canopies are constructed to achieve such coupling between LAI and TFN. To what extent are competitive interactions between species important, and if so, do prevailing radiation conditions have an impact on species composition? Or is N allocation within single plants, as a response to light conditions more important in determining whole canopy properties? The answers to these questions have implications for the speed and extent to which plant communities can respond to changing climate. If the Arctic becomes cloudier, will plant N distributions become sub-optimal with respect to LAI? And if so, what would be the effects on Arctic GPP? How would species or communities respond in order to re-gain the optimal TFN distribution? On the basis of the data presented in this chapter, a plant canopy typical of Toolik with a LAI of 1.5 m^2 m^{-2} has a TFN content of 2.1 g N m^{-2}, if this canopy was subject to an increase in average diffuse radiation fraction from ca. 65 % to ca. 80 % the optimum TFN would increase to 3.7 m^2 m^{-2}. If TFN did increase in response, perhaps through re-allocation of N from below ground, this would cause a

significant shift in plant N distribution with potential consequences for other parts of the carbon and nitrogen cycles (through, for example, effects on litter quality and above and below ground C and N allocation).

I demonstrate a lack of significant plant functional type or site effects on the relationship between near-light saturated GPP, canopy light-use efficiency and LAI. These general relationships provide a basis for estimating GPP from remotely sensed LAI over the pan-Arctic without the need for spatial data of the distribution of vascular plant vegetation type. Site differences in the allocation of TFN with respect to LAI might be expected to affect how the canopy GPP light response is related to LAI, but the data provided no support for including site as an explanatory variable. This was probably partly due to the fact that GPP measurements were made at a larger scales, reducing the variation in LAI and TFN between plots, but also indicates that other sources of variation (such as temperature and vapour pressure deficient) are more important in explaining GPP than differences in the structural properties of canopies between sites and vegetation types.

The obvious next step would be to confirm the effects of radiation conditions on multi-species canopies, through detailed sampling of N with canopy height and with species, combined with direct (and long-term) monitoring of radiation conditions and canopy light extinction. This would help to unravel between-species versus within-species effects on whole canopy N distributions. Further research might also explore whether LAI-TFN coupling occurs as result of N limitation in Arctic ecosystems, or whether the relationship holds for other natural vegetation. Experiments which manipulate light conditions in combination with modelling studies could test hypotheses relating to canopy-level versus species-level responses to changing radiation conditions, and explore the impacts of predicted changes in radiation conditions on pan-Arctic GPP.

The annual GPP of Arctic bryophytes can be a significant fraction (up to 90%) of the annual GPP of Arctic dwarf shrub communities, with pre-growing season photosynthetic activity contributing significantly to bryophyte annual gross C uptake. Moss turf water content dynamics are not important for all bryophytes (e.g. species of *Sphagnum* and *Polytrichum*) in determining annual GPP, at least for periods without sustained low rainfall. Seasonal changes in photosynthetic capacity however, are important in determining annual GPP for these species.

I quantified the annual gross C uptake by patches of bryophyte species (*Polytrichum piliferum* and *Sphagnum fuscum*) in comparison to that of neighbouring dwarf shrub tundra

vegetation. A key finding was that cumulative annual GPP for moss patches can be a significant percentage of that for vascular plant communities (for *Polytrichum* and *Sphagnum* about 90 % and 30 % respectively of dwarf shrubs with peak season LAI of 2 m^2 m^{-2}). Annual C uptake per unit ground area of these magnitudes is surprising given the small stature and low standing biomass of mosses, but can be explained partly by the earlier onset and later termination of photosynthetic activity in both species. *Polytrichum* was also able to achieve very high rates of gross photosynthesis. Examination of the drivers of annual C uptake in these species showed that, contrary to our expectations, the water content of the moss turfs did not strongly affect annual sums although the period studied did not include periods of sustained low rainfall. We show however that the timing of seasonal changes in photosynthetic capacity (between the end of March and the beginning of June) has a significant impact on cumulative GPP for both bryophyte species.

The *Polytricaceae* and *Sphagnaceae* have evolved morphological adaptations to avoid tissue desiccation. This is in contrast to many mosses which are adapted to survive periods of desiccation and lose water freely from their tissues (for example, *Pleurozium schreberi* and other feather mosses). In *Polytrichum* species water can be transported upwards to the photosynthetic tissue through xylem-like vessels, the stems also grow up through a mat of dead material and tomentum (a felt-like coating of fine filaments on the outside of the stem). Presumably this mat increases water retention at the ground surface, over and above that of bare mineral soil. *Polytrichum* also has a wax like coating on the leaf surface which repels water in a similar way to vascular plant leaves. *Sphagnum* by contrast maintains tissue water content by storing large quantities of water within the capillary spaces between leaves and stems and within hollow cells within tissues. These alternative desiccation avoidance strategies have interesting implications for the seasonal development of photosynthetic activity. *Polytrichum* is able to photosynthesise at temperatures below zero, when the underlying substrate is frozen (high rates of photosynthesis have been maintained in Antarctic *P.alpestre* at -5 °C (Kennedy, 1993)). The lack of frozen water in and on the surface of the leaves allows photosynthesis to occur as long as some moisture can be absorbed from melting snow or humid air. Photosynthesis in *Sphagnum* however, is likely to be restricted due to the freezing of liquid water in and around the leaf surfaces, which may explain why rates of photosynthesis were very low for *Sphagnum* in April; much of the photosynthetic tissue was encased ice. The biochemical ability to photosynthesise at very low temperatures would therefore confer a greater advantage in terms of carbon gain in *Polytrichum* than in *Sphagnum*, and also in vascular plants which ultimately rely on water supplied from unfrozen soil.

The large sensitivity of bryophytes annual C uptake to the development of photosynthetic capacity highlights a need to properly represent the timing of the onset of bryophyte growing season in C models. We show that the beginning of the bryophyte growing season can be many weeks before leaf emergence in vascular plants, and is not necessarily the same for all kinds of mosses. For *Sphagnum* the date of the beginning of surface ground thaw provides a reasonable early constraint. For *Polytrichum* and perhaps for many other moss species, photosynthesis can occur well before surface ground temperatures exceed zero. Despite extensive research (much of it now 20-30 years old) into Arctic and Antarctic bryophyte ecology, there is a very little available information on the responses of bryophyte respiration and photosynthesis to low temperatures (i.e. over the range -10 °C to + 5 °C) and what drives increases in photosynthetic activity in the early season. There is a clear need for detailed field sampling of bryophyte GPP before, during and after the thaw period to fully understand the controls over bryophyte annual C gain.

II) The allocation and turnover of assimilated C in Arctic vegetation.

The presence of a bryophyte understory in shrub tundra vegetation has a significant impact on community level carbon use efficiency (CUE) and the fraction of ecosystem GPP which is allocated to above ground, versus below ground net primary productivity (NPP). There are large differences in C turnover and allocation between bryophyte species. In feather mosses C turnover is also strongly dependant on tissue moisture content.

Chapter four presents the results of a stable isotope labelling experiment which aimed to quantify the effect of a moss understory on CUE and C allocation at the community level. We use a ^{13}C pulse-labelling experiment to quantify the C turnover in *Sphagnum* and *Pleurozium*, and in a dwarf shrub community with a *Pleurozium* understory. The presence of a moss understory in the dwarf shrub vegetation increased the carbon use efficiency of the community by ca. 9 %. This chapter also demonstrated that C turnover in *Pleurozium* is strongly dependant on the moisture dynamics of moss tissues, which is turn was dependant on the frequency of precipitation. The lack of precipitation for several days following labelling meant that after being wetted to allow label uptake the *Pleurozium* mosses dried and substantially decreased their metabolic activity. We then measured an increase in the return of the ^{13}C label 10 days after labelling which was linked to a heavy rainfall event after several days of dry weather.

This chapter shows that it is not possible to properly represent the allocation and turnover of C in *Pleurozium* and other desiccation tolerant mosses without including a

representation of the water status of tissues. This could be achieved through modelling the moss energy balance, using meteorological data on incident radiation, relative humidity and air temperature. Additional information on the conductance of moss canopies, the albedo of difference types of moss surface, and the influences of the vascular canopy (which probably mediates the tissues moisture dynamics) would also be needed. The effect of mosses on the thermal and hydrological regime of soils is a key uncertainty in Arctic terrestrial ecosystem models, so research effort in this area would make a valuable contribution to understanding both plant and soil C dynamics.

Appendix 2 of the thesis provides some preliminary data on the effect of different moss species on surface energy balance. Differences in surface temperature which at times exceed 15 °C indicate that mosses can have dramatic effects on energy partitioning over very small spatial scales (the two patches measured being less than 2 m apart). The temperature differences between *Sphagnum* and *Pleurozium* presumably reflect differences in moisture status and therefore partitioning to latent energy fluxes. Measurements of surface temperature using infra-red thermometers may be a basis for monitoring the water content of feather mosses which is technically challenging because capacitance or time-domain reflectometry based moisture probes are not effective.

The results of this chapter show that, for the community studied, not including mosses as a distinct vegetation type in a model representation of vegetation C dynamics would lead to an underestimation of ecosystem CUE of 9 %, and an overestimation of the fraction of GPP allocated belowground of 17 %. To help put these numbers into a landscape context, we present data in Appendix 3 on the estimated % cover of bryophytes, and the land-surface cover based on classification of aerial photographs over an 4.5 km × 1.2 km area. The land-surface classification identified 48 % of the vegetated land surface as forested. Mire-forest transition (of the type in which we conducted the labelling experiment) accounted for 30 % of the non-forested land-surface, 60 % was classified as graminoid lawn or lichen dominated vegetation. Multiplying average estimated bryophyte cover (fig. 1, Appendix 3) by the fraction of the land-surface which is mire-forest transition (fig. 2, Appendix 3) provides a first order approximation to the total cover of *Sphagnum* over the surrounding landscape (4 %). The land-surface classification alone identified only 0.2 % of land-surface cover as *Sphagnum* due to masking by the vascular canopy, a 20 fold underestimation. These results emphasize the need for better spatial data on moss abundances and surface cover; and highlight the challenge of remote-sensing the abundance of plants which are often hidden from view.

Moss species differ in their patterns of carbon allocation and rates of turnover. These differences can be linked to growth form or strategy to maintain tissue water contents.

The final chapter of the thesis describes a new model of C turnover for *Polytrichum piliferum* and *Sphagnum fuscum*. The model was developed to explore differences in C allocation and turnover between the two species, and to enable robust quantification of confidence intervals on estimates of NPP:GPP ratios and C turnover rate. The model structure consisted of four pools for labile and structural C in photosynthetic and stem tissues with photosynthetic, respiration, translocation and litter fluxes.

A surprising result of this analysis was that the central estimate of C incorporation in the aboveground tissues of *Polytrichum piliferum* was only 23 % of GPP. We were unable to quantify the percentage of GPP allocated to NPP in deeper tissues and developing shoots, but argue this is unlikely to be more than 10 %. This means that whole plant CUE in *P. piliferum* < 33 %; which is lower than the expected 40 - 60 % for vascular plants, and also lower than for other moss species (68 – 71 %) for *Sphagnum* sect. *Acutifolia* and (62 – 81 %) for *Pleurozium schreberi*. Why bryophyte species would have such widely varying CUE is unknown. In particular why is CUE so low for *Polytrichum?* Why would a plant respire such a large proportion of its assimilated carbon? One answer is that building and maintaining highly photosynthetically active tissues demands greater respiratory ATP and C skeleton generation. In chapter 3 we show that this species can match the productivity of dwarf shrubs on the per meter ground area basis. In chapter 4 we show that there appears to be a negative trend in bryophyte CUE with increasing productivity, though it could be argued that this trend is largely driven by the low CUE of *P. piliferum*. An alternative hypothesis is that the respiratory pathway of *Polytrichum* is less *efficient* at generating the respiratory products necessary for metabolism and growth, so requires greater total respiratory activity. This could occur if partitioning to non-ATP generating respiratory pathways, for example the alternative oxidase (AOX) pathway, accounts for a high proportion of respiratory activity. Partitioning to alternative respiratory metabolic pathways in higher plants has been linked to the prevention of oxidative damage under stress (Bartoli *et al.*, 2005). Perhaps *Polytrichum* which is often not associated with a vascular canopy and is therefore unshaded, requires high AOX activity to prevent damage due to high light levels. AOX activity has also been associated with thermogenesis in plants (the ability to raise tissue temperatures above ambient) as an adaptation to frost damage avoidance (Minorsky, 2003). In chapter 3 we observed early melting of snow over *Polytrichum* patches in April, which we assumed were due to the high

albedo of *Polytrichum* surface compared to the surrounding snow. Could *Polytrichum piliferum* be a candidate for the first ever documented case of a thermogenic in bryophytes?

Concluding remarks

A common theme throughout the work of this thesis has been the effect of species or species types on the way ecosystems function. The first chapter showed that vascular plant canopies converge towards general functional relationships despite large variability between species. In further chapters I demonstrate differences in function between moss species; in terms of gross C flux, C allocation and turnover, and surface energy balance. Attempts to incorporate mosses into C models at landscape scales must somehow take these functional differences into account, a challenge considering the vast spatial heterogeneity in both bryophyte abundance and species composition, confounded by the difficulties inherent in remotely sensing either. A promising approach may be to focus on categorising moisture regulation strategies (for example drought avoidance vs. tolerance) which can then potentially link the position of bryophyte in the landscape to their function.

References

ACIA (2005) *Arctic Climate Impact Assessment - Scientific Report* Cambridge University Press.

Albrizio, R. & Steduto, P. (2003) Photosynthesis, respiration and conservative carbon use efficiency of four field grown crops. *Agricultural and Forest Meteorology*, **116**, 19-36.

Amthor, J.S. (2000) The McCree-de Wit-Penning de Vries-Thornley respiration paradigms: 30 years later. *Annals of Botany*, **86**, 1-20.

Anisimov, O.A., Vaughan, D.G., Callaghan, T.V., Furgal, C., Marchant, H., Prowse, T.D., Vilhjálmsson, H., & Walsh, J.E. (2007) *Polar regions (Arctic and Antarctic).* Cambridge University Press, Cambridge.

Anten, N.P.R., Schieving, F., & Werger, M.J.A. (1995) Patterns of Light and Nitrogen Distribution in Relation to Whole Canopy Carbon Gain in C-3 and C-4 Monocotyledonous and Dicotyledonous Species. *Oecologia*, **101**, 504-513.

Arndal, M.F., Illeris, L., Michelsen, A., Albert, K., Tamstorf, M., & Hansen, B.U. (2009) Seasonal Variation in Gross Ecosystem Production, Plant Biomass, and Carbon and Nitrogen Pools in Five High Arctic Vegetation Types. *Arctic Antarctic And Alpine Research*, **41**, 164-173.

Arneth, A., Harrison, S.P., Zaehle, S., Tsigaridis, K., Menon, S., Bartlein, P.J., Feichter, J., Korhola, A., Kulmala, M., O'Donnell, D., Schurgers, G., Sorvari, S., & Vesala, T. (2010) Terrestrial biogeochemical feedbacks in the climate system. *Nature Geoscience*, **3**, 525-532.

Ayres, E., van der Wal, R., Sommerkorn, M., & Bardgett, R.D. (2006) Direct uptake of soil nitrogen by mosses. *Biology Letters*, **2**, 286-288.

Baddeley, J.A., Woodin, S.J., & Alexander, I.J. (1994) Effects of Increased Nitrogen and Phosphorus Availability on the Photosynthesis and Nutrient Relations of 3 Arctic Dwarf Shrubs from Svalbard. *Functional Ecology*, **8**, 676-685.

Bartoli, C.G., Gomez, F., Gergoff, G., Guiamet, J.J., & Puntarulo, S. (2005) Up-regulation of the mitochondrial alternative oxidase pathway enhances photosynthetic electron transport under drought conditions. *Journal of Experimental Botany*, **56**, 1269-1276.

Bekryaev, R.V., Polyakov, I.V., & Alexeev, V.A. (2010) Role of Polar Amplification in Long-Term Surface Air Temperature Variations and Modern Arctic Warming. *Journal of Climate*, **23**, 3888-3906.

Benscoter, B.W. & Vitt, D.H. (2007) Evaluating feathermoss growth: a challenge to traditional methods and implications for the boreal carbon budget. *Journal of Ecology*, **95**, 151-158.

Beringer, J., Lynch, A.H., Chapin, F.S., Mack, M., & Bonan, G.B. (2001) The representation of arctic soils in the land surface model: The importance of mosses. *Journal of Climate*, **14**, 3324-3335.

Bloom, A.A., Palmer, P.I., Fraser, A., Reay, D.S., & Frankenberg, C. (2010) Large-Scale Controls of Methanogenesis Inferred from Methane and Gravity Spaceborne Data. *Science*, **327**, 322-325.

Bond, B.J., Farnsworth, B.T., Coulombe, R.A., & Winner, W.E. (1999) Foliage physiology and biochemistry in response to light gradients in conifers with varying shade tolerance. *Oecologia*, **120**, 183-192.

Bowling, D.R., Pataki, D.E., & Randerson, J.T. (2008) Carbon isotopes in terrestrial ecosystem pools and CO2 fluxes. *New Phytologist*, **178**, 24-40.

Bret-Harte, M.S., Shaver, G.R., Zoerner, J.P., Johnstone, J.F., Wagner, J.L., Chavez, A.S., Gunkelman, R.F., Lippert, S.C., & Laundre, J.A. (2001) Developmental plasticity allows Betula nana to dominate tundra subjected to an altered environment. *Ecology*, **82**, 18-32.

Brown, J., Miller, P.C., Tieszen, L.L., & Bunnell, F.L. (1980) An Arctic Ecosystem: The coastal tundra at Barrow, Alaska. . In US IBP Synthesis Series, Vol. 12, pp. 571. Dowden, Hutchinson, and Ross, Stroudsburg, PA.

Campioli, M. (2008) Carbon allocation in ecosystems: an experimental and modelling approach for tundra and forest vegetations, Universiteit Gent, Gent.

Campioli, M., Michelsen, A., Samson, R., & Lemeur, R. (2009a) Seasonal variability of leaf area index and foliar nitrogen in contrasting dry-mesic tundras. *Botany-Botanique*, **87**, 431-442.

Campioli, M., Samson, R., Michelsen, A., Jonasson, S., Baxter, R., & Lemeur, R. (2009b) Nonvascular contribution to ecosystem NPP in a subarctic heath during early and late growing season. *Plant Ecology*, **202**, 41-53.

Cannell, M.G.R. & Thornley, J.H.M. (2000) Modelling the components of plant respiration: Some guiding principles. *Annals of Botany*, **85**, 45-54.

Carleton, T.J. & Dunham, K.M.M. (2003) Distillation in a boreal mossy forest floor. *Canadian Journal of Forest Research-Revue Canadienne De Recherche Forestiere*, **33**, 663-671.

Chapin, F.S., BretHarte, M.S., Hobbie, S.E., & Zhong, H.L. (1996) Plant functional types as predictors of transient responses of arctic vegetation to global change. *Journal of Vegetation Science*, **7**, 347-358.

Chapin, F.S., McFarland, J., McGuire, A.D., Euskirchen, E.S., Ruess, R.W., & Kielland, K. (2009) The changing global carbon cycle: linking plant-soil carbon dynamics to global consequences. *Journal of Ecology*, **97**, 840-850.

Chapin, F.S., McGuire, A.D., Randerson, J., Pielke, R., Baldocchi, D., Hobbie, S.E., Roulet, N., Eugster, W., Kasischke, E., Rastetter, E.B., Zimov, S.A., & Running, S.W. (2000) Arctic and boreal ecosystems of western North America as components of the climate system. *Global Change Biology*, **6**, 211-223.

Chapin, F.S. & Oechel, W.C. (1983) Photosynthesis, Respiration, and Phosphate Absorption by Carex-Aquatilis Ecotypes Along Latitudinal and Local Environmental Gradients. *Ecology*, **64**, 743-751.

Chapin, F.S., Oechel, W.C., Vancleve, K., & Lawrence, W. (1987) The Role of Mosses in the Phosphorus Cycling of an Alaskan Black Spruce Forest. *Oecologia*, **74**, 310-315.

Chapin, F.S., Shaver, G.R., Giblin, A.E., Nadelhoffer, K.J., & Laundre, J.A. (1995) Responses Of Arctic Tundra To Experimental And Observed Changes In Climate. *Ecology*, **76**, 694-711.

Chapin, F.S., Sturm, M., Serreze, M.C., McFadden, J.P., Key, J.R., Lloyd, A.H., McGuire, A.D., Rupp, T.S., Lynch, A.H., Schimel, J.P., Beringer, J., Chapman, W.L., Epstein, H.E., Euskirchen, E.S., Hinzman, L.D., Jia, G., Ping, C.L., Tape, K.D., Thompson, C.D.C., Walker, D.A., & Welker, J.M. (2005) Role of land-surface changes in Arctic summer warming. *Science*, **310**, 657-660.

Christensen, J.H., Hewitson, B., Busuioc, A., Chen, A., Gao, X., Held, I., Jones, R., Kolli, R.K., Kwon, W.-T., Laprise, R., Rueda, V.M., Mearns, L., Menéndez, C.G., Räisänen, J., Rinke, A., Sarr, A., & Whetton, P. (2007). Regional Climate Projections. In *Climate Change 2007: The Physical Science Basis. Contribution of Working Group I to the Fourth Assessment Report of the Intergovernmental Panel on Climate Change* (eds S. Solomon, D. Qin, M. Manning, Z. Chen, M. Marquis, K.B. Averyt, M. Tignor & H.L. Miller). Cambridge University Press, Cambridge, United Kingdom and New York, USA.

Christiansen, H.H. (2004) Meteorological control on interannual spatial and temporal variations in snow cover and ground thawing in two northeast greenlandic circumpolar-active-layer-monitoring (CALM) sites. *Permafrost and Periglacial Processes*, **15**, 155-169.

Collins, N.J. & Oechel, W.C. (1974) Pattern of Growth and Translocation of Photosynthate in a Tundra Moss, Polytrichum-Alpinum. *Canadian Journal of Botany-Revue Canadienne De Botanique*, **52**, 355-363.

Cornelissen, J.H.C., Lang, S.I., Soudzilovskaia, N.A., & During, H.J. (2007a) Comparative cryptogam ecology: A review of bryophyte and lichen traits that drive biogeochemistry. *Annals of Botany*, **99**, 987-1001.

Cornelissen, J.H.C., van Bodegom, P.M., Aerts, R., Callaghan, T.V., van Logtestijn, R.S.P., Alatalo, J., Chapin, F.S., Gerdol, R., Gudmundsson, J., Gwynn-Jones, D., Hartley, A.E., Hik, D.S., Hofgaard, A., Jonsdottir, I.S., Karlsson, S., Klein, J.A., Laundre, J., Magnusson, B., Michelsen, A., Molau, U., Onipchenko, V.G., Quested, H.M., Sandvik, S.M., Schmidt, I.K., Shaver, G.R., Solheim, B., Soudzilovskaia, N.A., Stenstrom, A., Tolvanen, A., Totland, O., Wada, N., Welker, J.M., & Zhao, X.Q. (2007b) Global negative vegetation feedback to climate warming responses of leaf litter decomposition rates in cold biomes. *Ecology Letters*, **10**, 619-627.

Davidson, E.A. & Janssens, I.A. (2006) Temperature sensitivity of soil carbon decomposition and feedbacks to climate change. *Nature*, **440**, 165-173.

Dawson, T.E., Mambelli, S., Plamboeck, A.H., Templer, P.H., & Tu, K.P. (2002) Stable isotopes in plant ecology. *Annual Review of Ecology and Systematics*, **33**, 507-559.

DeLucia, E.H., Drake, J.E., Thomas, R.B., & Gonzalez-Meler, M. (2007) Forest carbon use efficiency: is respiration a constant fraction of gross primary production? *Global Change Biology*, **13**, 1157-1167.

Denman, K.L., Brasseur, G., Chidthaisong, A., Ciais, P., Cox, P.M., Dickinson, R.E., Hauglustaine, D., Heinze, C., Holland, E., Jacob, D., Lohmann, U., Ramachandra, S., Dias, P.L.d.S., Wofsy, S.C., & Zhang, X. (2007). Couplings Between Changes in the Climate System and Biogeochemistry. In *Climate Change 2007: The Physical Science Basis. Contribution of Working Group I to the Fourth Assessment Report of the Intergovernmental Panel on Climate Change* (eds S. Solomon, D. Qin, M. Manning, Z. Chen, M.

Marquis, K.B. Averyt, M.Tignor & H.L. Miller). Cambridge University Press, Cambridge, United Kingdom and New York, NY, USA.

Dilks, T.J.K. & Proctor, M.C.F. (1979) Photosynthesis, Respiration and Water-Content in Bryophytes. *New Phytologist*, **82**, 97-&.

Dormann, C.F. & Woodin, S.J. (2002) Climate change in the Arctic: using plant functional types in a meta-analysis of field experiments. *Functional Ecology*, **16**, 4-17.

Dorrepaal, E., Aerts, R., Cornelissen, J.H.C., Callaghan, T.V., & van Logtestijn, R.S.P. (2004) Summer warming and increased winter snow cover affect Sphagnum fuscum growth, structure and production in a sub-arctic bog. *Global Change Biology*, **10**, 93-104.

Dorrepaal, E., Toet, S., van Logtestijn, R.S.P., Swart, E., van de Weg, M.J., Callaghan, T.V., & Aerts, R. (2009) Carbon respiration from subsurface peat accelerated by climate warming in the subarctic. *Nature*, **460**, 616-U79.

Douma, J., van Wijk, M.T., Lang, S.I., & Shaver, G.R. (2007) The contribution of mosses to the carbon and water exchange of arctic ecosystems: quantification and relationships with system properties. *Plant, Cell and Environment*, **30**, 1205-1215.

Ebinger, C.K. & Zambetakis, E. (2009) The geopolitics of Arctic melt. *International Affairs*, **85**, 1215-+.

Ellsworth, D.S. & Reich, P.B. (1993) Canopy Structure and Vertical Patterns of Photosynthesis and Related Leaf Traits in a Deciduous Forest. *Oecologia*, **96**, 169-178.

Erbs, D.G., Klein, S.A., & Duffie, J.A. (1982) Estimation of the Diffuse-Radiation Fraction for Hourly, Daily and Monthly-Average Global Radiation. *Solar Energy*, **28**, 293-302.

Evans, J.R. (1989) Photosynthesis and Nitrogen Relationships in Leaves of C-3 Plants. *Oecologia*, **78**, 9-19.

Fenner, N., Ostle, N., Freeman, C., Sleep, D., & Reynolds, B. (2004) Peatland carbon afflux partitioning reveals that Sphagnum photosynthate contributes to the DOC pool. *Plant and Soil*, **259**, 345-354.

Field, C. (1983) Allocating Leaf Nitrogen for the Maximization of Carbon Gain - Leaf Age as a Control on the Allocation Program. *Oecologia*, **56**, 341-347.

Forbes, B.C., Fauria, M.M., & Zetterberg, P. (2010) Russian Arctic warming and 'greening' are closely tracked by tundra shrub willows. *Global Change Biology*, **16**, 1542-1554.

Forland, E.J. & Hanssen-Bauer, I. (2000) Increased precipitation in the Norwegian Arctic: True or false? *Climatic Change*, **46**, 485-509.

Fox, A., Williams, M., Richardson, A.D., Cameron, D., Gove, J.H., Quaife, T., Ricciuto, D., Reichstein, M., Tomelleri, E., Trudinger, C.M., & Van Wijk, M.T. (2009) The REFLEX project: Comparing different algorithms and implementations for the inversion of a terrestrial ecosystem model against eddy covariance data. *Agricultural and Forest Meteorology*, **149**, 1597-1615.

Friedlingstein, P., Cox, P., Betts, R., Bopp, L., Von Bloh, W., Brovkin, V., Cadule, P., Doney, S., Eby, M., Fung, I., Bala, G., John, J., Jones, C., Joos, F., Kato, T., Kawamiya, M., Knorr, W., Lindsay, K., Matthews, H.D., Raddatz, T., Rayner, P., Reick, C., Roeckner, E., Schnitzler, K.G., Schnur, R., Strassmann, K., Weaver, A.J., Yoshikawa, C., & Zeng, N. (2006) Climate-carbon cycle feedback analysis: Results from the (CMIP)-M-4 model intercomparison. *Journal of Climate*, **19**, 3337-3353.

Frolking, S., Goulden, M.L., Wofsy, S.C., Fan, S.M., Sutton, D.J., Munger, J.W., Bazzaz, A.M., Daube, B.C., Crill, P.M., Aber, J.D., Band, L.E., Wang, X., Savage, K., Moore, T., & Harriss, R.C. (1996) Modelling temporal variability in the carbon balance of a spruce/moss boreal forest. *Global Change Biology*, **2**, 343-366.

Gaberščik, A. & Martinčič, A. (1987) Seasonal Dynamics of Net Photosynthesis and Productivity of *Sphagnum Papillosum*. *Lindbergia*, **13**, 105-110.

Gaston, K.J. (2000) Global patterns in biodiversity. *Nature*, **405**, 220-227.

Gautier, D.L., Bird, K.J., Charpentier, R.R., Grantz, A., Houseknecht, D.W., Klett, T.R., Moore, T.E., Pitman, J.K., Schenk, C.J., Schuenemeyer, J.H., Sorensen, K., Tennyson, M.E., Valin, Z.C., & Wandrey, C.J. (2009) Assessment of Undiscovered Oil and Gas in the Arctic. *Science*, **324**, 1175-1179.

Gifford, R.M. (1994) The Global Carbon-Cycle - a Viewpoint on the Missing Sink. *Australian Journal of Plant Physiology*, **21**, 1-15.

Gifford, R.M. (2003) Plant respiration in productivity models: conceptualisation, representation and issues for global terrestrial carbon-cycle research. *Functional Plant Biology*, **30**, 171-186.

Gornall, J.L., Jonsdottir, I.S., Woodin, S.J., & Van der Wal, R. (2007) Arctic mosses govern below-ground environment and ecosystem processes. *Oecologia*, **153**, 931-941.

Goulden, M.L. & Crill, P.M. (1997) Automated measurements of CO2 exchange at the moss surface of a black spruce forest. *Tree Physiology*, **17**, 537-542.

Gower, S.T., Krankina, O., Olson, R.J., Apps, M., Linder, S., & Wang, C. (2001) Net primary production and carbon allocation patterns of boreal forest ecosystems. *Ecological Applications*, **11**, 1395-1411.

Griffis, T.J., Rouse, W.R., & Waddington, J.M. (2000) Interannual variability of net ecosystem CO2 exchange at a subarctic fen. *Global Biogeochemical Cycles*, **14**, 1109-1121.

Groendahl, L., Friborg, T., & Soegaard, H. (2007) Temperature and snow-melt controls on interannual variability in carbon exchange in the high Arctic. *Theoretical and Applied Climatology*, **88**, 111-125.

Grogan, P. & Jonasson, S. (2005) Temperature and substrate controls on intra-annual variation in ecosystem respiration in two subarctic vegetation types. *Global Change Biology*, **11**, 465-475.

Grogan, P. & Jonasson, S. (2006) Ecosystem CO_2 production during winter in a Swedish subarctic region: the relative importance of climate and vegetation type. *Global Change Biology*, **12**, 1479-1495.

Gu, L.H., Baldocchi, D., Verma, S.B., Black, T.A., Vesala, T., Falge, E.M., & Dowty, P.R. (2002) Advantages of diffuse radiation for terrestrial ecosystem productivity. *Journal Of Geophysical Research-Atmospheres*, **107**.

Hallinger, M., Manthey, M., & Wilmking, M. (2010) Establishing a missing link: warm summers and winter snow cover promote shrub expansion into alpine tundra in Scandinavia. *New Phytologist*, **186**, 890-899.

Hansen, J., Ruedy, R., Sato, M., & Lo, K. (2010) Global Surface Temperature Change. *Reviews of Geophysics*, **48**.

Harley, P.C., Tenhunen, J.D., Murray, K.J., & Beyers, J. (1989) Irradiance and Temperature Effects on Photosynthesis of Tussock Tundra Sphagnum Mosses from the Foothills of the Philip Smith Mountains, Alaska. *Oecologia*, **79**, 251-259.

Hartley, I.P., Hopkins, D.W., Garnett, M.H., Sommerkorn, M., & Wookey, P.A. (2008) Soil microbial respiration in arctic soil does not acclimate to temperature. *Ecology Letters*, **11**, 1092-1100.

Hicklenton, P.R. & Oechel, W.C. (1977) Influence of Light-Intensity and Temperature on Field Carbon-Dioxide Exchange of Dicranum-Fuscescens in Subarctic. *Arctic And Alpine Research*, **9**, 407-419.

Hikosaka, K. & Hirose, T. (1998) Leaf and canopy photosynthesis of C-3 plants at elevated CO2 in relation to optimal partitioning of nitrogen among photosynthetic components: theoretical prediction. *Ecological Modelling*, **106**, 247-259.

Hill, G.B. & Henry, G.H.R. (2011) Responses of High Arctic wet sedge tundra to climate warming since 1980. *Global Change Biology*, **17**, 276-287.

Hirose, T. (2005) Development of the Monsi-Saeki theory on canopy structure and function. *Annals of Botany*, **95**, 483-494.

Hirose, T. & Werger, M.J.A. (1987) Maximizing Daily Canopy Photosynthesis with Respect to the Leaf Nitrogen Allocation Pattern in the Canopy. *Oecologia*, **72**, 520-526.

Hobbie, S.E., Schimel, J.P., Trumbore, S.E., & Randerson, J.R. (2000) Controls over carbon storage and turnover in high-latitude soils. *Global Change Biology*, **6**, 196-210.

Holland, M.M. & Bitz, C.M. (2003) Polar amplification of climate change in coupled models. *Climate Dynamics*, **21**, 221-232.

Hollinger, D.Y. (1996) Optimality and nitrogen allocation in a tree canopy. *Tree Physiology*, **16**, 627-634.

Hollister, R.D., Webber, P.J., & Bay, C. (2005) Plant response to temperature in Northern Alaska: Implications for predicting vegetation change. *Ecology*, **86**, 1562-1570.

Hooper, D.U., Cardon, Z.G., Chapin, F.S., III, & Durant, M. (2002) Corrected calculations for soil and ecosystem measurements of CO_2 flux using the LI-COR 6200 portable photosynthesis system. *Oecologia*, **132**, 1-11.

Hudson, J.M.G. & Henry, G.H.R. (2010) High Arctic plant community resists 15 years of experimental warming. *Journal of Ecology*, **98**, 1035-1041.

Huemmrich, K.F., Gamon, J.A., Tweedie, C.E., Oberbauer, S.F., Kinoshita, G., Houston, S., Kuchy, A., Hollister, R.D., Kwon, H., Mano, M., Harazono, Y., Webber, P.J., & Oechel, W.C. (2010a) Remote sensing of tundra gross ecosystem productivity and light use efficiency under varying temperature and moisture conditions. *Remote Sensing of Environment*, **114**, 481-489.

Huemmrich, K.F., Kinoshita, G., Gamon, J.A., Houston, S., Kwon, H., & Oechel, W.C. (2010b) Tundra carbon balance under varying temperature and moisture regimes. *Journal of Geophysical Research-Biogeosciences*, **115**.

Ise, T., Litton, C.M., Giardina, C.P., & Ito, A. (2010) Comparison of modeling approaches for carbon partitioning: Impact on estimates of global net primary production and equilibrium biomass of woody vegetation from MODIS GPP. *Journal of Geophysical Research-Biogeosciences*, **115**.

Jia, G.S.J., Epstein, H.E., & Walker, D.A. (2003) Greening of arctic Alaska, 1981-2001. *Geophysical Research Letters*, **30**.

Jia, G.S.J., Epstein, H.E., & Walker, D.A. (2009) Vegetation greening in the canadian arctic related to decadal warming. *Journal of Environmental Monitoring*, **11**, 2231-2238.

Johansson, T., Malmer, N., Crill, P.M., Friborg, T., Akerman, J.H., Mastepanov, M., & Christensen, T.R. (2006) Decadal vegetation changes in a northern peatland, greenhouse gas fluxes and net radiative forcing. *Global Change Biology*, **12**, 2352-2369.

Kammer, A., Hagedorn, F., Shevchenko, I., Leifeld, J., Guggenberger, G., Goryacheva, T., Rigling, A., & Moiseev, P. (2009) Treeline shifts in the Ural mountains affect soil organic matter dynamics. *Global Change Biology*, **15**, 1570-1583.

Karlsson, P.S. (1989) Insitu Photosynthetic Performance of 4 Coexisting Dwarf Shrubs in Relation to Light in a Subarctic Woodland. *Functional Ecology*, **3**, 481-487.

Kennedy, A.D. (1993) Photosynthetic Response of the Antarctic Moss Polytrichum-Alpestre Hoppe to Low-Temperatures and Freeze-Thaw Stress. *Polar Biology*, **13**, 271-279.

Kwon, H.J., Oechel, W.C., Zulueta, R.C., & Hastings, S.J. (2006) Effects of climate variability on carbon sequestration among adjacent wet sedge tundra and moist tussock tundra ecosystems. *Journal of Geophysical Research-Biogeosciences*, **111**.

Litton, C.M. & Giardina, C.P. (2008) Below-ground carbon flux and partitioning: global patterns and response to temperature. *Functional Ecology*, **22**, 941-954.

Litton, C.M., Raich, J.W., & Ryan, M.G. (2007) Carbon allocation in forest ecosystems. *Global Change Biology*, **13**, 2089-2109.

Lloyd, C.R. (2001) The measurement and modelling of the carbon dioxide exchange at a high Arctic site in Svalbard. *Global Change Biology*, **7**, 405-426.

Longton, R.E. (1988) *Biology of Polar Bryophytes and Lichens* Cambridge University Press, Cambridge.

Lund, M., Lafleur, P.M., Roulet, N.T., Lindroth, A., Christensen, T.R., Aurela, M., Chojnicki, B.H., Flanagan, L.B., Humphreys, E.R., Laurila, T., Oechel, W.C., Olejnik, J., Rinne, J., Schubert, P., & Nilsson, M.B. (2010) Variability in exchange of CO2 across 12 northern peatland and tundra sites. *Global Change Biology*, **16**, 2436-2448.

Mack, M.C., Schuur, E.A.G., Bret-Harte, M.S., Shaver, G.R., & Chapin, F.S. (2004) Ecosystem carbon storage in arctic tundra reduced by long-term nutrient fertilization. *Nature*, **431**, 440-443.

McBean, G., Alekseev, G., Chen, D., Førland, E., Fyfe, J., Groisman, P.Y., King, R., Melling, H., Vose, R., & Whitfield, P.H. (2005). Arctic climate: past and present. In *Arctic Climate Impact Assessment: Scientific Report*, pp. 21–60. Cambridge University Press, Cambridge, UK.

McCutchan, C.L. & Monson, R.K. (2001) Effects of tissue-type and development on dark respiration in two herbaceous perennials. *Annals of Botany*, **87**, 355-364.

McGuire, A.D., Anderson, L.G., Christensen, T.R., Dallimore, S., Guo, L.D., Hayes, D.J., Heimann, M., Lorenson, T.D., Macdonald, R.W., & Roulet, N. (2009) Sensitivity of the carbon cycle in the Arctic to climate change. *Ecological Monographs*, **79**, 523-555.

McGuire, A.D., Chapin, F.S., III, Walsh, J.E., & Wirth, C. (2006) Integrated Regional Changes In Arctic Climate Feedbacks: Implications for the Global Climate System. *Annual Review of Environment and Resources*, **31**, 61-91.

McGuire, A.D., Clein, J.S., Melillo, J.K., Kicklighter, D.W., Meier, R.A., Vorosmarty, C.J., & Serreze, M.C. (2000) Modeling carbon responses of tundra ecosystems to historical and projected climate: sensitivity of pan-Arctic carbon storage to temporal and spatial variation in climate. *Global Change Biology*, **6**, 141-159.

McGuire, A.D., Hayes, D.J., Kicklighter, D.W., Manizza, M., Zhuang, Q., Chen, M., Follows, M.J., Gurney, K.R., McClelland, J.W., Melillo, J.M., Peterson, B.J., & Prinn, R.G. (2010) An analysis of the carbon balance of the Arctic Basin from 1997 to 2006. *Tellus Series B-Chemical and Physical Meteorology*, **62**, 455-474.

McKane, R.B., Rastetter, E.B., Shaver, G.R., Nadelhoffer, K.J., Giblin, A.E., Laundre, J.A., & Chapin, F.S. (1997a) Climatic effects on tundra carbon storage inferred from experimental data and a model. *Ecology*, **78**, 1170-1187.

McKane, R.B., Rastetter, E.B., Shaver, G.R., Nadelhoffer, K.J., Giblin, A.E., Laundre, J.A., & Chapin, F.S. (1997b) Reconstruction and analysis of historical changes in carbon storage in arctic tundra. *Ecology*, **78**, 1188-1198.

Meir, P., Kruijt, B., Broadmeadow, M., Barbosa, E., Kull, O., Carswell, F., Nobre, A., & Jarvis, P.G. (2002) Acclimation of photosynthetic capacity to irradiance in tree canopies in relation to leaf nitrogen concentration and leaf mass per unit area. *Plant Cell And Environment*, **25**, 343-357.

Miller, P.C., Oechel, W.C., Stoner, W.A., & Sveinbjornsson, B. (1976) Simulation of CO_2 Uptake and Water Relations of Four Arctic Bryophytes at Point Barrow, Alaska. *Photosynthetica*, **12**, 7-20.

Miller, P.C., Webber, P.J., Oechel, W.C., & Tieszen, L.L. (1980). Biophysical Processes and Primary Production In *An Arctic Ecosystem: the Coastal Tundra at Barrow, Alaska.* (eds J.M. Brown, P.C. Miller, L.L. Tieszen & F.L. Bunnell), pp. 66-101. Dowden, Hutchinson & Ross, Inc., Stroudsburg, PA.

Minorsky, P.V. (2003) The hot and the classic. *Plant Physiology*, **132**, 25-26.

Molau, U. (2010) Long-term impacts of observed and induced climate change on tussock tundra near its southern limit in northern Sweden. *Plant Ecology & Diversity*, **3**, 29-34.

Murray, K.J., Harley, P.C., Beyers, J., Walz, H., & Tenhunen, J.D. (1989) Water-Content Effects on Photosynthetic Response of Sphagnum Mosses from the Foothills of the Philip Smith Mountains, Alaska. *Oecologia*, **79**, 244-250.

Myneni, R.B., Keeling, C.D., Tucker, C.J., Asrar, G., & Nemani, R.R. (1997) Increased plant growth in the northern high latitudes from 1981 to 1991. *Nature*, **386**, 698-702.

Niinemets, U. (2007) Photosynthesis and resource distribution through plant canopies. *Plant Cell And Environment*, **30**, 1052-1071.

Niinemets, U. (2010) A review of light interception in plant stands from leaf to canopy in different plant functional types and in species with varying shade tolerance. *Ecological Research*, **25**, 693-714.

Oechel, W.C. (1976) Seasonal Patterns of Temperature Response of CO_2 Flux and Acclimation in Arctic Mosses Growing i*n Situ*. *Photosynthetica*, **10**, 447-456.

Oechel, W.C. & Collins, N.J. (1976) Comparative CO_2 Exchange Patterns in Mosses from 2 Tundra Habitats at Barrow, Alaska. *Canadian Journal of Botany-Revue Canadienne De Botanique*, **54**, 1355-1369.

Penny, M.G. & Bayfield, N.G. (1982) Photosynthesis in Desiccated Shoots of Polytrichum. *New Phytologist*, **91**, 637-645.

Ping, C.L., Michaelson, G.J., Jorgenson, M.T., Kimble, J.M., Epstein, H., Romanovsky, V.E., & Walker, D.A. (2008) High stocks of soil organic carbon in the North American Arctic region. *Nature Geoscience*, **1**, 615-619.

Polyakov, I.V., Alekseev, G.V., Bekryaev, R.V., Bhatt, U., Colony, R.L., Johnson, M.A., Karklin, V.P., Makshtas, A.P., Walsh, D., & Yulin, A.V. (2002) Observationally based assessment of polar amplification of global warming. *Geophysical Research Letters*, **29**.

Post, E., Forchhammer, M.C., Bret-Harte, M.S., Callaghan, T.V., Christensen, T.R., Elberling, B., Fox, A.D., Gilg, O., Hik, D.S., Hoye, T.T., Ims, R.A., Jeppesen, E., Klein, D.R., Madsen, J., McGuire, A.D., Rysgaard, S., Schindler, D.E., Stirling, I., Tamstorf, M.P., Tyler, N.J.C., van der Wal, R., Welker, J.,

Wookey, P.A., Schmidt, N.M., & Aastrup, P. (2009) Ecological Dynamics Across the Arctic Associated with Recent Climate Change. *Science*, **325**, 1355-1358.

Proctor, M.C.F. (2000) The bryophyte paradox: tolerance of desiccation, evasion of drought. *Plant Ecology*, **151**, 41-49.

Proctor, M.C.F. (2009). Physiological Ecology. In *Bryophyte Biology* (eds B. Goffinet & A.J. Shaw), pp. 273-269. Cambridge University Press, Cambridge.

Proctor, M.C.F., Raven, J.A., & Rice, S.K. (1992) Stable Carbon Isotope Discrimination Measurements in Sphagnum and Other Bryophytes - Physiological and Ecological Implications. *Journal of Bryology*, **17**, 193-202.

Qian, H.F., Joseph, R., & Zeng, N. (2010) Enhanced terrestrial carbon uptake in the Northern High Latitudes in the 21st century from the Coupled Carbon Cycle Climate Model Intercomparison Project model projections. *Global Change Biology*, **16**, 641-656.

Rastetter, E.B., Williams, M., Griffin, K.L., Kwiatkowski, B.L., Tomasky, G., Potosnak, M.J., Stoy, P.C., Shaver, G.R., Stieglitz, M., Hobbie, J.E., & Kling, G.W. (2010) Processing arctic eddy-flux data using a simple carbon-exchange model embedded in the ensemble Kalman filter. *Ecological Applications*, **20**, 1285-1301.

Reich, P.B. & Oleksyn, J. (2004) Global patterns of plant leaf N and P in relation to temperature and latitude. *Proceedings Of The National Academy Of Sciences Of The United States Of America*, **101**, 11001-11006.

Robroek, B.J.M., Schouten, M.G.C., Limpens, J., Berendse, F., & Poorter, H. (2009) Interactive effects of water table and precipitation on net CO2 assimilation of three co-occurring Sphagnum mosses differing in distribution above the water table. *Global Change Biology*, **15**, 680-691.

Roderick, M.L., Farquhar, G.D., Berry, S.L., & Noble, I.R. (2001) On the direct effect of clouds and atmospheric particles on the productivity and structure of vegetation. *Oecologia*, **129**, 21-30.

Rustad, L.E., Campbell, J.L., Marion, G.M., Norby, R.J., Mitchell, M.J., Hartley, A.E., Cornelissen, J.H.C., & Gurevitch, J. (2001) A meta-analysis of the response of soil respiration, net nitrogen mineralization, and aboveground plant growth to experimental ecosystem warming. *Oecologia*, **126**, 543-562.

Ryan, M.G., Gower, S.T., Hubbard, R.M., Waring, R.H., Gholz, H.L., Cropper, W.P., & Running, S.W. (1995) Woody Tissue Maintenance Respiration of 4 Conifers in Contrasting Climates. *Oecologia*, **101**, 133-140.

Rydin, H. & McDonald, A.J.S. (1985) Tolerance of Sphagnum to Water Level. *Journal of Bryology*, **13**, 571-578.

Sanderson, M.G., Hemming, D.L., & Betts, R.A. (2011) Regional temperature and precipitation changes under high-end (>= 4 degrees C) global warming. *Philosophical Transactions of the Royal Society a-Mathematical Physical and Engineering Sciences*, **369**, 85-98.

Schuur, E.A.G., Vogel, J.G., Crummer, K.G., Lee, H., Sickman, J.O., & Osterkamp, T.E. (2009) The effect of permafrost thaw on old carbon release and net carbon exchange from tundra. *Nature*, **459**, 556-559.

Shakhova, N., Semiletov, I., Leifer, I., Salyuk, A., Rekant, P., & Kosmach, D. (2010) Geochemical and geophysical evidence of methane release over the East Siberian Arctic Shelf. *Journal of Geophysical Research-Oceans*, **115**.

Shaver, G.R., Bret-Harte, S.M., Jones, M.H., Johnstone, J., Gough, L., Laundre, J., & Chapin, F.S. (2001) Species composition interacts with fertilizer to control long-term change in tundra productivity. *Ecology*, **82**, 3163-3181.

Shaver, G.R. & Chapin, F.S. (1980) Response to Fertilization by Various Plant Growth Forms in an Alaskan tundra: Nutrient accumulation and growth. *Ecology*, **61**, 662-675.

Shaver, G.R. & Chapin, F.S. (1986) Effect of fertilizer on production and biomass of tussock tundra, Alaska, U.S.A. *Arctic And Alpine Research*, **18**, 261-268.

Shaver, G.R. & Chapin, F.S. (1991) Production - Biomass Relationships And Element Cycling In Contrasting Arctic Vegetation Types. *Ecological Monographs*, **61**, 1-31.

Shaver, G.R., Giblin, A.E., Nadelhoffer, K.J., Thieler, K.K., Downs, M.R., Laundre, J.A., & Rastetter, E.B. (2006) Carbon turnover in Alaskan tundra soils: effects of organic matter quality, temperature, moisture and fertilizer. *Journal of Ecology*, **94**, 740-753.

Shaver, G.R., Street, L.E., Rastetter, E.B., Van Wijk, M.T., & Williams, M. (2007) Functional convergence in regulation of net CO2 flux in heterogeneous tundra landscapes in Alaska and Sweden. *Journal of Ecology*, **95**, 802-817.

Shipley, B., Lechoweicz, M.J., Wright, I., & Reich, P.B. (2006) Fundamental trade-offs generating the worldwide leaf economics spectrum. *Ecology*, **87**, 535-541.

Sitch, S., Huntingford, C., Gedney, N., Levy, P.E., Lomas, M., Piao, S.L., Betts, R., Ciais, P., Cox, P., Friedlingstein, P., Jones, C.D., Prentice, I.C., & Woodward, F.I. (2008) Evaluation of the terrestrial carbon cycle, future plant geography and climate-carbon cycle feedbacks using five Dynamic Global Vegetation Models (DGVMs). *Global Change Biology*, **14**, 2015-2039.

Sitch, S., McGuire, A.D., Kimball, J., Gedney, N., Gamon, J., Engstrom, R., Wolf, A., Zhuang, Q., Clein, J., & McDonald, K.C. (2007) Assessing the carbon balance of circumpolar Arctic tundra using remote sensing and process modeling. *Ecological Applications*, **17**, 213-234.

Sjogersten, S. & Wookey, P.A. (2009) The Impact of Climate Change on Ecosystem Carbon Dynamics at the Scandinavian Mountain Birch Forest-Tundra Heath Ecotone. *Ambio*, **38**, 2-10.

Skre, O. & Oechel, W.C. (1981) Moss Functioning in Different Taiga Ecosystems in Interior Alaska .1. Seasonal, Phenotypic, and Drought Effects on Photosynthesis and Response Patterns. *Oecologia*, **48**, 50-59.

Skre, O., Oechel, W.C., & Miller, P.M. (1983) Patterns of Translocation of Carbon in 4 Common Moss Species in a Black Spruce (Picea-Mariana) Dominated Forest in Interior Alaska. *Canadian Journal of Forest Research-Revue Canadienne De Recherche Forestiere*, **13**, 869-878.

Solomon, S., D. Qin, M. Manning, Z. Chen, M. Marquis, K.B. Averyt, Tignor, M., & Miller, H.L., eds. (2007) *Contribution of Working Group I to the Fourth Assessment Report of the Intergovernmental Panel on Climate Change*. Cambridge University Press, Cambridge, UK.

Sommerkorn, M. (2000) The ability of lichens to benefit from natural CO_2 enrichment under a spring snow-cover: a study with two arctic-alpine species from contrasting habitats. *Bibliotheca Lichenologica*, **75**, 365-380.

Sommerkorn, M., Bolter, M., & Kappen, L. (1999) Carbon dioxide fluxes of soils and mosses in wet tundra of Taimyr Peninsula, Siberia: controlling factors and contribution to net system fluxes. *Polar Research*, **18**, 253-260.

Spadavecchia, L., Williams, M., Bell, R., Stoy, P.C., Huntley, B., & van Wijk, M.T. (2008) Topographic controls on the leaf area index and plant functional type of a tundra ecosystem. *Journal of Ecology*, **96**, 1238-1251.

Starr, G. & Oberbauer, S.F. (2003) Photosynthesis of arctic evergreens under snow: Implications for tundra ecosystem carbon balance. *Ecology*, **84**, 1415-1420.

Steltzer, H. & Welker, J.M. (2006) Modeling the effect of photosynthetic vegetation properties on the NDVI-LAI relationship. *Ecology*, **87**, 2765-2772.

Street, L.E., Shaver, G.R., Williams, M., & Van Wijk, M.T. (2007) What is the relationship between changes in canopy leaf area and changes in photosynthetic CO2 flux in arctic ecosystems? *Journal of Ecology*, **95**, 139-150.

Sturm, M., Racine, C., & Tape, K. (2001) Increasing shrub abundance in the Arctic. *Nature*, **411**, 546-547.

Subke, J.A., Vallack, H.W., Magnusson, T., Keel, S.G., Metcalfe, D.B., Högberg, P., & Ineson, P. (2009) Short-term dynamics of abiotic and biotic soil (CO2)-C-13 effluxes after in situ (CO2)-C-13 pulse labelling of a boreal pine forest. *New Phytologist*, **183**, 349-357.

Sveinbjornsson, B. & Oechel, W.C. (1981) Controls on CO_2 exchange in two *Polytrichum* moss species. 2. The implications of belowground plant-parts on the whole-plant carbon balance. *Oikos*, **36**, 348-354.

Sveinbjornsson, B. & Oechel, W.C. (1983) The Effect of Temperature Preconditioning on the Temperature Sensitivity of Net Co2 Flux in Geographically Diverse Populations of the Moss Polytrichum-Commune. *Ecology*, **64**, 1100-1108.

Tape, K., Sturm, M., & Racine, C. (2006) The evidence for shrub expansion in Northern Alaska and the Pan-Arctic. *Global Change Biology*, **12**, 686-702.

Tarnocai, C., Canadell, J.G., Schuur, E.A.G., Kuhry, P., Mazhitova, G., & Zimov, S. (2009) Soil organic carbon pools in the northern circumpolar permafrost region. *Global Biogeochemical Cycles*, **23**.

Tast, J. (1991) Will the Norwegian Lemming Become Endangered If Climate Becomes Warmer. *Arctic And Alpine Research*, **23**, 53-60.

Thomas, R.J., Ryder, S.H., Gardner, M.I., Sheetz, J.P., & Nichipor, S.D. (1996) Photosynthetic function of leaf lamellae in Polytrichum commune. *Bryologist*, **99**, 6-11.

Thomas, R.J., Schiele, E.M., & Damberg, D.T. (1990) Translocation in Polytrichum-Commune (Bryophyta) .2. Clonal Integration. *American Journal of Botany*, **77**, 1569-1573.

Thomas, R.J., Schiele, E.M., & Scheirer, D.C. (1988) Translocation in Polytrichum-Commune (Bryophyta) .1. Conduction and Allocation of Photoassimilates. *American Journal of Botany*, **75**, 275-281.

Trenberth, K.E., Jones, P.D., Ambenje, P., Bojariu, R., Easterling, D., Tank, A.K., Parker, D., Rahimzadeh, F., Renwick, J.A., Rusticucci, M., Soden, B., & Zhai, P. (2007). Observations: Surface and Atmospheric Climate Change. In *Climate Change 2007: The Physical Science Basis. Contribution of Working Group I to the Fourth Assessment Report of the Intergovernmental Panel on Climate Change* (eds S. Solomon, D. Qin, M. Manning, Z. Chen, M. Marquis, K.B. Averyt, M. Tignor & H.L. Miller). Cambridge University Press, Cambridge, United Kingdom and New York, USA.

Trumbore, S. (2006) Carbon respired by terrestrial ecosystems - recent progress and challenges. *Global Change Biology*, **12**, 141-153.

Tuba, Z., Protor, M.C.F., & Csintalan, Z. (1998) Ecophysiological responses of homoiochlorophyllous and poikilochlorophyllous desiccation tolerant plants: a comparison and an ecological perspective. *Plant Growth Regulation*, **24**, 211-217.

Turetsky, M.R., Crow, S.E., Evans, R.J., Vitt, D.H., & Wieder, R.K. (2008) Trade-offs in resource allocation among moss species control decomposition in boreal peatlands. *Journal of Ecology*, **96**, 1297-1305.

Turetsky, M.R. & Wieder, R.K. (1999) Boreal bog Sphagnum refixes soil-produced and respired (CO2)-C-14. *Ecoscience*, **6**, 587-591.

Uchida, M., Kishimoto, A., Muraoka, H., Nakatsubo, T., Kanda, H., & Koizumi, H. (2010) Seasonal shift in factors controlling net ecosystem production in a high Arctic terrestrial ecosystem. *Journal of Plant Research*, **123**, 79-85.

van der Wal, R., Pearce, I.S.K., & Brooker, R.W. (2005) Mosses and the struggle for light in a nitrogen-polluted world. *Oecologia*, **142**, 159-168.

Van Iersel, M.W. (2003) Carbon use efficiency depends on growth respiration, maintenance respiration, and relative growth rate. A case study with lettuce. *Plant Cell And Environment*, **26**, 1441-1449.

van Wijk, M.T., Clemmensen, K.E., Shaver, G.R., Williams, M., Callaghan, T.V., Chapin, F.S., Cornelissen, J.H.C., Gough, L., Hobbie, S.E., Jonasson, S., Lee, J.A., Michelsen, A., Press, M.C., Richardson, S.J., & Rueth, H. (2004) Long-term ecosystem level experiments at Toolik Lake, Alaska, and at Abisko, Northern Sweden: generalizations and differences in ecosystem and plant type responses to global change. *Global Change Biology*, **10**, 105-123.

van Wijk, M.T., Williams, M., & Shaver, G.R. (2005) Tight coupling between leaf area index and foliage N content in arctic plant communities. *Oecologia*, **142**, 421-427.

Verbyla, D. (2008) The greening and browning of Alaska based on 1982-2003 satellite data. *Global Ecology and Biogeography*, **17**, 547-555.

Vitt, D.H. & Wieder, R.K. (2009). Bryophyte-dominated peatlands. In *Bryophyte Biology* (eds B. Goffinet & A.J. Shaw), pp. 357-392. Cambridge University Press, Cambridge.

Vogel, J., Schuur, E.A.G., Trucco, C., & Lee, H. (2009) Response of CO2 exchange in a tussock tundra ecosystem to permafrost thaw and thermokarst development. *Journal of Geophysical Research-Biogeosciences*, **114**.

Walker, D.A. (2000) Hierarchical subdivision of Arctic tundra based on vegetation response to climate, parent material and topography. *Global Change Biology*, **6**, 19-34.

Walker, M.D., Wahren, C.H., Hollister, R.D., Henry, G.H.R., Ahlquist, L.E., Alatalo, J.M., Bret-Harte, M.S., Calef, M.P., Callaghan, T.V., Carroll, A.B., Epstein, H.E., Jonsdottir, I.S., Klein, J.A., Magnusson, B., Molau, U., Oberbauer, S.F., Rewa, S.P., Robinson, C.H., Shaver, G.R., Suding, K.N., Thompson, C.C., Tolvanen, A., Totland, O., Turner, P.L., Tweedie, C.E., Webber, P.J., & Wookey, P.A. (2006) Plant community responses to experimental warming across the tundra biome. *Proceedings Of The National Academy Of Sciences Of The United States Of America*, **103**, 1342-1346.

Wallenstein, M.D., McMahon, S.K., & Schimel, J.P. (2009) Seasonal variation in enzyme activities and temperature sensitivities in Arctic tundra soils. *Global Change Biology*, **15**, 1631-1639.

Wania, R., Ross, I., & Prentice, I.C. (2009a) Integrating peatlands and permafrost into a dynamic global vegetation model: 1. Evaluation and sensitivity of physical land surface processes. *Global Biogeochemical Cycles*, **23**.

Wania, R., Ross, I., & Prentice, I.C. (2009b) Integrating peatlands and permafrost into a dynamic global vegetation model: 2. Evaluation and sensitivity of vegetation and carbon cycle processes. *Global Biogeochemical Cycles*, **23**.

Waring, R.H., Landsberg, J.J., & Williams, M. (1998) Net primary production of forests: a constant fraction of gross primary production? *Tree Physiology*, **18**, 129-134.

Warren, C.R. & Dreyer, E. (2006) Temperature response of photosynthesis and internal conductance to CO2: results from two independent approaches. *Journal of Experimental Botany*, **57**, 3057-3067.

Weih, M. & Karlsson, P.S. (2001) Growth response of Mountain birch to air and soil temperature: is increasing leaf-nitrogen content an acclimation to lower air temperature? *New Phytologist*, **150**, 147-155.

Williams, M., Bell, R., Spadavecchia, L., Street, L.E., & Van Wijk, M.T. (2008) Upscaling leaf area index in an Arctic landscape through multiscale observations. *Global Change Biology*, **14**, 1517-1530.

Williams, M. & Rastetter, E.B. (1999) Vegetation characteristics and primary productivity along an arctic transect: implications for scaling up. *Journal of Ecology*, **87**, 885-898.

Williams, M., Rastetter, E.B., Shaver, G.R., Hobbie, J.E., Carpino, E., & Kwiatkowski, B.L. (2001) Primary production of an arctic watershed: An uncertainty analysis. *Ecological Applications*, **11**, 1800-1816.

Williams, M., Schwarz, P.A., Law, B.E., Irvine, J., & Kurpius, M.R. (2005) An improved analysis of forest carbon dynamics using data assimilation. *Global Change Biology*, **11**, 89-105.

Williams, M., Street, L.E., van Wijk, M.T., & Shaver, G.R. (2006) Identifying Differences in Carbon Exchange among Arctic Ecosystem Types. *Ecosystems*, **9**, 288-304.

Williams, T.G. & Flanagan, L.B. (1996) Effect of changes in water content on photosynthesis, transpiration and discrimination against (CO2)-C-13 and (COO)-O-18-O-16 in Pleurozium and Sphagnum. *Oecologia*, **108**, 38-46.

Williams, T.G. & Flanagan, L.B. (1998) Measuring and modelling environmental influences on photosynthetic gas exchange in Sphagnum and Pleurozium. *Plant Cell And Environment*, **21**, 555-564.

Wilmking, M., Harden, J., & Tape, K. (2006) Effect of tree line advance on carbon storage in NW Alaska. *Journal of Geophysical Research-Biogeosciences*, **111**.

Wilson, J.A. & Coxson, D.S. (1999) Carbon flux in a subalpine spruce-fir forest: pulse release from Hylocomium splendens feather-moss mats. *Canadian Journal of Botany-Revue Canadienne De Botanique*, **77**, 564-569.

Wolf, A., Kozlov, M.V., & Callaghan, T.V. (2008) Impact of non-outbreak insect damage on vegetation in northern Europe will be greater than expected during a changing climate. *Climatic Change*, **87**, 91-106.

Woodin, S.J., van der Wal, R., Sommerkorn, M., & Gornall, J.L. (2009) Differential allocation of carbon in mosses and grasses governs ecosystem sequestration: a ^{13}C tracer study in the high Arctic. *New Phytologist*, **184**, 944-949.

Wookey, P.A., Aerts, R., Bardgett, R.D., Baptist, F., Brathen, K.A., Cornelissen, J.H.C., Gough, L., Hartley, I.P., Hopkins, D.W., Lavorel, S., & Shaver, G.R. (2009) Ecosystem feedbacks and cascade processes: understanding their role in the responses of Arctic and alpine ecosystems to environmental change. *Global Change Biology*, **15**, 1153-1172.

Wright, I.J., Reich, P.B., Westoby, M., Ackerly, D.D., Baruch, Z., Bongers, F., Cavender-Bares, J., Chapin, T., Cornelissen, J.H.C., Diemer, M., Flexas, J., Garnier, E., Groom, P.K., Gulias, J., Hikosaka, K., Lamont, B.B., Lee, T., Lee, W., Lusk, C., Midgley, J.J., Navas, M.L., Niinemets, U., Oleksyn, J., Osada, N., Poorter, H., Poot, P., Prior, L., Pyankov, V.I., Roumet, C., Thomas, S.C., Tjoelker, M.G., Veneklaas, E.J., & Villar, R. (2004) The worldwide leaf economics spectrum. *Nature*, **428**, 821-827.

Zhang, Y.J., Xu, M., Chen, H., & Adams, J. (2009) Global pattern of NPP to GPP ratio derived from MODIS data: effects of ecosystem type, geographical location and climate. *Global Ecology and Biogeography*, **18**, 280-290.

Appendix 1

This appendix contains moss biomass and percent cover data for the ABACUS field sites at Kevo and Abisko. Site descriptions are provided in Chapters 2, 3 & 4.

Methods

Mosses were harvested from 0.2 × 0.2 m harvest plots (these were the same plots sampled by other ABACUS work packages). All moss material was removed from the plots after the vascular plant canopy had been removed at ground level. A 0.1 × 0.1 m sub-sample was taken from the NW corner of each plot. This material was placed into a plastic bag. The remaining ¾ of the plot was then removed and placed into a second bag. The sub-sample was sorted into 'green' material and litter (including moss and vascular plant litter). Sorted material and the un-sorted remaining ¾ were then dried for at least 3 days at 70 °C. The total 'green' material for the whole plot was calculated according to the following formula:

$$M_{gT} = [M_{gS}/(M_{lS} + M_{gS})] \times M_R + M_{gS}$$

M_{gT} is total mass of green moss material in the plot (g), M_{gS} is mass of green material in the sub-sample (g), M_{lS} is mass of litter in the sub-sample (g), M_R is total mass of unsorted ¾ remainder of the plot (g).

The plots were sub-sampled to reduce the time required to sort the green moss material from litter and brown moss material (processing of one 0.1 × 0.1 m sub-sample could take up to 4hrs) . If there was only small amounts of moss material in the plot, or if the NW corner was judged to be unrepresentative, plots were not sub-sampled.

59 plots were harvested at Abisko, 66 plots were harvested at Kevo.

Percent cover of mosses was estimated after the vascular canopy was removed.

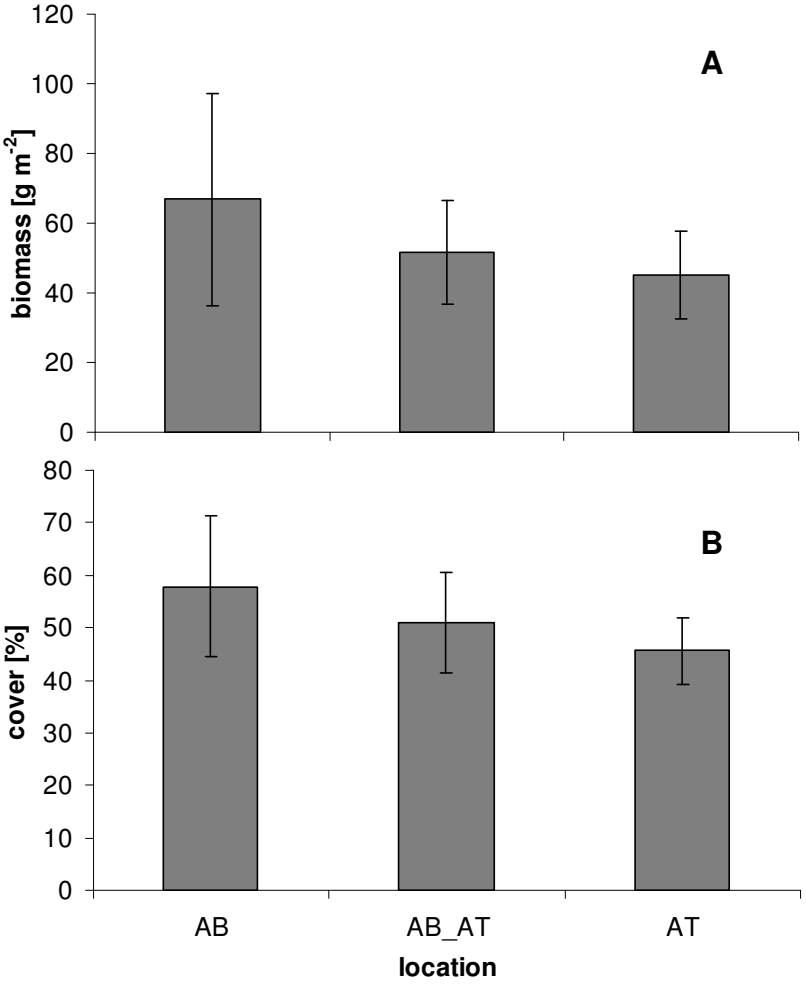

Figure 1a) Biomass (g m^{-2}) and b) estimated percent cover (%) of bryophytes (photosynthetic material only, based on visual assessment of greenness) at Abisko, Sweden. Data were obtained during July-August 2007 for 0.2 × 0.2 m^2 harvest plots. AB is birch forest, AB_AT is a ~ 2km long transect across birch forest tundra transition, AT is tundra

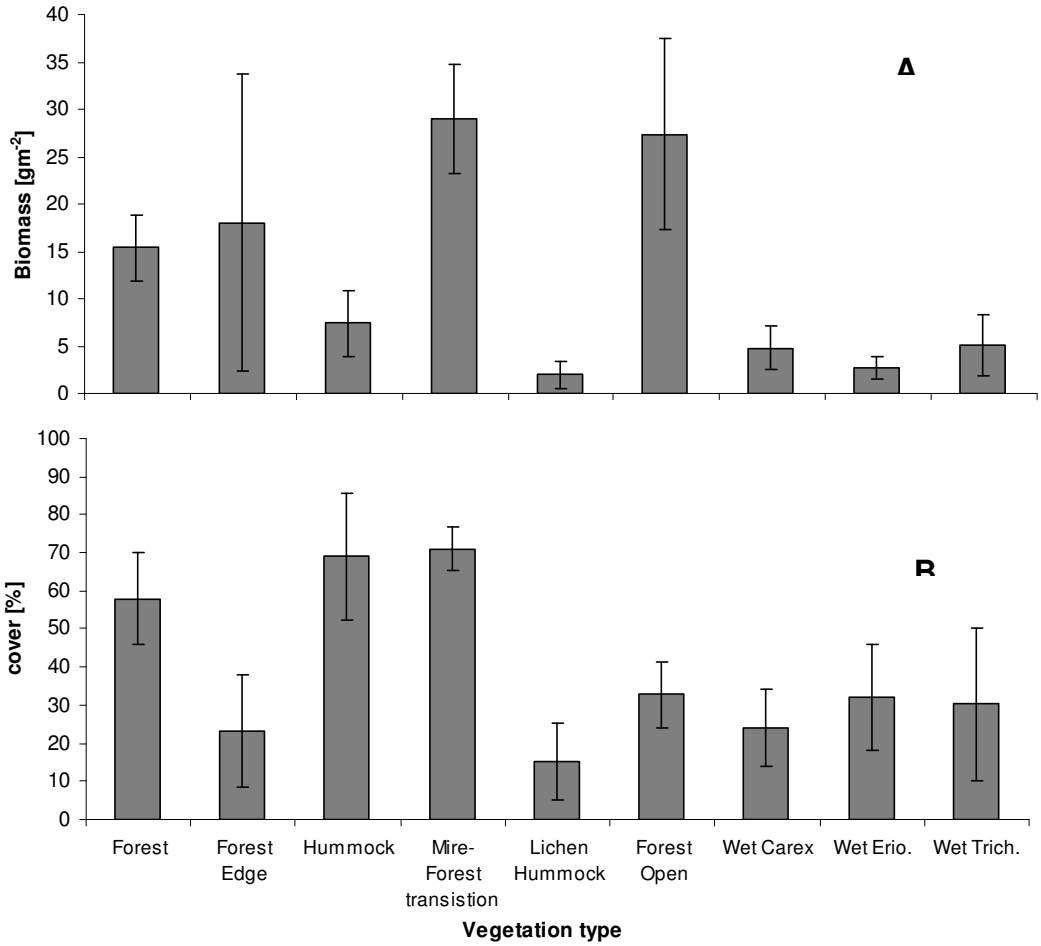

Figure 2a) Biomass (g m-2) and b) estimated percent cover (%) of bryophytes (photosynthetic material only, based on visual assessment of greenness) at Kevo, Finland. Data were obtained during July-August 2008 for 0.2 × 0.2 m2 harvest plots

Appendix 2

This appendix contains the results of an experiment designed to monitored the energy balance of bryophyte patches in Kevo, Finland. Data include bryophyte surface temperature, surface moisture, soil temperature and soil moisture from four plots at Kevo, Finland. A site description of Kevo is provided in Chapter 3.

Methods

Figure 1 The 'carpet' bryophyte patch instrumented with infra-red surface temperature sensor, air & moss (2 cm depth) thermocouples, soils moisture probe, and soil heat flux sensor.

Data were collected from one *Sphagnum* and one *Pleurozium* dominated patch located on the mire-forest transition. Two further patches were monitored within the birch forest; one *Pleurozium* dominated and one dominated by small acrocarpous moss species and leafy liverwort 'carpet' (Fig 1).

Data collected:

1. Moss surface temperature using precision Apogee infra-red temperature sensors (Apogee Instruments, Utah, USA). For these sensors the field of view (FOV) (for 90 % of the signal) was 34°. Sensors were mounted at an angle of 40°, 12 cm above the ground to measure moss patches of approximately 0.2×0.3 m^2.
2. Moss temperature ~ 3 cm depth below the moss surface, using type T thermocouples.
3. Air temperature at 5 cm above the moss surface using type T thermocouple, with radiation shield

4. Volumetric soil water content using ECH$_2$O soil moisture probes (Onset, Massachusetts, USA) inserted to approximately 6cm depth.
5. Soil heat flux using Thornthwaite Soils Heat Flux Disks, model 610 (C.W. Thornthwaite Associates, New Jersey, USA) inserted 2 -7 cm below the soil surface.
6. Relative humidity using HOBO Temperature and RH Smart Sensor (Onset, Massachusetts, USA)
7. Surface wetness using HOBO Leaf Wetness Smart Sensor (Onset, Massachusetts, USA)

Soil moisture, RH and surface wetness were logged at 5 min intervals using HOBO Micro Station data loggers (Onset, Massachusetts, USA). Surface temperature, moss and air temperature, soils heat flux were logged at 5 min intervals using Campbell CR1000 data loggers (Campbell Scientific, Utah, USA).

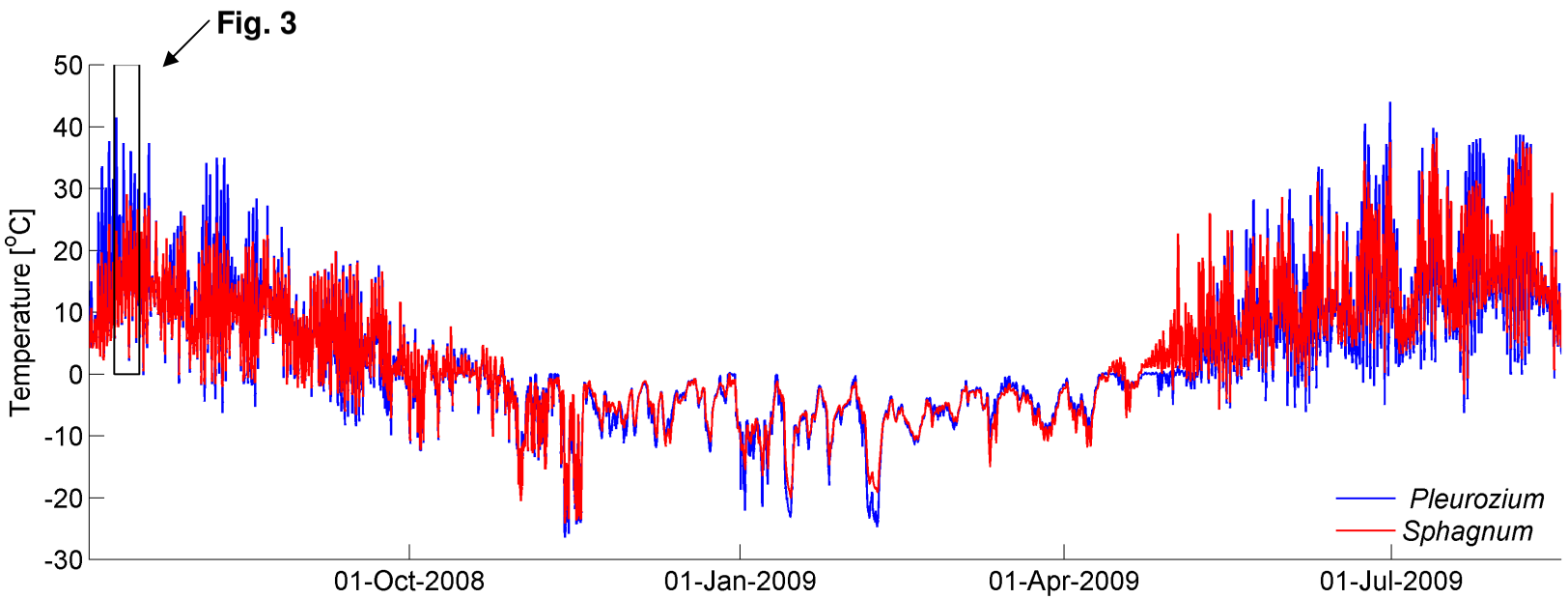

Figure 2. Surface temperature (°C) for *Sphagnum* and *Pleurozium* bryophyte patches from 4th July 2008 to 17th August 2009

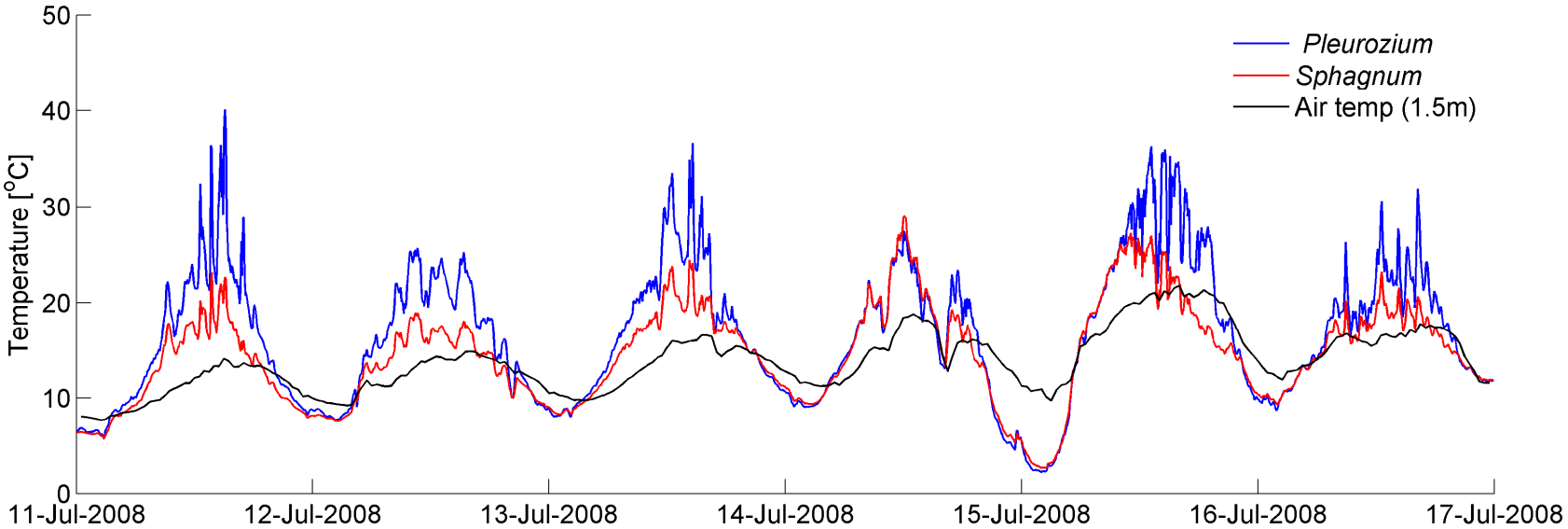

Figure 3. Surface temperature (°C) for *Sphagnum* and *Pleurozium* bryophyte patches from 11th July to 17th July 2008

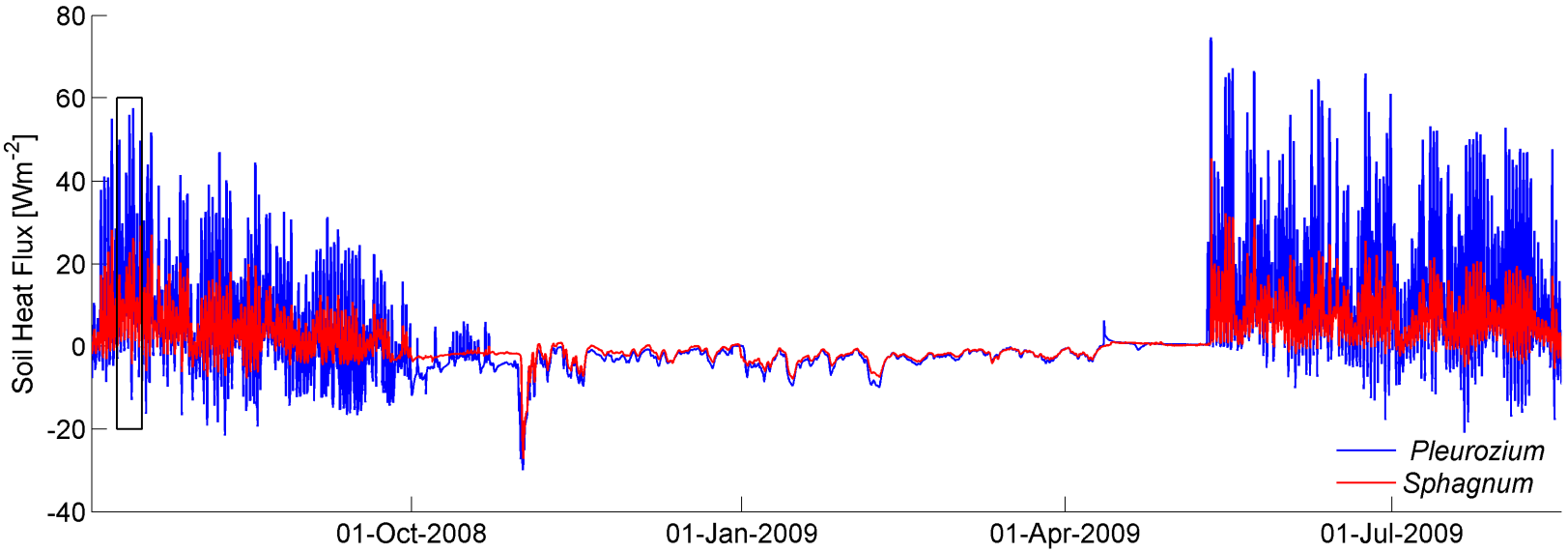

Figure 4. Soil heat flux (Wm-2) for Sphagnum and Pleurozium bryophyte patches from 4th July 2008 to 17th August 2009

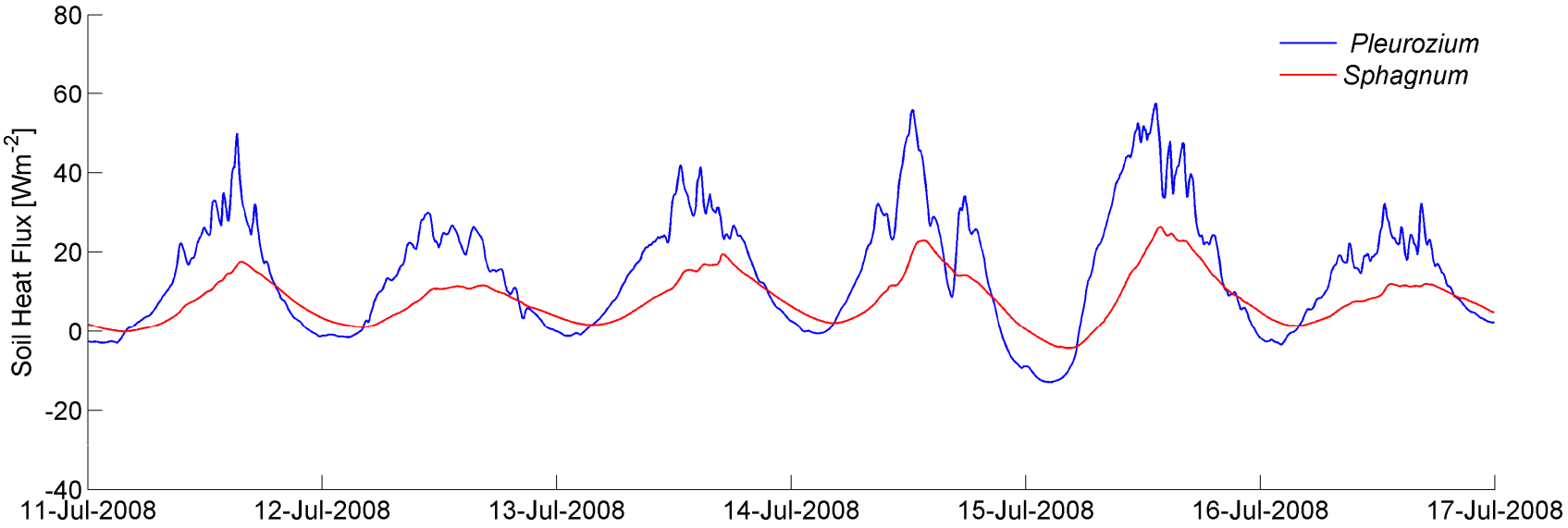

Figure 5. Soil heat flux (Wm^{-2}) for *Sphagnum* and *Pleurozium* bryophyte patches from 11th July to 17th July 2008

Appendix 3

This appendix contains spatial data quantifying the aerial cover of bryophytes within the surrounding landscape of the Kevo isotope labelling experiment (Chapter 5).

Methods

Aerial photography was used estimate the contribution of bryophytes and *Empetrum* heath to land surface cover over an area of 4.5 × 1.2 km surrounding the experimental site. The average altitude flown during photography was 290 m and the camera used a full frame Canon f1.4 lens with horizontal view angle of 40 ° and 4368 horizontal pixels. Each pixel is 0.048 m by 0.048 m. Images were analysed with Definiens Developer (München, Germany) to classify vegetation as graminoid lawn, vascular shrubs near water, sphagnum, lichen or birch forest (Fig 1. T. Hill, unpublished data).

We estimated aerial percent cover of mosses and vascular plants along three ~ 20 m × 2 m transects which ran between the edge of the open water, to the forest edge to characterise the 'vascular near water' land surface classification (Fig. 2). Each transect was divided into 1 m bands, which in turn were dived into 8 0.5 m × 0.5 m squares. We visually estimated the percent cover within each of the 8 squares and calculated a total for each band. Vascular % cover was converted to LAI using a general calibration relationship for the site ($R^2 = 0.71$) (B. Fletcher, unpublished data). Data are presented as averages for the 3 transects.

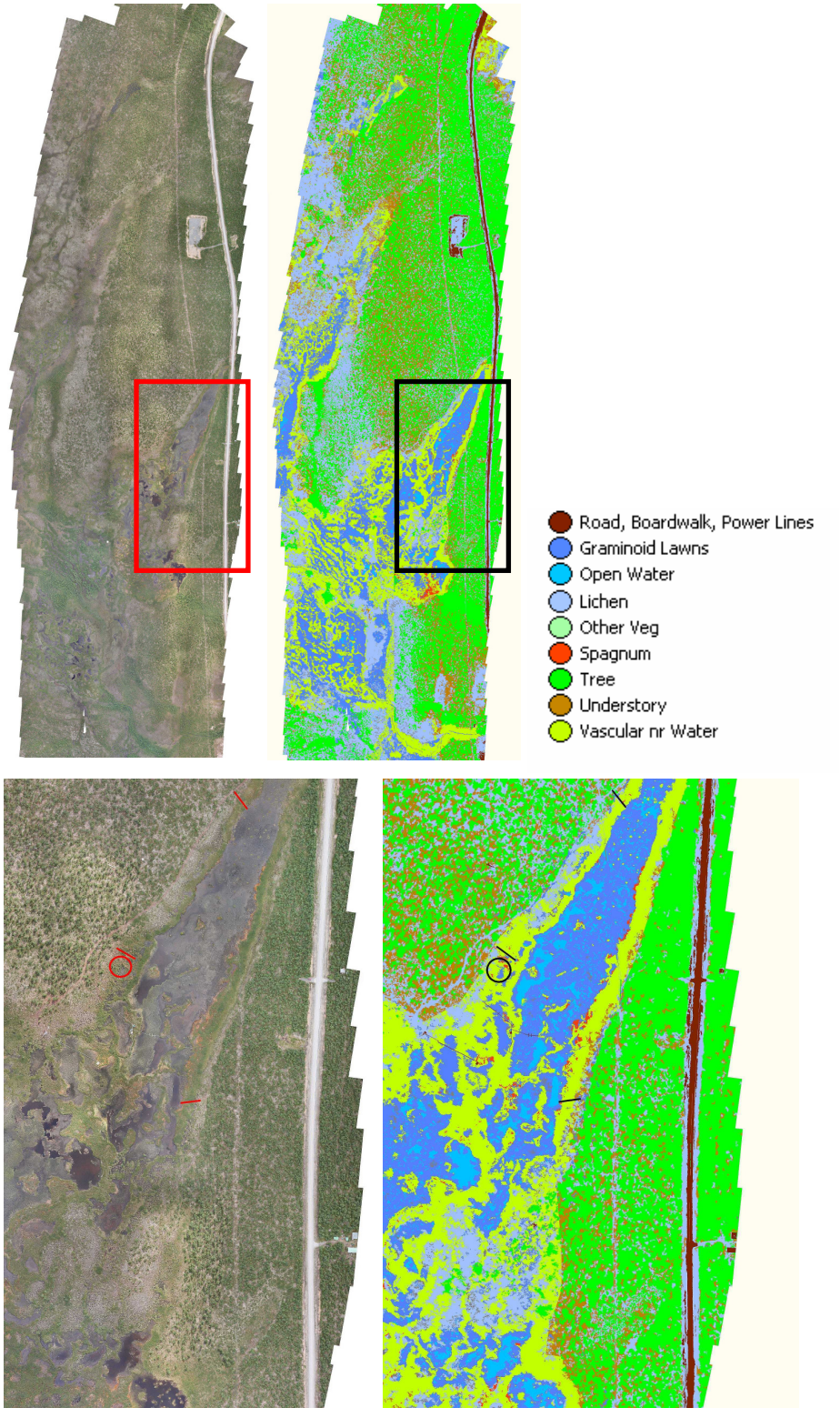

Figure 1 Aerial photography and land-cover classifications for the study area. Lines indicate location of the transects in which % cover was estimated. The isotope labelling experiment was conducted within the circled area

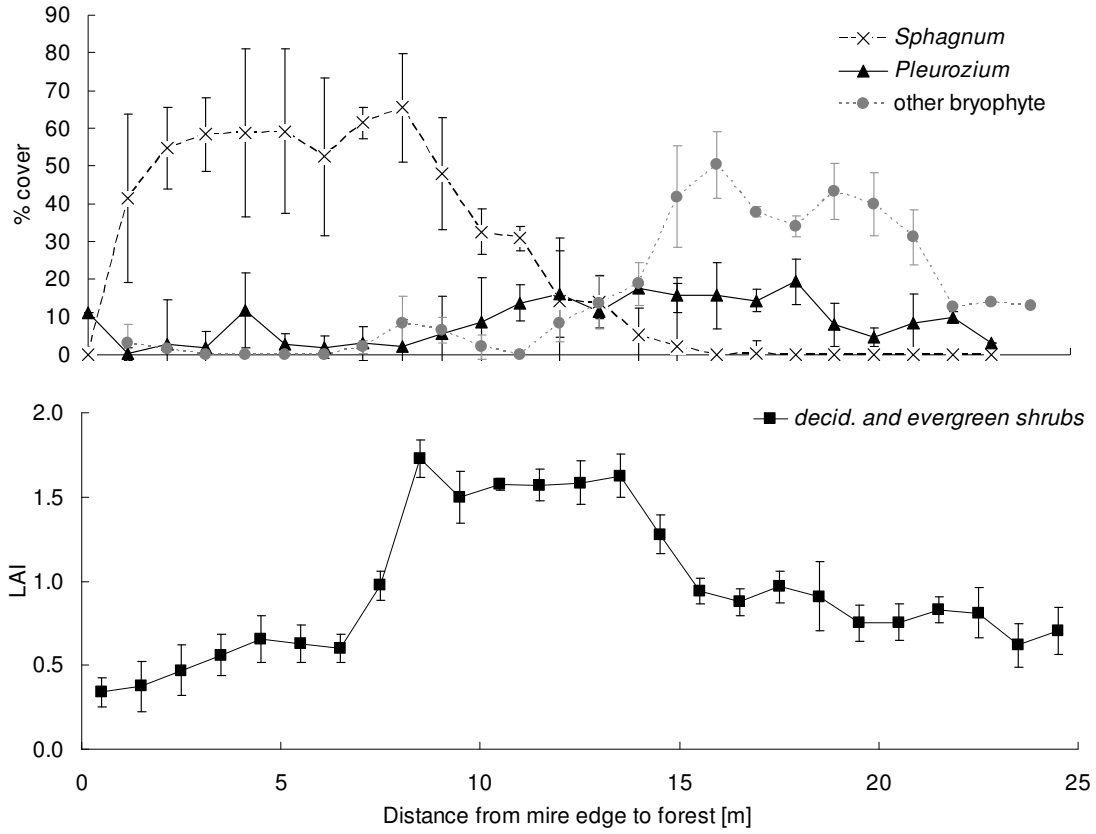

Figure 2 Estimated percent cover of Sphagnum, Pleurozium, and other bryophyte species b) LAI of deciduous and evergreen shrubs across the mire-forest transition

Appendix 4

Journal of Ecology 2007
95, 139–150

What is the relationship between changes in canopy leaf area and changes in photosynthetic CO_2 flux in arctic ecosystems?

L. E. STREET, G. R. SHAVER, M. WILLIAMS* and M. T. VAN WIJK†

*The Ecosystems Centre, Marine Biological Laboratory, Woods Hole, MA 02543, USA, *School of GeoSciences, Institute of Atmospheric and Environmental Sciences, University of Edinburgh, Edinburgh, EH9 3JN, UK, and †Plant Production Systems, Wageningen University, Plant Sciences, Haarweg 333, 6709 RZ Wageningen, the Netherlands*

Summary

1 The arctic environment is highly heterogeneous in terms of plant distribution and productivity. If we are to make regional scale predictions of carbon exchange it is necessary to find robust relationships that can simplify this variability. One such potential relationship is that of leaf area to photosynthetic CO_2 flux at the canopy scale.

2 In this paper we assess the effectiveness of canopy leaf area in explaining variation in gross primary productivity (GPP): (i) across different vegetation types; (ii) at various stages of leaf development; and (iii) under enhanced nutrient availability. To do this we measure net CO_2 flux light response curves with a 1×1 m chamber, and calculate GPP at a photosynthetic photon flux density (PPFD) of 600 μmol m^{-2} s^{-1}.

3 At a subarctic site in Sweden, we report 10-fold variation in GPP among natural vegetation types with leaf area index (LAI) values of 0.05–2.31 m^2 m^{-2}. At a site of similar latitude in Alaska we document substantially elevated rates of GPP in fertilized vegetation.

4 We can explain 80% of the observed variation in GPP in natural vegetation (including vegetation measured before deciduous leaf bud burst) by leaf area alone, when leaf area is predicted from measurements of normalized difference vegetation index (NDVI).

5 In fertilized vegetation the relative increase in leaf area between control and fertilized treatments exceeds the relative increase in GPP. This suggests that higher leaf area causes increased self-shading, or that lower leaf nitrogen per unit leaf area causes a reduction in the rate of photosynthesis.

6 The results of this study indicate that canopy leaf area is an excellent predictor of GPP in diverse low arctic tundra, across a wide range of plant functional types.

Key-words: Alaska, Arctic tundra, carbon balance, CO_2 flux, gross primary productivity, landscape heterogeneity, leaf area index, light response, normalized difference vegetation index, Sweden

Journal of Ecology (2007) **95**, 139–150
doi: 10.1111/j.1365-2745.2006.01187.x

Introduction

Climate change is predicted to affect high latitudes both sooner and more intensely than the rest of the globe. Significant warming has already been observed in arctic regions, together with increased precipitation, thawing of permafrost and earlier snow melt; in Alaska, for example, winter temperatures have increased by up to 3–4 °C in the past 50 years (ACIA 2004). Regional arctic warming will feed back on the global climate system if large amounts of carbon presently stored in terrestrial ecosystems are released in to the atmosphere (Oechel *et al*. 1993). This release may result from enhanced soil microbial activity due to higher temperatures or a lowering of the water table (Oechel & Billings 1992; McGuire *et al*. 2000). The concurrent increase in nitrogen mineralization, however, may stimulate plant growth in what are generally nutrient-limited systems (Shaver & Chapin 1980, 1986; Chapin *et al*. 1995). Combined with warmer, longer growing seasons, enhanced plant carbon sequestration may offset losses of carbon from the soil. Studies have already indicated that the composition of arctic vegetation is changing

*Correspondence: L. E. Street (tel. +1 508 289 7757; fax +1 508 457 1548; e-mail lstreet@mbl.edu).

(Myneni *et al*. 1997; Sturm *et al*. 2001), so it is important to understand how structural and compositional differences in vegetation will affect ecosystem processes. Quantification of the balance between plant productivity and ecosystem respiration in the arctic is critical to accurate forecasting of future climate scenarios.

Predicting plant productivity in the arctic is difficult due to the highly heterogeneous nature of tundra vegetation; within a single small catchment communities may range from unproductive dry heath on exposed hillcrests to dense, highly productive woody shrubs near water tracks (Walker *et al*. 1994). These communities differ markedly in biomass, leaf area and functional type composition (systems dominated by graminoids, deciduous and evergreen shrubs, are all common). It is well established that leaf level photosynthetic characteristics vary within and between individuals, species and functional types (Oberbauer & Oechel 1989; Shaver & Chapin 1995), so in order to make landscape-scale carbon budgeting feasible it is necessary to find simplifying relationships that hold for whole ecosystems. One useful emergent ecosystem property is the tight relationship between leaf area and total canopy nitrogen that exists in low arctic vegetation regardless of species composition (Williams & Rastetter 1999; van Wijk *et al*. 2005). This relationship suggests that the environment imposes strict controls on plant canopy development, such that, on average throughout the canopy at peak season, nitrogen per unit leaf area remains constant despite considerable differences within and among species (Stoner *et al*. 1982). Canopy nitrogen and leaf area have been shown to be major long-term controls on arctic plant productivity (Williams & Rastetter 1999), so it follows that if a tightly constrained leaf area index (LAI)–N relationship exists across communities, a similar universal relationship may exist for leaf area and gross primary productivity (GPP) itself.

In this paper we assess the importance of leaf area in controlling carbon uptake through time and space and in a scenario of enhanced nutrient availability. We ask whether the relationship between leaf area and GPP is the same, regardless of vegetation type, leaf developmental stage, or increased nutrient availability. To answer these questions, we describe the results of a uniquely detailed CO_2 flux survey covering a wide range of vegetation types, at two low arctic sites on opposite sides of the globe. Previous studies using similar chamber measurement techniques have focused on fluxes during peak season (Boelman *et al*. 2003; Williams *et al*. 2006) or in just one vegetation type (Shaver *et al*. 1998; Johnson *et al*. 2000). For the first time, we present data from northern Sweden that covers the period from leaf bud burst and expansion, through peak season to early senescence. In northern Alaska we compare five distinct tundra types with and without 15+ years of N and P fertilization. We hypothesize that: (i) total canopy leaf area explains variation in GPP between vegetation types; (ii) total canopy leaf area explains seasonal increases in GPP; and (iii) leaf area explains increases in GPP as a result of fertilization. Alternative scenarios are: (i) GPP of whole canopies is determined solely by species or growth form level differences in photosynthesis; at the canopy scale light penetration through differently structured canopies (i.e. shrub vs. graminoid) could also influence GPP; (ii) changes in photosynthetic capacity *per unit leaf area* or increases in self-shading within canopies also affect the relationship between leaf area and GPP; and (iii) differences in GPP between control and fertilized vegetation are at least in part due to changes in light environment, species composition or photosynthetic capacity per unit leaf area.

Materials and methods

THE STUDY AREAS

Flux measurements in Sweden were conducted at the STEPPS site (68°18′ N, 18°51′ E, elevation 710 m) (http://www.dur.ac.uk/stepps.project/) near the Abisko Scientific Research Station on the southern shore of Lake Torneträsk, about 200 km north of the arctic circle. Annual precipitation at the site is 225–475 mm, average annual temperature −1 °C and average July temperature 11 °C (van Wijk *et al*. 2005). The STEPPS site is located approximately 7 km due south of the research station on a north-facing slope above the tree line. Soils are typically well drained without continuous permafrost. We measured ecosystem CO_2 flux in 15 1 × 1 m plots in five vegetation types classified by the dominant vascular plant species (Table 1). '*Betula*' and '*Salix*' vegetation types grew close together on a sheltered bank and both had ericaceous understory vegetation. Maximum canopy height reached approximately 0.8 m. The 'dry heath' was on an exposed ridge and consisted of sparse patches of prostrate ericaceous shrubs and scattered forbs between cryptogamic crust and rock. '*Empetrum* heath' was situated below the shrub sites and was less well drained, with almost continuous cover of *Empetrum hermaphroditum* Hagerup. The 'wet sedge' vegetation was still further down the slope and dominated by *Carex* species. All plots were within 100 m of each other.

In Alaska we made flux measurements within the long-term Ecological Research Site at Toolik Lake, in the northern foothills of the Brooks Range (68°38′ N, 149°34′ W, elevation 760 m). Annual precipitation at Toolik is 200–400 mm, Annual temperature −10 °C, and average July temperature 14 °C (van Wijk *et al*. 2005). Fertilization experiments have been running at Toolik for more than 15 years; site and methodological descriptions can be found in Hobbie *et al*. (2005). We made measurements in control and fertilized treatments of moist acidic tussock (MAT), non-acidic tussock (NAT), non-acidic non-tussock (NANT), wet sedge, and heath vegetation (Walker *et al*. 1994; Hobbie *et al*. 2002; Gough & Hobbie 2003; Hobbie *et al*. 2005). All sites were within *c*. 2 km of each other. MAT has soil pH around 4 and overlies surfaces that

Table 1 Average aerial percentage cover of the dominant plant species, lichen and moss in 1 × 1 m flux plots in each vegetation type at Toolik in 2004 and Abisko in 2005

Site	Vegetation	Treatment	No. flux plots	Dominant vascular plant species (average percentage cover in August)
Toolik, Alaska	MAT	Control	4	*Eriophorum* and *Carex* species (25), *Rubus chamaemorus* (15), *Betula nana* (14), *Vaccinium vitis-idaea* (6), *Ledum palustre* (8), moss (10), lichen (6)
		Fert	4	*B. nana* (55), *R. chamaemorus* (48), moss (3), lichen (< 1)
	NAT	Control	4	*Eriophorum* and *Carex* spp. (21), *Cassiope tetragona* (14), *Salix reticulata* (12), *Dryas octopetala* (5), moss (37), lichen (7)
		Fert	4	*Eriophorum* and *Carex* spp. (48), *Salix reticulata* (6), *Draba* spp. (8), *Dryas octopetala* (5), moss (11), lichen (< 1)
	NANT	Control	4	*Eriophorum* & *Carex* spp. (19), *Cassiope tetragona* (14), *Dryas octopetala* (21), *Salix* spp. (7), moss (26), lichen (10)
		Fert	4	Grass (75), *Salix* spp. (15), *Equisetum* spp. (8), moss (< 1), lichen (< 1)
	Sedge	Control	4	*Eriophorum* and *Carex* spp. (53), moss (15), lichen (< 1)
		Fert	4	*Eriophorum* and *Carex* spp. (40), grass (23), moss (17), lichen (< 1)
	Heath	Control	4	*Arctostaphylos alpina* (19), *Ledum palustre* (14), *V. vitis-idaea* (16), *E. nigrum* (10), moss (< 1), lichen (18)
		Fert	4	*Hierochloe alpina* (44), *B. nana* (49), moss (2), lichen (2)
Abisko, Sweden	*Betula*	–	3	*B. nana* (63), *E. hermaphroditum* (19), *V. vitis-idaea* (9), *Lycopodium* spp. (9), *V. uliginosum* (9), moss (17), lichen (< 1)
	Salix	–	3	*Salix glauca* (43), *E. hermaphroditum* (56), *V. vitis-idaea* (15), *B. nana* (19), *Juniperus communis* (18), *V. myrtilus* (18), moss (18), lichen (< 1)
	Empetrum heath	–	3	*E. nigrum* (73), *V. uliginosum* (10), *B. nana* (12), *R. chamaemorus* (5), moss (15), lichen (< 1)
	Sedge	–	3	*Carex* spp. (50), *E. nigrum* (37), *Andromeda polifolia* (10), moss (37), lichen (< 1)
	Dry heath	–	3	*E. nigrum* (22), *B. nana* (5), *V. uliginosum* (8), cryptogamic crust (45), moss (4)

are 50 000–120 000 years old. The dominant species are the tussock-forming sedge, *Eriophorum vaginatum* L., with ericaceous shrubs such as *Betula nana* L., *Ledum palustre* L. and *Vaccinium vitis-idaea* L. Fertilization of MAT doubled leaf area, with *B. nana* becoming dominant. Moss cover decreased (Shaver *et al*. 2001). NAT and NANT sites overlie glacial surfaces aged 11 500–20 000 years, with soil pH of 5.5–7. Non-acidic sites have lower plant biomass but greater species richness, and *B. nana* is absent (Hobbie *et al*. 2002). Fertilization of NAT resulted in increased biomass without loss of species richness (Gough *et al*. 2002; Hobbie *et al*. 2005). Wet sedge vegetation is dominated by rhizomatous sedges, mostly *Carex* and *Eriophorum* species. Five years of fertilization increased wet sedge above ground biomass two- to fourfold (Shaver *et al*. 1998; Boelman *et al*. 2005). Heath vegetation is characterized by ericaceous shrubs such as *Vaccinium uliginosum* L. and *Loiseleuria procumbens* L. Soils are well drained, with an upper organic mat 0–0.05 m thick and annual thaw depth > 1 m. Annual net primary productivity increased with fertilization; a tussock forming grass, *Hierochloe alpina* Sw. ex Willd, replaced prostrate shrubs (Gough *et al*. 2002).

CO_2 FLUX MEASUREMENT

We measured the response of net ecosystem CO_2 exchange to manipulated light on 1 × 1 m plots. In Sweden in 2005 we measured 15 plots in five vegetation types during four rounds of field measurements (7–11 June, 16–17 June, 26–30 June and 10–15 August), the first of which was before leaf bud break. In Alaska during 2004 we measured 20 plots in control and fertilized treatments of five vegetation types, one to two times between 26 June and 8 July and 22 July and 4 August (Table 1).

To measure CO_2 fluxes we used a LI-COR 6400 portable photosynthesis system (LI-COR Inc., Lincoln, Nebraska, USA) connected to a 1 × 1 × 0.25 m Plexiglas chamber (Williams *et al*. 2006). In late season 2004 we used a LI-COR 6200 and corrected CO_2 fluxes for the effects of water vapour flux according to the methods of Hooper *et al*. (2002). We placed the chamber on top of a 1-m^2 aluminium frame base, with a rubber gasket on both surfaces to ensure an airtight seal. The base was supported approximately 0.05–0.20 m above the ground by steel legs driven down to the permafrost. We attached a plastic skirt to the bottom of the base to enclose the volume between the base and the ground surface; at the ground surface we weighted the skirt with heavy chains pushed down onto the moss layer. This method enabled us to move the chamber from site to site with minimal disturbance to the surface of the organic mat. The air inside the chamber was mixed using four small fans, which we ran for 30–60 s before taking the first measurement. To provide an estimate of total chamber volume we measured the height of the chamber base above the ground in a grid of 36 points. We then added the volume of the air space within the base to that of the chamber itself.

To create a light response curve we took two to three net CO_2 flux measurements at full light, followed by one to two measurements at several (usually three) successive levels of shading, followed by three measurements in full darkness. We shaded the chamber using one to three layers of plastic window screening or mosquito netting and used an opaque tarpaulin to block all light from the chamber. We assumed the mosquito netting was not selective in its transmission of the different wavelengths of PAR. Flux measurements under complete darkness represent ecosystem respiration. Each flux measurement lasted 45–60 s, the LI-COR 6400 recording CO_2 and H_2O concentrations every 1–2 s. We lifted the chamber between flux measurements to allow internal conditions to return to ambient. The LI-COR 6400 also recorded photosynthetic photon flux density (PPFD) inside the chamber, as well as air temperature and pressure. After completing the light response curve we took five regularly spaced measurements of soil temperature at 5 cm depth. We also measured soil volumetric water content at five points using a Hydrosense handheld soil moisture probe (Campbell Scientific, Logan, Utah, USA) inserted where possible to the maximum depth of 20 cm. We adjusted the soil moisture data using a calibration developed across a wide range of soil types found near Toolik Lake (J. Powers, unpublished data).

VEGETATION CHARACTERIZATION

At each plot we took measurements of canopy reflectance and calculated a normalized difference vegetation index (NDVI) using the formula:

$$\mathrm{NDVI} = (R_{\mathrm{nir}} - R_{\mathrm{vis}})/(R_{\mathrm{nir}} + R_{\mathrm{vis}}) \qquad \text{eqn 1}$$

where R_{NIR} is reflectance at a wavelength of 0.725–1.0 μm and R_{VIS} is reflectance at 0.56–0.68 μm (Boelman *et al*. 2003). At Toolik in 2004 we used a Skye portable field sensor (Skye Instruments Ltd, Llandrindod Wells, UK), which measures total reflected light in the wavebands specified in equation 1. At Abisko in 2005 we used a Unispec spectral analyser (PP systems, Haverhill, Massachusetts, USA), which records complete reflectance spectra from 0.3 mm to 1.0 mm, but used only the reflectance in the appropriate wavebands. We took measurements in a regular grid of nine points with both instruments, holding each sensor at a vertical height such that the field of view was approximately 0.04 m^2. The two instruments agreed well in cross-calibration. The relationship between Skye sensor NDVI and Unispec NDVI, both measured on 89 1 × 1 m flux plots, was Skye NDVI = 0.92 × Unispec NDVI + 0.051, $R^2 = 0.94$.

To use NDVI to predict LAI of the flux plots we destructively measured the leaf area of 81 independent 0.04 m^2 plots and developed an NDVI-LAI calibration curve. After taking an NDVI measurement we removed all the leaf material from the plot and then sorted by species in the laboratory. We measured leaf area of each species using a scanner and WinRhizo/WinFolia software (Regent Instruments Inc, Ste-Foy, Canada). At Abisko in 2005 we took a total of 40 harvests, approximately one-third of which were taken in mid-June, in late June and in August. At Toolik in 2004 we took 18 harvests in fertilized plots. We used data from 23 harvests from 2003 in unfertilized vegetation at Toolik, using the same methods (the same data used by Williams *et al*. 2006). We estimated absolute aerial cover in each flux plot by species for all vascular plants (i.e. total cover can be > 100%). We did this by placing a 5 × 5 string grid (each square = 0.04 m^2) over the plot, and visually estimating cover. In 2004 we estimated cover by species in each square, then calculated an average species cover for the entire plot. In 2005 we estimated cover for each species in turn, counting a running total of percentage cover ($^1/_4$ of a square = 1% of total plot) in squares 1 through to 25. We also noted bryophyte cover, bare ground, cryptogamic crust, rock and standing water. At Toolik in 2004 we estimated cover in each flux plot once, while at Abisko we estimated cover each time a light response curve was measured.

DATA ANALYSIS

CO_2 fluxes are calculated from the change in chamber CO_2 concentration though time according to the formula:

$$F_c = \frac{\rho \cdot V \cdot \mathrm{d}C/\mathrm{d}t}{A} \qquad \text{eqn 2}$$

where F_c is net CO_2 flux (μmol m^{-2} s^{-1}), ρ is air density (mol m^{-3}), V is the chamber CO_2 volume (m^3), $\mathrm{d}C/\mathrm{d}t$ is the slope of chamber CO_2 concentration against time (μmol mol^{-1} s^{-1}) and A is the chamber surface area (m^2). The light response of net CO_2 exchange, or net ecosystem productivity (NEP), is modelled as a rectangular hyperbola with a term for ecosystem respiration:

$$\mathrm{NEP} = \mathrm{ER} - \frac{P_{\max} \cdot I}{k + I} \qquad \text{eqn 3}$$

where $P_{\max}$ is the rate of light saturated photosynthesis (μmol CO_2 m^{-2} s^{-1}), k is the half-saturation constant of photosynthesis (μmol PAR m^{-2} s^{-1}), I is the incident PPFD (μmol PAR m^{-2} s^{-1}) and ER is ecosystem respiration (μmol CO_2 m^{-2} s^{-1}). Ecosystem respiration can then be subtracted to produce a light response curve of gross primary productivity (GPP):

$$\mathrm{GPP} = \frac{P_{\max} \cdot I}{k + I} \qquad \text{eqn 4}$$

E_0, the initial slope of the light response curve or quantum efficiency (μmol CO_2 μmol^{-1} PAR), and LCP, the light compensation point (μmol PAR m^{-2} s^{-1}) are calculated as:

$$E_0 = \frac{P_{\max}}{k} \qquad \text{eqn 5}$$

$$\mathrm{LCP} = \frac{\mathrm{ER} \cdot k}{P_{\max} - \mathrm{ER}} \qquad \text{eqn 6}$$

Table 2 Best-fit exponential regression parameters and root mean squared errors of prediction (RMSE) for the LAI-NDVI relationships used to predict LAI (equation 7). The regressions were calculated using data from 81 0.2×0.2 m harvests, classified according to species composition

Vegetation type	*a*	*b*	*n*	R^2	RMSE
Betula	0.0132	6.271	22	0.79	0.58
Salix glauca	0.0323	5.625	11	0.89	0.26
Empetrum heath	0.0259	5.087	7	0.48	0.26
Dry heath	0.0137	5.446	8	0.43	0.11
Tussock	0.0064	7.210	10	0.85	0.27
Sedge	0.1516	2.663	18	0.50	0.22
Grass	–	–	5	–	–
All data	0.0148	6.192	81	0.75	0.36

To make comparisons of photosynthetic activity between plots it is necessary to take account of the large differences in GPP that occur under changing light. To do this each light curve was used to predict photosynthesis at 600 μmol m^{-2} s^{-1} PPFD (GPP_{600}). GPP_{600} values were also normalized by predicted leaf area for each flux plot to give GPP per unit leaf area at 600 μmol m^{-2} s^{-1} PPFD (GPP_{600L}).

The LAI of each flux plot was predicted from NDVI using the equation:

$$LAI = a \cdot e^{(b \cdot NDVI)} \qquad \text{eqn 7}$$

where *a* and *b* are parameters specific to each vegetation type (Table 2).

STATISTICAL ANALYSIS

For the Abisko data, we analysed seasonal changes in LAI, GPP_{600} and GPP_{600L} using repeated measures ANOVA in SYSTAT 11.0, with vegetation type as the between-subject factor and date of measurement as the within-subject factor. The average date of each measurement round is used to account for irregularity of spacing between dates. Univariate results are presented. We analysed LAI, GPP_{600} and GPP_{600L} at Toolik using two-way ANOVA in SYSTAT 11.0, with vegetation type and treatment as factors. Data were natural log transformed prior to each ANOVA analysis. Simple contrasts between treatments within each vegetation type were used to examine interaction effects in more detail.

Results

LEAF AREA AND NDVI

NDVI and leaf area were strongly correlated overall with an R^2 of 0.75. As expected, NDVI saturated at high LAI, reaching a maximum value of approximately 0.86. As a result, the exponential model tended to underestimate leaf area at high NDVI, though only two plots (both in fertilized MAT) had NDVI greater than 0.85. Combining all the harvest data and using a single exponential regression led to biased estimates of leaf area due to differences in the LAI-NDVI relationship between vegetation types (Fig. 1a). Sedge plots, for example, generally had higher leaf area than dry heath plots at a given NDVI. This may have been due to the presence of sedge leaf litter, which obscured live green material or moss cover, which contributed to the NDVI signal. Harvests dominated by *Salix glauca* L. also had consistently higher LAI than *Betula* plots at the same NDVI; this was caused by a covering of pale hairs on *S. glauca* leaves, which made them appear grey-green. Harvests were therefore grouped by vegetation type (*Betula*, *Salix glauca*, sedge, dry heath, *Empetrum* heath, tussock or grass, based on dominant species and harvest location) in order to predict leaf area. Table 2 gives

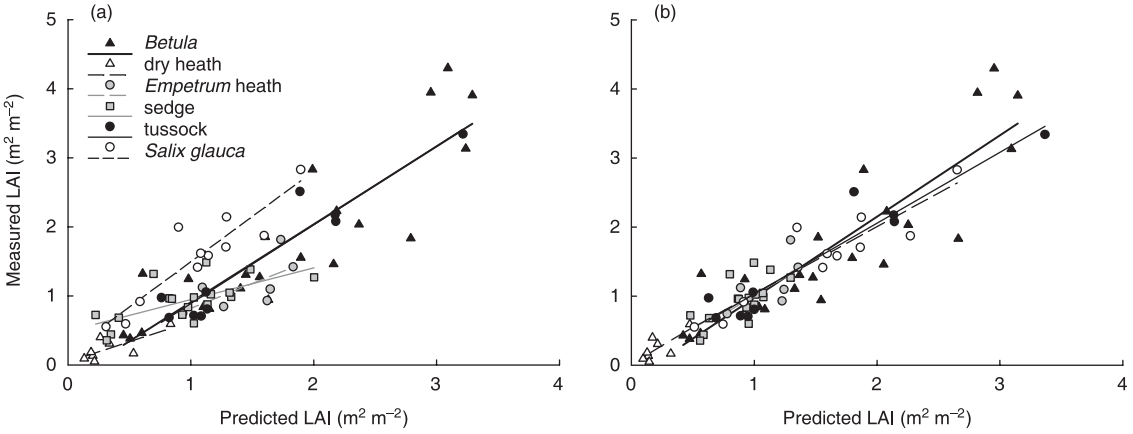

Fig. 1 Predicted LAI vs. measured LAI for 81 0.20×0.20 m harvests from Abisko & Toolik in 2003–05. Each panel shows the same data. In (a) the overall best-fit exponential relationship between LAI and NDVI (equation 7, Table 2) for all 81 harvests is used to predict LAI (*x*-axis). In (b) *separate* exponential relationships between LAI and NDVI for each vegetation type (Table 2) are used to predict LAI (*x*-axis). In both panels the best-fit linear regression of predicted vs. measured LAI is plotted for each of the six vegetation types. R^2 of predicted vs. measured LAI for *all* 81 harvest data points in (a) = 0.74 and (b) = 0.84 (overall regression lines are not shown). Harvests were classified as representative of '*Betula*', '*Salix*', 'sedge', 'dry heath', '*Empetrum* heath', '*Salix glauca*' or 'tussock' vegetation depending on species composition and harvest location.

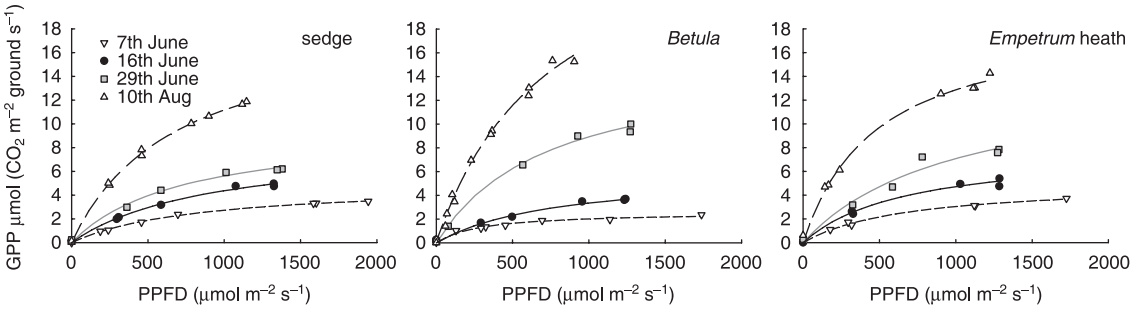

Fig. 2 Response of GPP to photosynthetic photon flux density (PPFD) for three flux plots dominated by sedge, *Betula nana* and *Empetrum* heath vegetation at Abisko in 2005. Light response curves were measured on each plot four times during the growing season.

best-fit parameters, R^2 and RMSE values for equation 7 for each vegetation type individually and for all data combined. Using vegetation-specific regression relationships to predict LAI explains 10% more of the total variation in LAI (Fig. 1b). Separating LAI-NDVI data by site or date (early or late season) of harvest did not result in similar improvements in precision. Grass harvests covered only a very small range in LAI so it was not possible to fit a useful regression equation. Instead, the overall regression was used to predict LAI and the result multiplied by a factor of 1.6; on average, grass-dominated harvests had 1.6 times more leaf area than predicted by the overall model.

SEASONAL PATTERNS AT ABISKO

GPP showed a clear saturating response to light at all sites and time periods, with the average RMSE of prediction for all light curves = 0.20 µmol C m^{-2} ground s^{-1} (Fig. 2). Ecosystem respiration (ER) and air temperature were exponentially related ($R^2 = 0.35$), but there was no relationship between air temperature and GPP_{600}, LCP or E_0. Plots with high LAI and GPP also had the highest ER. Multiple regression of air temperature and LAI against ER explains 52% of the variation across all vegetation types and time periods (see Appendix S1 in Supplementary Material). There were significant differences in GPP_{600} between vegetation types ($P < 0.0005$) and dates of measurement ($P < 0.005$; Fig. 3a). In early June before leaf break GPP_{600} was low for all vegetation, between 0.4 and 2.9 µmol C m^{-2} ground s^{-1}. By August GPP_{600} had increased in all plots, but those dominated by *Betula* and *Salix* increased the most, to 10.6–14.8 µmol C m^{-2} ground s^{-1}. This led to a strong interaction between date and vegetation type ($P < 0.0005$; Fig. 3a).

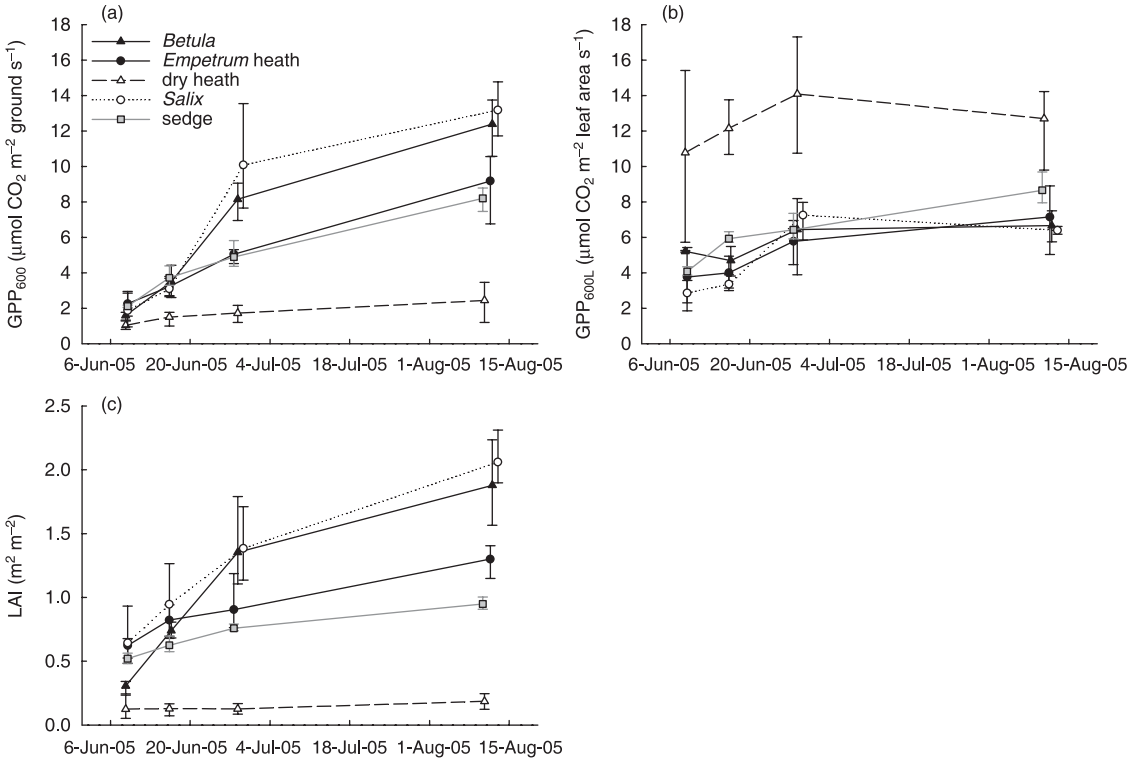

Fig. 3 (a) Estimated GPP_{600}, (b) estimated GPP_{600L} and (c) predicted leaf area, measured in five vegetation types, four times through the growing season at Abisko. Bars show ranges for each vegetation type.

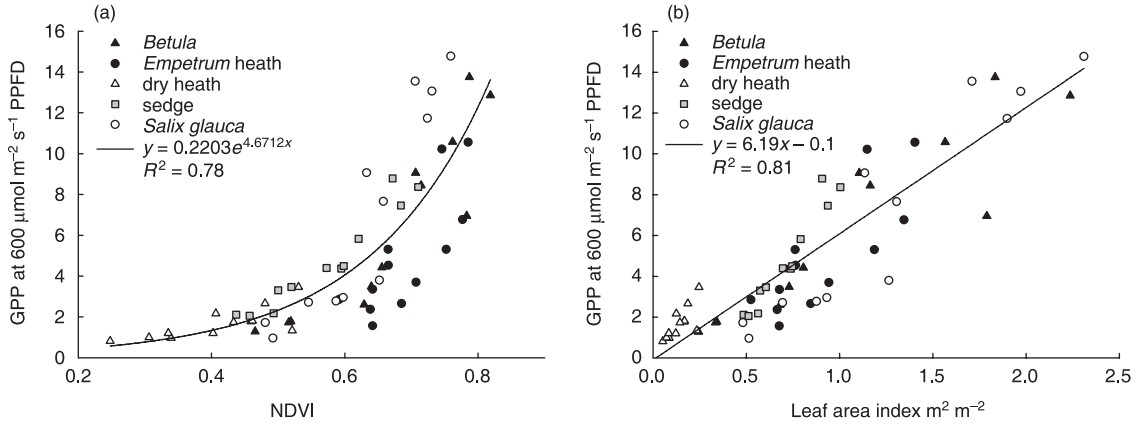

Fig. 4 The relationship between GPP_{600} and (a) NDVI and (b) predicted LAI for all flux plots at Abisko. Each point represents one measurement made on one plot; 15 plots were each measured four times between early June and mid-August ($n = 60$).

Leaf area index varied 30-fold across plots and sampling dates, from a minimum of 0.07 in dry heath vegetation in early season to 2.31 in *Salix* plots in August (Fig. 3c). Before leaf bud break, *Empetrum* heath, sedge and *Salix* plots all had leaf area index above 0.5 due to the presence of evergreen species (all *Salix* plots had *E. nigrum* and *V. vitis-idaea* in the understory; one had *Juniperus communis* L.). Leaf area increased in all vegetation types through the season, with the greatest increase in deciduous shrub plots; on average LAI in *Betula* and *Salix* plots increased three- to fivefold by August (Fig. 3c). Dry heath vegetation had very low LAI, which increased by less than 0.1 $m^2\ m^{-2}$. Across all plots and time periods 75% of the variation in GPP_{600} was explained by NDVI (Fig. 4a), translating to a strong linear relationship between leaf area and GPP_{600}. After leaf development in August LAI explained 90% of the variation in GPP_{600} across vegetation types. Across all vegetation types and measurement periods, LAI explained 81% of the variation in GPP_{600} (Fig. 4b).

Average GPP_{600} per unit leaf area (GPP_{600L}) showed a statistically significant change through time ($P < 0.0005$), but there appears to be only a slight overall increase in GPP_{600L} through the season (Fig. 3b). GPP_{600L} values for the dry heath plots are obvious outliers. This could be due to the presence of cryptogamic crust and lichen, which covered around 45% of the surface of these plots. Cryptogamic crusts are very dark green or black in colour, and lichens are often almost white, yet both are still potentially photosynthetically active. If NDVI (greenness) is used to predict leaf area but the carbon uptake by non-vascular plants is not accounted for, then GPP per unit leaf area will be overestimated. Although photosynthesis by crust and lichens is presumably low, vascular leaf area was also very low in the dry heath plots. The reflective properties of the 'background', including exposed soil and rock, will also influence the NDVI signal, particularly in very open canopies. Large standard errors for dry heath plots reflect the greater sensitivity of GPP_{600L} to errors in LAI prediction at very low values. GPP_{600L} is the same between vegetation types if dry heath plots are excluded from analysis ($P > 0.20$). At peak season in August the coefficient of variation in GPP_{600} across all 15 plots was 47%, but in GPP_{600L} was only 19% (excluding dry heath). Spatial heterogeneity in carbon uptake is therefore substantially reduced if expressed per unit canopy leaf area. The relative importance of canopy leaf area vs. GPP_{600L} in *seasonal* changes in GPP_{600} can also be compared. For example, in *Betula* plot 1, GPP_{600L} increased by 11% between June and August, while LAI increased by 600%; leaf area explains six times more of the increase in carbon uptake than GPP_{600L}. On average for deciduous shrub plots, the contribution of leaf area is 3.2 times that of GPP_{600L}. In evergreen-dominated communities the contribution of the two factors is approximately equal, on average (see Appendix S1).

FERTILIZER ADDITION AT TOOLIK

The leaf area of flux plots in fertilized treatments was greater than that of control treatments in all vegetation types ($P < 0.0005$; Fig. 5c). LAI in control plots ranged from 0.27 $m^2\ m^{-2}$ in NANT to 1.41 $m^2\ m^{-2}$ in MAT and in fertilized flux plots from 0.92 $m^2\ m^{-2}$ in wet sedge to 2.82 $m^2\ m^{-2}$ in MAT. The largest differences in LAI between control and fertilized treatments corresponded to dramatic shifts in species composition and dominance; in MAT vegetation *B. nana* replaced a mix of functional types (graminoid, deciduous and evergreen shrubs and forbs), while in NANT tall stands of grasses dominated almost exclusively compared with diverse short-stature vegetation in control plots. Sedge and NAT vegetation, by contrast, had more similar LAI and more similar species composition between treatments (Table 1).

There was no significant response of GPP_{600} to air or soil temperature at Toolik. ER was exponentially related to air temperature in fertilized plots but not in control plots ($R^2 = 0.53$ and $R^2 = 0.06$, respectively) and ER rates were higher in fertilized plots (see Appendix S2). GPP_{600} was also greater in fertilized plots ($P < 0.0005$), with a highly significant interaction between treatment and vegetation type ($P < 0.0005$; Fig. 5a). NANT vegetation had both the highest and lowest GPP_{600},

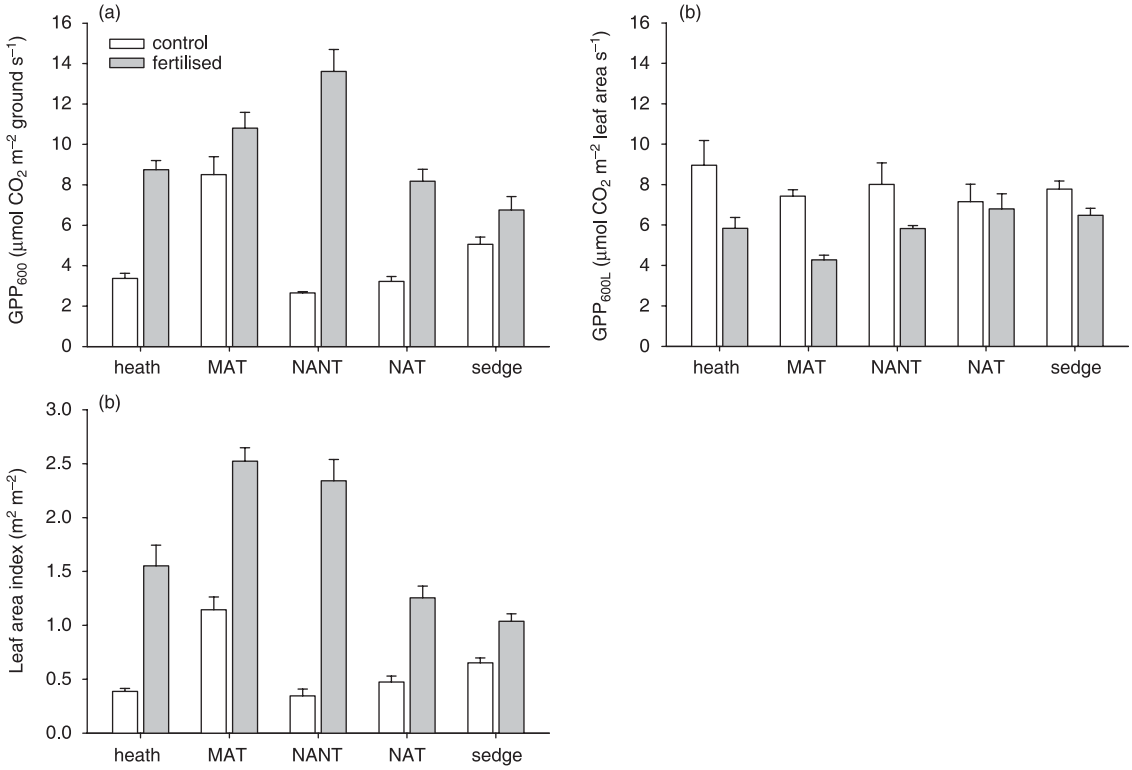

Fig. 5 (a) GPP_{600}, (b) GPP_{600L} and (c) leaf area index for control and fertilized treatments at Toolik 2004, averaged across measurement rounds. MAT = moist acidic tussock, NANT = non-acidic non-tussock, NAT = non-acidic tussock. Bars show standard errors.

with averages of 13.6 μmol C m^{-2} s^{-1} and 2.6 μmol C m^{-2} s^{-1} in the fertilized and control treatments, respectively. GPP_{600L} in fertilized treatments of heath, MAT and NANT vegetation was significantly lower than control plots, i.e. the relative increase in leaf area as a result of fertilization exceeded the relative increase in photosynthesis. GPP_{600L} in sedge and NAT fertilized vegetation was also lower than control treatments, but not significantly so (Fig. 5b, Table 3).

GPP_{600} and NDVI show a very similar relationship at Toolik and Abisko, though NANT plots consistently had higher GPP_{600} relative to NDVI (Fig. 6a). These were

Table 3 Results of simple contrasts between control and fertilized plots (control minus fertilized) within each vegetation type at Toolik Lake in 2004. ***$P < 0.005$, **$P < 0.05$, *$P < 0.1$, NS = non-significant

Vegetation type	LAI (m^2 m^{-2})	GPP_{600} (μmol CO_2 m^{-2} ground s^{-1})	GPP_{600L} (μmol CO_2 m^{-2} LA s^{-1})
Heath	***	***	***
Mat	***	**	***
Nant	***	***	*
Nat	***	***	NS
Sedge	***	**	NS

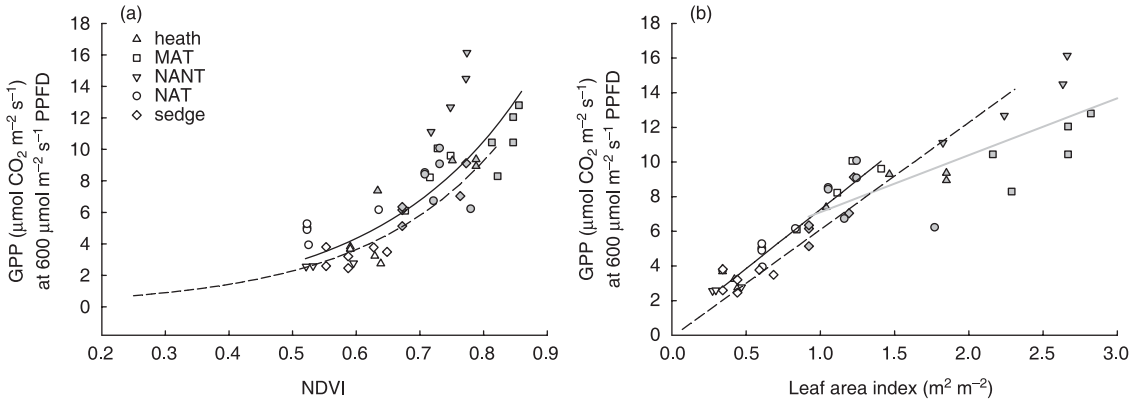

Fig. 6 (a) Relationship between GPP_{600} and NDVI for control and fertilized flux plots at Toolik 2004. Dashed line shows the same relationship for Abisko 2005. Filled symbols are fertilized plots. (b) Relationship between GPP_{600} and LAI for control and fertilized flux plots at Toolik 2004. Filled symbols are fertilized plots. Grey line is the best-fit linear regression for Toolik 2004 fertilized plots only ($R^2 = 0.63$), solid line is for Toolik 2004 control plots only ($R^2 = 0.89$). Dashed line is for Abisko 2005.

graminoid-dominated plots, which had lower NDVI at high given leaf area, presumably due to very different canopy level properties (Steltzer & Welker 2006). This was accounted for in the calculation of leaf area (see methods section). Up to LAI of 1.5 m^2 m^{-2} the slope of the linear relationship between GPP_{600} and LAI for control plots at Toolik and all plots at Abisko (over the whole season) is not significantly different ($P = 0.38$), though GPP_{600} is slightly greater at Toolik than at Abisko ($P = 0.02$; Fig. 6b). Average GPP_{600L} after full leaf expansion had occurred is not significantly different between sites (at Toolik in July, and at Abisko in August, GPP_{600L} was 7.8 ± 0.36 and 7.2 ± 0.39 μmol C m^{-2} LA s^{-1}, respectively). However, above leaf area index of 1.5 m^2 m^{-2} the relationship between GPP_{600} and LAI in fertilized plots at Toolik begins to deviate from linear (Fig. 6b); this is reflected in lower GPP_{600L} in fertilized plots (Fig. 5b).

Discussion

LEAF AREA CONTROLS CO_2 UPTAKE

By fitting CO_2 flux light response curves and estimating GPP at constant irradiance, we were able to investigate seasonal and spatial patterns in GPP. The results highlight the importance of leaf area as the primary driver of photosynthesis in arctic systems. At peak leaf area in August, 90% of the variation in GPP across five vegetation types was explained by leaf area alone. This correlation is remarkable considering clear differences in community composition (Table 1) and the range in leaf-level photosynthetic activity between individual species; P_{max} values near Toolik Lake range from 6 to 20 μmol CO_2 m^{-2} leaf s^{-1} in common tundra species (Oberbauer & Oechel 1989). At the canopy level, differences between species become unimportant because communities are assembled in such a way that GPP at a given *canopy* leaf area is tightly constrained (Fig. 3b). The underlying mechanism may be strict environmental controls over canopy nitrogen allocation. Van Wijk *et al*. (2005) found a constant ratio of 1.9 g N m^{-2} leaf across a wide range of vegetation types at peak season at Toolik and Abisko. Leaf area and N are key biotic controls on photosynthesis (Williams & Rastetter 1999), so coupling between them would constrain ecosystem photosynthesis in relation to canopy leaf area as demonstrated (Fig. 4b).

GPP at Abisko increased by an order of magnitude between early June and mid-August in deciduous shrub-dominated plots, the most rapid increase coinciding with early season leaf expansion. GPP in graminoid and evergreen-dominated communities increased more gradually; both vegetation types were photosynthetically active before deciduous leaves emerged but did not attain such high rates of GPP by August. Where leaf area was very low on dry, exposed ridges GPP was also very low and only increased slightly (Fig. 3a). Spatial patterns in ecosystem carbon uptake are therefore community dependent and change over time such that heterogeneity between 'patches' in the landscape increases as canopies develop. Not all of the increase in GPP through time is attributable to increases in leaf area, however; we have shown that average GPP *per unit leaf area* increases up to two- to threefold by peak season (Fig. 3c). There are currently no data available on the LAI-N relationship during canopy development. Do canopies converge on the optimum 1.9 g N m^{-2} LA at peak season and is early season canopy N less than 1.9 g N m^{-2} LA? If not, what is the explanation for increases in average canopy GPP per unit leaf area through the season?

In evergreen-dominated communities we show that increases in GPP_{600L} and increases in LAI contribute equally to seasonal increases in GPP_{600}. This is because throughout the growing season evergreen canopy development involves both new leaf production, 're-activation' of previous year's leaves, and leaf senescence. *E. hermaphroditum* leaves at Abisko, for example, survive over three seasons and are then shed (Kudo *et al*. 2001). On average, evergreen leaf photosynthetic capability increases slightly through the season, but the increase in leaf area is less dramatic than in deciduous species, where canopy development is characterized by the emergence and expansion of a single leaf cohort. Despite these differences in leaf life span, the average increase in GPP_{600L} is very similar across vegetation types (Fig. 3b). Leaf area is a more important factor in determining GPP, explaining 80% of observed variation through space *and time* (Fig. 4b).

LEAF AREA AND GPP RESPONSE TO FERTILIZATION

Unexpectedly, rates of photosynthesis per unit leaf area were lower in fertilized treatments (Fig. 5b), i.e. relative increases in leaf area *exceeded* relative increases in GPP. Harvest results by Shaver *et al*. (2001) suggest that canopy nitrogen per unit leaf area is lower in fertilized MAT plots than control plots, despite an increase in tissue nitrogen concentration by mass. The decrease in N per unit leaf area is mostly the result of increased dominance by *Betula nana*, which has much higher specific leaf area (leaf area per unit mass). If the ratio of leaf area to canopy nitrogen optimizes productivity in natural vegetation, then this would suggest that MAT has not (yet) reached an optimum canopy structure in response to fertilizer addition. Detailed investigation of the LAI-N relationship in treatment plots of different ages would provide insight into whether vegetation is converging to some optimal N:LA ratio, and the speed of that response. Self-shading may also explain some or all of the observed depression in GPP per unit leaf area. Although lower GPP_{600L} rates were not evident at Abisko at comparably high LAI (Fig. 6b), the loss of species diversity associated with fertilization may affect canopy structure such that light capture becomes limiting only at Toolik.

GPP in fertilized vegetation was higher than in controls (Fig. 5a) but the more productive plots also tended to have greater ecosystem respiration, offsetting some of the increase in plant carbon uptake. Although the data presented here are insufficient to provide an annual carbon budget, it is known that 20 years of fertilization of MAT vegetation at Toolik Lake has resulted in substantial net carbon *loss*, despite a doubling of above-ground net primary production. This net loss is caused by stimulation of decomposition in organic and mineral soils below 5 cm depth (Mack *et al*. 2004). Enhanced respiration in long-term fertilizer experiments in wet sedge vegetation may be due to the combination of increased litter input, increased root biomass, or thicker soil organic mats (Shaver *et al*. 1998; Johnson *et al*. 2000; Boelman *et al*. 2003).

THE ROLE OF MOSSES

Throughout this study we have effectively assumed that the contribution of mosses to both NDVI and ecosystem CO_2 fluxes is zero. In reality, they are a significant part of tundra plant communities. Moss biomass can contribute up to 35% of total above-ground biomass in tussock and shrub tundra, and 50% in wet sedge tundra (Shaver & Chapin 1991). It is possible that the loss of moss cover as a result of nutrient addition leads to the apparently lower GPP per unit leaf area in fertilized plots, as mosses were included in the flux measurements but not in the estimation of leaf area. The largest change in moss cover between treatments at Toolik was in NANT vegetation, where moss cover decreased from an average of 26% to < 1% with fertilization (Table 1).

At Abisko in 2005, J. C. Douma (unpublished data) found a strong negative linear relationship between the contribution of mosses to total system GPP and the LAI of vascular plants, across a variety of tundra types. Control NANT vegetation also had the lowest leaf area index (0.35 m^2 m^{-2}; Fig. 5c), so the change in moss cover is likely to have the biggest impact in this vegetation type. In the study by Douma, at vascular LAI of 0.4 m^2 m^{-2} and moss cover of 100% beneath the vascular canopy, mosses contributed around 60% of the total GPP measured. At LAI of 1.0 m^2 m^{-2} and moss cover of 100%, mosses contributed around 25% of GPP. If the same relationship applies to NANT control plots, as a rough estimate with only 26% moss cover, moss GPP_{600} might account for 15% of total system GPP_{600}. Without mosses, the GPP_{600L} value would then decrease from 8.0 to 6.6 μmol C m^{-2} LA s^{-1}. This is still higher than the average GPP_{600L} in fertilized NANT plots, but clearly mosses can be important when leaf area is low. In control MAT vegetation where LAI values are above 1.0 m^2 m^{-2}, moss photosynthesis is much less important and cannot fully explain the reduction in GPP_{600L} with fertilization.

The role of mosses will be particularly important in early season when shading by vascular plants is at a minimum. Applying J.C. Douma's results to our data at Abisko suggests that in early June the contribution of mosses would be highest in *Betula* (lowest leaf area) and wet sedge vegetation (highest moss cover). For *Betula* plots with average LAI of 0.3 m^2 m^{-2} and moss cover of 17%, accounting for moss photosynthesis reduces average GPP_{600L} by about 10%. In wet sedge vegetation, with LAI of 0.5 m^2 m^{-2} and moss cover of 37%, the reduction in GPP_{600L} would be approximately 15%; 3.9 μmol C m^{-2} LA s^{-1} including mosses, and 3.3 μmol C m^{-2} LA s^{-1} without mosses. This is still well within the range of GPP_{600L} values measured across all vegetation types during early season, although moss productivity could account for some of the unexplained variation in GPP_{600L} between vegetation types.

NDVI AND LEAF AREA

NDVI has been used extensively in production models as a measure of leaf area. We have shown, however, that when using NDVI data measured on scales that match the spatial scale of variation in vegetation type, 'calibrating' NDVI to leaf area in each vegetation type separately increases precision (Fig. 1a,b). This is due to differences in leaf colour and canopy structure between vegetation types dominated by different species or growth forms (Steltzer & Welker 2006). The presence of moss also represents a potential source of error in the NDVI-LAI relationship as mosses contribute to the NDVI signal but were not quantified as a part of vascular leaf area. It was necessary in this study to account for as much noise in the LAI-NDVI relationship as possible, in order to understand differences in LAI *between* vegetation types. For scaling up and averaging *across* vegetation types is has been shown that a single LAI-NDVI relationship can be acceptable (van Wijk & Williams 2005). For example, in this study if a single LAI-NDVI relationship is used to predict LAI at Abisko, there is still a strong positive relationship between GPP_{600} and LAI ($GPP_{600} = 5.45 \times LAI + 0.47$) but the R^2 value falls to 0.69.

We have shown that leaf area is an excellent predictor of ecosystem photosynthesis in the low arctic, regardless of vegetation type. This simplifies the task of regional carbon budgeting as it removes the need for detailed ground surveys and aggregation of species level data into ecosystem models. Expressing GPP per unit leaf area substantially reduces spatial heterogeneity in ecosystem photosynthesis. We conclude that leaf area is a good predictor of GPP (i) across different vegetation types and (ii) through the stages of leaf development. Differences between species are unimportant, though there is evidence for increases in per unit leaf area photosynthesis through the season. However, vegetation that is responding to manipulated nutrient conditions does not follow the same rules as natural vegetation. Under enhanced nutrients, leaf area is still related to GPP but the relationship differs from that in 'normal' vegetation. The LAI-GPP relationship for fertilized plots at

Toolik Lake and control plots at Abisko diverges above 1.5 m^2 m^{-2}. The cause could be self-shading within the canopy, fertilization affecting canopy structure such that self-shading occurs at Toolik Lake but not at Abisko. The divergence in LAI-GPP could also be related to the divergence of LAI-N relationships between Swedish and Alaskan vegetation at high leaf area, as demonstrated by van Wijk *et al*. (2005). The cause and generality of this phenomenon needs further research; if a warmer climate results in increases in soil fertility then adapting vegetation may also have lower rates of photosynthesis per unit canopy leaf area.

Acknowledgements

This work was supported by grants from the US National Science Foundation to the Marine Biological Laboratory including grants # OPP-0352897, DEB-0423385 and DEB-0444592. We thank Brooke Kaye, Bob Douma, Celine Ronfort, Beth Bernhardt, Joe Powers, Carrie McCalley and Catherine Thompson for their dedication in the field. Jim Laundre at the MBL and the staff at Toolik Field Station and Abisko Scientific Research Station gave us invaluable support. We also thank Ed Rastetter for his helpful comments and advice.

References

ACIA (2004) *Impacts of a Warming Arctic: Arctic Climate Impact Assessment*. Cambridge University Press, Cambridge.

Boelman, N.T., Stieglitz, M., Griffin, K.L. & Shaver, G.R. (2005) Inter-annual variability of NDVI in response to long-term warming and fertilization in wet sedge and tussock tundra. *Oecologia*, **143**, 588–597.

Boelman, N.T., Stieglitz, M., Rueth, H.M., Sommerkorn, M., Griffin, K.L., Shaver, G.R. *et al.* (2003) Response of NDVI, biomass, and ecosystem gas exchange to long-term warming and fertilization in wet sedge tundra. *Oecologia*, **135**, 414–421.

Chapin, F.S., Shaver, G.R., Giblin, A.E., Nadelhoffer, K.J. & Laundre, J.A. (1995) Responses of arctic tundra to experimental and observed changes in climate. *Ecology*, **76**, 694–711.

Gough, L. & Hobbie, S.E. (2003) Responses of moist non-acidic arctic tundra to altered environment: productivity, biomass and species richness. *Oikos*, **103**, 204–216.

Gough, L., Wookey, P.A. & Shaver, G.R. (2002) Dry heath arctic tundra responses to long-term nutrient and light manipulation. *Arctic Antarctic and Alpine Research*, **34**, 211–218.

Hobbie, S.E., Gough, L. & Shaver, G.R. (2005) Species compositional differences on different-aged glacial landscapes drive contrasting responses of tundra to nutrient addition. *Journal of Ecology*, **93**, 770–782.

Hobbie, S.E., Miley, T.A. & Weiss, M.S. (2002) Carbon and nitrogen cycling in soils from acidic and nonacidic tundra with different glacial histories in northern Alaska. *Ecosystems*, **5**, 761–774.

Hooper, D.U., Cardon, Z.G., Chapin, F.S. III & Durant, M. (2002) Corrected calculations for soil and ecosystem measurements of CO_2 flux using the LI-COR 6200 portable photosynthesis system. *Oecologia*, **132**, 1–11.

Johnson, L.C., Shaver, G.R., Cades, D.H., Rastetter, E., Nadelhoffer, K., Giblin, A. *et al.* (2000) Plant carbon–nutrient interactions control CO_2 exchange in Alaskan wet sedge tundra ecosystems. *Ecology*, **81**, 453–469.

Kudo, G., Molau, U. & Wada, N. (2001) Leaf-trait variation of tundra plants along a climatic gradient: an integration of responses in evergreen and deciduous species. *Arctic, Antarctic, and Alpine Research*, **33**, 181–190.

Mack, M.C., Schuur, E.A.G., Bret-Harte, M.S., Shaver, G.R. & Chapin, F.S. (2004) Ecosystem carbon storage in arctic tundra reduced by long-term nutrient fertilization. *Nature*, **431**, 440–443.

McGuire, A.D., Clein, J.S., Melillo, J.K., Kicklighter, D.W., Meier, R.A., Vorosmarty, C.J. *et al.* (2000) Modeling carbon responses of tundra ecosystems to historical and projected climate: sensitivity of pan-Arctic carbon storage to temporal and spatial variation in climate. *Global Change Biology*, **6**, 141–159.

Myneni, R.B., Keeling, C.D., Tucker, C.J., Asrar, G. & Nemani, R.R. (1997) Increased plant growth in the northern high latitudes from 1981 to 1991. *Nature*, **386**, 698–702.

Oberbauer, S.F. & Oechel, W.C. (1989) Maximum CO_2 assimilation rates of vascular plants on an Alaskan arctic tundra slope. *Holarctic Ecology*, **12**, 312–316.

Oechel, W.C. & Billings, W.D. (1992) *Effects of Global Change on the Carbon Balance of Arctic Plants and Ecosystems*. Academic Press, New York.

Oechel, W.C., Hastings, S.J., Vourlitis, G., Jenkins, M., Riechers, G. & Grulke, N. (1993) Recent change of Arctic tundra ecosystems from a net carbon dioxide sink to a source. *Nature*, **361**, 520–523.

Shaver, G.R., Bret-Harte, S.M., Jones, M.H., Johnstone, J., Gough, L., Laundre, J. *et al.* (2001) Species composition interacts with fertilizer to control long-term change in tundra productivity. *Ecology*, **82**, 3163–3181.

Shaver, G.R. & Chapin, F.S. III (1980) Response to fertilization by various plant growth forms in an Alaskan tundra: nutrient accumulation and growth. *Ecology*, **61**, 662–675.

Shaver, G.R. & Chapin, F.S. III (1986) Effect of fertilizer on production and biomass of tussock tundra, Alaska, USA. *Arctic and Alpine Research*, **18**, 261–268.

Shaver, G.R. & Chapin, F.S. (1991) Production–biomass relationships and element cycling in contrasting arctic vegetation types. *Ecological Monographs*, **61**, 1–31.

Shaver, G.R. & Chapin, F.S. (1995) Long-term responses to factorial, NPK fertilizer treatment by Alaskan wet and moist tundra sedge species. *Ecography*, **18**, 259–275.

Shaver, G.R., Johnson, L.C., Cades, D.H., Murray, G., Laundre, J.A., Rastetter, E.B. *et al.* (1998) Biomass and CO_2 flux in wet sedge tundras: responses to nutrients, temperature, and light. *Ecological Monographs*, **68**, 75–97.

Steltzer, H. & Welker, J.M. (2006) Modeling the effect of photosynthetic vegetation properties on the NDVI-LAI relationship. *Ecology*, **87**, 2765–2772.

Stoner, W.A., Miller, P. & Miller, P.C. (1982) Seasonal dynamics and standing crops of biomass and nutrients in a subarctic tundra vegetation. *Holarctic Ecology*, **5**, 172–179.

Sturm, M., Racine, C. & Tape, K. (2001) Increasing shrub abundance in the Arctic. *Nature*, **411**, 546–547.

Walker, M.D., Walker, D.A. & Auerbach, N.A. (1994) Plant communities of a tussock landscape in the Brooks Range Foothills, Alaska. *Journal of Vegetation Science*, **5**, 843–866.

van Wijk, M.T. & Williams, M. (2005) Optical instruments for measuring leaf area index in low vegetation: application in arctic ecosystems. *Ecological Applications*, **15**, 1462–1470.

van Wijk, M.T., Williams, M. & Shaver, G.R. (2005) Tight coupling between leaf area index and foliage N content in arctic plant communities. *Oecologia*, **142**, 421–427.

Williams, M. & Rastetter, E.B. (1999) Vegetation characteristics and primary productivity along an arctic transect: implications for scaling up. *Journal of Ecology*, **87**, 885–898.

Williams, M., Street, L.E., van Wijk, M.T. & Shaver, G.R. (2006) Identifying differences in carbon exchange among arctic ecosystem types. *Ecosystems*, **9**, 288–304.

Received 2 June 2006
revision accepted 8 September 2006
Handling Editor: Malcolm Press

Supplementary material

The following supplementary material is available for this article:

Appendix S1 Table of best fit parameters, NDVI, leaf area and environmental conditions for each NEP light response curve measured at Abisko in 2005.

Appendix S2 Table of best fit parameters, NDVI, leaf area and environmental conditions for each NEP light response curve measured at Toolik Lake in 2004.

This material is available as part of the online article from:

http://www.blackwell-synergy.com/doi/full/10.1111/j.1365–2745.2006.01187.x

Please note: Blackwell Publishing is not responsible for the content or functionality of any supplementary materials supplied by the authors. Any queries (other than missing material) should be directed to the corresponding author for the article.